

EFFICIENT SEPARATION OF BENZENE AND  
CYCLOHEXANE BY LIQUID-LIQUID EXTRACTION USING  
EMERGING SOLVENTS AND THEIR BINARY MIXTURES

MUHAMMAD ZULHAZIMAN BIN MAT SALLEH

FACULTY OF ENGINEERING  
UNIVERSITY OF MALAYA  
KUALA LUMPUR

2019

**EFFICIENT SEPARATION OF BENZENE AND  
CYCLOHEXANE BY LIQUID-LIQUID EXTRACTION  
USING EMERGING SOLVENTS AND THEIR BINARY  
MIXTURES**

**MUHAMMAD ZULHAZIMAN BIN MAT SALLEH**

**THESIS SUBMITTED IN FULFILMENT OF THE  
REQUIREMENTS FOR THE DEGREE OF DOCTOR OF  
PHILOSOPHY**

**DEPARTMENT OF CHEMICAL ENGINEERING  
FACULTY OF ENGINEERING  
UNIVERSITY OF MALAYA  
KUALA LUMPUR**

**2019**

**UNIVERSITY OF MALAYA**  
**ORIGINAL LITERARY WORK DECLARATION**

Name of Candidate: Muhammad Zulhaziman Bin Mat Salleh

Matric No: KHA 150027

Name of Degree: Doctor of Philosophy

Title of Thesis: Efficient separation of benzene and cyclohexane by liquid–liquid extraction using emerging solvents and their binary mixtures.

Field of Study: Green technology

I do solemnly and sincerely declare that:

- (1) I am the sole author/writer of this Work;
- (2) This Work is original;
- (3) Any use of any work in which copyright exists was done by way of fair dealing and for permitted purposes and any excerpt or extract from, or reference to or reproduction of any copyright work has been disclosed expressly and sufficiently and the title of the Work and its authorship have been acknowledged in this Work;
- (4) I do not have any actual knowledge nor do I ought reasonably to know that the making of this work constitutes an infringement of any copyright work;
- (5) I hereby assign all and every rights in the copyright to this Work to the University of Malaya (“UM”), who henceforth shall be owner of the copyright in this Work and that any reproduction or use in any form or by any means whatsoever is prohibited without the written consent of UM having been first had and obtained;
- (6) I am fully aware that if in the course of making this Work I have infringed any copyright whether intentionally or otherwise, I may be subject to legal action or any other action as may be determined by UM.

Candidate’s Signature

Date:

Subscribed and solemnly declared before,

Witness’s Signature

Date:

Name:

Designation:

**EFFICIENT SEPARATION OF BENZENE AND CYCLOHEXANE BY  
LIQUID–LIQUID EXTRACTION USING EMERGING SOLVENTS AND  
THEIR BINARY MIXTURES**

**ABSTRACT**

The separation of benzene and cyclohexane is difficult to perform via conventional distillation because of their close boiling points. The use of conventional technology in industry suffers from several disadvantages such as process complexity, high capital and operating costs, and high energy consumption. Ionic liquids (ILs) and deep eutectic solvents (DESs) are two types of emerging solvents being widely studied in many applications. In this study, 40 DESs and more than 200 ILs were separately screened using COSMO-RS program for the separation of benzene and cyclohexane by liquid–liquid extraction process. The screening was evaluated based on the comparison of selectivity, capacity, and performance index; all derived from the activity coefficient at infinite dilution. The actual performance of the top-screened solvents, i.e. 5 DESs and 4 ILs was validated via experimental liquid–liquid extraction process at 25 °C and under 1 atm. The selected DESs in this study, namely tetrabutylammonium bromide:sulfolane, TBABr:Sulf (1:7); tetrabutylammonium bromide:triethylene glycol, TBABr:TEG (1:4); methyltriphenylphosphonium bromide:triethylene glycol, MTPPBr:TEG (1:4); methyltriphenylphosphonium bromide:1,2-propanediol, MTPPBr:PD (1:4); and choline chloride:triethylene glycol ChCl:TEG (1:4), were proved to be feasible extracting solvents. Despite the small benzene distribution ratio, an effective extraction using TBABr:Sulf (1:7) was still achievable through a multistage process, where 97% of benzene were extracted after nine extraction stages. In addition, TBABr:Sulf (1:7) can be easily recovered and regenerated back into the next extraction cycle. After four cycles, the recycled DES was as effective as the fresh one; the extracted benzene was constantly

higher than 98 %. The analysis of extraction mechanism proved that the TBABr:Sulf (1:7) conserves its structure in the presence of benzene, thus prevents the solubilisation of sulfolane in the raffinate phase. In the study of extraction using IL, four ILs, namely 1-ethyl-3-methylimidazolium acetate,  $C_2mimAc$ ; 1-ethyl-3-methylimidazolium dicyanamide,  $C_2mimN(CN)_2$ ; 1-ethyl-3-methylimidazolium thiocyanate,  $C_2mimSCN$ ; and 1-ethyl-3-methylimidazolium bis(trifluoromethylsulfonyl)imide,  $C_2mimTf_2N$ , were selected based on the COSMO-RS preliminary screening. The new ternary LLE data for each IL was measured experimentally and correlated successfully with the NRTL model, where the root mean square deviation (RMSD) between experimental and calculated solubilities was less than 1%. On top of being commercially available at relatively low prices, the selected ILs showed effective extraction of benzene. The comparison of these ILs with other solvents in the literature proved their relative superiority with respect to extraction efficiency. Finally, mixtures of binary solvent were developed under the same condition by utilizing the high individual value of selectivity or distribution ratio of the single IL. Six new pseudo-ternary LLE data involving binary mixtures of [IL–organic solvent] or [IL–IL] were generated. Ethylene glycol was discovered as a good diluting agent with  $C_2mimTf_2N$ , indicating a potential cost saving. At the optimized mixing fraction, the mixture of [ $C_2mimTf_2N + C_2mimSCN$ ] produced the highest extraction performance, giving benzene distribution ratio of 0.96 and selectivity of 20.7. The mixing of different solvents has been proved to be a newly efficient and versatile method to further enhance the extraction performance.

**Keywords:** Ionic liquids, deep eutectic solvents, COSMO-RS, liquid–liquid extraction, aromatic–aliphatic

**PEMISAHAN CEKAP BENZENA DAN SIKLOHEKSANA SECARA  
PENGEKTRAKAN CECAIR-CECAIR MENGGUNAKAN PELARUT BAHARU  
DAN CAMPURAN BINARINYA**

**ABSTRAK**

Pemisahan campuran benzena dan sikloheksana adalah sukar untuk dilakukan melalui penyulingan konvensional disebabkan takat didih mereka yang berdekatan. Penggunaan teknologi konvensional di peringkat industri mempunyai beberapa kelemahan seperti kerumitan proses, modal dan kos operasi yang tinggi, serta penggunaan tenaga yang tinggi. Cecair ionik (IL) dan pelarut eutektik (DES) adalah dua jenis pelarut baharu yang dikaji secara meluas di dalam pelbagai aplikasi. Dalam kajian ini, 40 DES dan lebih 200 IL telah disaring secara berasingan menggunakan program COSMO-RS untuk pemisahan benzena dan sikloheksana melalui proses pengekstrakan cecair-cecair. Penyaringan ini dinilai berdasarkan kepada perbandingan selektiviti, kapasiti, dan indeks prestasi; di mana kesemuanya dikira berdasarkan pekali aktiviti pada pencairan infiniti. Prestasi sebenar pelarut-pelarut ini, iaitu 5 DES dan 4 IL telah disahkan melalui eksperimen pengekstrakan cecair-cecair pada suhu 25 °C dan tekanan 1 atm. DES-DES yang dipilih dalam kajian ini, iaitu *tetrabutylammonium bromide:sulfolane*, *TBABr:Sulf (1:7)*; *tetrabutylammonium bromide:triethylene glycol*, *TBABr:TEG (1:4)*; *methyltriphenylphosphonium bromide:triethylene glycol*, *MTPPBr:TEG (1:4)*; *methyltriphenylphosphonium bromide:1,2-propanediol*, *MTPPBr:PD (1:4)*; dan *choline chloride:triethylene glycol* *ChCl:TEG (1:4)* telah terbukti sebagai pelarut pengekstrak yang berkesan. Walaupun nisbah taburan benzena adalah kecil, pengekstrakan yang berkesan menggunakan *TBABr:Sulf (1:7)* masih dapat dicapai melalui proses bertahap, di mana 97% benzena telah berjaya diekstrak selepas sembilan tahap. Selain itu, *TBABr:Sulf (1:7)* juga boleh dirawat dan dikitar semula. Selepas empat kitaran, prestasi

DES masih seperti keadaan yang baharu kerana jumlah benzena yang diekstrak sentiasa melebihi 98%. Analisis mekanisme pengekstrakan membuktikan bahawa TBABr:Sulf (1:7) memelihara strukturnya dengan kehadiran benzena, lalu mengelakkan pelarutan sulfolane dalam lapisan rafinat. Dalam kajian pengekstrakan menggunakan IL, empat jenis IL iaitu *1-ethyl-3-methylimidazolium acetate*,  $C_2mimAc$ ; *1-ethyl-3-methylimidazolium dicyanamide*,  $C_2mimN(CN)_2$ ; *1-ethyl-3-methylimidazolium thiocyanate*,  $C_2mimSCN$ ; dan *1-ethyl-3-methylimidazolium bis(trifluoromethylsulfonyl)imide*,  $C_2mimTf_2N$  telah dipilih. Data LLE ternari yang baharu bagi setiap IL telah diperolehi secara eksperimen dan dikorelasikan dengan model NRTL dengan nilai RMSD kurang daripada 1%. Selain daripada boleh didapati secara komersil pada harga yang lebih rendah, IL-IL ini juga menunjukkan pengekstrakan benzena yang berkesan. Perbandingan IL-IL ini dengan pelarut-pelarut yang lain dalam literatur membuktikan keunggulan mereka dari aspek keberkesanan pengekstrakan. Akhir sekali, kaedah campuran binari pelarut telah dikembangkan pada kondisi yang sama dengan memanfaatkan ketinggian selektiviti dan nisbah penyebaran benzena dalam IL individu. Enam data LLE pseudo-ternari telah dihasilkan melibatkan campuran-campuran binari [IL–pelarut organik] atau [IL–IL]. Etilena glikol telah ditemui sebagai ejen pencairan yang baik terhadap  $C_2mimTf_2N$ , sekaligus menandakan potensi besar terhadap penjimatan kos. Pada nisbah campuran optimal, campuran [ $C_2mimTf_2N + C_2mimSCN$ ] menghasilkan prestasi pengekstrakan tertinggi, iaitu nisbah taburan benzena sebanyak 0.96 dan selektiviti bernilai 20.67. Pelarut campuran binari terbukti sebagai suatu kaedah baharu yang efisien serta versatil untuk meningkatkan lagi prestasi pengekstrakan.

**Kata kunci:** Cecair ionik, pelarut eutektik, COSMO-RS, pengekstrakan cecair–cecair, aromatic–alifatik

## ACKNOWLEDGEMENTS

First and foremost, my utmost gratitude to Allah SWT for granting me opportunity and strength to pursue this study, and for guiding me a bright path along the way.

Very special thanks to my two honorable supervisors, Professor Dr Mohd Ali Hashim and Associate Professor Dr Mohamed Kamel Hadj-Kali, for their undeniably great supervisions along this admission. Thank you for your patience and trust. I truly appreciate all the meaningful guidances and the valuable advices given to me.

Thank you to all members of UMCiL (University Malaya Centre for Ionic Liquids) for the continuous support and inspiration, especially to Dr Hanee Farzana, Dr Adeeb Hayyan, Dr Maan Hayyan, Dr Mohamed Khalid and Dr Muhammad AbdulHakim Alsaadi. To my colleagues Hamdi, Shahida, Shakilla, Ein, Ainul and Anis, thank you very much for the great moment we shared together in UMCiL.

From the bottom of my heart, I would like to dedicate my warmest thank to my parents, my wife and my family members for their love, support and continuous encouragement throughout the study.

To Mu'min and Mu'izz, thank you for being my awesome boys and for giving indirect motivations to your father here.

Last but not least, I would like to thank all other people who are directly and indirectly involved in assisting me along this study.

## TABLE OF CONTENTS

ABSTRACT.....	iii
ABSTRAK.....	v
ACKNOWLEDGEMENTS.....	vii
TABLE OF CONTENTS.....	viii
LIST OF FIGURES.....	xiii
LIST OF TABLES.....	xix
LIST OF SYMBOLS AND ABBREVIATIONS.....	xxii
LIST OF APPENDICES.....	xxv
<b>CHAPTER 1: INTRODUCTION.....</b>	<b>1</b>
1.1 Background.....	1
1.2 Problem statement.....	4
1.3 Objectives.....	6
1.4 Research methodology.....	7
1.5 Scope of study.....	8
1.6 Outline of thesis.....	9
<b>CHAPTER 2: LITERATURE REVIEW.....</b>	<b>10</b>
2.1 Benzene and cyclohexane.....	10
2.1.1 Properties of benzene and cyclohexane.....	10
2.1.2 Production and demand of benzene and cyclohexane.....	13
2.2 Industrial technologies to separate benzene–cyclohexane mixture.....	18

2.2.1	Azeotropic distillation .....	19
2.2.2	Extractive distillation .....	20
2.3	Ionic liquids .....	22
2.3.1	Overview of ILs.....	22
2.3.2	Review on the performance of ILs and organic solvents in extractive separation of benzene and cyclohexane .....	25
2.3.2.1	Performance of organic solvents .....	25
2.3.2.2	Progress of ILs .....	31
2.4	Deep eutectic solvents .....	38
2.4.1	Overview of DESs.....	38
2.4.2	Review on the potential of DESs in separation of benzene and cyclohexane 41	
2.4.2.1	Extractive performance of DESs in separation of aromatic–aliphatic mixtures .....	41
2.4.2.2	Comparison of extractive performance between DESs and organic solvents.....	45
2.4.2.3	Comparison of extractive performance between DESs and ILs	49
2.5	COSMO-RS programme .....	52
2.5.1	COSMO-RS theory .....	52
2.5.2	Highlights on application of COSMO-RS in separation processes.....	54
2.5.2.1	Activity coefficients at infinite dilution .....	55
2.5.2.2	The use of COSMO-RS to predict liquid–liquid phase equilibria involving ILs and DESs .....	58
2.6	The potential of modifying the solvent as a binary mixture.....	63
2.6.1	Overview of solvent binary mixture.....	63
2.6.2	Applications of solvent binary mixture in liquid–liquid extraction .....	64

2.7	Outcomes of literature review .....	69
<b>CHAPTER 3: METHODOLOGY .....</b>		<b>70</b>
3.1	Part 1: COSMO-RS prediction .....	71
3.1.1	Generation of COSMO-files .....	71
3.1.2	Molecular representation in COSMOthermX .....	71
3.1.3	Screening of DESs.....	72
3.1.4	Screening of ILs .....	76
3.1.5	The selectivity, capacity and performance index at infinite dilution .....	78
3.2	Part 2: LLE experiment .....	79
3.2.1	Materials .....	79
3.2.2	Synthesis of DESs .....	80
3.2.3	LLE experiments .....	81
3.2.4	Compositional analysis.....	81
3.2.5	Experimental selectivity and distribution ratio .....	82
3.2.6	Consistency tests using the Othmer-Tobis and Hand correlations.....	83
3.2.7	Correlation of LLE data .....	83
3.3	Part 3: Binary mixing of ILs.....	85
3.3.1	Mixing operation .....	85
3.3.2	Determination of optimized binary ratio .....	86
3.3.3	Quaternary LLE experiments .....	86
<b>CHAPTER 4: RESULTS AND DISCUSSION .....</b>		<b>88</b>
4.1	Extractive separation of benzene and cyclohexane using DESs .....	88
4.1.1	DES ranking from $C^\infty$ and $S^\infty$ .....	88
4.1.2	Molecular interactions .....	90
4.1.2.1	Analysis of $\sigma$ -profiles.....	90

4.1.2.2	Analysis of $\sigma$ -potentials.....	93
4.1.3	Effects of salt:HBD ratio.....	94
4.1.4	Ternary liquid-liquid equilibrium.....	96
4.1.5	NRTL regression and consistency tests.....	100
4.1.6	Experimental selectivity and distribution ratio.....	102
4.1.7	Analysis of extraction mechanism using $^1\text{H}$ NMR.....	104
4.1.8	Comparison between COSMO-RS prediction and experimental measurement.....	106
4.1.9	Number of extraction stages.....	107
4.1.10	Regeneration of DESs.....	108
4.2	Extractive separation of benzene and cyclohexane using ILs.....	109
4.2.1	COSMO-RS screening.....	109
4.2.1.1	$\sigma$ -profiles of industrial organic solvents and ILs.....	109
4.2.1.2	$C^\infty$ , $S^\infty$ and $PI^\infty$ .....	111
4.2.1.3	Selection of ILs for experimental validation.....	114
4.2.2	Settling time study.....	116
4.2.3	Ternary LLE data.....	117
4.2.4	Comparison between COSMO-RS and experimental results.....	121
4.2.5	Comparison of the selected ILs with other solvents.....	125
4.2.6	NRTL correlation.....	127
4.3	Extractive separation of benzene and cyclohexane using binary ILs.....	129
4.3.1	Mixing of IL with organic solvents.....	129
4.3.2	Mixing of an IL with another IL.....	134
4.3.3	Comparison between the mixed and pure solvents.....	142
4.3.4	The NRTL modelling.....	144
4.4	General insights on the economic and environmental benefits.....	146

<b>CHAPTER 5: CONCLUSION AND RECOMMENDATIONS .....</b>	<b>147</b>
5.1 Conclusion .....	147
5.1.1 The feasibility of using COSMO-RS for solvent screening.....	147
5.1.2 DESs as a cheaper alternative.....	148
5.1.3 The superior performance of ILs.....	148
5.1.4 The potential of binary ILs mixture .....	149
5.2 Recommendations.....	150
REFERENCES.....	152
LIST OF PUBLICATIONS AND CONFERENCE PROCEEDINGS.....	167
List of main publications in journals: .....	167
List of other publications during this admission:.....	168
List of papers presented in conferences: .....	168
APPENDIX .....	174

## LIST OF FIGURES

Figure 2.1: Heats of hydrogenation from cyclohexane to cyclohexene, 1,3-cyclohexadiene, and benzene .....	10
Figure 2.2: The structure of a benzene molecule in view of (a) electrostatic potential map and (b) resonance structure .....	11
Figure 2.3: Structure of cyclohexane in view of (a) a flat hexagon and (b) the most-stable chair conformation .....	12
Figure 2.4: Structure and energy levels of cyclohexane conformers, and the energy required for this ring-flipping process .....	13
Figure 2.5: Main applications of benzene .....	15
Figure 2.6: Hydrogenation of benzene to produce cyclohexane .....	17
Figure 2.7: Separation of benzene and cyclohexane by azeotropic distillation using acetone and water .....	20
Figure 2.8: Separation of benzene and cyclohexane by extractive distillation using furfural .....	21
Figure 2.9 Number of publications in the topic of ILs since 1990 .....	23
Figure 2.10: Example of common cations and anions of ILs .....	23
Figure 2.11: The range of distribution ratio for organic solvents from literature .....	29
Figure 2.12: The range of selectivity for organic solvents from literature .....	29
Figure 2.13: Number of annual publications in the topic of DESs since the year 2000.	39
Figure 2.14: Structure of some compounds that can form DESs: (a) salts and (b) HBDs .....	40
Figure 2.15: The selectivity range for some ternary systems involving organic solvents/DESs + aromatics + aliphatics. ....	47
Figure 2.16: The distribution ratio range for some ternary systems involving organic solvents/DESs + aromatics + aliphatics. ....	48
Figure 2.17: Comparative performance of ILs and DESs in the separation of benzene– <i>n</i> -hexane .....	50

Figure 2.18: Comparative performance of ILs and DESs in the separation of toluene–heptane .....	50
Figure 2.19: Comparative performance of ILs and DESs in the separation of thiophene–heptane .....	51
Figure 2.20: Conductor like screening model process: (a) a water molecule in its original form, (b) the molecule inside a molecular shape cavity in a continuum medium, (c) screening charges on the cavity surface. ....	52
Figure 2.21: Separation factors, $\alpha$ (selectivity) and distribution ratio, $D$ of toluene versus mole fraction of $C_4pyBF_4$ in the mixed IL solvents ( $\phi_3$ ) for two pseudo-ternary systems: (a) n-heptane (1) + toluene (2) + ( $C_4pyBF_4$ + $C_4pyTF_2N$ ) and (b) n-heptane (1) + toluene (2) + ( $C_4pyBF_4$ + $C_4mpyTF_2N$ ) at 313.15 K and atmospheric pressure (García et al., 2012b, 2012d) .....	65
Figure 4.1: Selectivity of DESs at infinite dilution.....	88
Figure 4.2: Capacity of DESs at infinite dilution.....	89
Figure 4.3: Performance index of DESs at infinite dilution.....	89
Figure 4.4: $\sigma$ -profiles benzene, cyclohexane and DESs with high $S^\infty$ .....	90
Figure 4.5: $\sigma$ -profiles of benzene, cyclohexane and DESs with high $C^\infty$ .....	91
Figure 4.6: $\sigma$ -potential of DESs with $C^\infty$ and $PI^\infty$ .....	94
Figure 4.7: Effect of Salt:HBD ratio towards DESs' $C^\infty$ , $S^\infty$ and $PI^\infty$ . The black, grey and white colours represent MTPPBr:PD, TBABr:TEG and MTPPBr:TEG, respectively. 96	
Figure 4.8: Ternary phase diagrams for TBABr:Sulf (1:7) + benzene + cyclohexane at 298.15 K and 1 atm: –●–, experimental; --○--, COSMO-RS; and ·×·, NRTL .....	98
Figure 4.9: Ternary phase diagrams for TBABr:TEG (1:4) + benzene + cyclohexane at 298.15 K and 1 atm: –●–, experimental; --○--, COSMO-RS; and ·×·, NRTL .....	98
Figure 4.10: Ternary phase diagrams for MTPPBr:TEG (1:4) + benzene + cyclohexane at 298.15 K and 1 atm: –●–, experimental; --○--, COSMO-RS; and ·×·, NRTL.....	99
Figure 4.11: Ternary phase diagrams for MTPPBr:PD (1:4) + benzene + cyclohexane at 298.15 K and 1 atm: –●–, experimental; --○--, COSMO-RS; and ·×·, NRTL .....	99
Figure 4.12: Ternary phase diagrams for ChCl:TEG (1:4) + benzene + cyclohexane at 298.15 K and 1 atm: –●–, experimental; --○--, COSMO-RS; and ·×·, NRTL .....	100

Figure 4.13: Distribution ratio as a function of benzene concentration in the raffinate phase. The solid-full and dashed-empty data represent the experimental and COSMO-RS results, respectively. The symbols of square, circle, triangle, diamond and star represent TBABr:Sulf (1:7), TBABr:TEG (1:4), MTPPBr:TEG (1:4), MTPPBr:PD (1:4) and ChCl:TEG (1:4), respectively. ....	102
Figure 4.14: Selectivity as a function of benzene concentration in the raffinate phase. The solid-full and dashed-empty data represent the experimental and COSMO-RS results, respectively. The symbols of square, circle, triangle, diamond and star represent TBABr:Sulf (1:7), TBABr:TEG (1:4), MTPPBr:TEG (1:4), MTPPBr:PD (1:4) and ChCl:TEG (1:4), respectively. ....	103
Figure 4.15: <sup>1</sup> H NMR spectra of TBABr:Sulf (1:7) and its constituents, in the presence of 20% benzene. ....	105
Figure 4.16: HPLC chromatograms of benzene in the raffinate phase for different extraction stages with TBABr:Sulf (1:7) .....	107
Figure 4.17: Extraction percentage of benzene using TBABr:Sulf (1:7) after different regeneration cycle. ....	108
Figure 4.18: $\sigma$ -profiles of benzene, cyclohexane and industrial organic solvents .....	109
Figure 4.19: $\sigma$ -profiles of benzene, cyclohexane and ILs with cyclic cations .....	110
Figure 4.20: Capacity of the screened ILs at infinite dilution: $\blacktriangle$ , $C_n\text{mim}^+$ ; $\blacklozenge$ , $C_n\text{mpyr}^+$ ; $\bullet$ , $C_n\text{mpyrro}^+$ ; $\blacksquare$ , $C_n\text{mpip}^+$ and the fill colors of green, red, blue and black indicate the cation alkyl length (n) from ethyl, butyl, hexyl and octyl, respectively. ....	111
Figure 4.21: Selectivity of the screened ILs at infinite dilution: $\blacktriangle$ , $C_n\text{mim}^+$ ; $\blacklozenge$ , $C_n\text{mpyr}^+$ ; $\bullet$ , $C_n\text{mpyrro}^+$ ; $\blacksquare$ , $C_n\text{mpip}^+$ and the fill colors of green, red, blue and black indicate the cation alkyl length (n) from ethyl, butyl, hexyl and octyl, respectively. ....	112
Figure 4.22: $S^\infty$ vs $C^\infty$ for the screened ILs in this study .....	113
Figure 4.23: Performance index of the screened ILs at infinite dilution: $\blacktriangle$ , $C_n\text{mim}^+$ ; $\blacklozenge$ , $C_n\text{mpyr}^+$ ; $\bullet$ , $C_n\text{mpyrro}^+$ ; $\blacksquare$ , $C_n\text{mpip}^+$ and the fill colors of green, red, blue and black indicate the cation alkyl length (n) from ethyl, butyl, hexyl and octyl, respectively. ....	114
Figure 4.24: Molar concentration of individual species in extract phase versus time after extraction .....	117
Figure 4.25: Ternary LLE diagram for $C_2\text{mimAc}$ + benzene + cyclohexane at 25 °C and 1 atm. The symbols are represented by: $-\blacktriangle-$ , experimental; $--\Delta--$ , COSMO-RS; and $\cdots\times\cdots$ , NRTL. ....	119

Figure 4.26: Ternary LLE diagram for $C_2mimN(CN)_2$ + benzene + cyclohexane at 25 °C and 1 atm. The symbols are represented by: $\blacktriangle$ , experimental; $\Delta$ , COSMO-RS; and $\times$ , NRTL.....	119
Figure 4.27: Ternary LLE diagram for $C_2mimSCN$ + benzene + cyclohexane at 25 °C and 1 atm. The symbols are represented by: $\blacktriangle$ , experimental; $\Delta$ , COSMO-RS; and $\times$ , NRTL. ....	120
Figure 4.28: Ternary LLE diagram for $C_2mimTf_2N$ + benzene + cyclohexane at 25 °C and 1 atm. The symbols are represented by: $\blacktriangle$ , experimental; $\Delta$ , COSMO-RS; and $\times$ , NRTL. ....	120
Figure 4.29: Distribution ratio of benzene versus mole fraction of benzene in raffinate phase for five ternary systems in this study. The solid and dashed lines indicate experimental and COSMO-RS data, respectively.....	123
Figure 4.30: Selectivity of ILs versus mole fraction of benzene in raffinate phase for five ternary systems in this study. The solid and dashed lines indicate experimental and COSMO-RS data, respectively. ....	123
Figure 4.31: Distribution ratio of organic solvents, ILs and DESs for the extractive separation of benzene and cyclohexane .....	125
Figure 4.32: Selectivity of organic solvents, ILs and DESs for the extractive separation of benzene and cyclohexane.....	126
Figure 4.33: Selectivity of solvent ( $\blacksquare$ ) and distribution ratio of benzene ( $\blacktriangle$ ) versus molar fractions of an IL in the respective binary IL mixtures for the pseudo-ternary systems of benzene + cyclohexane + [ $C_2mimSCN$ + DMF] at 25 °C and 1 atm. The solid and dashed lines indicate the experimental and calculated data, respectively. The red line refers to the selectivity and distribution ratio for sulfolane at the same condition. ....	129
Figure 4.34: Selectivity of solvent ( $\blacksquare$ ) and distribution ratio of benzene ( $\blacktriangle$ ) versus molar fractions of an IL in the respective binary IL mixtures for the pseudo-ternary systems of benzene + cyclohexane + [ $C_2mimTf_2N$ + EG] at 25 °C and 1 atm. The solid and dashed lines indicate the experimental and calculated data, respectively. The red line refers to the selectivity and distribution ratio for sulfolane at the same condition. ....	130
Figure 4.35: Ternary LLE involving the mixture of [ $C_2mimSCN$ + DMF] in comparison with the individual $C_2mimSCN$ or DMF. ....	132
Figure 4.36: Ternary LLE involving the mixture of [ $C_2mimTf_2N$ + EG] in comparison with the individual $C_2mimTf_2N$ or EG.....	133
Figure 4.37: Selectivity of solvent ( $\blacksquare$ ) and distribution ratio of benzene ( $\blacktriangle$ ) versus molar fractions of an IL for the pseudo-ternary systems of benzene + cyclohexane + [ $C_2mimSCN$ + $C_2mimTf_2N$ ] at 298 °C and 1 atm. The solid and dashed lines indicate the	

experimental and calculated data, respectively. The red line refers to the selectivity and distribution ratio for sulfolane at the same condition..... 135

Figure 4.38: Selectivity of solvent (—■—) and distribution ratio of benzene (—▲—) versus molar fractions of an IL for the pseudo-ternary systems of benzene + cyclohexane + [C<sub>2</sub>mimN(CN)<sub>2</sub> + C<sub>2</sub>mimTf<sub>2</sub>N] at 298 °C and 1 atm. The solid and dashed lines indicate the experimental and calculated data, respectively. The red line refers to the selectivity and distribution ratio for sulfolane at the same condition..... 135

Figure 4.39: Selectivity of solvent (—■—) and distribution ratio of benzene (—▲—) versus molar fractions of an IL for the pseudo-ternary systems of benzene + cyclohexane + [C<sub>2</sub>mimSCN + C<sub>2</sub>mimN(CN)<sub>2</sub>] at 298 °C and 1 atm. The solid and dashed lines indicate the experimental and calculated data, respectively. The red line refers to the selectivity and distribution ratio for sulfolane at the same condition..... 136

Figure 4.40: Selectivity of solvent (—■—) and distribution ratio of benzene (—▲—) versus molar fractions of an IL for the pseudo-ternary systems of benzene + cyclohexane + [C<sub>2</sub>mimN(CN)<sub>2</sub> + C<sub>2</sub>mimAc] at 298 °C and 1 atm. The solid and dashed lines indicate the experimental and calculated data, respectively. The red line refers to the selectivity and distribution ratio for sulfolane at the same condition..... 136

Figure 4.41: Ternary plots involving the mixture of [C<sub>2</sub>mimSCN + C<sub>2</sub>mimTf<sub>2</sub>N] in comparison with the individual IL: —▲—, experimental (IL mixture); --▲--, COSMO-RS (IL mixture); ··×··, NRTL (IL mixture); --○--, pure C<sub>2</sub>mimSCN and --□--, pure C<sub>2</sub>mimTf<sub>2</sub>N ..... 140

Figure 4.42: Ternary plots involving the mixture of [C<sub>2</sub>mimN(CN)<sub>2</sub> + C<sub>2</sub>mimTf<sub>2</sub>N] in comparison with the individual IL: —▲—, experimental (IL mixture); --▲--, COSMO-RS (IL mixture); ··×··, NRTL (IL mixture); --○--, pure C<sub>2</sub>mimN(CN)<sub>2</sub> and --□--, pure C<sub>2</sub>mimTf<sub>2</sub>N ..... 140

Figure 4.43: Ternary plots involving the mixture of [C<sub>2</sub>mimSCN + C<sub>2</sub>mimN(CN)<sub>2</sub>] in comparison with the individual IL: —▲—, experimental (IL mixture); --▲--, COSMO-RS (IL mixture); ··×··, NRTL (IL mixture); --○--, pure C<sub>2</sub>mimSCN and --□--, pure C<sub>2</sub>mimN(CN)<sub>2</sub>..... 141

Figure 4.44: Ternary plots involving the mixture of [C<sub>2</sub>mimN(CN)<sub>2</sub> + C<sub>2</sub>mimAc] in comparison with the individual IL: —▲—, experimental (IL mixture); --▲--, COSMO-RS (IL mixture); ··×··, NRTL (IL mixture); --○--, pure C<sub>2</sub>mimN(CN)<sub>2</sub> and --□--, pure C<sub>2</sub>mimAc..... 141

Figure 4.45: Distribution ratio of benzene using [IL + organic solvent] mixtures in comparison with the respective pure ones. .... 142

Figure 4.46: Selectivity of [IL + organic solvent] mixtures in comparison with the respective pure ones. .... 143

Figure 4.47: Distribution ratio of benzene using binary mixture of ILs in comparison with the respective pure ILs. .... 143

Figure 4.48: Selectivity of [IL + IL] mixtures in comparison with the respective pure ILs. .... 144

University of Malaya

## LIST OF TABLES

Table 2.1: Physical properties of benzene and cyclohexane (Villaluenga & Tabe-Mohammadi, 2000).....	13
Table 2.2: Common processes to separate aromatic–aliphatic mixtures and their operational suitability (Brandrup, 1989).....	19
Table 2.3: The conventional organic solvents studied in the separation of benzene and cyclohexane by liquid-liquid extraction.....	28
Table 2.4: Vapor pressure of organic solvents used in the separation of benzene and cyclohexane.....	30
Table 2.5: Performance of ILs previously studied for the separation of benzene and cyclohexane.....	37
Table 2.6: Summary of DESs used for the separation of aromatic compounds from n-hexane (at P =101.325 kPa) .....	43
Table 2.7: Summary of DESs used for the separation of aromatic compounds from n-heptane (at P =101.325 kPa) .....	44
Table 2.8: DES used for the separation of aromatic compounds from n-octane (at P =101.325 kPa).....	44
Table 2.9: Extractive separation of aromatic and aliphatic using DESs or organic solvents .....	45
Table 2.10: Summary of ILs used for the separation of aromatic–aliphatic mixtures (at 101.325 kPa) .....	49
Table 2.11: Equations and constants in COSMO-RS .....	54
Table 2.12: The RMSD value between the experimental and COSMO-RS data for separation of aromatic–aliphatic mixtures using DESs .....	61
Table 2.13: The use of mixed solvents for the separation of aliphatic and aromatic compounds .....	68
Table 3.1: List of the selected DESs for COSMO-RS screening.....	73
Table 3.2: List of cations for the screening of ILs .....	76
Table 3.3: List of anions for the screening of ILs .....	77
Table 3.4: ILs used in the LLE experiments .....	79

Table 3.5: DES constituents involved in synthesis and LLE experiments .....	79
Table 3.6: Details of benzene and cyclohexane used in LLE experiments.....	80
Table 3.7: <sup>1</sup> HNMR solvents used for compositional analysis.....	80
Table 3.8: DESs synthesized in this work.....	80
Table 4.1: Molar composition of tie-lines with the distribution ratio and selectivity data for the ternary systems investigated in this work.....	97
Table 4.2: NRTL parameters for the ternary systems (benzene + cyclohexane + DES) with RMSD between experimental and calculated data. ....	101
Table 4.3: Parameters of Othmer–Tobias and Hand correlation for each ternary system and the values of regression coefficient R <sup>2</sup> .....	101
Table 4.4: The top 15 ILs according to COSMO-RS screening by C <sup>∞</sup> , S <sup>∞</sup> and PI <sup>∞</sup> ....	115
Table 4.5: Molar composition of the tie-lines with the distribution ratio and selectivity data for benzene (1) + cyclohexane (2) + ILs (3) at 25 °C and 1 atm.....	118
Table 4.6: Parameters of Othmer-Tobias and Hand correlation for each ternary system and the values of regression coefficient, R <sup>2</sup> .....	121
Table 4.7: Molar composition of the tie-lines predicted by COSMO-RS for benzene (1) + cyclohexane (2) + ILs (3) at 25 °C and 1 atm .....	124
Table 4.8: RMSD values between the tie lines of COSMO-RS and experimental approaches.....	124
Table 4.9: Binary interaction parameters in NRTL regression for the ternary systems in this study with RMSD between experimental and calculated data. ....	128
Table 4.10: Molar composition of the tie-lines with the distribution ratio and selectivity data for benzene (1) + cyclohexane (2) + DMF or EG (3) at 25 °C and 1 atm.....	131
Table 4.11: Molar composition of the tie-lines with the distribution ratio and selectivity data for benzene (1) + cyclohexane (2) + [IL (3) + DMF or EG (4)] at 25 °C and 1 atm .....	132
Table 4.12: The selectivity and distribution ratio using pure ILs for 10 wt % of benzene in benzene-cyclohexane feed mixture.....	134
Table 4.13: Molar composition of the tie-lines with the distribution ratio and selectivity data for benzene (1) + cyclohexane (2) + binary mixture of ILs (3) at 25 °C and 1 atm .....	139

Table 4.14: Binary interaction parameters in NRTL regression for the ternary systems in this study with RMSD between experimental and calculated data ..... 145

University of Malaya

## LIST OF SYMBOLS AND ABBREVIATIONS

IL	:	Ionic liquid
DES	:	Deep eutectic solvent
HBA	:	Hydrogen bond acceptor
HBD	:	Hydrogen bond donor
LLE	:	Liquid-liquid equilibrium
GCM	:	Group contribution method
UNIQUAC	:	Universal quasichemical
UNIFAC	:	Universal quasichemical functional group activity coefficients
TBABr	:	Tetrabutylammonium bromide
MTPPBr	:	Methyltriphenylphosphonium
TEG	:	Triethylene glycol
PD	:	1,2-propanediol
Sulf	:	Sulfolane
RMSD	:	Root mean square deviation
COSMO-RS	:	Conductor-like Screening Model for Real Solvent
NMR	:	Nuclear magnetic resonance
NRTL	:	Non-Random Two-Liquid
DMF	:	Dimethylformamide
DMSO	:	Dimethylsulfoxide
EG	:	Ethylene glycol
EC	:	Ethylene carbonate
KSCN	:	Potassium thiocyanate
NFM	:	<i>N</i> -formylmorpholine
ACV	:	Acyclovir

AAD	:	Average absolute deviation
DFT	:	Density functional theory
TZVP	:	Triple- $\zeta$ Zeta Valence Potential
HPLC	:	High performance liquid chromatography
ppm	:	Parts per million
GLC	:	Gas liquid chromatography
$D$	:	Distribution ratio
$C^\infty$	:	Capacity at infinite dilution
$D_{Bz}$	:	Distribution ratio of benzene
$S$	:	Solvent selectivity
$S^\infty$	:	Solvent selectivity at infinite dilution
$PI^\infty$	:	Performance index at infinite dilution
$\sigma$	:	Screening charge density
$\mu$	:	Chemical potential
$E_{misfit}$	:	Electrostatic misfit energy
$E_{hb}$	:	Hydrogen bond interaction energy
$E_{vdw}$	:	Van Der Waals interaction energy
$\gamma$	:	Activity coefficient
$\gamma^\infty$	:	Activity coefficient at infinite dilution
$\Delta H^{E,\infty}$	:	Infinite dilution partial excess enthalpy
$x_{Bz}$	:	Molar concentration of benzene
$x_{Cy}$	:	Molar concentration of cyclohexane
$x_{IL}$	:	Molar concentration of IL
$x_{DES}$	:	Molar concentration of DES
$\tau_{ij}$ or $\tau_{ji}$	:	Binary interaction parameters
$\alpha_{ij}$	:	Non-randomness parameter

$M$  : Number of tie-lines

$\text{Å}$  : Angstrom unit

University of Malaya

## LIST OF APPENDICES

Appendix A: COSMO-RS prediction data involving  $C^\infty$ ,  $S^\infty$ ,  $PI^\infty$ ,  $\sigma$ -profile,  $\sigma$ -potential and LLE tie lines.

Appendix B:  $^1H$  NMR spectroscopy of samples from extract and raffinate layers

University of Malaya

## CHAPTER 1: INTRODUCTION

### 1.1 Background

Benzene and cyclohexane are two valuable products being widely processed in petrochemical industry. Benzene is an aromatic hydrocarbon which is commonly used as a raw material to synthesize compounds such as styrene, phenol, cyclohexane, anilines and alkylbenzenes. Cyclohexane, on the other hand, has the important usage in its conversion into intermediate cyclohexanone, which is then used as a feedstock for nylon precursors. Cyclohexane is also used in paints and varnishes as a solvent in plastic industry. Cyclohexane can be produced by several methods, one of which by direct distillation of crude gasoline cut. Nevertheless, the increasing demand of cyclohexane and the issue of low product purity in the traditional process drives a necessity for new processes. At present, nearly all cyclohexane is produced by catalytic hydrogenation of benzene (Robert & Dang, 1971; Weissermel & Arpe, 2007). In this process, the cyclohexane with high purity can only be produced under a complex process control which involves complex heat integration and economic study (Kassel, 1956). Therefore, this separation usually produces a mixture of benzene and cyclohexane. The unreacted benzene in the reactor's effluent must be removed to produce pure cyclohexane. However, the separation of benzene and cyclohexane is regarded as the most important and most difficult process in petrochemical industry. It is difficult to separate them by conventional distillation because both have similar properties and close boiling points.

The current technologies for this separation are azeotropic distillation and extractive distillation. In azeotropic distillation, a strongly polar entrainer is usually introduced to form an azeotrope mixture with cyclohexane (Shiau & Yu, 2009). The mixture then alters the vapor-liquid equilibrium curve. On the other hand, extractive distillation uses the entrainer to reduce the volatility of benzene (Albrecht, 1989). Despite their applications in industry, both processes suffer from complexity and high energy consumption.

Besides, these processes are carried out by adding the third compound, where the removal of the third compound from distillate will encounter higher process complexity and cost (Villaluenga & Tabe-Mohammadi, 2000). With all these factors, the need to find innovative separation of benzene and cyclohexane emerges.

Ionic liquids (ILs) have become an increasingly popular class of solvent in the last decades since their potential application in many industrial processes becomes more diverse. ILs are compounds consisting of cations and anions which exist as a liquid at low temperature (below 100 °C). Compared to other solvents, most ILs are non-flammable, non-volatile and thermally stable over a wide range of temperature. The final IL product can also be designed with tailored properties to be used in specific purpose, which is the main reason for it being called 'designer solvent' (Holbrey & Seddon, 1999). As there are many types of cation and anion, a huge combination is available to form enormous number of ILs. Despite these advantages, the main challenges in ILs are the expensive price and being not universally green towards environment. In fact, the toxicity of ILs has been extensively studied that the term 'green solvent' is arguable and does not apply to all types of ILs (Thuy Pham, Cho, & Yun, 2010). These factors drive the research community to investigate other new environmentally benign alternatives.

Recently, a new class of solvent which is called deep eutectic solvents (DESs) has been identified as a promising alternative in many separation issues. Beginning from the first preparation method, DES starts to be widely acknowledged as a new class of IL analogue because they share many characteristics and properties with ILs, especially being liquid at ambient temperature (Tang & Row, 2013; Zhang et al., 2012). Besides, they also have other appreciable advantages over ILs such as low production cost, environmentally benign and easier preparation with no purification step. DES is a eutectic mixture of complimentary salt with hydrogen bond donor that produces a liquid having

much lower melting points than the raw materials. Although DES is acknowledged for its advantages, there has been no available information on their potential use in the separation of benzene and cyclohexane.

The essential step before applying IL or DES in industry is the solid knowledge of its thermodynamic properties. In liquid-liquid extraction process, the aim to find ILs or DESs that perform high selectivity and high extraction capacity is unachievable without LLE database. The acquisition of this database information through experimental work is impractical because of the huge number of possible combinations between different cations and anions (for ILs) or salts and complexing agents (for DESs). This suggests the need of assistive tools, or faster but effective methods. Recently, a useful predictive methodology to describe thermophysical properties was developed (Klamt & Eckert, 2000). Known as Conductor-like Screening Model for Real Solvent (COSMO-RS), it has attracted much attention and gained tremendous influence in research activity due to its ability to describe thermodynamic properties and behavior of solvents, including ILs and DESs (Diedenhofen & Klamt, 2010).

The computational prediction validated with experimental results will produce vigorous information on thermodynamic properties that enables the discovery of an effective way to separate benzene and cyclohexane. This study investigates the potential of the emerging solvents (ILs and DESs) for the separation of benzene and cyclohexane. It involves the screening and selection of potential ILs and DESs, the experimental validation, and the solvent modification through binary mixtures.

## 1.2 Problem statement

The separation of benzene and cyclohexane from their mixture is difficult to perform via conventional distillation because of their close boiling points, i.e. 80.1 °C for benzene and 80.74 °C for cyclohexane. The conventional techniques employed for the separation of benzene and cyclohexane from their mixture includes the azeotropic distillation and the extractive distillation. However, despite their usage at an industrial scale, both processes suffer from serious disadvantages, such as process complexity, high capital and operating costs, and high energy consumption (Johann G Stichlmair & Fair, 1998). Besides, these processes are carried out by adding the third compound as an entrainer, whereby the removal of the third compound from distillate will encounter higher process complexity and cost (Villaluenga & Tabe-Mohammadi, 2000). In addition, the separation technology depends on the concentration of aromatic content in the feed stream. The concentrations of benzene at high range (> 90 %), medium range (65-90 %) and lower range (20-65 %) are typically suitable to be treated with azeotropic distillation, extractive distillation and liquid-liquid extraction, respectively. However, for production of cyclohexane through hydrogenation process, the unreacted benzene is normally in low concentration (<20 %) (K. Weissermel, 2003). This implies that there is no suitable separation technology available for this concentration.

Liquid-liquid extraction (LLE) is an interesting technique as it is a simple process that can be operated under mild condition. However, the use of organic solvents as the extracting agents are undesired because they are usually volatile, toxic and flammable. Meanwhile, although ILs and DESs are the potential alternatives which possess many advantages, there is limited information on their use as the solvents for the extractive separation of benzene and cyclohexane (Villaluenga & Tabe-Mohammadi, 2000). The use of ILs in the separation of benzene and cyclohexane is scarcely studied, while the use of DESs for this process is totally unexplored. In liquid-liquid extraction process, the aim

to find ILs or DESs that perform high selectivity and high extraction capacity is unachievable without LLE database. The acquisition of this database information through experimental work is impractical because it is tedious and costly. This suggests the need of assistive tools or faster screening methods. The necessity of screening process is motivated by the idea that many other ILs having high extracting performances might remain undiscovered. This is due to numerous cation and anion being available, which makes the selection of potential ILs through experimental work a time-consuming and expensive method (Plechkova & Seddon, 2008). Therefore, an extensive investigation of applying ILs and DESs in the separation of benzene and cyclohexane could provide an alternative solution to the issues mentioned.

### 1.3 Objectives

The objectives of this research are:

- 1) To investigate the potential of DESs in the extractive separation of benzene and cyclohexane using computational screening and experimental validation.
- 2) To investigate the potential of ILs in the extractive separation of benzene and cyclohexane through computational screening and experimental validation.
- 3) To study the thermodynamic phase behavior and the performance of the selected ILs and DESs in the separation of benzene and cyclohexane via liquid–liquid extraction process.
- 4) To apply the macroscopic thermodynamic models in correlating the experimental data for potential use in design calculation.
- 5) To study the feasibility of combining the top-ranked ILs into a series of binary mixtures in improving the extraction performance.

#### 1.4 Research methodology

The methodologies adopted to achieve the research objectives are:

- 1) Qualitative and quantitative screening of potential ILs and DESs using COSMO-RS programme and literature survey.
- 2) Acquiring the selected ILs and DESs through laboratory synthesis or commercial purchase.
- 3) Ternary liquid-liquid extraction (LLE) experiments for the systems containing the selected ILs or DESs, benzene and cyclohexane.
- 4) Prediction of ternary phase equilibria using COSMO-RS.
- 5) Sampling and compositional analysis of the extraction mixtures using nuclear magnetic resonance (NMR) spectroscopy.
- 6) Performing consistency tests for the experimental LLE data using the Othmer-Tobias and Hand correlations to validate the compositional profile.
- 7) Correlation of the experimental LLE data with the Non-Random Two-Liquid (NRTL) model.
- 8) Determination of optimum molar ratio for the binary IL-IL mixture through LLE experiments and ideal mixing calculations.
- 9) Generation of phase equilibria involving the pseudo-ternary systems of binary ILs, benzene and cyclohexane.

## 1.5 Scope of study

This research aims to provide recommendation of suitable ILs and DESs to be used as the extracting solvents in the separation of benzene from its mixture with cyclohexane. Solvent is a core aspect in liquid-liquid extraction process. Thus, the selection of the most suitable solvent plays an important role in achieving a feasible extraction process. The understanding of molecular interactions between solvent and solute is vital in selecting the correct solvent for the extraction process. The selection of ILs and DESs as the extractive solvents based on predictive methods, such as COSMO-RS, provides deep insights on the molecular interaction between the solvents and the benzene. Ternary liquid–liquid equilibrium experiments were performed to investigate the performance of the selected ILs and DESs in the separation of benzene and cyclohexane, and to validate the calculation results. To improve the extraction performance, the selected ILs can be developed further by combining them into a series of binary mixtures. Binary solvent mixing is potentially a promising method to enhance the extraction efficiency as the individual performance of the two solvents is well compromised.

## 1.6 Outline of thesis

This thesis is composed by the following chapters:

Chapter 1 is an introductory section which includes the brief background of the separation of benzene and cyclohexane, problems encountered in the current technologies, research objectives, research methodologies and the scope of work.

Chapter II provides a literature review about the contexts and challenges in the separation of benzene and cyclohexane. This includes the description of properties, production and demands of benzene and cyclohexane as well as the evaluation of current technologies being applied in industry. Next, the reports on the application of ILs and DESs as the alternative solvents for this separation are reviewed and summarized. Finally, the feasibility of solvent modification through binary mixture is reviewed.

Chapter III explains the details of each methodology which includes the screening of ILs and DESs using COSMO-RS, ternary and quaternary LLE experiments, compositional analysis using NMR spectroscopy, prediction of phase equilibria using COSMO-RS, consistency tests using Othmer-Tobias and Hand correlations, and correlation of experimental data with NRTL model.

Chapter IV discusses the results obtained and highlights the important findings of this research.

Chapter V provides the outcomes, recommendations, achievements and conclusions of this research.

## CHAPTER 2: LITERATURE REVIEW

### 2.1 Benzene and cyclohexane

#### 2.1.1 Properties of benzene and cyclohexane

Benzene is a nonpolar aromatic hydrocarbon, volatile, colourless and flammable liquid with a characteristic of odour and high chemical stability (Villaluenga & Tabe-Mohammadi, 2000). The stability of benzene can be estimated by the heat of partial hydrogenation from cyclohexane to benzene (Figure 2.1). The heat of hydrogenation from cyclohexane to cyclohexene and to 1,3-cyclohexadiene is -118 kJ/mol and -230 kJ/mol, respectively. Theoretically, the expected heat of hydrogenation from cyclohexane to benzene is -356 kJ/mol. However, the actual value is only -206 kJ/mol, indicating that benzene is more stable than expected by 150 kJ/mol.

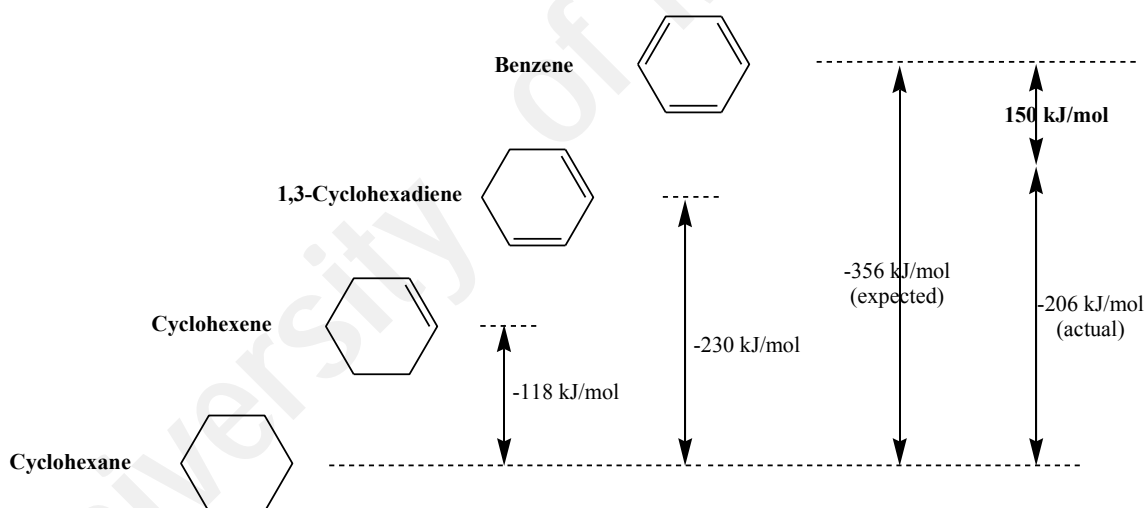


**Figure 2.1: Heats of hydrogenation from cyclohexane to cyclohexene, 1,3-cyclohexadiene, and benzene**

In view of molecular structure, benzene is a planar molecule with the shape of a hexagon constituted by six-member ring. The angle of all C–C–C bonds is  $120^\circ$ . The hydrogen-carbon bond length is  $1.09 \text{ \AA}$  and carbon bonds have equal lengths of  $1.39 \text{ \AA}$ , which is an intermediate between single bond ( $1.54 \text{ \AA}$ ) and double bond carbon-carbon ( $1.34 \text{ \AA}$ ) (McMurry, 2011). All the six carbon atoms are  $sp^2$ -hybridized, and each carbon has a  $p$ -orbital perpendicular to the plane of the ring. The electrostatic potential map of

benzene shows that the electron density in all six carbon–carbon bonds is identical, as illustrated in Figure 2.2(a). Due to the delocalization of six electron pairs in benzene ring, the enhanced chemical stability of benzene is attributed by the resonant structure. Because of *p*-orbitals, it is not possible to define the three localized  $\pi$ -bonds with the six  $\pi$ -electrons, resulting in the  $\pi$ -electrons being freely move through the entire ring. This is represented by two resonance forms, as shown in Figure 2.2 (b). Both forms are typically represented by a circle to indicate the equivalence of the carbon-carbon bonds. More information on atomic orbitals and chemical stability of benzene can be found elsewhere (McMurry, 2011).

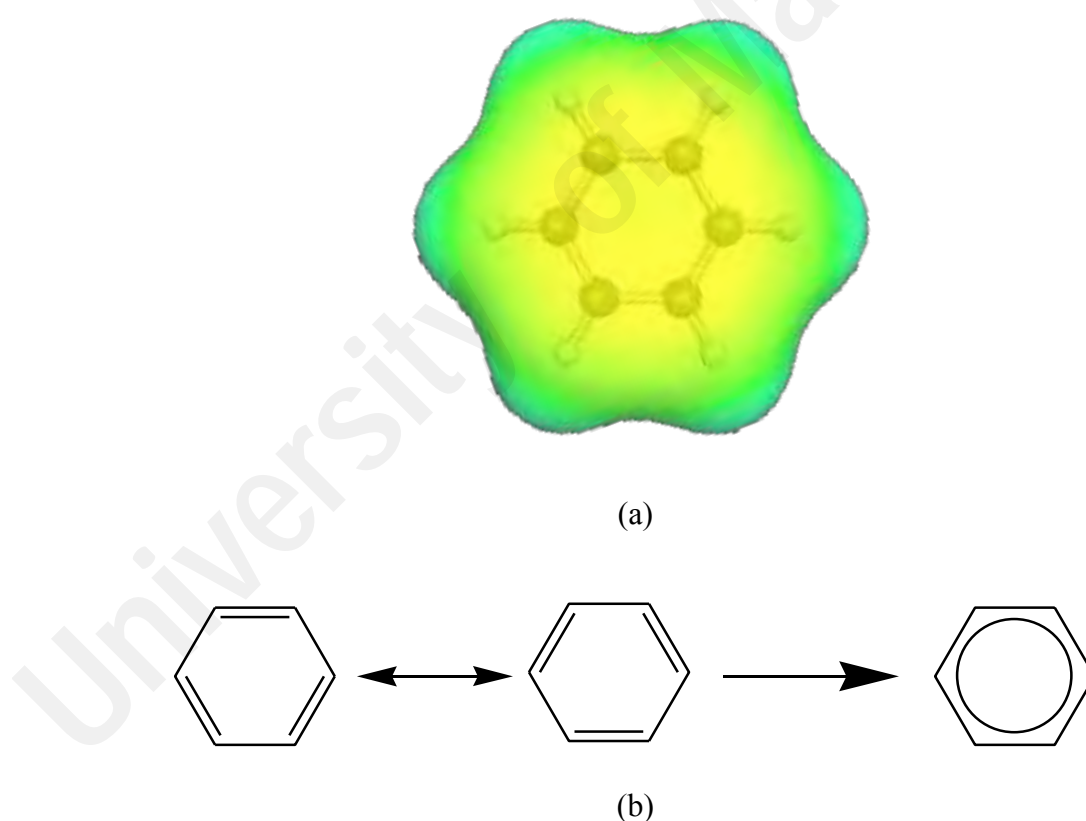


**Figure 2.2: The structure of a benzene molecule in view of (a) electrostatic potential map and (b) resonance structure**

Cyclohexane is a colourless, flammable, water-insoluble, non-corrosive and non-polar liquid possessing a pungent odour (Villaluenga & Tabe-Mohammadi, 2000). The six carbons in its structure is in the form of ring so that each carbon is connected to a  $\text{CH}_2$ ,

rather than  $\text{CH}_3$ . Cyclohexane can be quickly recognized by a flat hexagon, as shown in Figure 2.3(a). However, the planar hexagon does not represent the actual atomic arrangement as it would forcibly require very high energy state and violate the convergence of molecular energy. Cyclohexane is therefore further characterized by the non-planar conformational structures, where C–C–C bond angles are tetrahedrally near  $109.5^\circ$ , and all the neighbouring C–H bonds are staggered. The most stable structural arrangement is known as the “chair conformation”. This term is given because of its similarity to a lounge chair with a back, seat and footrest (Figure 2.3 (b)).



**Figure 2.3: Structure of cyclohexane in view of (a) a flat hexagon and (b) the most-stable chair conformation**

Another cyclohexane conformation is called “boat conformation”, where the so-called footrest of the chair flips upward, creating a boat-like structure. In boat conformation, all atoms are eclipsed which creates high energy state. This energy strain could be reduced by twisting into a slightly more stable form, known as twist or skew boat. Cyclohexane conformation with the highest possible energy state is called half-chair. More information on the conformational analysis of cyclohexane can be found elsewhere (Carroll, 2011; Johnson et al., 1961). The structural conformations of cyclohexane and their relative energy state is summarized in Figure 2.4.

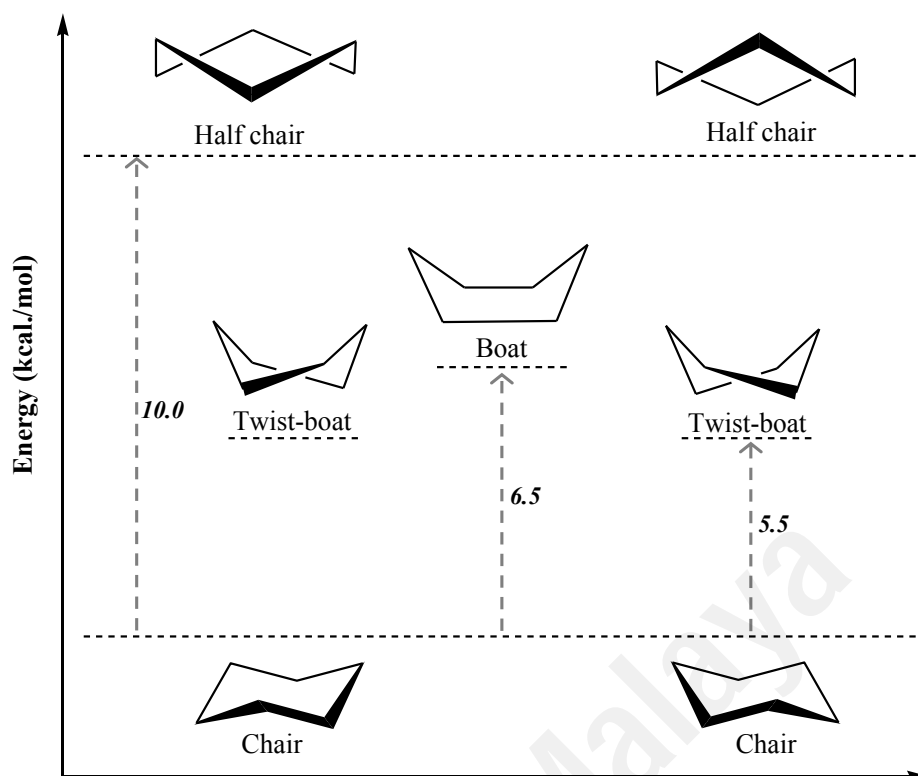


**Figure 2.4: Structure and energy levels of cyclohexane conformers, and the energy required for this ring-flipping process**

The physical properties of benzene and cyclohexane are summarized in Table 2.1.

**Table 2.1: Physical properties of benzene and cyclohexane (Villaluenga & Tabe-Mohammadi, 2000)**

Properties	Benzene	Cyclohexane
Freezing point (°C)	5.533	6.554
Boiling point (°C)	80.100	80.738
Density at 25 °C (g. cm <sup>-3</sup> )	0.8737	0.7786
Refractive index at 25	1.4979	1.4262
Viscosity (absolute) at	0.647	0.980
Surface tension at 25	28.18	25.3
Critical temperature	289.45	281.0

### 2.1.2 Production and demand of benzene and cyclohexane

Since 1950s, the production of benzene from petroleum feedstocks has been very successful and accounts for about 95% of all benzene obtained (Fruscella, 2000). In fuel

processing, several methods have been adopted to produce benzene, including crude oil cracking, naphtha reforming, toluene disproportionation, and toluene hydrodealkylation (Bank, 2017).

In crude oil cracking, the raw petroleum is vaporized and added with steam before it is passed through into a furnace at temperatures around 870 °C. The resulting mixture of hydrocarbons, known as pyrolysis gas, is then treated with alcohol to extract benzene and other aromatic compounds. Then, fractional distillation is used to further separate benzene and other compounds.

Naphtha reforming is another benzene production method but with a pre-treatment process, where the sulphurous impurities in naphtha feed are firstly removed. The naphtha is then mixed with hydrogen at nearly 500 °C and 5 atm, where catalytic hydroforming process takes place. As a result, the aliphatic hydrocarbons are converted into the corresponding aromatic compounds. For instance, *n*-hexane is converted into benzene. This is followed by a final distillation to separate the different compounds.

In toluene disproportionation, the toluene is mixed with hydrogen before it is catalytically converted into a mixture of benzene and xylene. Benzene and xylene are then separated through distillation, and the toluene is recycled into the feed.

Toluene hydrodealkylation is another way to produce benzene using toluene as a feedstock. In this process, toluene and hydrogen are compressed inside a catalytic reactor between 20 to 60 atm, and the mixture is heated up to 650 °C. This process converts the toluene–hydrogen mixture into benzene–methane mixture. The remaining hydrogen is recycled, and the benzene is distilled out from methane. Benzene can also be produced by dealkylation of alkyl aromatics (toluene, xylenes, or longer chain alkyl aromatics), where the methyl radical is replaced by hydrogen atom to produce benzene (Fang et al., 2008).

Benzene is by far the most important aromatic petrochemical raw material with versatile end-use pattern, as illustrated in Figure 2.5. The core use of benzene is as a raw material to synthesize important chemicals such as ethyl benzene (styrene), 55.6 %; cumene (phenol), 22.4%; cyclohexane (nylon), 13.5 %; nitrobenzene (aniline), 5 %; and detergent alkylates, alkylbenzenes and chlorobenzenes (detergents) (3%) (Kent, 2013). These intermediates are then used to produce different speciality of chemicals, pharmaceuticals, plastics, resins, dyes, and pesticides. Ultimately, benzene is the key-controller to the chain values of other chemicals such as styrenics, nylons, polycarbonate, phenol-formaldehyde and polyurethanes.

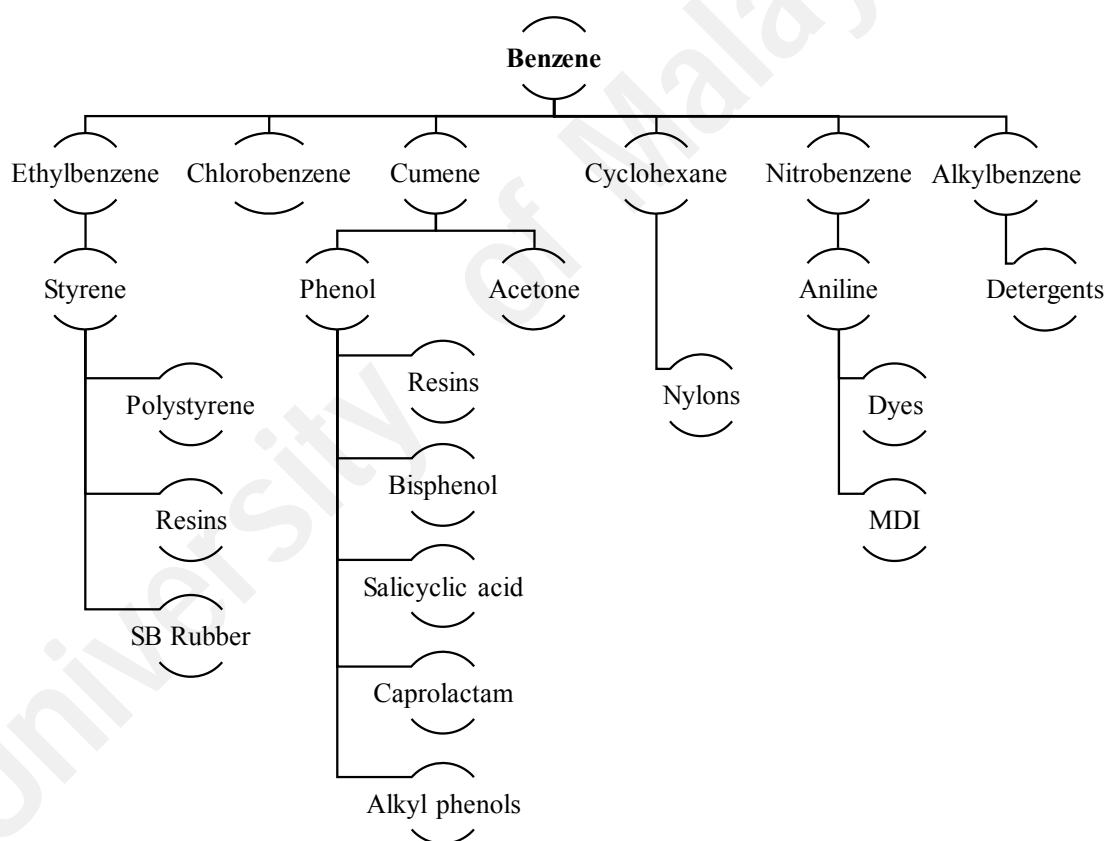


**Figure 2.5: Main applications of benzene**

The stability of benzene has made it an excellent solvent in chemical processes. In IL research, benzene was used as an effective solvent to synthesize 1-butyl-6-methylquinolinium dicyanamide ( $C_4mquinN(CN)_2$ ); a novel IL with high performance of removing aromatic sulphur compounds from fuels (Wilfred, Man, & Chan, 2013).

However, due to its toxic properties, especially being highly carcinogenic, it has been almost entirely replaced by less harmful materials.

The world consumption of benzene is dominated by two of its major derivatives, i.e. ethylbenzene and cumene, accounting nearly 70 % of its overall consumption. The global demand has been growing steadily despite a slow economic situation over the last five years. High demand of benzene was mainly observed in China, United States and Western Europe. In addition, South Korea, Japan and Middle East countries are among the important customers (Markit, 2017a). China has increasingly emerged to give important influence on the benzene market and this trend is expected to continue in future (Feng, 2004). In fact, high demand of benzene in Asia-Pacific region is caused by the rapid growth of petrochemical industries in China, and the economic performance in China will remain as a vital driver for benzene consumption. While the global benzene consumption is forecasted to grow at an average rate of 2-3% per year, the annual consumption in China has already increased at nearly 9 % from 2011-16 (Markit, 2017a).

Cyclohexane was traditionally produced by fractional distillation of naphtha. However, this process brought critical challenges involving process efficiency and cyclohexane demand. Firstly, fractional distillation of naphtha produced many components with similar boiling points, making the separation difficult. Secondly, this process encountered low purity of cyclohexane, i.e. only 85%. In addition, the production of high quality cyclohexane was unlikely. Only Phillips Petroleum has achieved the required purity of cyclohexane but with advanced technology that combined distillation of naphtha and isomerization of methyl-cyclopentane to cyclohexane (Chauvel & Lefebvre, 1989; Villaluenga & Tabe-Mohammadi, 2000). This challenge drove the production of cyclohexane through another process called hydrogenation of benzene (Figure 2.6). Later, hydrogenation of benzene became the main method due to its

simplicity and high efficiency. At present, nearly all benzene is produced by hydrogenation of cyclohexane (Vangelis et al., 2010).

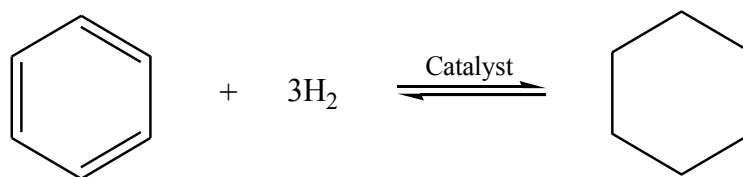


**Figure 2.6: Hydrogenation of benzene to produce cyclohexane**

Due to the stable resonance resulting from the strong  $\pi$ -conjugation in the benzene ring, the hydrogenation must be performed at high temperatures ( $>100$  °C) and high initial  $H_2$  pressure ( $>30$  atm). This leads to unavoidable problems of undesired byproducts and complicated steps to purify the products. To enhance the conversion rate and purity of cyclohexane, the process underwent some developments such as the variation of physical state (liquid phase or vapor phase hydrogenation) (Hayes, 1972; Larkin, Templeton, & Champion, 1993), and the application of catalysts. The development of catalyst has taken place since 1930 when some monometallic catalysts such as nickel, platinum and palladium were firstly introduced (Bancroft & George, 1930). However, the complete hydrogenation of benzene to cyclohexane with acceptable rates remain a challenge until the present day (Tonbul, Zahmakiran, & Özkar, 2014). Recently, the discovery of bimetallic catalysts has attracted the research communities to explore the bimetallic combinations. This was contributed by the synergistic effect between the two metals. One of the remarkable combinations was the Ru–Pt bimetallic catalyst deposited on a zeolite-type MOF (MIL-101), which gave benzene hydrogenation to cyclohexane up to  $>99\%$  yield (Liu et al., 2015).

Cyclohexane is mainly used to make cyclohexanol and cyclohexanone. These intermediates are then used as precursors to produce two important chemicals, i.e. caprolactam and adipic acid, which are then used to generate Nylon 6 and Nylon 6.6.

Caprolactam is estimated to continuously account more than 55% of the total demand for cyclohexane. Nonetheless, caprolactam can also be produced from another competing feedstock, i.e. phenol. This has affected the global demand of cyclohexane, where it is expected to decrease in the next few years. Cyclohexane is also notably supplied worldwide for various solvent applications such as in paints, resins, varnish and oil, and as a plasticiser. The United States, Western Europe and China are the main capacity centers for global demand of cyclohexane. China, being the highest cyclohexane consumer, has accounted 40 % of the total demand (Markit, 2017b). While the cyclohexane is mainly used for caprolactam production in China, the demand in United States is driven more by adipic acid. Despite the growing uncertainty, especially from the competing feedstock of caprolactam, the global demand for cyclohexane has been stable since 2005 (Tefera, 2006). Moreover, the global demand is forecasted to grow about 2.6 % annually, where most of it will continue to occur in China.

## **2.2 Industrial technologies to separate benzene–cyclohexane mixture**

At present, nearly all cyclohexane is produced by catalytic hydrogenation of benzene, which usually produces a mixture of benzene and cyclohexane. The unreacted benzene in the reactor's effluent must be removed to produce pure cyclohexane. The challenge of separating benzene-cyclohexane mixture comes from the closeness of their physical properties. It is erroneous to separate them through a simple distillation process because of three factors: (i) the difference of boiling points is only 0.64 °C, (ii) the nearly a close-boiling system of their vapor–liquid equilibria, and (iii) they form azeotrope at 45 vol % cyclohexane (Villaluenga & Tabe-Mohammadi, 2000). This entails the development of advanced technologies to suit the separation at industrial scale. For the separation of benzene and cyclohexane, two methods are viable, namely extractive distillation and azeotropic distillation. However, both technologies are only feasible at a certain concentration of benzene, as summarized in Table 2.2 for the removal of benzene, toluene

and xylene (BTX). Although LLE is suitable for separating low concentrations of benzene (20–65 %), there is still no industrial process available for concentrations less than 20 wt %.

**Table 2.2: Common processes to separate aromatic–aliphatic mixtures and their operational suitability (Brandrup, 1989)**

<b>Method</b>	<b>Separation problem</b>	<b>Requirements for economical operation</b>
Azeotropic distillation	BTX separation from pyrolysis gas	High aromatic contents (>90 %)
Extractive distillation	BTX separation from pyrolysis gas	Medium aromatic content (65-90 %)
Liquid–liquid extraction	BTX separation from reformat gas	Low aromatic content (20-65 %)

### 2.2.1 Azeotropic distillation

In azeotropic distillation, the separation is generally carried out by adding a strongly polar solvent that forms azeotrope with one of the two components and alters the phase diagram of the binary mixture. The azeotrope mixture is collected at the overhead of the first distillation column and the solvent is recycled using the second distillation column. The second component is then recovered at the bottom of the second distillation column.

Specifically for benzene and cyclohexane, the separation can be facilitated by adding a polar solvent like acetone, acetonitrile or isopropanol. Taking acetone as an example, acetone will form azeotrope with cyclohexane at 77% cyclohexane, with a boiling point of 53.2 °C (Shiau & Yu, 2009). As shown in Figure 2.7, the acetone–cyclohexane azeotrope flows into the overhead of the distillation column while benzene is collected at the bottom. From the overhead, the azeotrope mixture is then fed into an extraction

column where acetone is washed with water. As cyclohexane is insoluble in water, nearly pure cyclohexane is collected at the bottom. Finally, water–acetone mixture is separated in the second distillation column. Acetone is recycled back to the first distillation column, while water to the extraction column.

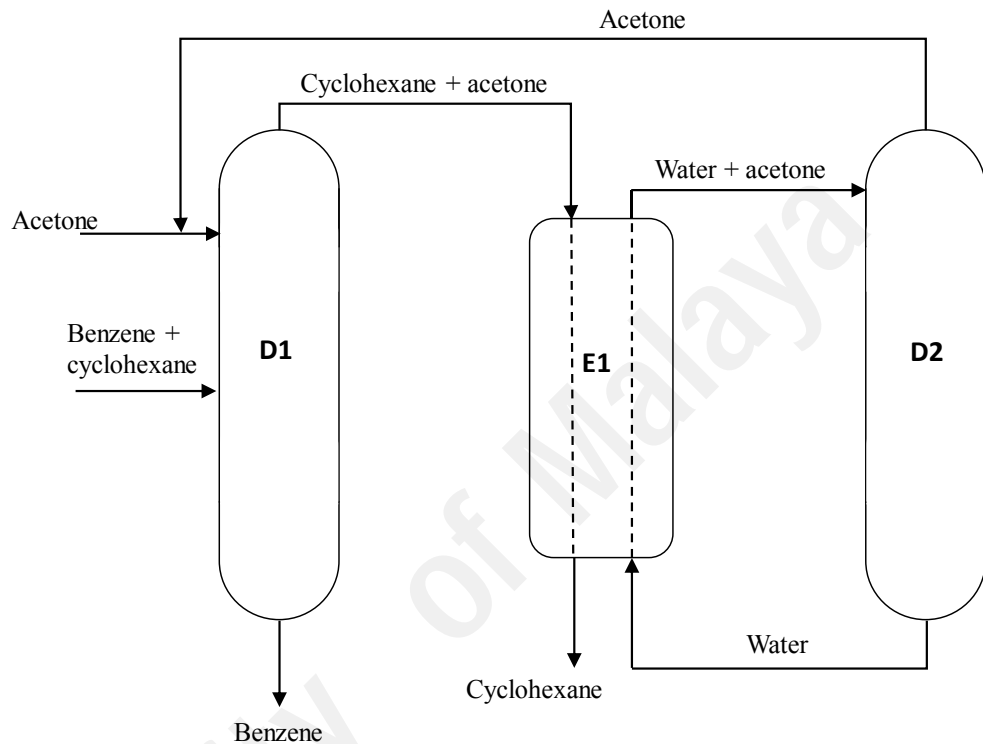


**Figure 2.7: Separation of benzene and cyclohexane by azeotropic distillation using acetone and water**

### 2.2.2 Extractive distillation

The extractive distillation is principally similar to azeotropic distillation because both use solvents for the separation. However, extractive distillation uses a relatively stable solvent with high boiling point. In general, a solvent is used to reduce the relative volatility of one component. The other component is distilled overhead, and the bottom mixture is fed into a stripping column for separation. In the case of separating benzene–cyclohexane mixture, the solvent selectively interacts with benzene and shifts the vapor–liquid equilibria. This process is as shown in Figure 2.8, taking furfural as an example (Albrecht, 1989).

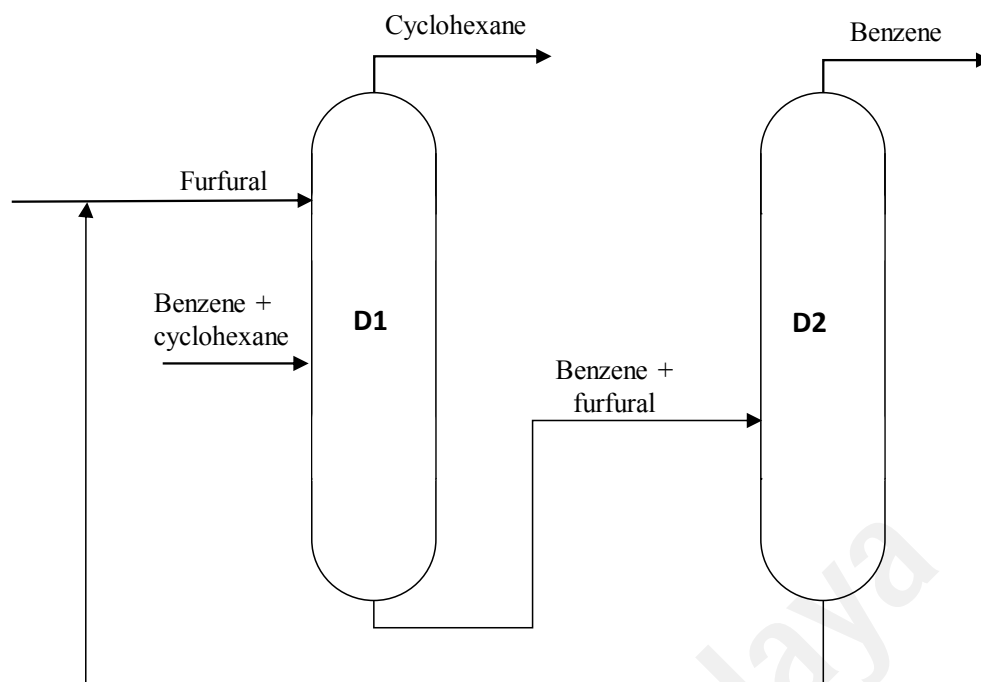


**Figure 2.8: Separation of benzene and cyclohexane by extractive distillation using furfural**

Furfural, which is highly selective for benzene, is added to the mixture to shift the vapor–liquid equilibrium. The mixture of furfural and benzene flows to the bottom and enters the second distillation column while cyclohexane is distilled overhead. In the second column, benzene is distilled overhead, and furfural is recycled back to the first column. Another typical solvent used in extractive distillation of benzene and cyclohexane is N-formylmorpholine. Extractive distillation was reportedly less energy intensive than azeotropic distillation because of lower energy consumption and it allows flexible selection of the solvents (Sucksmith, 1982). For the separation of benzene and cyclohexane, the combination of two or three conventional solvents has been applied to enhance the feasibility of extractive distillation (Yin et al., 2010; Zhang, Shi-Min, & Zhang, 2006). However, the extractive distillation still suffers from high capital and operating cost, high process complexity, requiring the secondary distillation and the limited range of feed compositions. This became the driving force for a research into other convenient solvents or alternative separation processes.

As a summary, both industrial processes are the state of the art but their application is associated with challenges, especially with regards to high cost and process complexity. Therefore, a more pragmatic approach for the development of cleaner separation technologies would be the search of viable alternatives to replace the traditional solvents. At the forefront of this is the ILs.

## **2.3 Ionic liquids**

### **2.3.1 Overview of ILs**

The field of ILs including their properties and synthesis reactions have been widely reviewed by the earlier researchers (Holbrey & Seddon, 1999; Seddon, 1997; Welton, 1999). ILs are formed by the combination of cations and anions, and they exist as a liquid at low temperature (below 100 °C). In general, ILs consist of a salt where one or both ions are large, and the cation has a low degree of symmetry. These factors tend to reduce the lattice energy of the crystalline form of the salt, and hence lower the melting point (Earle & Seddon, 2000). Comparing to the other solvents, they are exceptionally non-flammable, non-volatile, potentially environmental-benign, and chemically and thermally stable over a wide range of temperatures.

The interest in these molten salts advanced after the development of binary ILs from mixtures of aluminium (III) chloride and N-alkylpyridinium (Chum et al., 1975) and 1, 3-dialkylimidazolium chloride (Boon et al., 1986). At end of 1990s, the interest in ILs tremendously ascended, resulting into an exponential increase of publications in the topic of ILs (Figure 2.9). A detailed review of the historical development of ILs can be found elsewhere (Plechkova & Seddon, 2008).

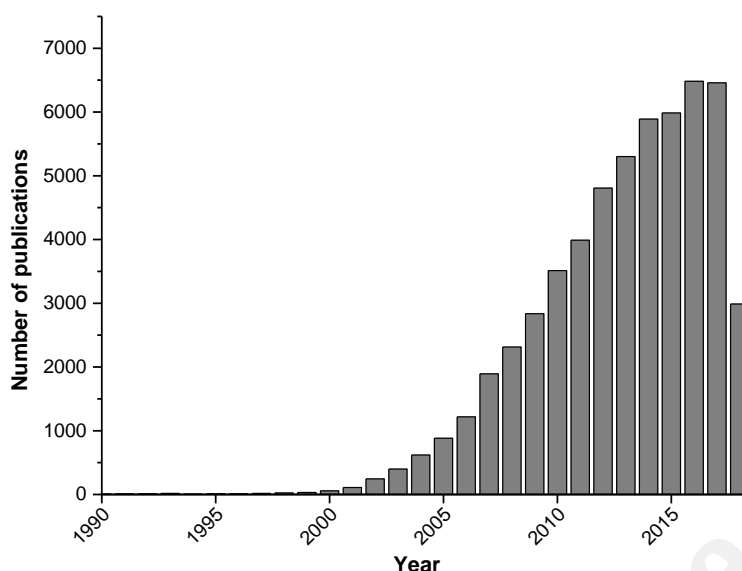


**Figure 2.9** Number of publications in the topic of ILs since 1990

ILs are typically based on the bulky organic cations with the charge balanced by organic or inorganic anions. Although there are many types of cations that are possible to form ILs, the most commonly studied cations are imidazolium, pyridinium, N,N,N-alkylammonium and N,N,N-alkylphosphonium. The anions, in contrast, are usually the weakly basic inorganic or organic compounds with a diffused or protected negative charge. Some examples of the common cations and anions are shown in Figure 2.10.

<b>Cation</b>	 imidazolium	 pyridinium	 ammonium	 ammonium
<b>Anion</b>	 acetate	 thiocyanate	 dicyanamide	 chloride
	 tetrafluoroborate	 hexafluorophosphate	 nitrate	 methanesulfonate

**Figure 2.10:** Example of common cations and anions of ILs

There is a huge number of ILs available, regardless of by commercial purchase or through synthesis procedure. Therefore, the advantages of ILs combined with their availability will create a huge potential of applications in various fields as reported in numerous articles since the last decades. Most of the studies explored ILs as an alternative and new type of solvent to replace the conventional ones. Some review articles have also concisely explained the applications of ILs in several research fields, such as in separation processes (Berthod, Ruiz-Ángel, & Carda-Broch, 2008; Kubota & Goto, 2006), electrochemistry (Hagiwara & Lee, 2007), bio-chemical reactions (Dichiarante et al., 2007; Moniruzzaman et al., 2010), catalysis (Shen et al., 2008), sensor (Shvedene, Chernyshov, & Pletnev, 2008) and tribology (Minami, 2009).

Another interesting characteristic of ILs is their versatility and wide choice of selection. In fact, the research community called the IL as the “designer” solvent because the properties of the resulting IL (such as melting point, viscosity, density, and hydrophobicity) can be accustomed, designed, or adjusted by simple changes in the ion structure to suit an individual reaction type (Earle & Seddon, 2000; Plechkova & Seddon, 2007). Apart from that, the term “Task Specific Ionic Liquids” (TSILs) was introduced to express the ability of ILs tailored for specific properties or reactivities by utilizing the functional groups attached to the cation (H. Davis, 2004). For instance, Lee et al. had demonstrated the synthesis of imidazolium based TSILs and their specific applications in various chemical processes.

The overview above can be considered as a strong motivation to explore the progress of using IL, particularly in the separation of benzene and cyclohexane. A few research groups had reported some significant results. However, as presented in the following sections, it is still necessary to discover new opportunities in selecting the suitable ILs.

### **2.3.2 Review on the performance of ILs and organic solvents in extractive separation of benzene and cyclohexane**

The solvents used for the separation of benzene and cyclohexane can be viewed as twofold, i.e. organic solvents and ILs. The common practice of researchers dealing with solvent discovery is to set the performance of organic solvents as a benchmark. Thus, for the separation of benzene and cyclohexane, it is necessary to firstly review the performance of organic solvents before analyzing the performance of ILs.

#### **2.3.2.1 Performance of organic solvents**

Organic solvents are widely used in many chemical processes at industrial scale, mostly due to easy supply and low prices. Organic solvents can be defined as a chemical class of compounds that are used regularly in commercial industries. These solvents exist in liquid form at room temperature and share a common C-H structure that consists of low molecular weight, high lipophilicity and high volatility. Some common types of organic solvents are alcohols, ketones, glycols, esters, ethers, aldehydes and more. Despite the availability of many organic solvents, researchers have restricted the selection criteria for their usage in the extractive separation of benzene and cyclohexane. This is reflected in the published articles where only some of the organic solvents were considered for experimental study.

The early experimental work for the determination of phase equilibria in the separation of aromatic-aliphatic mixtures, including benzene-cyclohexane, was reported using sulfolane (De Fré & Verhoeve, 1976). Aspi et al. (1998) then studied the feasibility of dimethylformamide (DMF) with various concentrations (10, 20, 30 and 50 %) of ethylene glycol (EG) as the extracting solvents. The solvent-blending principle here was motivated by the idea of combining two solvents: one with high solvent capacity (i.e. DMF) and another with high selectivity (i.e. EG). Although the LLE data was tabulated, there was

no further evaluation in terms of extraction efficiency by the means of distribution ratio and selectivity (Aspi et al., 1998). Nevertheless, it is interesting to note that after this finding, the later works seemingly investigated the other organic solvents that were inferred from DMF and EG. For instance, Reza et al. (2011) studied the effect of higher temperature towards the extractive ability of ethylene glycol. The extraction using ethylene glycol was claimed as a possible approach since the selectivity was higher than unity, but the benzene is found more soluble in cyclohexane than in ethylene glycol (M. Reza, Lotfollahi, & Asl, 2011).

In addition, two articles have reported the same approach, which is by replacing ethylene glycol from Aspi et al.'s work with potassium thiocyanate (KSCN) (Dong, Yang, & Zhang, 2010b; Song, Lin, & You, 2014b). As a result, this combination successfully formed a complex solvent system (DMF-KSCN), which was claimed a very cheap and highly selective solvent. In the first work, the maximum mixing ratio for KSCN:DMF was found at 17:83 because the KSCN was salted out when the ratio was higher. Thus, the experimental works were carried out below this ratio and the results were presented in two separate articles i.e. 10:90, 15:85, 16:84, 17:83 (Dong, Yang, & Zhang, 2010b) and 5:95, 8:92, 10:90, 15:85 (Song, Lin, & You, 2014b). The quaternary phase equilibria of DMF-KSCN + benzene + cyclohexane also showed significant increase in selectivity. In addition, the same research group also found NaSCN as another good co-solvent with DMF which produced relatively high selectivity (Dong et al., 2013a).

Mohsen-Nia et al (2006) carried out another method by replacing ethylene glycol with ethylene carbonate. Ethylene carbonate is a water-soluble compound that was reportedly a suitable solvent in the recovery of aromatics from alkane mixtures. Due to this application, the ethylene carbonate was evaluated in the determination of ternary LLE for the extraction of benzene, toluene and m-xylene from cyclohexane. As a comparison,

despite the reduced selectivity, the distribution ratio of benzene using the ethylene carbonate was higher than that with ethylene glycol. The extraction of benzene was also more efficient than toluene and m-xylene because of higher selectivity (Mohsen-Nia & Doulabi, 2006)..

The extractive separation of benzene and cyclohexane was studied by Ghannad et al. (2011) using N-formylmorpholine (NFM). The NMF was selected as it was reported as a good solvent in the extraction of aromatics from non-aromatic hydrocarbons. It was found that the extraction at higher temperature is less effective as the selectivity and distribution ratio were reduced (S. Ghannad et al., 2011).

In contrast to the complex solvents reported in the quaternary systems, Yang et al. (2015) recently proclaimed that a very common organic solvent could be more competitive. Furthermore, the organic solvents could even be more competitive than ILs since the ILs are commonly too expensive. Thus, they had selected dimethylsulfoxide (DMSO) for the determination of LLE phase equilibria in DMSO + benzene + cyclohexane system. The result showed good insight in terms of economical view and process simplicity. Apart from being simple and cheaper, the DMSO also showed comparable selectivity with some imidazolium based ILs (Yang et al., 2015).

Table 2.3 summarizes the research progress in the use of organic solvents for the separation of benzene and cyclohexane, while Figure 2.12 and Figure 2.13 show the range of selectivity and distribution ratio, respectively. It is worth to note that the distribution ratio of benzene using the reported organic solvents was less than unity. It means at equilibrium, the concentration of benzene in the cyclohexane-rich phase was higher than in the solvent-rich phase. This result indicates that multistage extraction is required to achieve efficient separation. Conversely, the extraction is still possible since the selectivity was far above unity.

**Table 2.3: The conventional organic solvents studied in the separation of benzene and cyclohexane by liquid-liquid extraction**

Extracting solvents	T (K)	P (atm)	D range	S range	Reference
Sulfolane	298.15	1	0.52 – 0.85	1.81 – 16.16	(De Fré & Verhoeve, 1976)
N,N-Dimethylformamide	303.15	1	0.86 – 0.92	1.60 – 3.00	(Aspi et al., 1998)
Ethylene glycol	303.15	1	0.13 – 0.27	9.52 – 47.53	(Aspi et al., 1998)
N,N-Dimethylformamide + ethylene glycol	303.15	1	0.25 – 0.80*	2.03 – 5.70*	(Aspi et al., 1998)
Ethylene carbonate	303.15	1	0.34 – 0.49	3.92 – 9.30	(Mohsen-Nia & Doulabi, 2006)
N,N-dimethylformamide + potassium thiocyanate	303.15	1	0.30 – 0.86*	2.77 – 11.36*	(Dong, Yang, & Zhang, 2010b)
Ethylene glycol	308.15	1	0.10 – 0.30	9.10 – 30.0	(M. Reza, Lotfollahi, & Asl, 2011)
N-formylmorpholine	303.15	1	0.59 – 0.74	3.94 – 24.88	(S. Ghannad et al., 2011)
N,N-dimethylformamide + sodium thiocyanate	303.15	1	0.08 – 0.4	2.45 – 11.99*	(Dong et al., 2013a)
N,N-dimethylformamide + potassium thiocyanate	298.15	1	0.62 – 0.9	2.32 – 20.74*	(Song, Lin, & You, 2014b)
Dimethylsulfoxide	303.15	1	0.57 – 0.71	4.84 – 14.06	(Yang et al., 2015)

\*taken as a combined range from different mass fractions of the two components

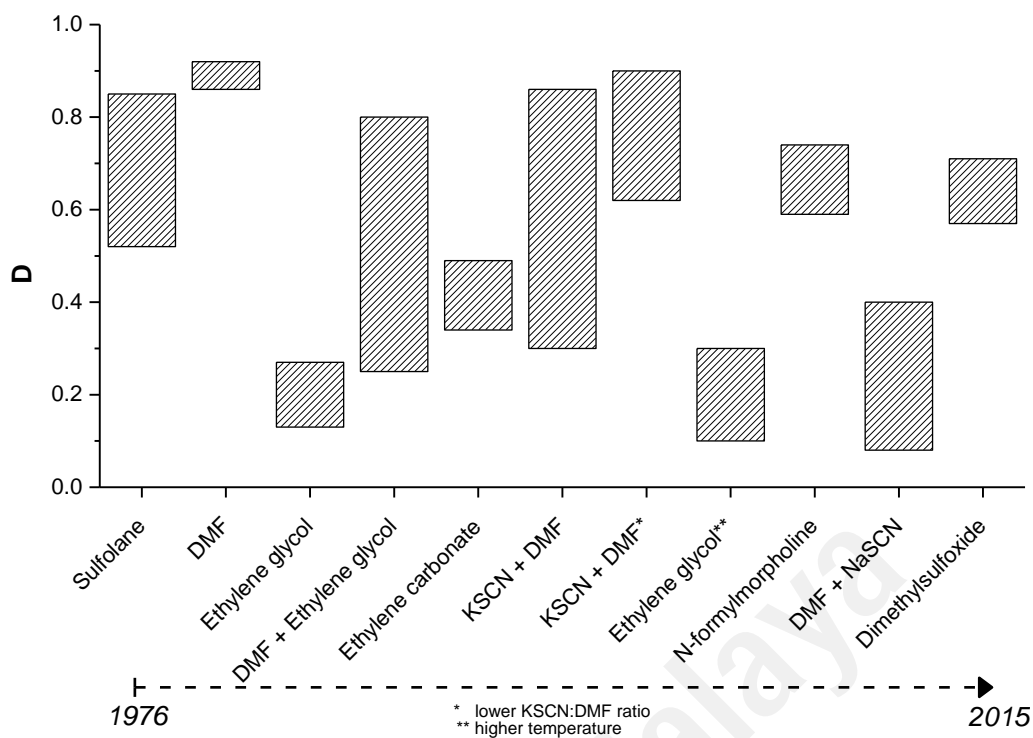


Figure 2.11: The range of distribution ratio for organic solvents from literature

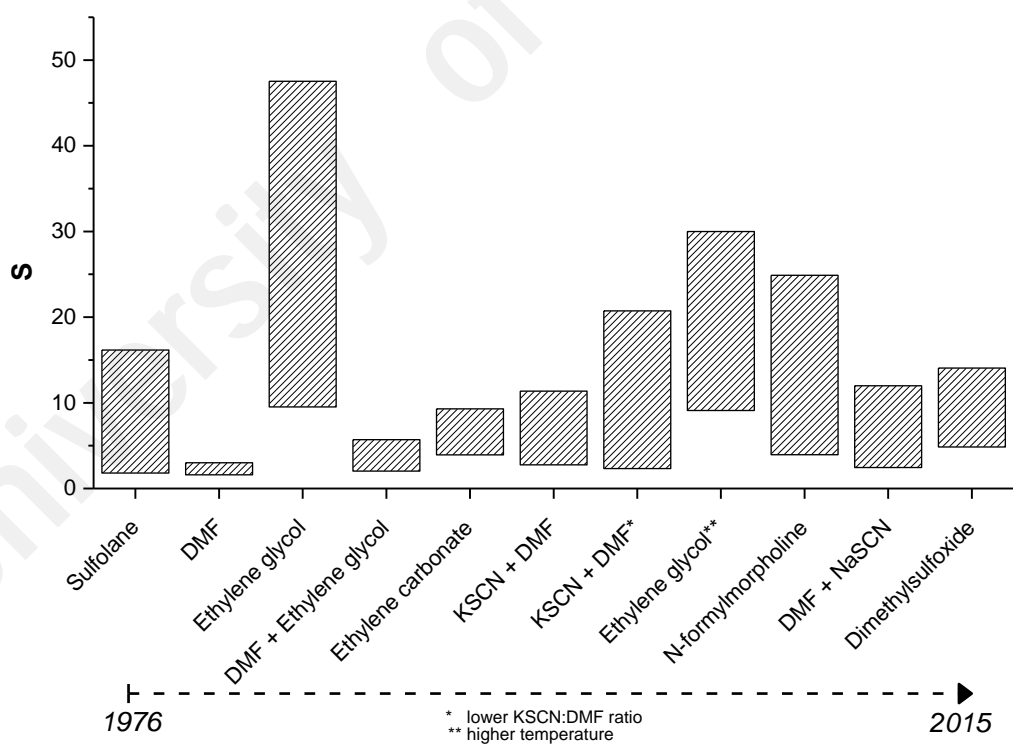
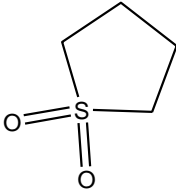
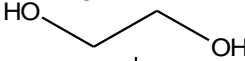
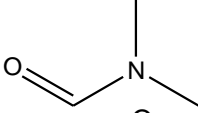
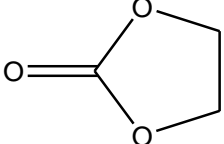
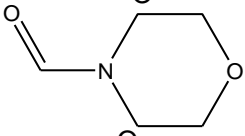
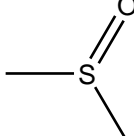


Figure 2.12: The range of selectivity for organic solvents from literature

It is interesting to note the benefit of using each organic solvent in the works discussed above. Their specific reason for solvent selection also propagated into different modification to the nature of the extracting solvent. Despite this result, the continuous application of organic solvents at industrial scale is arguable. Thus, it is important to find other green solvents as alternatives. The use of organic solvents is associated with negative impact towards the environment. For example, dimethylsulfoxide produces a very unpleasant smell upon biological degradation. In addition, it was reported that ethylene glycol, sulfolane and dimethylsulfoxide are dangerous to the environment as they have mutagenic properties, or more specifically the ability to induce genetic changes in DNA (Wypych, 2001). The organic solvents are also usually volatile and toxic. Table 2.4 shows the values of vapor pressure for the solvents that were previously studied in the separation of benzene and cyclohexane. For the other organic solvents, their physical properties and toxicology profiles can be found elsewhere (Cheremisinoff, 2003).

**Table 2.4: Vapor pressure of organic solvents used in the separation of benzene and cyclohexane**

Solvent	Structure	Vapor pressure (hPa)
Sulfolane		0.0083 (27.6 °C)
Ethylene glycol		0.092 (25 °C)
N,N-dimethylformamide		3.5 (20 °C)
Ethylene carbonate		0.013 (25 °C)
N-formylmorpholine		0.03 (20 °C)
Dimethylsulfoxide		0.61 (25 °C)

### 2.3.2.2 Progress of ILs

The most important advantage of ILs over organic solvents is their infinitesimal or negligible vapor pressure (Seddon, 1995). This exclusive property makes IL as difficult or nearly impossible to be distilled or vaporized. Only several ILs were reported as possible to be vaporized and re-condensed without significant decomposition, but at severe operating temperature and pressure (Earle et al., 2006). Therefore, the use of IL as a solvent could result into easier solvent recovery or regeneration, such as using distillation and liquid-liquid extraction. For this reason, the extractive separation of benzene and cyclohexane using several types of ILs have been explored.

Wang et al. (2008) has studied several ILs for the extractive separation of benzene and cyclohexane, and these works were presented in two articles. In the first article, two ILs, namely 1-methyl-3-methylimidazolium dimethylphosphate ( $C_1\text{mimDMP}$ ) and 1-ethyl-3-methylimidazolium diethylphosphate ( $C_2\text{mimDEP}$ ), were claimed as promising solvents for the extraction of benzene from its mixture with cyclohexane. The comparison of both ternary diagrams showed that the extraction performance was related to three characteristics of the solvents: polarity, aromaticity and size of anion (Wang et al., 2008b).

It is known that N-methylimidazole (Mim), N-ethylimidazole (Eim) have an excellent ability for the extraction of thiophene derivatives from fuels due to  $\pi$ - $\pi$  interaction between aromatic rings and thiophene. Inspired by this idea, Wang et al. (2008) have studied both in their second article and added one IL i.e. 1-hexyl-3-methylimidazolium dibutylphosphate ( $C_6\text{mimDBP}$ ) for comparison. The selectivity of Mim, Eim and  $C_6\text{mimDBP}$  was found in the range of 423.6–10.7, 5.4–1.5 and 2.3–1.3, respectively. Again, the outcome from this work confirmed the effects of polarity and aromaticity of the extracting solvent towards the extraction efficiency. The solute-solvent interaction

was enhanced by the interaction between the planar rings of benzene and imidazole molecules via two ways i.e. polar-induced polar and  $\pi$ - $\pi$  interaction. As the cyclohexane is a non-aromatic and non-polar molecule, the selectivity for benzene increased (Wang et al., 2008a). This also supports the other results that showed the significantly high values of selectivity for benzene using solvents with high polarity and low miscibility with cyclohexane, such as N-formylmorpholine (S. Ghannad et al., 2011) and ethylene carbonate (Mohsen-Nia & Doulabi, 2006). The selectivity of C<sub>6</sub>mimDBP was then compared with the previous result involving C<sub>1</sub>mimDMP. This comparison revealed that the IL with bigger size of anion may reduce its solubility in benzene + cyclohexane mixture, thus reducing the selectivity (Wang et al., 2008b).

González et al. (2010) investigated 1-ethyl-3-methylimidazolium ethylsulfate (C<sub>2</sub>mimEtSO<sub>4</sub>) as an extracting solvent for the separation of benzene from its mixture with three types of cyclic hydrocarbons, i.e. cyclohexane, methylcyclohexane and cyclooctane at 298.15 K and under atmospheric pressure. It was observed that increasing the number of carbon atom of cycloalkane produced the ternary diagrams with higher miscibility region in the order of cyclohexane < methylcyclohexane < cyclooctane. Therefore, it was concluded that the selectivity of IL to extract benzene was also affected by the size of the cycloalkane. In particular, for C<sub>2</sub>mimEtSO<sub>4</sub> + benzene + cyclohexane system, the experimental distribution ratio and selectivity were in the range of 0.45–0.63 and 10.38–19.85, respectively (E. J. González et al., 2010).

Apart from the nature of hydrocarbon, the same author also investigated the effect of different aromatic compounds in the extractive separation of benzene, toluene and ethylbenzene from their mixture with cyclohexane using 1-ethyl-3-methylpyridinium ethylsulfate (C<sub>2</sub>mpyrEtSO<sub>4</sub>). It was concluded that the solubility of aromatic compounds in C<sub>2</sub>mpyrEtSO<sub>4</sub> decreased in the order of benzene > toluene > ethylbenzene. This

demonstrated that the presence of radicals in the aromatic compounds will negatively affect the extraction process. Although the process was highly selective, high number of extraction stages was recommended because the distribution ratio was less than unity (E. González et al., 2010b).

The extractive separation of benzene and cyclohexane using 1-butyl-3-methylimidazolium hexafluorophosphate ( $C_4mimPF_6$ ) as the solvent gave the selectivity values in the range of 20–60 and showed indirect trend of selectivity at higher temperatures (Lu, Yang, & Luo, 2010).

Calvar et al. (2011) studied numerous ternary systems for the separation of aromatic and aliphatic mixture at 298.15 K and under atmospheric pressure using two ILs, namely 1-butyl-3-methylimidazolium bis(trifluoromethylsulfonyl)imide ( $C_4mimTf_2N$ ) and 1-butyl-3-methylimidazolium methylsulfate ( $C_4mimMeSO_4$ ). The ternary systems investigated were *n*-hexane/*n*-heptane/cyclohexane + benzene +  $C_4mimMeSO_4$ , *n*-hexane/cyclohexane + benzene +  $C_4mimTf_2N$  and *n*-hexane + toluene +  $C_4mimTf_2N$  (Calvar et al., 2011). Focusing on the separation of benzene and cyclohexane, the selectivity of  $C_4mimTf_2N$  was less than those with  $C_2mimEtSO_4$ ,  $C_2mpyrEtSO_4$  and  $C_4mimPF_6$ . However, as illustrated in Table 2.5, the distribution ratio was exceptionally higher than the other ILs studied previously. Furthermore, at higher concentration of benzene, the distribution ratio was also higher than unity and correspondingly produced positive slopes. This indicates that benzene has higher affinity in the IL layer than in the cyclohexane layer (Calvar et al., 2011).

As mentioned previously, the effect of solvent mixing was firstly studied by Aspi et al. (1998) which involved the combination of two organic compounds, namely dimethylformamide and ethylene glycol (Aspi et al., 1998). Interestingly, instead of using organic compounds, Salem et al. (2012) used two ILs ( $MimBF_4$  and  $C_1mimDMP$ ) which

were blended to form a quaternary system (Salem, Shen, & Li, 2012). However, it is noteworthy that the solvent mixing study by Aspi et al. (1998) was done by considering two organic solvents in which one having high selectivity and another having high distribution ratio, while Salem et al. (2012) introduced  $C_{1mim}DMP$  to dissolve the  $MimBF_4$ , which has high selectivity but is solid at room temperature. Although the approaches in both groups were different, solvent mixing was confirmed as a very good technique to enhance the extraction performance. This can be seen by the remarkable increase in selectivity and distribution ratio of the mixed solvent in both cases.

Zhout et al. (2012) studied the effect of alkyl chain on imidazolium cation by investigating the performance of 1-alkyl-3-methylimidazolium hexafluorophosphate ( $C_nmimPF_6$ ) ( $n=4, 5, 6$ ) in the separation of benzene and cyclohexane mixture. These ILs are easy to prepare and available commercially. The benzene distribution ratio increased in the order of  $C_4mimPF_6 < C_5mimPF_6 < C_6mimPF_6$ , while the selectivity decreased through this order. The noteworthy finding was that  $C_4mimPF_6$  possesses an extremely high solvent selectivity at low composition (<15%) of benzene in the raffinate phase, which concludes that it is suitable for deep separation of benzene and cyclohexane (Zhou et al., 2012a).

The extractive separation of benzene and cyclohexane was also further studied by Zhou et al. (2012) in their next article by considering the lower concentration of benzene (15 mol %). Regarded as a deep separation process, this study used three ILs, namely 1-butyl-3-methylimidazolium tetrafluoroborate ( $C_4mimBF_4$ ), 1-butylpyridinium tetrafluoroborate ( $C_4pyrBF_4$ ) and 1-butyl-3-methylimidazolium thiocyanate ( $C_4mimSCN$ ). These ILs were selected because imidazolium- and pyridinium-based ILs with  $BF_4^-$  or  $N(CN)_2^-$  anions were reportedly good solvents for the separation of aromatic and aliphatic hydrocarbons. The result showed that the overall extraction efficiency

increased in the order of  $C_4\text{mimSCN} < C_4\text{pyrBF}_4 < C_4\text{mimBF}_4$ . This trend was supported with the analysis of  $\sigma$ -profiles and cation-anion interaction in COSMO-RS programme, which concluded that  $\text{BF}_4^-$  and imidazolium were better ions than  $\text{SCN}^-$  and pyridinium, respectively (Zhou et al., 2012b).

Gómez et al. (2014) used a simple but high potential IL, i.e. 1-ethylpyridinium ethylsulfate ( $C_2\text{pyEtSO}_4$ ) for the extraction of benzene from benzene–cyclohexane mixture (Gómez et al., 2014). The selectivity of this IL was higher than most of other ILs in the previous works, but still lower than the system containing  $C_2\text{mpyrEtSO}_4$  at low molar concentration ( $< 0.4$ ) of benzene in the raffinate phase (E. González et al., 2010b). In addition, it was found that the solvent selectivity was affected by the structural nature of the cyclic hydrocarbon: increased by higher alkyl chain or the presence of methyl group and decreased by the presence of double bond. It should be noted that the  $C_2\text{pyEtSO}_4$  in this study was selected because of easy preparation, market availability, and its satisfactory results in the separation of benzene from its mixture with *n*-hexane/ *n*-heptane (Gómez et al., 2010a), and octane/nonane (Gómez et al., 2010b). Since there is a huge number of ILs available, this selection technique is therefore infinitesimal and nearly random. This would suggest the significance of a preliminary selection stage by considering cations and anions that form the ILs.

The first investigation on the use of computational software to perform a preliminary screening of several ILs was done by considering a combination of 12 cations and 22 anions (Lyu et al., 2014b). This study comprehensively investigated three major aspects of solvent evaluation: preliminary screening using COSMO-RS, experimental validation and conceptual design of the extraction process. For the screening input, the tetrachloroaluminate anion ( $\text{AlCl}_4^-$ ) was also introduced which aimed to validate the effect of delocalized electron. The screening result proved that any cations combined with

$\text{AlCl}_4^-$  showed higher benzene distribution ratio and performance index. Thus, it was concluded that anions with delocalized electron can promote the extraction efficiency. Furthermore, the agreements with other works were also observed, where the anion with highly delocalized electron will form  $\pi$ -complexation with aromatics (Zhang et al., 2007), as well as facilitate aromatics to share the positive charge of the cation (Meindersma, Hansmeier, & de Haan, 2010). The quantum chemical calculations by Lyu et al. (2014) further showed that there were not only strong bonds between anion and benzene, but also comparable CH- $\pi$  and  $\pi$ - $\pi$  interactions between the cation and benzene.  $\text{AlCl}_4^-$  has higher interaction with benzene because compared to  $\text{BF}_4^-$ , it has weaker interaction with  $\text{Bmim}^+$  (Lyu et al., 2014b).

Table 2.5 summarizes the ILs studied previously and their corresponding performances in the extractive separation of benzene and cyclohexane.

**Table 2.5: Performance of ILs previously studied for the separation of benzene and cyclohexane**

Extracting solvents	T (K)	P (atm)	D range	S range	Reference
N-methylimidazole	298.2	1	0.74 – 0.92	10.76 – 402.85	(Wang et al., 2008a)
N-ethylimidazole	298.2	1	0.95 – 1.05	1.47 – 5.43	(Wang et al., 2008a)
C <sub>6</sub> mimDBP	298.2	1	–	1.3 – 2.3	(Wang et al., 2008a)
C <sub>1</sub> mimDMP	298.2	1	–	2.9 – 3.6	(Wang et al., 2008b)
C <sub>1</sub> mimDMP	313.2	1	–	3.0 – 4.4	(Wang et al., 2008b)
C <sub>2</sub> mimDEP	298.2	1	–	2.5 – 4.3	(Wang et al., 2008b)
C <sub>2</sub> mimDEP	313.2	1	–	2.6 – 3.7	(Wang et al., 2008b)
C <sub>2</sub> mimEtSO <sub>4</sub>	298.15	1	0.45 – 0.63	10.4 – 19.9	(E. J. González et al., 2010)
C <sub>2</sub> mpyrEtSO <sub>4</sub>	298.15	1	0.54 – 0.66	9.59 – 27.0	(E. González et al., 2010b)
C <sub>4</sub> mimPF <sub>6</sub>	298.15	1	–	26.6 – 33.8	(Lu, Yang, & Luo, 2010)
C <sub>4</sub> mimTf <sub>2</sub> N	298.15	1	0.82 – 1.85	3.81 – 9.78	(Calvar et al., 2011)
C <sub>1</sub> mimDMP	298.2	1	0.31 – 0.53	0.67 – 5.25	(Salem, Shen, & Li, 2012)
MimBF <sub>4</sub>	338.2	1	0.09 – 0.12	0.26 – 2.22	(Salem, Shen, & Li, 2012)
BmimPF <sub>6</sub>	298.15	1	0.62 – 1.38	6.6 – 49.4	(Zhou et al., 2012a)
PmimPF <sub>6</sub>	298.15	1	0.81 – 1.24	2.2 – 38.3	(Zhou et al., 2012a)
HmimPF <sub>6</sub>	298.15	1	0.83 – 1.36	2.2 – 25.6	(Zhou et al., 2012a)
BmimBF <sub>4</sub>	298.15	1	0.61 – 0.77	3.3 – 80.4	(Zhou et al., 2012b)
BpyrBF <sub>4</sub>	298.15	1	0.50 – 0.68	2.8 – 50.0	(Zhou et al., 2012b)
BmimSCN	298.15	1	0.39 – 0.79	2.7 – 31.8	(Zhou et al., 2012b)
EpyEtSO <sub>4</sub>	298.15	1	0.38 – 0.45	17.36 – 24.77	(Gómez et al., 2014)
BmimAlCl <sub>4</sub>	298.15	1	0.91 – 1.26	13.63 – 21.76	(Lyu et al., 2014b)

## **2.4 Deep eutectic solvents**

### **2.4.1 Overview of DESs**

About fifteen years ago, a new group of solvents was introduced for the first time as DESs (Abbott et al., 2003). DESs have been progressively explored and applied as new solvents in many fields. Recently, DESs were found as potential solvents to replace conventional organic solvents for the separation of aromatics from aliphatic hydrocarbons. DESs are now widely termed as a new class of IL analogue because they share many characteristics and properties with ILs. Despite the similar properties, DESs still cannot be considered as ILs. This is due to the difference in ionic nature, i.e. DESs are not entirely composed of ionic species, and DESs can also be produced from non-ionic species. Although the use of ILs in the separation of aromatic and aliphatic is expected to consume less energy and lower processing steps, the applications are still limited by their expensive prices and being not universally green. On the other hand, DESs has gained a special attention by the scientific community due to their two remarkable advantages over ILs, i.e. being cheaper and easier to synthesize. In addition, DESs derived from choline chloride gather many additional advantages, such as easier storage (inertness with water) and they are mostly biodegradable, biocompatible and non-toxic (Zhang et al., 2012). These advantages have rapidly increased their applications as a solvent in numerous fields. Since the beginning of this century, research works involving DESs has been increasing exponentially (Figure 2.13).

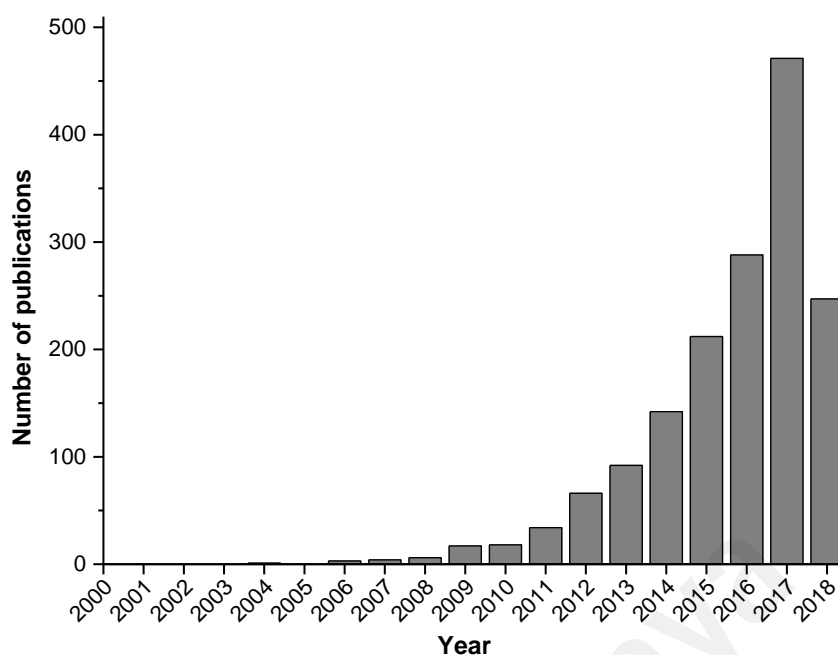
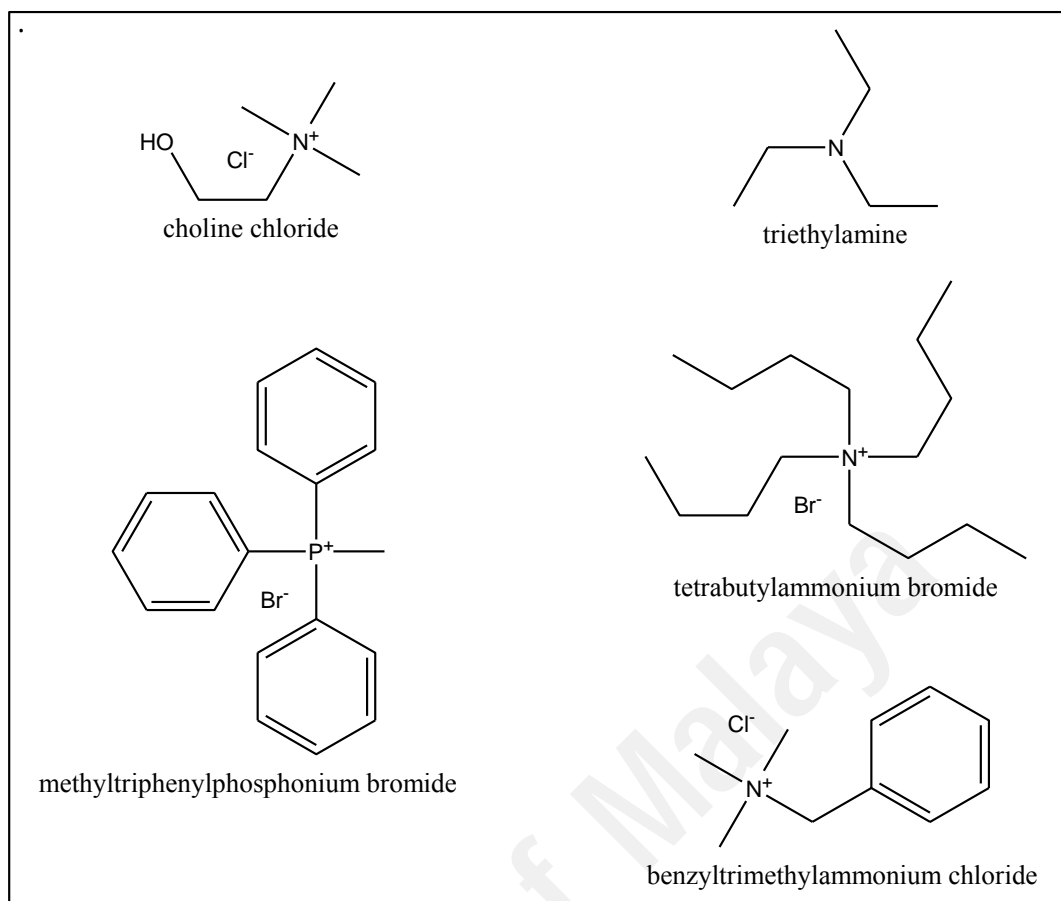
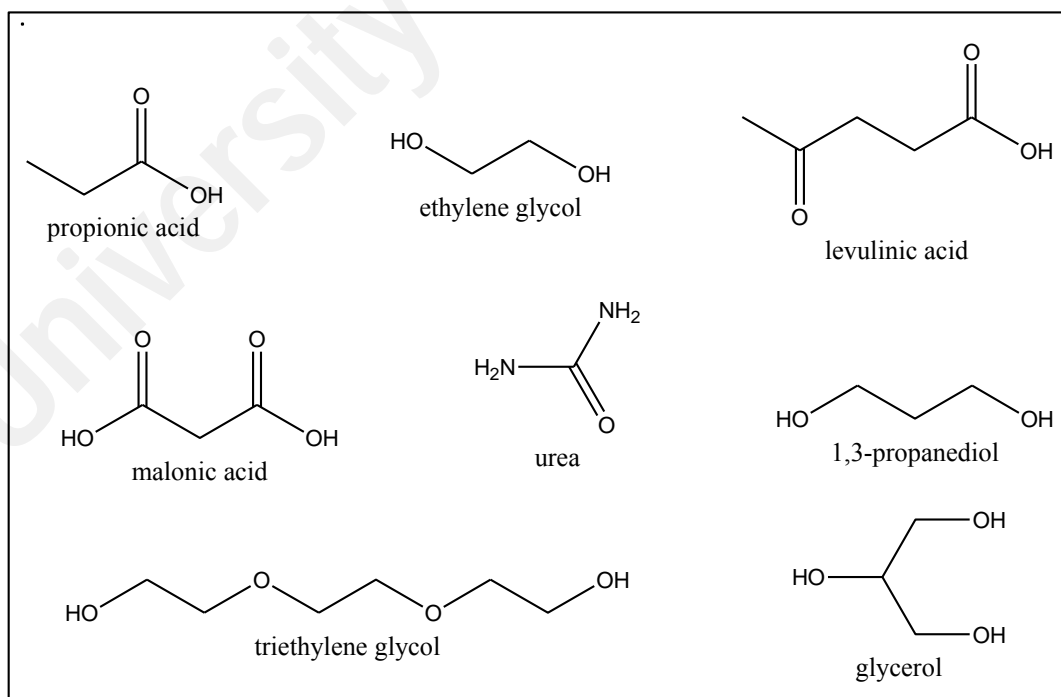


**Figure 2.13: Number of annual publications in the topic of DESs since the year 2000.**

In general, a DES is synthesized by mixing various molar ratio of two or more ingredients which results in a eutectic with much lower melting point than that of each individual ingredient. An example of a common DES is the combination of choline chloride with urea, which forms a eutectic mixture when 1 mole of choline chloride is mixed with 2 moles of urea (Abbott et al., 2004). DES is constituted by bulky and nonsymmetric ions that have low lattice energy and hence low melting points (Smith, Abbott, & Ryder, 2014). They are usually obtained by complexation of two entities, i.e. salt or hydrogen bond acceptor (HBA) and hydrogen bond donor (HBD). On one hand, the salt cation is principally any ammonium, phosphonium or sulfonium types, while the salt anion is generally a halide anion. On the other hand, the HBD is usually a Lewis or Brønsted acid. The lower melting point of DES relative to the individual compounds is attributed by the charge delocalization via hydrogen bonding between salt anion and hydrogen-donor moiety in HBD. Figure 2.14 shows the structure of some salts and HBDs that are commonly used to synthesize DESs.



(a)



(b)

**Figure 2.14: Structure of some compounds that can form DESs: (a) salts and (b) HBDs**

## 2.4.2 Review on the potential of DESs in separation of benzene and cyclohexane

DESs are well recognized for their advantages, such as easy to synthesize, cheaper materials and wide range of selection. This promotes a progressive research on their usage in various applications, including in the separation of aromatic and aliphatic hydrocarbons. However, there has been no article that specifically reports the performance of DESs in the separation of benzene and cyclohexane. Due to this reason, this section surveys the existing data for a more general application, i.e. the use of DESs in the separation of other aromatic–aliphatic hydrocarbon systems. This is still in line with the original scope of this study (benzene and cyclohexane) – as benzene is in fact an aromatic hydrocarbon, while cyclohexane is an aliphatic hydrocarbon that is in cyclic nature. The ternary systems presented in this section involves different mixture combinations arise from several types of aromatic (eg: benzene, toluene, xylene) and aliphatics (eg: hexane, heptane, octane).

### 2.4.2.1 Extractive performance of DESs in separation of aromatic–aliphatic mixtures

The feasibility of two different DESs as novel extracting solvents for the separation of benzene from *n*-hexane was tested by Rodriguez et al. (2015). Two different types of DES were tested i.e. tetrahexylammonium bromide (THABr) with ethylene glycol and glycerol at molar ratio of 1:2. The ternary LLE data showed that DESs are the promising extracting agents for the industrial purification of naphtha streams containing diluted aromatic (Rodriguez, Requejo, & Kroon, 2015)..

Sander et.al. (2016) studied 6 systems of three compounds with choline chloride:urea (ChCl:Ur) and choline chloride:glycerol (ChCl:Gly) at molar ratio of 1:2 The results proposed that (ChCl:Gly) has better potential as an extracting solvent for the separation of pyridine from its mixture with *n*-hexane (Sander et al., 2016).

Kareem et al. (2013) studied the extraction of toluene from toluene-heptane mixture using ethyltriphenylphosphonium based DESs. Six DESs were synthesized by mixing ethyltriphenylphosphonium iodide (ETPPI) with either ethylene glycol or sulfolane. The LLE data showed that the DES ETPPI:Sulf (1:4) gave enhanced purification competency at 30 °C. The selectivities observed in the study were higher than those reported for sulfolane in commercial applications (Kareem et al., 2013). Similar work was carried out by Mulyono et al. (2014), who reported the feasibility of using ammonium-based DESs for the separation of BTEX (benzene, toluene, ethylbenzene and xylenes) from n-octane using DESs (Mulyono et al., 2014).

Oliveira et al. (2013) observed remarkably high selectivities and distribution coefficients for chlorine chloride based DESs with three different types of HBD, i.e, ethylene glycol, levulinic acid and glycerol which proves them as promising alternatives to ILs in the extraction of ethanol from ethanol–heptane mixtures (Oliveira et al., 2013). The same group tested DESs based on three different salts, namely choline chloride, benzylcholine chloride and tetrabutylammonium chloride with levulinic acid as HBD (Salt:HBD, 1:2) for the separation of toluene from n-heptane at 298.15K. It was concluded that the introduction of a more hydrophobic HBA in the DES promotes the improvement of the distribution coefficient, while manipulating the aromaticity of the DES leads to higher selectivity (Gouveia et al., 2016).

Recently, Hadj-Kali et al. (2016) investigated the potential of four DESs based on tetrabutylammonium bromide (TBABr) or methyltriphenylphosphonium bromide (MTPPBr) (as typical salts) with ethylene glycol, triethylene glycol or sulfolane (as the HBDS) for the separation of thiophene from a model diesel of n-heptane. The study showed that the sulfolane-based DES (TBABr:Sulf) (1:7) resulted the best extraction efficiency, 35%, outperforming the other DESs studied. Furthermore, the extraction

efficiency could be improved up to 98% after five extraction cycles (Hadj-Kali et al., 2016).

The equilibrium data in the systems involving some DESs for the separation of aromatic compound from its mixture with *n*-hexane, *n*-heptane and *n*-octane are summarized in Table 2.6, Table 2.7 and Table 2.8, respectively.

**Table 2.6: Summary of DESs used for the separation of aromatic compounds from n-hexane (at P =101.325 kPa)**

Aromatic	DES	D	S	T (K)	Ref
Benzene	TMACl:Gly (1:2)	0.01–0.02	6.88–51.82	298.2	(Mahmoudi & Lotfollahi, 2010)
	TEACl:Gly (1:2)	0.08–0.1	21.13–137.0		
	TEACl:EG (1:2)	0.19–0.32	28.64–174.0		
	TBACl:EG (1:2)	0.49–0.55	2.70–17.75		
	THACl:Gly (1:2)	0.42–0.49	1.76–7.35		
	THACl:EG (1:2)	0.74–0.86	1.59–4.28		
Benzene	ChCl:Glucose (1:1)	0.04–0.12	13.58–36.05	298.15	(Kurnia et al., 2016)
Toluene	ChCl:Glucose (1:1)	0.02–0.05	6.05–14.27		
Pyridine	ChCl:Glucose (1:1)	0.23–0.66	12.74–177.16		
o-cresol	Imidazole	5.76–74.51	20.9–1759	303.15	(Jiao et al., 2016)
	Imidazole	3.88–79.61	10.4–1652	313.15	
m-cresol	Imidazole	9.94–119.80	31–5943	303.15	
	Imidazole	6.99–195.1	21.5–48478	313.15	
Benzene	MTPPBr:EG (1:4)	0.12–0.27	12.36–98.27	300.15	(M. A. Kareem et al., 2012)
	MTPPBr:EG (1:4)	0.17–0.92	15.87–87.09	308.15	
	MTPPBr:EG (1:4)	1.04–2.50	18.39–93.68	318.15	
	MTPPBr:EG (1:6)	0.79–2.25	28.38–55.83	300.15	
	MTPPBr:EG (1:6)	0.32–0.5	32.99–83.64	308.15	
	MTPPBr:EG (1:6)	0.43–1.16	4.94–19.27	318.15	
	MTPPBr:EG (1:8)	0.31–0.55	13.66–49.09	318.15	

**Table 2.7: Summary of DESs used for the separation of aromatic compounds from n-heptane (at P =101.325 kPa)**

Aromatic	DES	D	S	T (K)	Ref
Toluene	ChlCl:LevA (1:2)	0.095–0.13	9.47–23.90	298.15	(Gouveia et al., 2016)
	BzChlCl:LevA (1:2)	0.16–0.34	12.31–39.11		
	N <sub>444</sub> Cl:LevA (1:2)	0.48–0.74	0.60–13.41		
Toluene	MTPPBr:EG (1:4)	0.23–0.29	12.6–48.5	308.15	(Naik et al., 2016)
	MTPPBr:Gly (1:4)	0.14–0.22	1.2–21.6		
Quinoline	MTPPBr:EG (1:4)	5.92–35.27	142.4–3344.2		
	MTPPBr:Gly (1:4)	7.83–16.66	463.5–2539.2		
Thiophene	TBABr:EG (1:4)	0.23–0.33	8.79– 30.22	298.15	(Hadj-Kali et al., 2016)
	MTPPBr:EG (1:4)	0.27–0.37	10.12–37.54		
	TBABr:TEG (1:4)	0.30–0.46	7.33–51.95		
	TBABr:Sulf (1:7)	0.76–0.66	13.77–41.87		
Toluene	TBPBr:EG (1:2)	0.54–0.95	4.00–15.38	313.15	(M. Kareem et al., 2012)
	TBPBr:EG (1:2)	0.48–0.57	3.81–7.48	323.15	
	TBPBr:EG (1:2)	0.495–0.65	3.64–7.95	333.15	
	TBPBr:Sulf (1:2)	0.74–0.83	4.39–9.87	323.15	
	TBPBr:Sulf (1:2)	0.73–0.82	4.08–8.50	333.15	

**Table 2.8: DES used for the separation of aromatic compounds from n-octane (at P =101.325 kPa)**

Aromatic	DES	D	S	T (K)	Ref
Toluene	TBABr:Sulf (1:4)	0.47–0.57	8.3–25.7	298.15	(Mulyono et al., 2014)
m-xylene	TBABr:Sulf (1:4)	0.32–0.55	3.2–27.2		
Benzene	TBABr:Sulf (1:4)	0.31–0.74	9.2–46.4		
Ethyl benzene	TBABr:Sulf (1:4)	0.45–0.58	6.0–8.7		

In Table 2.6 to 2.8, the extraction efficiency is evaluated through selectivity and distribution ratio. These measurements are obtained from measured experimental molar compositions of each component in the extract (DES-rich) and raffinate (aliphatic-rich)

phases. For a given DES-aromatic-aliphatic ternary system, we can classify DES, aromatic and aliphatic compounds as the solvent, solute and carrier, respectively. The distribution ratio of solute describes its distribution behavior between the extract and raffinate phase at equilibrium. A similar definition applies to the distribution ratio of carrier. In this particular separation, the distribution ratio of solute is more important because aromatic compounds represent the targeted component to be extracted. Conversely, the selectivity evaluates the ability of solvent to extract aromatic compounds only, rather than extracting aromatic and aliphatic compounds altogether.

#### 2.4.2.2 Comparison of extractive performance between DESs and organic solvents

The results of the DESs and organic solvents used in the extractive separation of aromatic and aliphatic compounds are summarized in Table 2.9. The information from Table 2.9 was then extracted into Figure 2.16 and Figure 2.17 to obtain a clear comparison between DESs and organic solvents used in a specific system.

**Table 2.9: Extractive separation of aromatic and aliphatic using DESs or organic solvents**

Aromatic + Aliphatic	Organic Solvent	D	S	T (K)	References
Benzene + n-hexane	Sulfolane	0.49–0.72	7.21–20.14	308–318	(Mahmoudi & Lotfollahi, 2010)
Benzene + n-hexane	TEACl:EG (1:2)	0.19–0.32	28.64–174.03	298	(Rodriguez et al., 2017)
Benzene + n-hexane	TMACl:Gly (1:2)	0.01–0.02	6.88–51.82	298	(Rodriguez et al., 2017)
Benzene + n-hexane	NFM	0.56–0.78	4.21–18.81	303–313	(Mahmoudi & Lotfollahi, 2010)
Benzene + n-hexane	50% Sulfolane+ 50% NFM	0.60–0.67	8.55–39.85	298–308	(Mahmoudi & Lotfollahi, 2010)
Benzene + n-hexane	ChCl:Glucose (1:1)	0.04–0.12	13.58–36.05	298	(Kurnia et al., 2016)
Benzene + n-hexane	MTPPBr:EG (1:4)	0.12–0.27	12.36–98.27	300	(M. A. Kareem et al., 2012)
Benzene + cyclohexane	EG	0.10–0.29	9.10–29.95	298–318	(M. Reza, Lotfollahi, & Asl, 2011)
Benzene + cyclohexane	TBABr:Sulf (1:7)	0.20–0.24	4.97–13.69	298	(Salleh et al., 2017c)

**Table 2.9, continued**

<b>Aromatic + Aliphatic</b>	<b>Organic Solvent</b>	<b>D</b>	<b>S</b>	<b>T (K)</b>	<b>References</b>
Benzene + cyclohexane	NFM	0.59–0.76	3.26–24.88	303–313	(Seyedein Ghannad, Lotfollahi, & Haghghi Asl, 2011)
Benzene + cyclohexane	MTPPBr:TEG (1:4)	0.10–0.12	4.28–13.39	298	(Salleh et al., 2017c)
Toluene + heptane	Ethylene glycol	0.027–0.067	7.16–48.32	303–313	(Haghnazarloo et al., 2013)
Toluene + heptane	MTPPBr:EG (1:4)	0.23–0.29	12.6–48.5	308	(Naik et al., 2016)
Toluene + <i>n</i> -heptane	EC	0.22–0.31	7.65–13.28	313	(Mohsen-Nia et al., 2005)
<i>m</i> -xylene + <i>n</i> -heptane	Sulfolane	0.24–0.42	2.23–9.49	303–313	(Mohsen-Nia et al., 2005)
<i>m</i> -xylene + <i>n</i> -heptane	EC	0.12–0.17	6.08–10.75	313	(Mohsen-Nia et al., 2005)
<i>m</i> -xylene + <i>n</i> -heptane	Sulfolane + EC (50:50)	0.17–0.47	2.12–11	313	(Mohsen-Nia et al., 2005)
<i>m</i> -xylene + <i>n</i> -Octane	DMSO	0.31–0.75	1.72–10.74	298–303	(Mohsen-Nia et al., 2005)
<i>m</i> -xylene + <i>n</i> -Octane	TBABr:Sulf (1:4)	0.32–0.55	3.2–27.2	298	(Mulyono et al., 2014)
Toluene + cyclohexane	Ethylene carbonate	0.20–0.53	2.09–5.01	313	(Mohsen-Nia et al., 2005)
<i>n</i> -xylene + cyclohexane	Ethylene carbonate	0.11–0.18	0.78–4.56	313	(Mohsen-Nia et al., 2005)
Toluene + <i>n</i> -octane	Ethylene carbonate	0.19–0.40	5.71–19.27	313	(Mohsen-Nia et al., 2005)
Toluene + <i>n</i> -octane	Ethylene glycol	0.22–0.33	6.73–33.93	295–307	(Mohsen-Nia, Mohammad Doulabi, & Manousiouthakis, 2008)
Toluene + <i>n</i> -heptane	Sulfolane + EC (50:50)	0.30–0.56	2.98–18.91	313	(Mohsen-Nia et al., 2005)
<i>n</i> -xylene + <i>n</i> -heptane	NFM	0.39–0.77	1.12–3.70	298–353	(Chen, Ye, & Hao, 2007)
Benzene + methylcyclohexane	NFM	0.24–0.60	1.51–3.29	293–333	(Chen, Ye, & Wu, 2007)
Benzene + Hexadecane	acetonitrile	0.33–0.81	6.16–147.45	298	(You, Jeong, & Park, 2015)
Toluene+ Hexadecane	acetonitrile	0.52–0.79	6.43–51.97	298	(You, Jeong, & Park, 2015)

Table 2.9, continued

Aromatic + Aliphatic	Organic Solvent	D	S	T (K)	References
p-xylene+ Hexadecane	acetonitrile	0.41–0.62	4.9–171	298	(You, Jeong, & Park, 2015)
Benzene + Hexadecane	2-methoxyethanol	0.53–0.83	5.11–192.40	298	(You, Jeong, & Park, 2015)
Toluene + Hexadecane	2-methoxyethanol	0.45–0.85	2.62–128.82	298	(You, Jeong, & Park, 2015)
P-Xylene + Hexadecane	2-methoxyethanol	0.32–0.64	2.67–38.69	298	(You, Jeong, & Park, 2015)
Ethylbenzene + trimethylpentane	NFM	0.31–0.79	1.72–15.74	303-323	(Wang, Xia, & Ma, 2012)

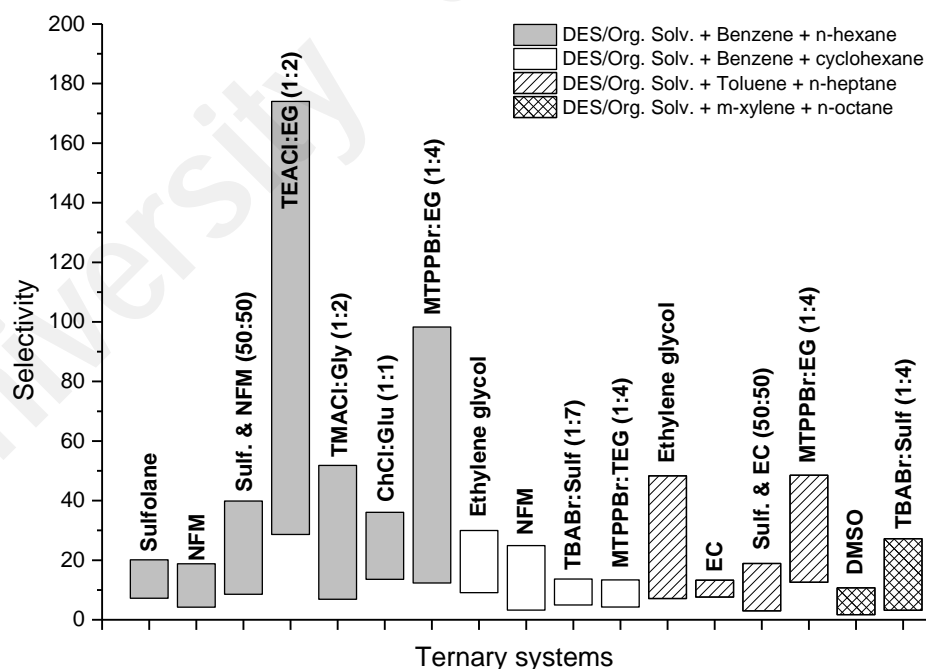
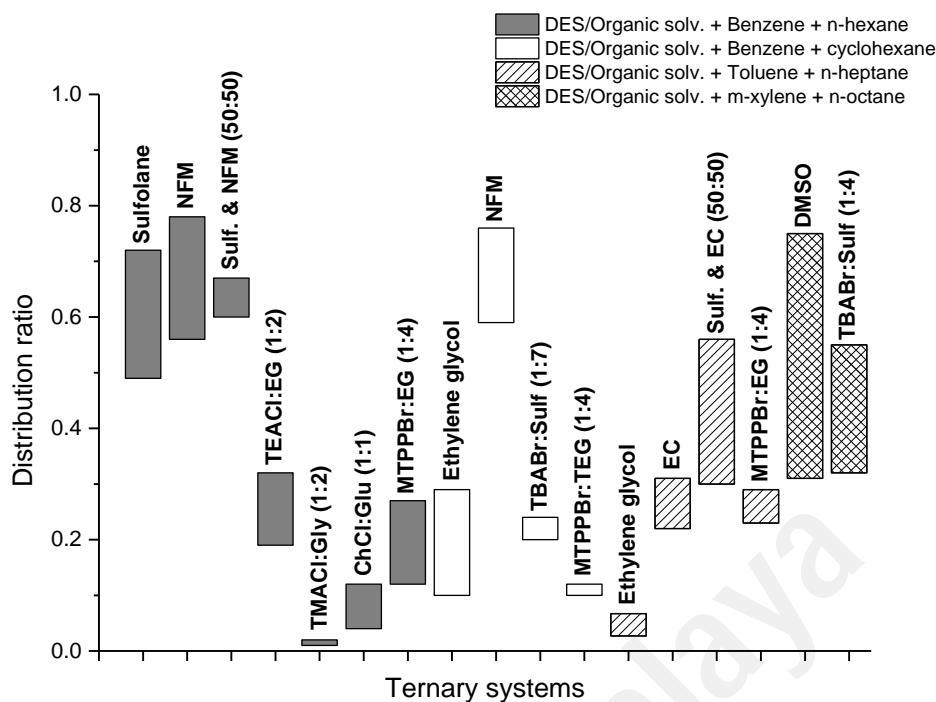


Figure 2.15: The selectivity range for some ternary systems involving organic solvents/DESS + aromatics + aliphatics.



**Figure 2.16: The distribution ratio range for some ternary systems involving organic solvents/DESs + aromatics + aliphatics.**

As seen in Figure 2.16, the highest selectivity for benzene-hexane system was observed with TEACl:EG (1:2) DES, followed by MTPPBr:EG (1:4) and TMACl:Gly (1:2) (Rodriguez et al., 2017). However, these selectivity values were traded off, where the values of distribution ratio were relatively lower than sulfolane, NFM and mixture of both (Mahmoudi & Lotfollahi, 2010).

Similarly, although NFM exhibited the highest value of distribution ratio, it has the lowest selectivity compared to sulfolane and all DESs. In general, this trend is also observable in other aromatic-aliphatic system, where the distribution ratio for all types of solvents (both DESs and organic solvents) were less than unity, but the selectivity of DESs were more superior than the organic solvents. Therefore, it can be concluded that the use of DES will enhance the selectivity but reduce the distribution ratio. This means the application of DES in the separation of aromatic and aliphatic will give the lower extraction stages than organic solvent, but with higher solvent-to-feed ratio. This finding

would make the DESs more favorable because of their negligible vapor pressure and being less hazardous to the environment.

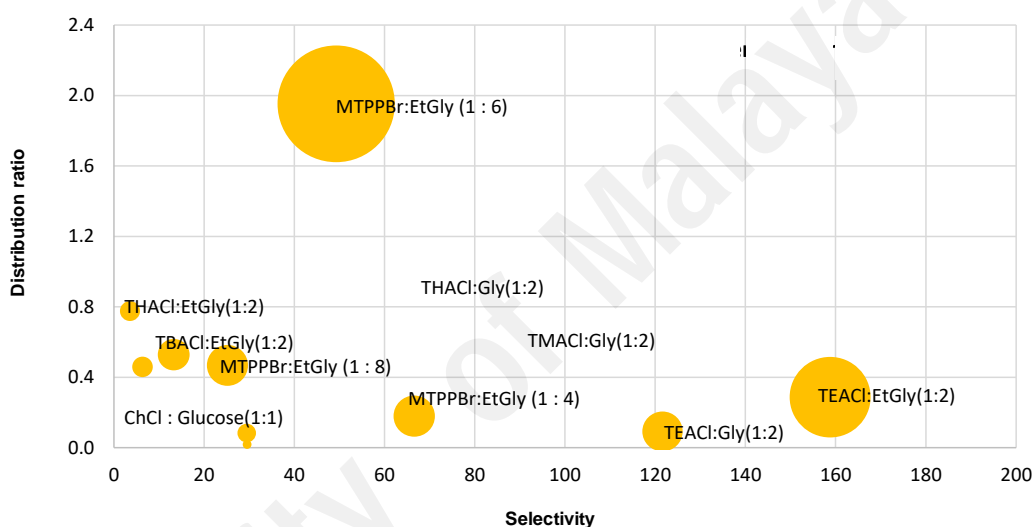
### 2.4.2.3 Comparison of extractive performance between DESs and ILs

Table 2.10 shows the summary of ILs that were used in some of the previous works for the separation of aromatic–aliphatic systems.

**Table 2.10: Summary of ILs used for the separation of aromatic–aliphatic mixtures (at 101.325 kPa)**

Aromatic + aliphatic	IL	D	S	T (K)	References
Toluene + <i>n</i> -heptane	C <sub>2</sub> mimN(CN) <sub>2</sub>	0.27–0.32	32.9–72	313.2	(Larriba et al., 2013a)
	C <sub>4</sub> mimN(CN) <sub>2</sub>	0.43–0.477	16.4–45.7		
	C <sub>2</sub> mimTCM	0.441–0.579	18.9–47		
Thiophene + <i>n</i> -heptane	C <sub>2</sub> mimSCN	0.63–0.76	106.5–1598.5	298.15	(Kędra-Królik, Fabrice, & Jaubert, 2011)
	C <sub>2</sub> mimSCN	0.6–0.74	119–497.3	303.15	
	C <sub>1</sub> mimMePO <sub>4</sub>	0.26–0.44	18.9–1756.2	298.15	
	TEMAMeSO <sub>4</sub>	0.05–0.09	9.3–102	298.15	
Pyridine + <i>n</i> -heptane	C <sub>2</sub> mimSCN	1.12–3.85	6.8–1208.9	298.15	
	C <sub>1</sub> mimMePO <sub>4</sub>	0.37–1.19	6.3–49.6	298.15	
Benzene + <i>n</i> -hexane	C <sub>4</sub> mimTf <sub>2</sub> N	0.82–1.79	2.73–17.39	298.15	(Alberto et al., 2007)
	C <sub>8</sub> mimTf <sub>2</sub> N	0.92–1.9	1.51–7.35		
	C <sub>10</sub> mimTf <sub>2</sub> N	0.96–2.21	1.19–5.45		
	C <sub>12</sub> mimTf <sub>2</sub> N	0.99–1.83	1.16–3.54		
Benzene + <i>n</i> -hexane	C <sub>2</sub> mimTf <sub>2</sub> N	0.76–1.37	4.85–33.56	289.15	(Arce et al., 2007)
	C <sub>2</sub> mimTf <sub>2</sub> N	0.76–1.2	4.6–27.77	313.15	
Toluene + <i>n</i> -heptane	Sulfolane	0.28–0.51	4.63–31.01	313.2	(Meindersma, Podt, & de Haan, 2006)
		0.32–0.56	3.71–24.91	348.2	
	C <sub>1</sub> bupyBF <sub>4</sub>	0.43–0.52	12.14–53.09	313.2	
		0.36–0.49	16.85–39.32	348.2	
Ethylbenzene + <i>n</i> -hexane	C <sub>4</sub> mimNO <sub>3</sub>	0.14–0.17	4.67–22.42	298.15	(Mokhtarani et al., 2016)
Ethylbenzene + <i>n</i> -heptane		0.14–0.25	5.89–40.2		

To compare ILs' and DESs' extraction capabilities, the consideration was only given to the systems where both solvents were applied for the same operating conditions. As a result, this restriction allowed the comparison only for three cases, i.e. benzene–*n*-hexane (Figure 2.17), toluene–heptane (Figure 2.18) and thiophene–heptane (Figure 2.19). The selectivity in these figures is plotted against the distribution ratio for each specific solvent with the size of the circle being proportional to the performance index. For fair comparison, the analysis was limited for solute mole fraction in the range of (0 ~ 0.2).



**Figure 2.17: Comparative performance of ILs and DESs in the separation of benzene–*n*-hexane**

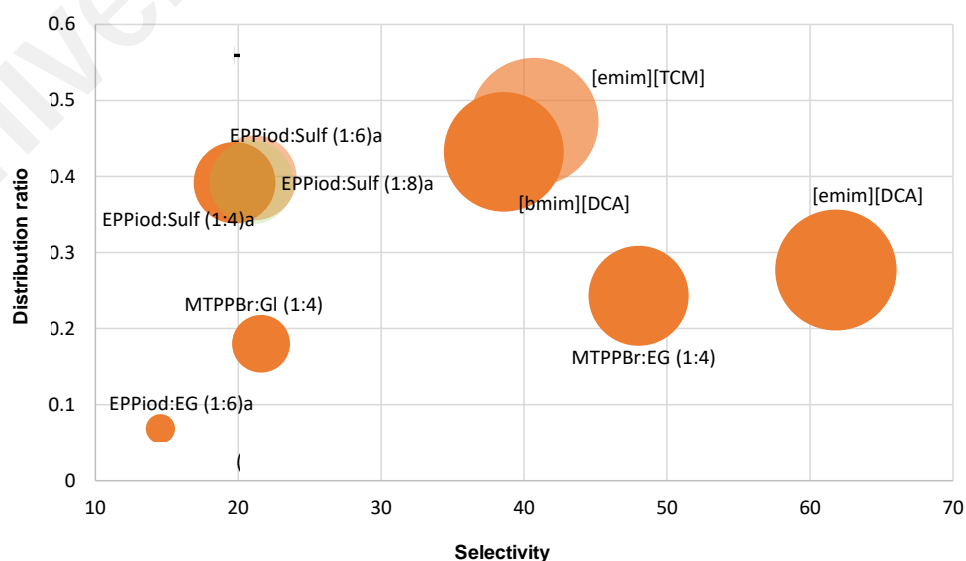


**Figure 2.18: Comparative performance of ILs and DESs in the separation of toluene–heptane**

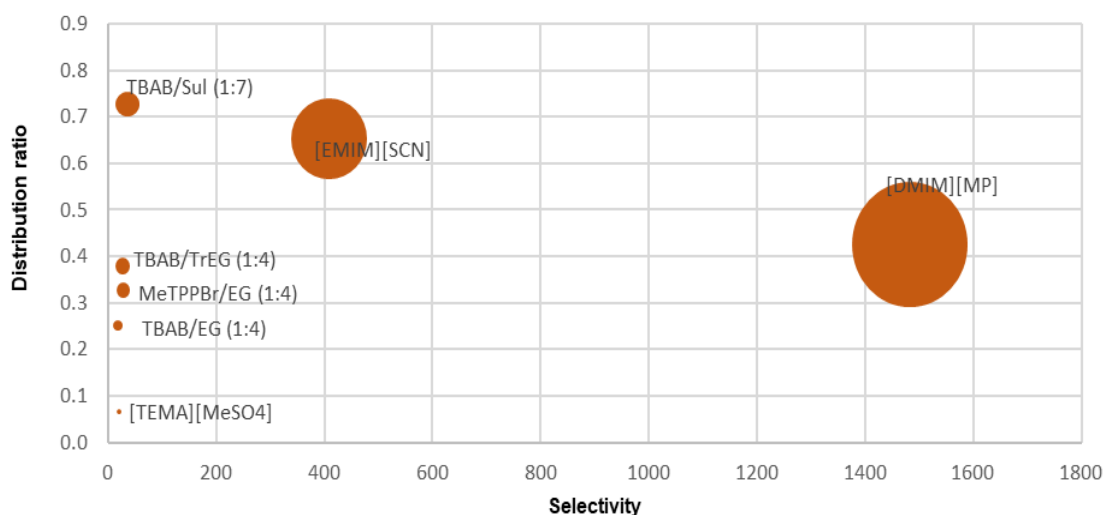


**Figure 2.19: Comparative performance of ILs and DESs in the separation of thiophene–heptane**

As seen in Figure 2.17, MTPPBr:EG (1:6) gave the largest performance index but lower selectivity. In contrast, TEACl:EG (1:2) has the second largest PI but with selectivity being higher than that using MTPPBr:EG (1:6). The DESs rather showed similar size of performance index that were much lower than those in ILs. In Figure 2.18, although C<sub>2</sub>mimTCM possess the maximum PI, other ILs such C<sub>4</sub>mimN(CN)<sub>2</sub> and C<sub>4</sub>mimN(CN)<sub>2</sub> showed reasonable separation efficiency. In addition, extractive performance of ILs/DES in toluene–heptane was relatively lower than those in benzene–*n*-hexane and thiophene–*n*-heptane. It is obvious in Figure 2.19 that C<sub>1</sub>mimMePO<sub>4</sub> offered the best performance index with a very distinguished selectivity factor.

In conclusion, it can be observed as a general remark from all the three figures, that ILs outperformed DESs for the separation of aromatic and aliphatic compounds. This is contributed by all means of extraction performance, i.e., distribution ratio, selectivity and performance index. Only TBABr:Sulf (1:7) showed a slight exception, where the distribution ratio was higher than both ILs.

## 2.5 COSMO-RS programme

### 2.5.1 COSMO-RS theory

COSMO-RS (Conductor-like Screening Model for Real Solvent) has attracted much attention and gained great influence in research activity due to its ability to describe thermodynamic properties and behaviour of ILs (Klamt, 2005). It is a model which combines two methods, i.e. (i) quantum chemical considerations in the form of a conductor-like-screening tool, and (ii) statistical thermodynamics. This enables the determination and prediction of thermodynamic properties without requiring experimental data.

In COSMO module, the solute molecule is placed inside a cavity in a dielectric continuum medium, which in this theory, is viewed as the solvent. Consequently, a cavity is formed in the midst of a perfect conductor with some specific atomic dimensions. The molecule's inherent moments then draw charges from the surroundings to the surface of the cavity to cancel the resulting electric field within the conductor. The charge induced at the surface is then calculated and termed as the screening charge. This creates the formation of local screening charge density ( $\sigma$ ), which describes the induced charge on the surface of the molecule if the molecule is embedded in a perfect conductor. A brief illustration of conductor like screening model is represented in Figure 2.20 (Klamt, 2005).

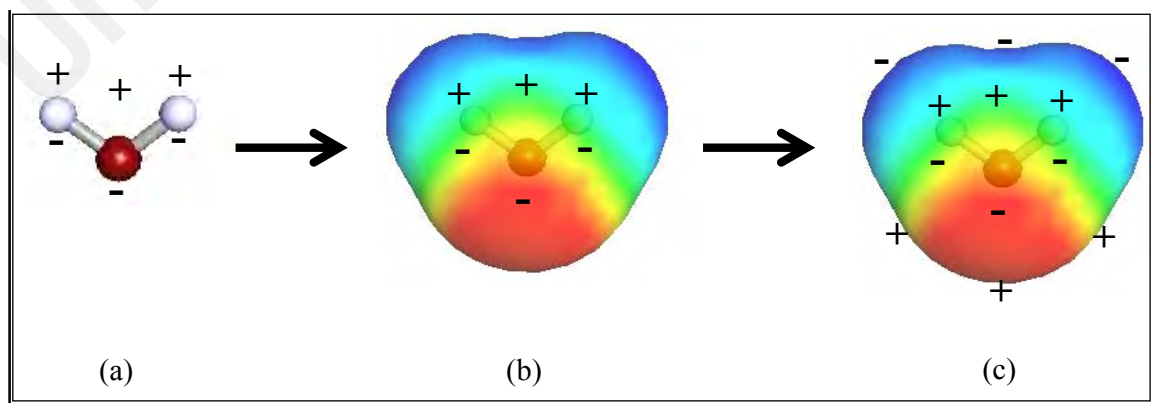


**Figure 2.20: Conductor like screening model process: (a) a water molecule in its original form, (b) the molecule inside a molecular shape cavity in a continuum medium, (c) screening charges on the cavity surface.**

As the energy from the solute electron density and geometry is optimized, the molecule is then converged into an optimal state inside a conductor, which is regarded as the reference point for the subsequent COSMO-RS calculations. The resulting energies, geometries, and screening charge densities are saved inside a specific compilation format, known as the cosmo file. The electrostatic misfit and hydrogen bonding are the main interaction energies being calculated in COSMO-RS.

The activity coefficient of any component in the mixture is calculated by Eq. 2.1:

$$\gamma_S^X = \exp\left\{\frac{\mu_S^X - \mu_X^X}{RT}\right\} \quad \text{Eq. 2.1}$$

where  $\mu_X^X$  is the chemical potential of compound X in the reference state of the pure compound.  $\mu_S^X$  is the chemical potential of compound X in the system S which can be calculated by integration of  $\mu_s(\delta)$  over the surface of the compound, as shown in Eq. 2.2.

$$\mu_S^X = \mu_{C,S}^X + \int \rho^X \mu_s(\delta) d\delta \quad \text{Eq. 2.2}$$

where  $\mu_{C,S}^X$  is the combinatorial term to take into account the size and shape differences of the molecules in the system. The chemical potential of the surface segments  $\mu_s(\delta)$  is calculated by Eq. 2.3:

$$\mu_s(\delta) = -\frac{RT}{\alpha_{eff}} \ln \left[ \int \rho_s(\delta') \exp\left(\frac{1}{RT(\alpha_{eff}\mu_s(\delta') - E_{misfit}(\delta, \delta') - E_{hb}(\delta, \delta'))}\right) \right] \quad \text{Eq. 2.3}$$

This set of COSMO-RS equations gives the chemical potential of all components in a mixture, which enables the estimation of several thermodynamic properties, such as activity coefficients, selectivities, distribution ratios and phase equilibria. The detailed derivations have been described by the developers elsewhere (Klamt, 2005; Klamt & Eckert, 2000), where the main resulting equations applied in COSMO-RS and their constants are summarized in Table 2.11.

**Table 2.11: Equations and constants in COSMO-RS**

Measurement	Mathematical expressions
Electrostatic misfit energy	$E_{misfit}(\sigma, \sigma') = \alpha_{eff} \frac{\alpha'}{2} (\sigma + \sigma')^2$
Hydrogen Bond interaction energy	$E_{hb} = \alpha_{eff} c_{hb} \min(0, \sigma\sigma' + \sigma_{hb}^2)$
Van Der Waals interaction energy	$E_{vdw} = \alpha_{eff} (\tau_{vdw} + \tau'_{vdw})$
Chemical potential of a segment	$\mu_s(\sigma) = -RT \ln \left[ \int d\sigma' p_s(\sigma) \times \exp \left\{ -\frac{1}{2} \alpha' (\sigma + \sigma')^2 - \mu_s(\sigma') / RT \right\} \right]$
Activity coefficient of a segment	$\ln \gamma_s(\sigma) = -\ln \left[ \int d\sigma' p_s(\sigma) \gamma_s(\sigma') \times \exp \left\{ \frac{-\alpha_{eff} e(\sigma, \sigma')}{RT} \right\} \right]$
Activity coefficient of a solute $i$ in an ensemble S	$\ln \gamma_{i/S}(\sigma) = \ln \gamma_{i/S}^{res} + \ln \gamma_{i/S}^{comb}$
Residual activity coefficient	$\ln \gamma_{i/S}^{res}(\sigma) = -n_i \left[ \int d\sigma' p_i(\sigma) \{ \ln \gamma_s(\sigma') - \gamma_i(\sigma') \} \right] + \ln \gamma_{i/S}^{comb}$
	$\ln \gamma_{i/S}^{comb} = \ln \frac{\phi_i}{x_i} + \frac{z}{2} q_i \ln \frac{\theta_i}{\phi_i} + l_i - \frac{\phi_i}{x_i} \sum x_j l_j$
Combinatorial activity coefficient	$\theta_i = \frac{x_i q_i}{\sum_j x_j q_j} \quad \phi_i = \frac{x_i r_i}{\sum_j x_j r_j} \quad l_i = \frac{z}{2} ((r_i - q_i) - (r_i - 1))$
$\sigma$ -profile of a mixture	$p_s(\sigma) = \sum_{i \in S} x_i p^{x_i}(\sigma)$
Constants	
$\alpha'$	General constant
$\alpha_{eff}$	Effective contact area
$c_{hb}$	Interaction strength coefficient
$\sigma_{hb}$	Polarization charge density threshold for hydrogen bond
$\tau_{vdw}$	Element-specific parameter for dispersion coefficient

### 2.5.2 Highlights on application of COSMO-RS in separation processes

COSMO-RS has been widely used to predict the thermodynamic behavior of molecular species in many field of applications. This section highlights only two prediction fields that are related to this study, namely, activity coefficients at infinite dilution and liquid–liquid equilibria.

### 2.5.2.1 Activity coefficients at infinite dilution

Activity coefficient at infinite dilution ( $\gamma^\infty$ ) is a useful measurement for the selection of solvent to be used in extractive distillation process. The value of  $\gamma^\infty$  describes the thermodynamic behavior of the solute that is fully surrounded by solvent molecules. In the case of IL as a solvent, the value of  $\gamma^\infty$  is strongly related to the affinity of solute towards the IL resulting from the competition of molecular interactions between IL-solute and IL-IL. Meanwhile, the solute-solute interaction has been negligible because at infinite dilution, the amount of solvent (IL) is considered as too large. Therefore, the difference in  $\gamma^\infty$  for a pair of solute is associated with the selectivity of IL to achieve the separation.

The activity coefficient at infinite dilution can be measured by several experimental methods such as the traditional gas-liquid chromatography (GLC) (Gruber et al., 1997). In this method, the liquid is effectively spread out in a gas chromatography column over a very small depth, implying a very large surface to volume ratio. In addition, activity coefficients at infinite dilution can also be measured by the stripping technique (Lerol et al., 1977). The stripping technique is based on the analysis of solute elution with time, in which, the solute is stripped from the solution by a constant flow of inert gas. Both methods can be considered as fast and reliable way to measure activity coefficient at infinite dilution. However, regardless of their advantages of being fast and accurate, it is still impractical to experimentally measure the values of  $\gamma^\infty$  for a pool of ILs. The measurements would be limited by the substantial cost, time and energy required, as the ILs are commonly expensive and there is a huge number of ILs available. This restriction supports the necessity to measure  $\gamma^\infty$  computationally, in which COSMO-RS has been proven as a reliable method.

For the solvent screening using COSMO-RS, the prediction of  $\gamma^\infty$  for solutes in solvents is much faster, cheaper and easier than the experimental methods. Moreover,

unlike the traditional Group Contribution Methods (GCMs), COSMO-RS is independent on the availability of group interaction parameters, making it a less-hassle alternative. The only limitation of COSMO-RS is the availability of individual component parameters which includes the conformer properties, energy convergence and molecular convergence.

Several works have been performed to investigate the accuracy of COSMO-RS in predicting the  $\gamma^\infty$  values in various solute-solvent mixture. Putnam et al (2003) compared the accuracy of COSMO-RS with two of the traditional GCMs, i.e. UNIFAC and Modified UNIFAC by calculating  $\gamma^\infty$  for over 400 binary systems involving organic solutes and water. The results proved that COSMO-RS constantly gave good estimations for most of the mixtures tested (Putnam et al., 2003). This result can be well expected because COSMO-RS was initially developed for neutral solvents.

Later, the first attempt of using COSMO-RS for prediction of  $\gamma^\infty$  involving ILs was done by the team of COSMO-RS developer, where the  $\ln \gamma^\infty$  for 38 organic compounds in three ILs were calculated. The RMSD were 0.524 ( $C_4\text{mpyBF}_4$ ), 0.426 ( $C_2\text{mimTf}_2\text{N}$ ) and 0.278 ( $C_1\text{eimTf}_2\text{N}$ ), indicating good agreement between COSMO-RS prediction and experimental data (Diedenhofen, Eckert, & Klamt, 2003). Banerjee et al (2006) used COSMO-RS to predict  $\gamma^\infty$  of common organic compounds in three trihexyl-tetradecyl-phosphonium (THTDPh) based ILs. The absolute average deviation (AAD) for each ILs were 9% (THTDPh-Cl), 8% (THTDPh- $\text{BF}_4$ ) and 16% (THTDPh- $\text{Tf}_2\text{N}$ ) (Banerjee & Khanna, 2006). Most of the results supported the feasibility of COSMO-RS as an assisting qualitative tool, which is greatly useful for fast solvent screening.

A comprehensive review has been recently reported by Paduszynski (2017) who evaluated the COSMO-RS in predicting the activity coefficient at infinite dilution of molecular solutes in ILs. The predicted data was compared with the experimental data

pool gathered from 41868 data points, 233 ILs and 150 solutes. An impact of chemical family of both IL and molecular solute on the accuracy of COSMO-RS predictions was qualitatively and quantitatively analyzed. Interestingly, the qualitative trends of  $\gamma^\infty$  as a function of chemical structure of ILs were observed to be related (Paduszynski, 2017).

Apart from the fundamental understanding of behavior of ILs at molecular level, the value of  $\gamma^\infty$  can also be extended into other derived properties. Paduszynski (2017) extended the  $\gamma^\infty$  values into two additional derived properties, namely infinite dilution partial excess enthalpy ( $\Delta H^{E,\infty}$ ) and infinite dilution selectivity ( $S^\infty$ ). It was observed that nearly 70 % of all data sets were qualitatively correct in the prediction of ( $\Delta H^{E,\infty}$ ). In contrast, the predictions of  $S^\infty$  showed large deviations, indicating the need of special treatment of representing the molecules prior to using COSMO-RS for the given separation problem (Paduszynski, 2017). Kurnia et al. (2014) extended the  $\gamma^\infty$  measurements as a factor to design cation and anion to form three IL with enhanced capacity of water absorption. The strong basic anions combined with a cation that possesses weak cation–anion hydrogen bonding interaction was found to dramatically increase the affinity toward water molecules (Kurnia, Pinho, & Coutinho, 2014). Lotfi et al. (2017) extended the  $\ln \gamma$  values to predict the solubility of a sparingly soluble drug known as acyclovir (ACV) in a wide variety of ILs. Good qualitative agreement was observed between the predicted solubility and the experimental results. In addition, the dissolution ability of ILs towards ACV was found to be controlled by its anion, indicating a potential of discovering many new ILs for dissolving sparingly soluble drug molecules (Lotfi et al., 2017).

### 2.5.2.2 The use of COSMO-RS to predict liquid–liquid phase equilibria involving ILs and DESs

LLE data is essential to understand the mutual solubilities between the species involved during the extraction process. To perform the liquid–liquid extraction process at industrial scale, LLE data is critically needed for the design and optimization of extraction column. The acquisition of complete phase equilibria through experimental measurement is impractical as it requires endless commitment of cost, energy and time. A more efficient way is by forecasting a general picture of LLE phase equilibria, which is commonly done by ruling the phase behavior and developing the predictive model. This is the main reason in justifying the massive amount of experimental effort being put to measure the LLE data in many liquid–liquid extraction processes since the last decades.

Ferreira et al. (2011 & 2012) has demonstrated a comprehensive overview of COSMO-RS performance in predicting the LLE involving ILs in two scenarios: binary systems of IL with hydrocarbon (Ferreira et al., 2011), and ternary systems of ILs with aromatic and aliphatic hydrocarbons (Ferreira et al., 2012). In binary systems, most of the results proved the ability of COSMO-RS to correctly describe the experimental trends for the binary mixture of ILs with hydrocarbons (*n*-hexane, cyclohexane, benzene), alkanes (from pentane to decane), aromatics (benzene, alkylsubstituted benzenes, and xylene isomers), and cycloalkanes (cyclohexane and cyclopentane). This has successfully enabled the qualitative analysis of molecular factors that affect the solubility, for instance, the alkyl length of cations or anions (Ferreira et al., 2011). Similarly, in ternary systems, COSMO-RS prediction showed good agreement with experimental data in generating tie-lines of ternary LLE diagrams involving numerous ILs (formed by 22 cations and 20 anions), aromatic hydrocarbons (benzene, toluene, ethylbenzene, propylbenzene, butylbenzene, *o*-xylene, *m*-xylene) and aliphatic hydrocarbons (from *n*-hexane to hexadecane, cyclohexane, methylcyclohexane, and cyclooctane) (Ferreira et al., 2012).

Wlazlo et al. (2016) recently made comparison between the COSMO-RS predictions and experimental data for ternary LLE of 13 ternary systems of IL–methanol–heptane, IL–thiophene–heptane and IL–benzothiophene–heptane. This work revealed that the prediction of LLE using COSMO-RS can be limited by the overestimation and underestimation of the measured values. This was reflected by discrepancies and failure of prediction in some ternary systems, where the IL–thiophene/benzothiophene–heptane system being the most inaccurate (Wlazło et al., 2016).

Despite the limitation case mentioned above, COSMO-RS still remains an acceptable and widely used method by researchers until the present day, where the most regular purpose is for the *a priori* solvent screening. This is supported by extensive use of COSMO-RS in predicting the LLE data for ternary systems involved in three major separation issues in industry, i.e. desulfurization of fuel (Anantharaj & Banerjee, 2013; Ferreira et al., 2014; Song et al., 2016), separation of aromatic and aliphatic hydrocarbons (Domínguez et al., 2014; Manohar et al., 2013; Potdar, Anantharaj, & Banerjee, 2012), and denitrogenation of fuels (Hizaddin et al., 2015; Salleh et al., 2017a; Verdía et al., 2017).

Apart from ILs, COSMO-RS was also recently used to study the phase behavior of ternary systems involving DESs. Following the discovery of DESs in 2003 (Abbott et al., 2003), researchers has gained great advantage of using COSMO-RS to investigate the new properties and new potential of DESs in many application fields.

Gouveia et al. (2016) used COSMO-RS as an assistive tool to investigate the potential of levulinic acid-based DESs (with choline chloride, ChCl; benzylcholine chloride, BzChCl, and tetrabutylammonium chloride, N<sub>4444</sub>Cl as the salts) to function as azeotrope breakers. COSMO-RS was found as capable to quantitatively predict the LLE phase behavior, tie-lines, distribution ratio and selectivity in ternary systems studied.

Interestingly, the RMSD values for each system were very low, i.e., 3.9 % ([N<sub>4444</sub>]Cl:LA), 0.9% (ChCl:LA) and 0.6% (BzChCl:LA) (Gouveia et al., 2016). Hadj-kali et al. (2017) recently reviewed and concluded the feasibility of using COSMO-RS to predict ternary LLE diagrams for various types of aromatic–aliphatic separations (Hadj-Kali et al., 2017).

Mulyono et al. (2014) used COSMO-RS to predict the ternary tie-lines for ternary systems involving TBABr:Sulf DES + benzene/toluene/ethylbenzene/xylene + *n*-octane. Although the RMSD values were considerably high (6.5–12.7 %), qualitative agreement of tie lines, aromatic distribution ratio and selectivity was constantly observed between experimental results and the COSMO-RS data (Mulyono et al., 2014). In the field of fuel denitrogenation using DESs, COSMO-RS was used by Hizaddin et al. (2014) to predict the ternary tie lines for the ternary systems ethylbenzene + *n*-octane + (tetrabutylammonium-based DESs with pyridine, or ethylene glycol, or mixture of both). From the five ternary systems studied, the average RMSD between COSMO-RS and experimental data was only 3.7% (Hizaddin et al., 2014). These results strongly supported the capability of COSMO-RS in predicting phase equilibria involving DESs.

It is important to study the accuracy of COSMO-RS to predict the LLE involving DESs, as DESs are the new generation of solvents that require careful molecular representation. From literature survey, it was observed that although the reported ternary systems were supported by the thermodynamic correlations such as NRTL, most of them scarcely included the prediction of tie lines using COSMO-RS. Therefore, considering COSMO-RS as a priori approach, the reliability of COSMO-RS prediction has to be examined solely based on the reported experimental data in literature. The prediction of COSMO-RS tie lines was conducted by taking one feed composition that lies on the tie lines, knowing that any points on the line will give similar molar concentration of each species in both phases at equilibrium. Table 2.12 showed the RMSD between

experimental and COSMO-RS data for separation of aromatic–aliphatic mixtures using DESs. The graphical plots of these predictions are available in Appendix A. The average RMSD in the studied ternary systems was 3.73. This demonstrated the accuracy of COSMO-RS in predicting phase equilibria involving DESs.

**Table 2.12: The RMSD value between the experimental and COSMO-RS data for separation of aromatic–aliphatic mixtures using DESs**

<b>Ternary systems</b>	<b>T (K)</b>	<b>Reference</b>	<b>RMSD (%)</b>
<i>n</i> -Hexane + benzene + TBACl:EG (1:2)	298.2	(Rodriguez et al., 2017)	5.50
<i>n</i> -Hexane + benzene + TEACl:EG (1:2)	298.2	(Rodriguez et al., 2017)	6.63
<i>n</i> -Hexane + benzene + THACl:EG (1:2)	298.2	(Rodriguez et al., 2017)	4.20
<i>n</i> -Hexane + benzene + TMACl:Gly (1:2)	298.2	(Rodriguez et al., 2017)	6.91
<i>n</i> -Hexane + benzene + TEACl:Gly (1:2)	298.2	(Rodriguez et al., 2017)	8.08
<i>n</i> -Hexane + benzene + THACl:Gly (1:2)	298.2	(Rodriguez et al., 2017)	3.85
<i>n</i> -Hexane + benzene + ChCl:LA (1:2)	298.15	(Gonzalez et al., 2013)	1.62
<i>n</i> -Hexane + benzene + ChCl:LA (1:2)	308.15	(Gonzalez et al., 2013)	5.34
<i>n</i> -Hexane + benzene + ChCl:LA (1:2)	318.15	(Gonzalez et al., 2013)	5.78
<i>n</i> -Hexane + benzene ChCl:Gly (1:2)	298.15	(Gonzalez et al., 2013)	2.21
<i>n</i> -Heptane + toluene + ETPPI:EG (1:6)	333.15	(Kareem et al., 2013)	1.42
<i>n</i> -Heptane + toluene + ETPPI:EG (1:8)	333.15	(Kareem et al., 2013)	1.33
<i>n</i> -Heptane + toluene + ETPPI:EG (1:10)	333.15	(Kareem et al., 2013)	1.69
<i>n</i> -Heptane + toluene + ETPPI:Sulf (1:4)	333.15	(Kareem et al., 2013)	3.20
<i>n</i> -Heptane + toluene + ETPPI:EG (1:6)	333.15	(Kareem et al., 2013)	2.97
<i>n</i> -Heptane + toluene + ETPPI:EG (1:8)	333.15	(Kareem et al., 2013)	2.27

**Table 2.12, continued**

<b>Ternary systems</b>	<b>T (K)</b>	<b>Reference</b>	<b>RMSD (%)</b>
<i>n</i> -Heptane + toluene + MTPPBr:EG (1:4)	308.15	(Naik et al., 2016)	1.24
<i>n</i> -Heptane + quinoline + MTPPBr:EG (1:4)	308.15	(Naik et al., 2016)	8.83
<i>n</i> -Heptane + toluene + MTPPBr:Gly (1:4)	308.15	(Naik et al., 2016)	1.89
<i>n</i> -Heptane + quinoline + MTPPBr:Gly (1:4)	308.15	(Naik et al., 2016)	9.91
<i>n</i> -Hexane + benzene + THABr:EG (1:2)	298.15	(Rodriguez, Requejo, & Kroon, 2015)	1.91
<i>n</i> -Hexane + benzene + THABr:EG (1:2)	308.15	(Rodriguez, Requejo, & Kroon, 2015)	1.23
<i>n</i> -Hexane + benzene + THABr:Gly (1:2)	298.15	(Rodriguez, Requejo, & Kroon, 2015)	2.02
<i>n</i> -Hexane + benzene + THABr:Gly (1:2)	308.15	(Rodriguez, Requejo, & Kroon, 2015)	1.58
<i>n</i> -Hexane + benzene + ChCl:Glu (1:1)	298.15	(Gouveia et al., 2016)	1.07
<i>n</i> -Hexane + toluene + ChCl:Glu (1:1)	298.15	(Gouveia et al., 2016)	0.93
<i>n</i> -Hexane + benzene + MTPPBr:TEG (1:4)	300.15	(M. Kareem et al., 2012)	7.12

## **2.6 The potential of modifying the solvent as a binary mixture**

### **2.6.1 Overview of solvent binary mixture**

In liquid-liquid extraction process, it is ideal to use an extracting solvent that gathers high values for both selectivity and distribution ratio. Nevertheless, it is nearly impossible to achieve this by using a single solvent. Numerous reports found that the distribution ratio of an extracting solvent, in most cases, showed an inverse relation with the selectivity. This relation creates difficulty to obtain ILs with high values for both selectivity and distribution ratio. A contrary evaluation always presents during the solvent-screening process from either one of these properties. Therefore, the design and modification of the solvent being used is an important research gap to achieve this purpose.

Particularly for ILs, the attempt to optimize the properties of ILs for a given application can be considered as a good innovation by the researchers. In summary, three attempts have been made by research communities to obtain IL(s) with high selectivity and distribution ratio (García et al., 2012b):

- 1) searching for new and unusual ILs,
- 2) mixing with green co-solvents, and
- 3) mixing of ILs.

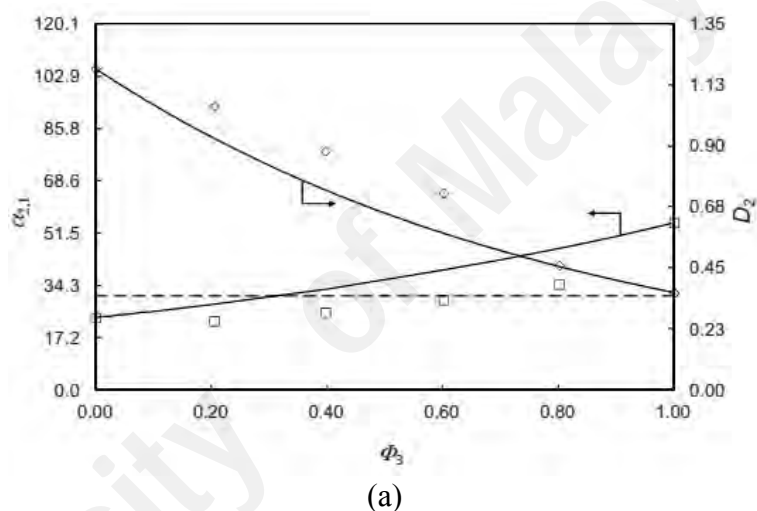
In this study, the third option is considered as a motivating option as the results of computational screening would be further developed. Solvent mixing has gained special attention in extractive separation of aromatic and aliphatic compounds. It is done by mixing one solvent possessing high aromatic/aliphatic selectivity with another solvent having high solute distribution ratio. With the objective of enhancing extraction efficiency, this technique has been investigated not just for conventional solvents but also for ILs. The mixing of organic solvents has been previously described in Section 2.4.2.1.

For the mixing of ILs, the first application was investigated in 2011 for the purpose of converting biomass (cellulose) to sustainable chemicals such as 2-(diethoxymethyl)furan, an important and useful intermediate (Long et al., 2011). Although the mixing of IL seems to be a huge step in ILs research, the progress of this technique in the separation of aromatic and aliphatic compounds was not very rapid. In fact, for the separation of benzene and cyclohexane, the mixing of ILs has never been investigated.

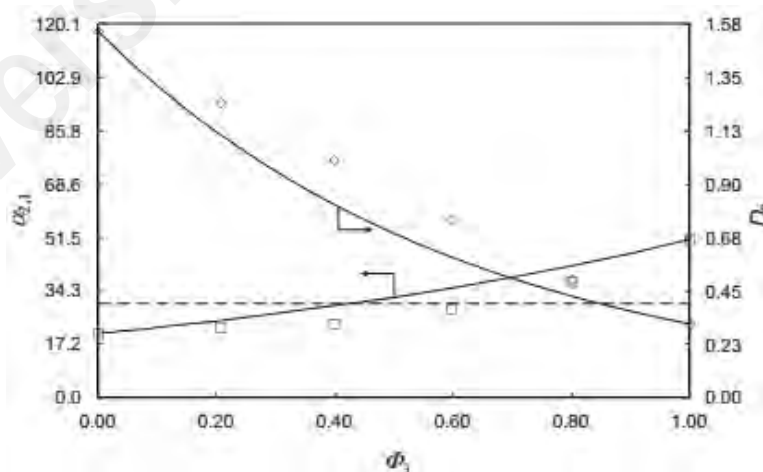
### 2.6.2 Applications of solvent binary mixture in liquid–liquid extraction

As for the separation of benzene and cyclohexane, the mixing of organic solvents was previously studied by a number of researchers involving N,N-dimethylformamide + ethylene glycol (Aspi et al., 1998), N,N-dimethylformamide + KSCN (Dong, Yang, & Zhang, 2010b; Song, Lin, & You, 2014b), and N,N-dimethylformamide + NaSCN (Dong et al., 2013a). As mentioned, the IL mixing was never investigated for the separation of benzene and cyclohexane. In contrast, good findings of using IL-IL mixture were rather reported in other aromatic–aliphatic systems. This was demonstrated by a remarkable work of mixing 1-ethyl-3-methylpyridinium bis(trifluoromethylsulfonyl)imide ( $C_2mpyrTf_2N$ ) and 1-ethyl-3-methylimidazolium dicyanamide ( $C_2mimN(CN)_2$ ) in the separation of toluene from its mixture with n-heptane, 2,3-dimethylpentane or cyclohexane (Clough et al., 2015). The same IL-IL mixture was also further investigated to separate toluene from its mixture with other hydrocarbons, namely n-hexane, n-octane and n-nonane (Larriba et al., 2013b). The results on these studies concluded that the extraction efficiency and physical properties of [IL-IL] mixture gave the intermediate values between the pure ILs. Most importantly, the [IL-IL] mixture also gave higher extractive properties than sulfolane, reflected by higher values of both selectivity and distribution ratio.

The same group of researchers also investigated other combination of [IL-IL] binary mixtures to separate toluene from n-heptane involving N-butylpyridinium bis(trifluoromethylsulfonyl)imide ( $C_4\text{pyrTf}_2\text{N}$ ), N-butylpyridinium tetrafluoroborate ( $C_4\text{pyrBF}_4$ ) and 1-butyl-4-methylpyridinium bis(trifluoromethylsulfonyl)imide ( $C_4\text{mpyrTf}_2\text{N}$ ) (García et al., 2012b, 2012d). The experimental data in this study was successfully correlated with logarithmic linear model for an ideal IL mixture. As seen in Figure 2.21, the mixture of ILs gave higher selectivity and distribution ratio when the mole fraction of  $C_4\text{pyBF}_4$  was approximately 0.7.



(a)



(b)

**Figure 2.21: Separation factors,  $\alpha$  (selectivity) and distribution ratio,  $D$  of toluene versus mole fraction of  $C_4\text{pyBF}_4$  in the mixed IL solvents ( $\phi_3$ ) for two pseudo-ternary systems: (a) n-heptane (1) + toluene (2) + ( $C_4\text{pyBF}_4$  +  $C_4\text{pyTf}_2\text{N}$ ) and (b) n-heptane (1) + toluene (2) + ( $C_4\text{pyBF}_4$  +  $C_4\text{mpyrTf}_2\text{N}$ ) at 313.15 K and atmospheric pressure (García et al., 2012b, 2012d)**

Arce et al. (2008) investigated the performance of a mutually immiscible IL system for the separation of aromatic compounds from the aliphatic/aromatic system. Mixing two ILs was found to enhance the efficiency of the extraction process. However, this would increase the complexity of separating the phases due to the formation of three phases, and the contact between the aliphatic/aromatic mixture and the IL would be small (Arce et al., 2008). Potdar et al. (2012) used different mixtures of ILs for the extraction of the aromatic compound from the aliphatic/aromatic mixture and found that the capacity of the mixed ILs was unsatisfactory (Potdar, Anantharaj, & Banerjee, 2012). As compared to a single IL, lower distribution ratio and selectivity values were achieved using the mixed IL. Larriba et al. (2014) used IL mixtures [1-ethyl-4-methylpyridinium bis-(trifluoromethylsulfonyl)imide ( $C_4mpyTf_2N$ ) and 1-ethyl-3-methylimidazolium dicyanamide ( $C_2mimN(CN)_2$ )] for the extraction of toluene from *n*-alkanes. Compared to sulfolane, the binary IL mixtures were found to provide substantially better extractive properties, particularly at lower mole fractions of toluene in the raffinate phase (Larriba et al., 2014).

Several other researchers (Navarro et al., 2016; Navarro et al., 2014, 2017) have also investigated the use of [ $C_4mpyTf_2N + C_2mimN(CN)_2$ ] mixture in the separation of aliphatic and aromatics. In addition, the mixture of IL with organic solvent has also been employed as an extractant for the separation of aromatic and aliphatic compounds. Manohar et al. used IL-acetonitrile extractant for the separation of benzene from *n*-hexane. However, high selectivities (~150) but low capacities were reported. Concerning the separation of aromatic compounds and cyclic hydrocarbon, the study using mixture of ILs is rather limited (Manohar, Banerjee, & Mohanty, 2013). Therefore, further efforts are necessary to find a promising IL mixture possessing high extraction performance that comes from the optimum value of selectivity and benzene distribution ratio.

Salem et al. (2012 ) reported the LLE data of [benzene + cyclohexane + two ILs) at different temperature and atmospheric pressure. They achieved lower distribution factor and selectivity of the IL mixture for benzene than that of pure IL (Salem, Chong, & Chun-xi, 2012). Mixture of organic solvents have also been investigated as an extractant for the separation of benzene from cyclohexane. DMF was used with different organic solvents to improve the separation efficiency of benzene (Dong et al., 2011; Dong et al., 2013b; Dong, Yang, & Zhang, 2010a; Salem, Chong, & Chun-xi, 2012; Song, Lin, & You, 2014a). For instance, DMF + potassium thiocyanate (KSCN) was employed as a potential extracting solvent for the separation of benzene and cyclohexane, where high selectivity of up to 11 was reported.

Table 2.13 summarizes the values of selectivity and distribution ratio for mixed solvents that have been reported for the separation of aromatic and aliphatic compounds.

**Table 2.13: The use of mixed solvents for the separation of aliphatic and aromatic compounds**

Binary mixture	Aromatic	Aliphatic	S range	D range	Ref.
C <sub>1</sub> mimBF <sub>4</sub> + C <sub>1</sub> mimDMP	Benzene	Cyclohexane	0.56–4.050	0.2–0.42	(Salem, Shen, & Li, 2012)
C <sub>1</sub> mimClO <sub>4</sub> + C <sub>1</sub> mimDMP			0.50–4.430	0.26–0.38	
DMF + KSCN			2.77–11.36	0.30–0.86	(Dong, Yang, & Zhang, 2010a)
DMF + NH <sub>4</sub> SCN			2.40–14.77	0.39–1.08	(Dong et al., 2011)
DMF + NaSCN			2.45–11.99	–	(Dong et al., 2013b)
C <sub>2</sub> mimEtSO <sub>4</sub> + acetonitrile	Benzene	<i>n</i> -Hexane	15.9–525.7	0.26–1.12	(Manohar, Banerjee, & Mohanty, 2013)
C <sub>2</sub> mimAc + acetonitrile			28.7–163.1	0.03–0.44	
C <sub>2</sub> mpyrTf <sub>2</sub> N + C <sub>2</sub> MIMN(CN) <sub>2</sub>	Toluene	<i>n</i> -hexane	27.7–66.60	0.27–1.04	(Larriba et al., 2014)
		<i>n</i> -octane	32.8–96.10	0.24–0.87	
		<i>n</i> -nonane	59.0–184.9	0.27–0.89	
C <sub>2</sub> mpyrTf <sub>2</sub> N + C <sub>2</sub> mimN(CN) <sub>2</sub>	Toluene	<i>n</i> -heptane	29.5–71.50	0.27–1.00	(Larriba et al., 2013c)
		2,3-Dimethylpentane	26.0–64.30	0.30–1.11	
		Cyclohexane	15.1–22.70	0.30–1.12	
C <sub>4</sub> pyrBF <sub>4</sub> + C <sub>4</sub> mpyrTf <sub>2</sub> N	Toluene	<i>n</i> -heptane	8.20–33.90	0.49–0.72	(García et al., 2012c)
C <sub>4</sub> pyrBF <sub>4</sub> + C <sub>4</sub> pyrTf <sub>2</sub> N			23.7–54.90	0.36–1.18	(García et al., 2012a)
C <sub>2</sub> mimTCM + C <sub>2</sub> mimN(CN) <sub>2</sub>			18.5–60.70	–	(González et al., 2016)

## 2.7 Outcomes of literature review

From the extensive literature review in this chapter, it is necessary to summarize the literature outcomes that can be regarded as important research gaps for the separation of benzene and cyclohexane. These outcomes are itemized as below:

1. Despite the research works carried out for over forty years, the separation of benzene and cyclohexane remains as a challenging process in petrochemical industry. It is critical to find alternative processes that can replace the conventional technologies as they are currently suffering from process complexity, high cost and high energy consumption.
2. For the production of cyclohexane through hydrogenation of benzene, the unreacted benzene in reactor effluent is normally in low concentration (<20 %). It is concluded from the literature that there is no suitable separation technology available for this aromatic concentration. Therefore, developing a new separation technology will provide significant contributions in meeting the demand of pure cyclohexane through efficient separation of benzene and cyclohexane mixture.
3. Liquid–liquid extraction is an interesting process for low concentration of aromatic compound. However, it is important to find feasible solvents as the organic solvents are volatile, toxic and flammable. ILs and DESs appear as the emerging solvents which demonstrated good potential in many applications. However, it is observed from the literature that only a few studies were conducted for the separation of benzene and cyclohexane using ILs. Moreover, the separation of benzene and cyclohexane using DESs was never studied at all.
4. In the previous works, the selected solvents (organic solvents or ILs) were usually used as a pure compound and their respective performances have been determined. Despite the reported performance of each solvent, efforts to enhance the extractive efficiency in each ternary system were hardly seen.

## CHAPTER 3: METHODOLOGY

The following methodologies were adopted to fulfil the research objectives:

- Part 1: Screening and selection of potential ILs and DESs using COSMO-RS program.  
The activity coefficient at infinite dilution ( $\gamma^\infty$ ) for each IL and DES with respect to the benzene and cyclohexane was predicted using COSMO-RS program. The values of  $\gamma^\infty$  were then used to calculate the capacity, selectivity and performance index at infinite dilution.
- Part 2: Liquid-liquid extraction experiments  
In order to generate the ternary phase equilibria of the ternary systems involving the selected ILs/DESs, benzene, and cyclohexane, liquid-liquid extractions for the separation of benzene and cyclohexane were conducted at 25 °C and under 1 atm. The results from these experiments were analyzed to validate the COSMO-RS screening results, thus evaluating the actual performance of the selected ILs and DESs. The results were also used to regress the NRTL model parameters of the ternary LLE systems to be used in process simulation and assess the industrial feasibility.
- Part 3: Improvement of extraction efficiency through solvent binary mixing  
The ILs were firstly ranked according to the experimental selectivity and distribution ratio. This ranking was used to produce a series of binary IL-IL pairs at optimized ratio, which aims to enhance the overall extraction efficiency.

In this chapter, each of these parts is described in detail.

### 3.1 Part 1: COSMO-RS prediction

#### 3.1.1 Generation of COSMO-files

The geometry optimisation of all species involved in this study was performed using the Turbomole programme package. The chemical structure of the target molecule was drawn first. Afterward, the geometry optimisation was performed at the Hartree–Fock level and 6-31G\* basis set. In order to use COSMO-RS as a screening tool, it is necessary to generate the *.cosmo* files of all components involved. The *.cosmo* file of a molecule contains information on the screening charge density ( $\sigma$ ) of the segmented molecule in a virtual conductor environment. The generation of *.cosmo* file was conducted through a single-point calculation by using density functional theory (DFT) with Becke–Perdew and the Triple- $\zeta$  Zeta Valence Potential (TZVP) basis set. Finally, the *.cosmo files* were exported to the COSMOthermX programme with the parameterisation BP\_TZVP\_C30\_1301.ctd.

#### 3.1.2 Molecular representation in COSMOthermX

The representation of ILs or DESs can be performed by adopting one of the three methods: (i) the metafile approach, (ii) the ion pair approach, and (iii) the electroneutral approach (Diedenhofen & Klamt, 2010). In metafile approach, ions are treated separately in the quantum chemistry COSMO calculations. The results of COSMO calculations of the cations and anions are combined into one file, known as meta-file. For the ion-pair approach, the COSMO-optimized structure of the ion-pair (cation-anion) is used. In electroneutral approach, the ILs or DESs are considered as completely dissociated ions (cation and anion) as separate molecules with respect to their mole ratio.

In this study, the electroneutral approach was adopted because it is the most appropriate and nearest to the actual nature of ILs or DESs. For ILs, the ions are treated as two different compounds in an equimolar mixture. For DESs, this approach was

considered according to the mole composition of their constituents. In liquid form, the constituents of DESs can be viewed as three distinct species, i.e. salt cation, salt anion and HBD. For instance, a DES with a salt:HBD molar ratio of 1: $n$  is represented by 1 mole of salt cation, 1 mole of salt anion and  $n$  mole of HBD. Compared to the representation of IL in COSMOthermX as 1:1 for its cation:anion ratio, the DES is represented as 1:1: $n$  for its cation:anion:HBD ratio.

### 3.1.3 Screening of DESs

The DESs studied in previous works involving different applications were collected from literature and shortlisted in Table 3.1, where they were reported liquids at  $T < 100$  °C. Since a single DES is composed of more than one molecule, employing its representation method in the COSMOtherm-X programme is crucial.

**Table 3.1: List of the selected DESs for COSMO-RS screening**

<b>No</b>	<b>Salt</b>	<b>HBD</b>	<b>Salt:HBD</b>	<b>Abbv.</b>
1	Choline tetrafluoroborate	Urea	1:2	ChBF <sub>4</sub> :Ur
2	Choline chloride	1, methyl urea	1:2	ChCl:MUr
3	Choline chloride	Acetamide	1:2	ChCl:Ac
4	Choline chloride	Tetramethyl urea	1:2	ChCl:TMUr
5	Choline chloride	Thio urea	1:2	ChCl:TUr
6	Choline chloride	Urea	1:2	ChCl:Ur
7	Choline chloride	Ethylene glycol	1:2	ChCl:EG
8	Choline chloride	Glycerol	1:1	ChCl:Gly
9	Choline chloride	Malonic acid	1:1	ChCl:MA
10	Choline chloride	Oxalic acid	1:1	ChCl:OA
11	Choline chloride	Phenylacetic acid	1:1	ChCl:PAC
12	Choline chloride	Phenylpropionic acid	1:1	ChCl:PPA
13	Choline chloride	Levulinic acid	1:2	ChCl:LA
14	Choline chloride	Itaconic acid	1:1	ChCl:IA
15	Choline chloride	Xylitol	1:1	ChCl:Xy
16	Choline chloride	D-sorbitol	1:1	ChCl:Sor
17	Choline chloride	D-isosorbide	1:2	ChCl:Iso
18	Choline chloride	Glucose	1:1	ChCl:Glu

**Table 3.1, continued**

<b>No</b>	<b>Salt</b>	<b>HBD</b>	<b>Salt:HBD</b>	<b>Abbv.</b>
19	Choline chloride	Triethylene glycol	1:4	ChCl:TEG
20	Choline nitrate	Urea	1:2	ChNO <sub>3</sub> :Ur
21	Methyltriphenylphosphonium bromide	Glycerol	1:2	MTPPBr:Gly
22	Methyltriphenylphosphonium bromide	Ethylene glycol	1:3	MTPPBr:EG
23	Methyltriphenylphosphonium bromide	1,2 Propanediol	1:4	MTPPBr:PD
24	Methyltriphenylphosphonium bromide	Tetraethylene glycol	1:4	MTPPBr:TEG
25	Benzyltriphenylphosphonium bromide	Glycerol	1:5	BTPPBr:Gly
26	Benzyltriphenylphosphonium bromide	Ethylene glycol	1:3	BTPPBr:EG
27	Benzyltriphenylphosphonium bromide	2,2,2- trifluoroacetamide	1:1	BTPPBr:TFA
28	N,N- diethylenethanolammonium chloride	Glycerol	1:2	DEEACl:Gly
29	N,N- diethylenethanolammonium chloride	Ethylene glycol	1:2	DEEACl:EG
30	N,N- diethylenethanolammonium chloride	2,2,2- trifluoroacetamide	1:2	DEEACl:TFA
31	Tetrabutylammonium bromide	Glycerol	1:4	TBABr:Gly
32	Tetrabutylammonium bromide	1,2 Propanediol	1:3	TBABr:PD
33	Tetrabutylammonium bromide	Sulfolane	1:7	TBABr:Sulf
34	Tetrabutylammonium bromide	Triethylene glycol	1:4	TBABr:TEG
35	Tetrabutylammonium chloride	Triethylene glycol	1:2	TBACl:TEG
36	Tetrabutylammonium chloride	Ethylene glycol	1:2	TBACl:EG

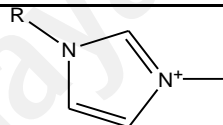
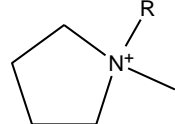
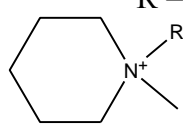
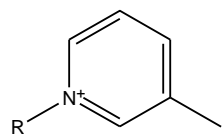
**Table 3.1, continued**

<b>No</b>	<b>Salt</b>	<b>HBD</b>	<b>Salt:HBD</b>	<b>Abbv.</b>
37	Tetrabutylammonium chloride	Glycerol	1:2	TBACl:Gly
38	Tetrabutylammonium chloride	Malonic acid	1:2	TBACl:MA
39	Tetramethylammonium chloride	Glycerol	1:2	TMACl:Gly
40	Tetramethylammonium chloride	Ethylene glycol	1:2	TMACl:EG

### 3.1.4 Screening of ILs

For the selection of cation, 4 types of cyclic cations were chosen: imidazolium, pyridinium, piperidinium and pyrrolidinium. As shown in Table 3.2, each of these cations was expanded into four kinds of methyl-alkyl group to study the effect of cation alkyl length. Meanwhile for the anion, 13 common and less complicated anions were shortlisted in Table 3.3.

**Table 3.2: List of cations for the screening of ILs**

No	Cation name	Abbreviation	Chemical structure
1	1-alkyl-3-methylimidazolium	$C_nMim^+$	 $R = 2, 4, 6, 8$
2	1-alkyl-1-methylpyrrolidinium	$C_nMpyrro^+$	 $R = 2, 4, 6, 8$
3	1-alkyl-1-methylpiperidinium	$C_nMpip^+$	 $R = 2, 4, 6, 8$
4	1-alkyl-3-methylpyridinium	$C_nMpyr^+$	 $R = 2, 4, 6, 8$

**Table 3.3: List of anions for the screening of ILs**

No	Name	Abbreviation	Chemical structure
1	Acetate	Ac <sup>-</sup>	
2	Benzoate	BzO <sup>-</sup>	
3	Tetrafluoroborate	BF <sub>4</sub> <sup>-</sup>	
4	Dicyanamide	N(CN) <sub>2</sub> <sup>-</sup>	
5	Ethylsulfate	EtSO <sub>4</sub> <sup>-</sup>	
6	Hydrogensulfate	HSO <sub>4</sub> <sup>-</sup>	
7	Nitrate	NO <sub>3</sub> <sup>-</sup>	
8	Octylsulfate	OcSO <sub>4</sub> <sup>-</sup>	
9	Hexafluoro-phosphate	PF <sub>6</sub> <sup>-</sup>	
10	Salicylate	Sal <sup>-</sup>	
11	Bis(trifluoromethyl-sulfonyl)imide	Tf <sub>2</sub> N <sup>-</sup>	
12	Thiocyanate	SCN <sup>-</sup>	
13	Methanesulfonate	MeSO <sub>3</sub> <sup>-</sup>	

### 3.1.5 The selectivity, capacity and performance index at infinite dilution

For predictions involving ILs and DESs, the electroneutral approach was adopted where the IL is assumed to undergo complete dissociation into its respective cation and anion, while the DES dissociates into its salt and hydrogen bond donors according to the molar ratio.

The activity coefficient at infinite dilution ( $\gamma^\infty$ ) was obtained from the *Chemical Potential* menu in the COSMO-RS software, where the mole fractions of benzene and cyclohexane were set to zero. The methods and calculations required to obtain activity coefficient at infinite dilution has been described in detail by its founder (Klamt, 2005). At infinite dilution, the capacity ( $C^\infty$ ) and selectivity ( $S^\infty$ ) of the IL are given by Eqs 3.1 and 3.2, respectively.

$$C^\infty = \frac{1}{\gamma_1^\infty} \quad \text{Eq. 3.1}$$

$$S^\infty = \frac{\gamma_2^\infty}{\gamma_1^\infty} \quad \text{Eq. 3.2}$$

where  $\gamma_1^\infty$  and  $\gamma_2^\infty$  are the activity coefficients at infinite dilution for benzene and cyclohexane, respectively. The performance index ( $PI$ ) of each IL or DES was calculated as a product of capacity and selectivity at infinite dilution using Eq. 3.3:

$$PI = C^\infty \times S^\infty = \left(\frac{1}{\gamma_1^\infty}\right) \times \left(\frac{\gamma_2^\infty}{\gamma_1^\infty}\right) = \left(\frac{\gamma_2^\infty}{(\gamma_1^\infty)^2}\right) \quad \text{Eq. 3.3}$$

## 3.2 Part 2: LLE experiment

### 3.2.1 Materials

The list of chemicals used in this study is given in Table 3.4 to 3.7. The ILs, DES constituents, benzene and cyclohexane were used as received without any further purification.

**Table 3.4: ILs used in the LLE experiments**

Chemical name	CAS No.	Supplier	Purity (wt %)	Abbreviation
1-ethyl-3-methylimidazolium acetate	143314-17-14	Sigma Aldrich	≥ 95.0	C <sub>2</sub> mimAc
1-ethyl-3-methylimidazolium dicyanamide	370865-89-7	Sigma Aldrich	98.0	C <sub>2</sub> mimN(CN) <sub>2</sub>
1-ethyl-3-methylimidazolium thiocyanate	331717-63-6	Merck	≥ 98.0	C <sub>2</sub> mimSCN
1-ethyl-3-methylimidazolium bis(trifluoromethylsulfonyl)imide	174899-82	Sigma Aldrich	≥ 98.0	C <sub>2</sub> mimTf <sub>2</sub> N

**Table 3.5: DES constituents involved in synthesis and LLE experiments**

Name	Formula	Supplier	Purity (wt %)	Abbreviation
Choline Chloride	67-48-1	Acros Organics	99.0	ChCl
Sulfolane	126-33-0	Acros Organics	99.0	Sulf
Triethylene glycol	112-27-6	Fluka	99.0	TEG
Methyltriphenylphosphonium bromide	1779-49-3	Acros Organics	98.0	MTPPBr
1,2 Propanediol	57-55-6	Loba Chemie	98.0	PD
Tetrabutylammonium bromide	1643-19-2	Loba Chemie	98.0	TBABr

**Table 3.6: Details of benzene and cyclohexane used in LLE experiments**

Name	CAS No.	Supplier	Purity (wt %)
Benzene	71-43-2	Merck	≥ 99.7
Cyclohexane	110-82-7	Merck	≥ 99.5

**Table 3.7: <sup>1</sup>HNMR solvents used for compositional analysis**

Name	CAS No.	Supplier	Purity (wt %)
Chloroform-D1	865-49-6	Merck	≥ 99.8 (deuteration degree)
Methanol-D4	811-98-3	Merck	≥ 99.8 (deuteration degree)

### 3.2.2 Synthesis of DESs

All DESs were prepared using the original method described by Abbott et al (2004) (Abbott et al., 2004). In this method, the salt was firstly mixed with the HBD for each DES in screw-capped bottles. Next, the bottles were stirred in an incubation shaker. Shaking was performed at a rotational speed of 200 rpm at a temperature of 90 °C until the formation of clear liquid was observed. The five DESs that were synthesized in this work are summarized in Table 3.8. To avoid any contamination, a fresh batch of DES was made for each LLE experiment. In each extraction, DES is regarded as a pseudo-pure species because it stays intact in the extract and no DES was observed in the raffinate.

**Table 3.8: DESs synthesized in this work**

Salt	HBD	Ratio	Abbreviation
Tetrabutylammonium bromide	Sulfolane	1:7	TBABr:Sulf (1:7)
Tetrabutylammonium bromide	Triethylene glycol	1:4	TBABr:TEG (1:4)
Methyltriphenylphosphonium bromide	Triethylene glycol	1:4	MTPPBr:TEG (1:4)
Methyltriphenylphosphonium bromide	1,2 Propanediol	1:4	MTPPB:PD (1:4)
Choline chloride	Triethylene glycol	1:4	ChCl:TEG (1:4)

### 3.2.3 LLE experiments

The feed mixture containing 10 wt% benzene in cyclohexane was first prepared inside a 20-mL screw-capped scintillation vial using an analytical balance with accuracy of  $\pm 0.0001$  g. This procedure was repeated for other concentrations of benzene (i.e., 20, 30, 40, 50, and 60 wt%) in the feed. Based on the binary composition, the total weight of the feed mixture was fixed at 2 g. The IL/DES was then mixed into every feed mixture in a 1:1 weight ratio. Parafilm was used to seal each vial so as to avoid component loss due to evaporation. The vials were then placed in an incubation shaker at 25 °C and 1 atm, where spring clamps were used to hold them in place while shaking. They were shaken at 200 rpm for 6 h. After stopping the mixing procedure, the mixture was left undisturbed for 12 h to reach equilibrium. This period was deemed to be sufficient based on a settling time study conducted to ensure that the equilibrium state was fully reached.

The ILs used are  $C_2mimAc$ ,  $C_2mimN(CN)_2$ ,  $C_2mimSCN$  and  $C_2mimTf_2N$  whereas the DESs used are TBABr:Sulf (1:7), TBABr:TEG (1:4), MTPPBr:TEG (1:4), MTPPBr:PD (1:4) and ChCl:TEG (1:4). A total of 15 ternary systems were investigated throughout this study, where each of the tie lines was plotted in line with the COSMO-RS prediction and the NRTL modelling.

### 3.2.4 Compositional analysis

For compositional analysis, a drop of the sample ( $\pm 0.035$  mL) was taken out from the extract and raffinate layers using a micropipette. For the extract layer, a bubble was purged from the micropipette tip to avoid cyclohexane contamination from the raffinate layer. This drop of sample was then dissolved in  $\pm 0.7$  mL of deuterated solvent placed inside an NMR tube. The sample and solvent in the tube were shaken carefully to form a homogenous mixture. To ensure homogeneity, the samples were dissolved in different solvents. Deuterated chloroform was used to dissolve all samples in the top layer and the

bottom layer of the C<sub>2</sub>mimAc system. On the other hand, the samples from the bottom layer of the C<sub>2</sub>mimN(CN)<sub>2</sub>, C<sub>2</sub>mimSCN, and C<sub>2</sub>mimTf<sub>2</sub>N systems were dissolved in deuterated methanol. Each NMR tube was tightly sealed with parafilm to avoid chemical loss. NMR 400 MHz Bruker spectrometer was used to obtain the <sup>1</sup>H NMR spectra of each component. The selected hydrogen peaks (chemical shifts in ppm) for calculation of the ternary composition are: benzene at ±7.35 (6H), cyclohexane at ±1.47 (12H), C<sub>2</sub>mimAc (3H) at 1.91, C<sub>2</sub>mimSCN (3H) at ±1.58, C<sub>2</sub>mimN(CN)<sub>2</sub> (3H) at ±1.56 and C<sub>2</sub>mimTf<sub>2</sub>N (3H) at 3.85. Eq. 3.4 was used to calculate the molar fraction of each component in both layers.

$$x_i = \frac{H_i}{\sum_{i=1}^3 H_i} \quad \text{Eq. 3.4}$$

where  $x_i$  is the concentration of a component  $i$  in mole fraction, and  $H_i$  is the peak area of a single hydrogen atom in component  $i$ .

For compositional analysis involving DESs, the samples taken from the top and bottom layers were analyzed using a high performance liquid chromatography (HPLC). Samples were diluted using acetonitrile. The HPLC Agilent 1100 series with a zorbax eclipse XDB-C8 column was used for analysis. The temperature of the column oven was set to 30 °C. The mobile phase included acetonitrile and distilled water, with a volume ratio of 3:1. The flow rate of the mobile phase was 1.4 mL min<sup>-1</sup> under a pressure of 120 bar. The uncertainty in the reported concentrations was estimated to be 0.001 wt% (10 ppm).

### 3.2.5 Experimental selectivity and distribution ratio

The distribution ratio of benzene ( $D_{Bz}$ ) and the solvent selectivity ( $S$ ) of each IL or DES were used to evaluate the extraction efficiency by employing Eqs. 3.5 and 3.6.

$$D_{Bz} = \frac{x_{Bz}^1}{x_{Bz}^2} \quad \text{Eq. 3.5}$$

$$S = \frac{x_{Bz}^1/x_{Cy}^1}{x_{Bz}^2/x_{Cy}^2} \quad \text{Eq. 3.6}$$

where  $x_{Bz}$  and  $x_{Cy}$  are the concentrations of benzene and cyclohexane, respectively. The superscripts 1 and 2 represent the extract and raffinate phase, respectively.

### 3.2.6 Consistency tests using the Othmer-Tobis and Hand correlations

For the experimental results, the consistency tests were conducted using the Hand (Hand, 1929) and the Othmer–Tobias (Othmer & Tobias, 1942) correlations. The following two correlations were used to obtain the Hand and Othmer–Tobias equations, respectively.

$$\ln \left( \frac{x_{Bz}''}{x_{Cyc}''} \right) = a + b \ln \left( \frac{x_{Bz}'}{x_{IL/DES}'} \right) \quad \text{Eq. 3.7}$$

$$\ln \left( \frac{1-x_{Cyc}'}{x_{Cyc}'} \right) = a + b \ln \left( \frac{1-x_{IL/DES}'}{x_{IL/DES}'} \right) \quad \text{Eq. 3.8}$$

where  $x_{Cyc}$ ,  $x_{Bz}$ , and  $x_{IL}$  represent the concentrations of cyclohexane, benzene and IL or DES, respectively. The superscript ' and '' refer to the extract and raffinate phases, respectively. The linearity of each plot (i.e. value of  $R^2$  close to unity) indicates excellent degree of consistency for the ternary LLE tie lines reported in this work.

### 3.2.7 Correlation of LLE data

In LLE calculations, an isothermal liquid-liquid flash is solved at a given temperature and pressure to obtain phase compositions. The flash calculation consists of Eq. 3.9 to 3.11:

$$\text{Material Balance:} \quad x_i - (1 - \omega)x_i^{L1} - \omega x_i^{L2} = 0, \quad i = 1, N_c \quad \text{Eq. 3.9}$$

$$\text{Equilibrium Equation:} \quad x_i^{L1} \gamma_i^{L1} - x_i^{L2} \gamma_i^{L2} = 0, \quad i = 1, N_c \quad \text{Eq. 3.10}$$

$$\text{Equation of Summation:} \quad \sum_i x_i^{L1} - \sum_i x_i^{L2} = 0 \quad \text{Eq. 3.11}$$

Here,  $\omega$  is the liquid–liquid splitting ratio;  $x_i$ , the amount of component  $i$  in the mixture;  $x_i^{L1}$ , the amount of component  $i$  in liquid phase  $L1$ ;  $x_i^{L2}$ , the amount of component  $i$  in liquid

phase  $L2$ ; and  $N_C$ , the number of constituents of the liquid phases. The parameters  $\gamma_i^{L1}$  and  $\gamma_i^{L2}$  are the activity coefficients of component  $i$  in  $L1$  and  $L2$ , respectively.

In this work, the activity coefficients were evaluated using the non-random two-liquid (NRTL) model (Renon & Prausnitz, 1968). This model was found to be useful for correlating the experimental LLE data of systems containing ILs without requiring any special modification. For a multicomponent system, the activity coefficient of component  $i$  is given by the general expression, shown in Eq. 3.12:

$$\ln \gamma_i = \frac{\sum_j \tau_{ji} G_{ji} x_j}{\sum_j G_{ji} x_j} + \sum_j \frac{G_{ji} x_j}{\sum_k G_{kj} x_k} \left( \tau_{ij} - \frac{\sum_k \tau_{kj} G_{kj} x_k}{\sum_k G_{kj} x_k} \right) \quad \text{Eq. 3.12}$$

with:  $\ln G_{ij} = -\alpha_{ij} \tau_{ij}$ ,  $\alpha_{ij} = \alpha_{ji}$  and  $\tau_{ii} = 0$

where  $\tau_{ij}$  and  $\tau_{ji}$  are binary interaction parameters and  $\alpha_{ij}$  is the non-randomness parameter.

The binary interaction parameters  $\tau_{ij}$  and  $\tau_{ji}$  were estimated by minimizing the root mean square deviation (RMSD) between calculated and experimental solubilities of each constituent in each phase using the Simulis<sup>®</sup> software package (Simulis<sup>®</sup> thermodynamics). The parameter  $\alpha_{ij}$  in the NRTL model measures the non-randomness in the mixture; i.e. the mixture is said to be completely random when  $\alpha_{ij}$  is zero. In this work,  $\alpha_{ij}$  was fixed equal to 0.20 for all binary combinations.

Tassios (1976) has eliminated any physical significance attributed to the parameter and has stated that the nonrandomness parameter is mainly an empirical parameter obtained by fitting the experimental data and may not follow the rules set out by Renon (Tassios, 1976). He has even showed that  $\alpha_{ij} = -1$  works in many cases. However, when the NRTL equation was derived, Renon and Prausnitz have suggested a relationship between the non-randomness parameter and Guggenheim's quasichemical approximation (Renon & Prausnitz, 1968). They have shown that  $\alpha$  is related to the inverse of the coordination number  $1/z$  that appeared in Guggenheim's expression. Since the coordination number

was typically found to be between 6 and 12, the non-randomness parameter was expected to vary in the range of 0.1–0.3, which was revised to 0.2–0.47 later.

Simulis® environment was utilized to achieve the model development (Simulis® & thermodynamics) where the third non-randomness parameter  $\alpha_{ij}$  was fixed at 0.20 and the interaction parameters  $\tau_{ij}$  and  $\tau_{ji}$  were estimated from “6M” experimental data points (where  $M$  represents the number of tie-lines) by minimizing the root mean square deviation (RMSD) between calculated and experimental solubilities of each constituent in each phase:

$$\text{RMSD (\%)} = 100 \times \left( \frac{1}{6M} \sum_i \sum_j \sum_k \left( s_{ijk}^{\text{exp}} - s_{ijk}^{\text{cal}} \right)^2 \right)^{1/2} \quad \text{Eq. 3.13}$$

where  $s$  is the solubility expressed in mole fraction and the subscripts  $i$ ,  $j$  and  $k$  designate the component, phase and tie line, respectively.

### 3.3 Part 3: Binary mixing of ILs

#### 3.3.1 Mixing operation

In the previous stage involving the extraction using ILs, the top four commercial ILs were found in the order of  $\text{C}_2\text{mimSCN} > \text{C}_2\text{mimN}(\text{CN})_2 > \text{C}_2\text{mimTf}_2\text{N} > \text{C}_2\text{mimAc}$  for selectivity, and  $\text{C}_2\text{mimTf}_2\text{N} > \text{C}_2\text{mimN}(\text{CN})_2 > \text{C}_2\text{mimAc} > \text{C}_2\text{mimSCN}$  for benzene distribution ratio. These ILs were then brought into a binary combination operation which considers the elimination of the binaries that contains the same IL, and the reversed ratio of the same IL pair. At the end of this operation, six sets of binary mixtures were ultimately produced for experimental validations:

- i) Highest  $S$  ( $\text{C}_2\text{mimSCN}$ ) + highest  $D_{bz}$  ( $\text{C}_2\text{mimTf}_2\text{N}$ )
- ii) 2<sup>nd</sup> highest  $S$  ( $\text{C}_2\text{mimN}(\text{CN})_2$ ) + highest  $D_{bz}$  ( $\text{C}_2\text{mimTf}_2\text{N}$ )
- iii) Highest  $S$  ( $\text{C}_2\text{mimSCN}$ ) + 2<sup>nd</sup> highest  $D_{bz}$  ( $\text{C}_2\text{mimN}(\text{CN})_2$ )
- iv) 2<sup>nd</sup> highest  $S$  ( $\text{C}_2\text{mimN}(\text{CN})_2$ ) + 3<sup>rd</sup> highest  $D_{bz}$  ( $\text{C}_2\text{mimAc}$ )

- v) Highest S (C<sub>2</sub>mimSCN) + 3<sup>rd</sup> highest D<sub>bz</sub> (C<sub>2</sub>mimAc)
- vi) 3<sup>rd</sup> highest S (C<sub>2</sub>mimTf<sub>2</sub>N) + 3<sup>rd</sup> highest D<sub>bz</sub> (C<sub>2</sub>mimAc)

### 3.3.2 Determination of optimized binary ratio

The optimization is carried out by selecting the binary molar ratio at which the curve of selectivity intersects with the curve of distribution ratio. This measurement was operated in twofold, i.e. by experimental LLE measurements, and by using the ideal IL mixing equation (Eq. 3.14)

$$\ln x_{i,ideal}^{I \text{ or } II} = \sum_j \phi_j \ln x_{i,j}^{I \text{ or } II} \quad \text{Eq. 3.14}$$

where  $x$  is the mole fraction,  $\phi$  is the molar ratio of binary ILs, superscripts I and II refer to the extract and raffinate phases, respectively. The subscript  $i$  refers to cyclohexane or benzene, while subscript  $j$  refers to the pure solvents (ILs or organic solvents). During the optimization, the feed concentration of benzene ( $X_{Bz,feed}$ ) was fixed at 10 wt%. The use of ideal mixing equation has been justified elsewhere when the binary mixture of N-butylpyridinium tetrafluoroborate (C<sub>4</sub>pyrBF<sub>4</sub>) and N-butylpyridinium bis(trifluoromethylsulfonyl)imide (C<sub>4</sub>pyrTf<sub>2</sub>N) was developed to separate toluene and *n*-heptane (García et al., 2012b). The logarithmic-linear model in Eq. 3.14 was predicted from the classical thermodynamic theory, where the solubility equilibrium is described in terms of the general expression for Henry's constant of a solute in a mixed-solvent system and the chemical potentials, which relate the solubility with the activity coefficients.

### 3.3.3 Quaternary LLE experiments

The optimized ratio obtained experimentally was used to investigate the quaternary LLE data involving [IL<sub>1</sub> + IL<sub>2</sub>] + benzene + cyclohexane. The quaternary LLE data was then simplified into a pseudo-ternary LLE data, where the molar concentrations of binary ILs were added. This was done to enable plotting the quaternary data into ternary diagrams. The liquid–liquid extraction experiments for these quaternary systems were

carried out using the same procedures described in section 3.2.3 to 3.2.5. In addition, as the two ILs have different molecular weights, the weight of each IL in the binary mixture was calculated so that the weight of mixture remained as 2g. This was carried out to ensure a consistent weight ratio between the top and bottom layers.

University of Malaya

## CHAPTER 4: RESULTS AND DISCUSSION

### 4.1 Extractive separation of benzene and cyclohexane using DESs

#### 4.1.1 DES ranking from $C^\infty$ and $S^\infty$

The results of DES screening are explained in terms of selectivity, capacity, and the PI at infinite dilution, which are depicted in Figure 4.1, Figure 4.2 and Figure 4.3, respectively. In this work, the capacity at infinite dilution ( $C^\infty$ ) was considered a decisive parameter for DES selection, because capacity was reported to give much greater influence on the cost of production than does the selectivity (Zahed A. H., 1992). The selection of HBDs can be observed to affect the selectivity, capacity, and PI of DESs in the separation of benzene and cyclohexane. For instance, as shown in Figure 4.1, the selectivity of five choline chloride-based DESs towards benzene at a constant ratio (1:2) is based on the ranking of  $\text{ChCl:Tur} \gg \text{ChCl:OA} > \text{ChCl:LA} > \text{ChCl:Mur}$ .

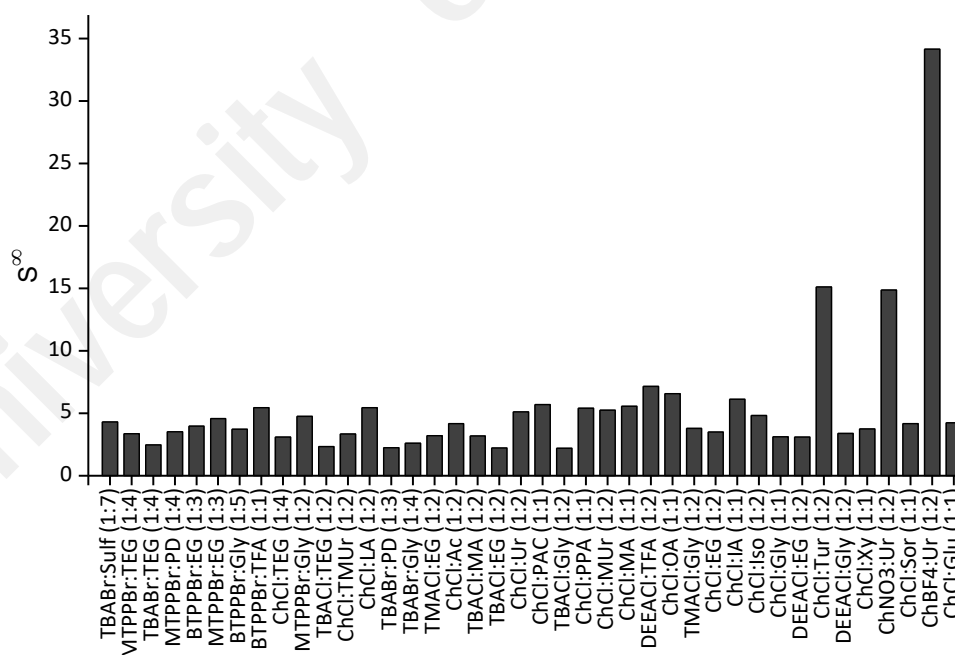


Figure 4.1: Selectivity of DESs at infinite dilution

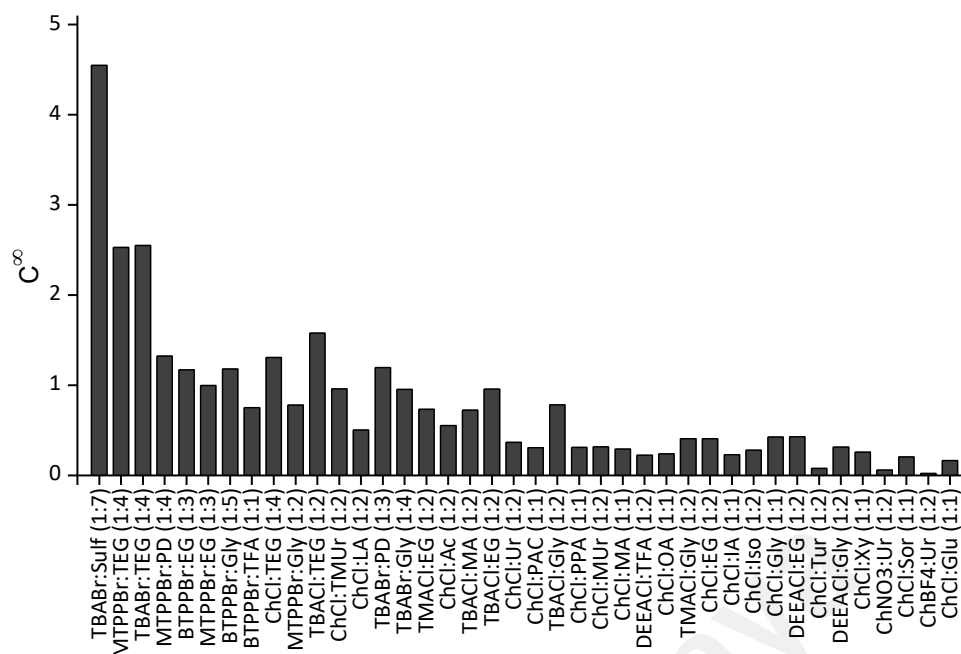


Figure 4.2: Capacity of DESs at infinite dilution

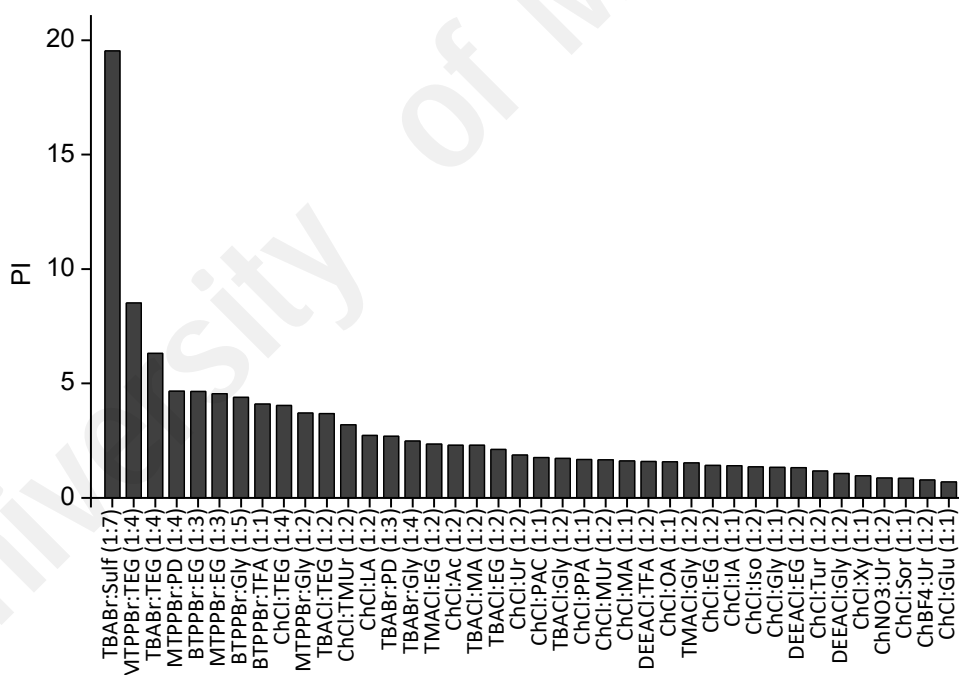


Figure 4.3: Performance index of DESs at infinite dilution

Apart from HBDs, the selection of salt also alters the selectivity of DESs. For example, Figure 4.1 shows that the selectivity of different salts with the same HBD (ethylene glycol) at a constant ratio (1:2) proceeds in the following order: ChCl:EG > TMACl:EG > DEEACl:EG > TBACl:EG. Three DESs with urea-based HBDs, namely ChBF<sub>4</sub>:Ur

(1:2) >> ChCl:Tur (1:2) > ChNO<sub>3</sub>:Ur (1:2), were found to have the highest selectivity among the other DESs. Five DESs with the highest capacity were ranked in the order of TBABr:Sulf (1:7) >> TBABr:TEG (1:4) > MTPPBr:TEG (1:4) > TBACl:TEG (1:2) > MTPPBr:PD (1:4) > ChCl:TEG (1:4). In addition, an inverse trend is typically observed when the same DESs are assessed according to their capacity and selectivity. This trend can be explained by the molecular interactions between the three species involved.

#### 4.1.2 Molecular interactions

##### 4.1.2.1 Analysis of $\sigma$ -profiles

In the  $\sigma$ -profile, when the screening charge density exceeds  $\pm 0.0084 \text{ e}\text{\AA}^{-2}$ , the molecule is considered sufficiently polar to induce hydrogen bonding. A higher absolute value of  $\sigma$  leads to a stronger compound as an HBD. The  $\sigma$ -profiles for DESs with high selectivity and high capacity were plotted in Figure 4.4 and Figure 4.5, respectively. Before analyzing the molecular interactions among the solvent (DES), solute (benzene), and carrier (cyclohexane), the polarity properties of the solute and carrier are first examined for efficient separation.

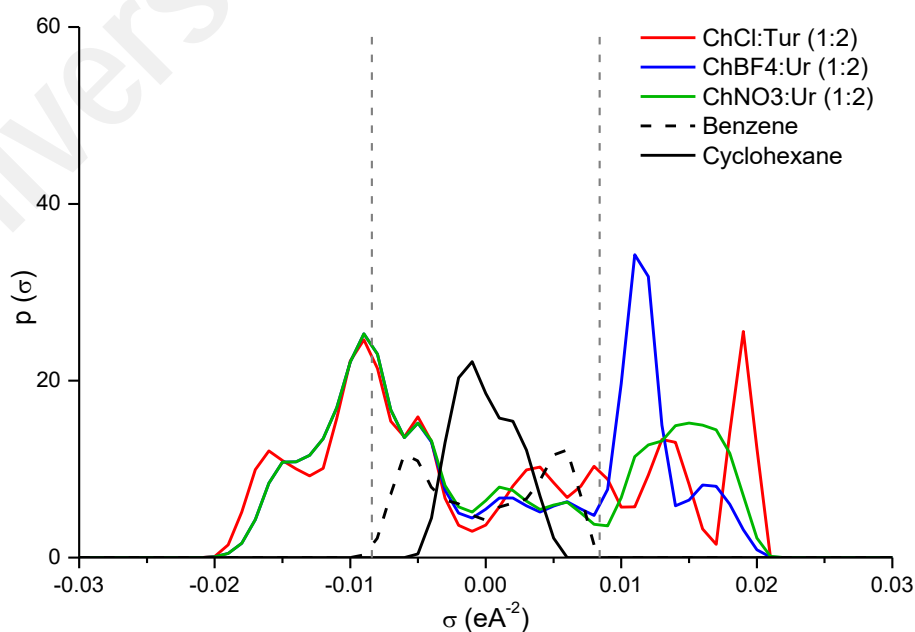
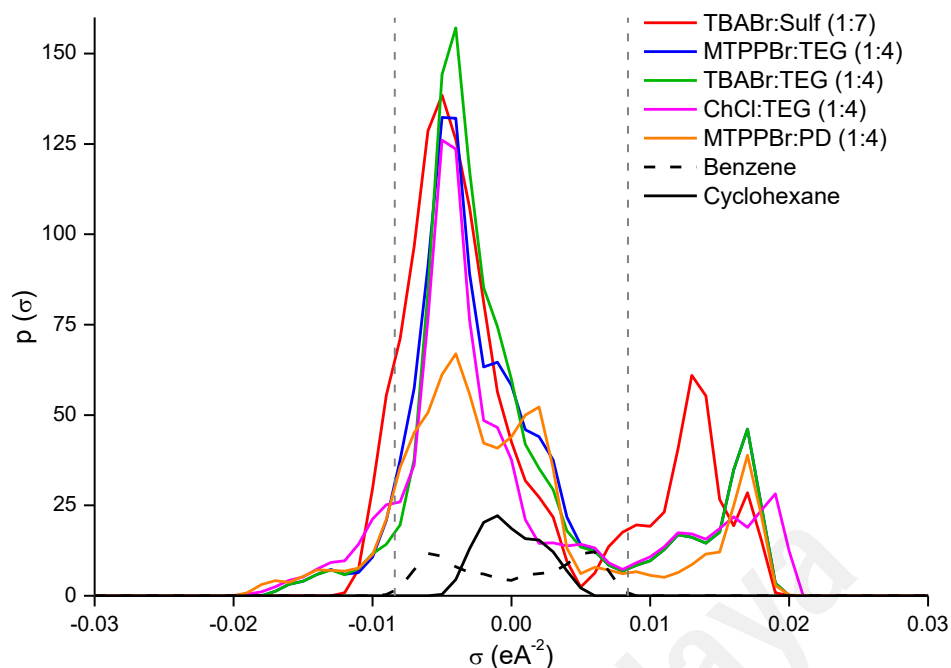


Figure 4.4:  $\sigma$ -profiles benzene, cyclohexane and DESs with high  $S^\infty$



**Figure 4.5:  $\sigma$ -profiles of benzene, cyclohexane and DESs with high  $C^\infty$**

As seen, the  $\sigma$ -profile of benzene clearly shows that its charge density results from two peaks within  $\pm 0.006 \text{ e}\text{\AA}^{-2}$ . This means that benzene is weak for hydrogen bond interactions and can also be classified as a nonpolar compound. The peak on the negative and positive  $\sigma$  is derived from the hydrogen and carbon atoms, respectively, in the benzene ring structure. The symmetrical shape of these two peaks indicates a favorable interaction between benzene and itself, explaining its high boiling points and surface tension. Apart from benzene, cyclohexane is also a strongly nonpolar molecule, because the two peaks are at  $-0.001 \text{ e}\text{\AA}^{-2}$  and  $0.002 \text{ e}\text{\AA}^{-2}$ , which are respectively derived from hydrogen and carbon atoms. Akin to benzene, the  $\sigma$ -profile of cyclohexane also has a near-symmetric shape, indicating a favorable interaction with itself. Since the  $\sigma$  values of benzene and cyclohexane are outside the hydrogen bond region ( $\pm 0.0084 \text{ e}\text{\AA}^{-2}$ ), the interactions between them arise from misfit energy.

DESs are typically synthesized from three types of compounds (i.e., salt cation (SC), salt anion (SA), and the HBD). To achieve high selectivity for benzene separation using a DES, it is ideal to find an SC with a symmetrical curve at  $0 \text{ e}\text{\AA}^{-2}$  with respect to the

right peak of benzene for both molecules to have a favorable interaction in the nonpolar region. As shown in Figure 4.4, ChCl:TUr, ChBF<sub>4</sub>:Ur, and ChNO<sub>3</sub>:Ur have one peak at  $-0.09 \text{ e\AA}^{-2}$ , which results in a favorable interaction with the right peak of benzene ( $0.006 \text{ e\AA}^{-2}$ ). This is the reason for the high selectivity of these three DESs as shown in Figure 4.1. Although the other potential DESs in Figure 4.5 also have the targeted peak, their peaks are substantially higher and are overlapping with the cyclohexane peaks. This overlap indicates that the DES interacts with both benzene and cyclohexane, resulting in low selectivity and high capacity. The same reason also applies to ChBF<sub>4</sub>:Ur, ChCl:TUr, and ChNO<sub>3</sub>:Ur which exhibited the highest selectivity values, but extremely low capacity (small overlapping curve with cyclohexane). The reasons for the highest value of  $C^\infty$  and the PI for TBABr:Sulf (1:7) are twofold, i.e., the hydrogen bond peak and the effect of the ratio). Comparing with other efficient DESs, TBABr:Sulf (1:7) only has a slight value of a negative screening charge density at  $\sigma < -0.0084 \text{ e\AA}^{-2}$ . As mentioned, the compound with any peak beyond this point acts as an HBD. As the  $\sigma$  becomes more negative, the peak is nearly nonexistent for TBABr:Sulf (1:7), leading to considerably fewer hydrogen bond interactions. As benzene does not interact through hydrogen bond, the high capacity of TBABr:Sulf (1:7) came from its interaction with benzene at the nonpolar region. For the second reason (the effect of the ratio), the higher ratio of sulfolane produces a higher peak area at  $0.005 \text{ e\AA}^{-2} < \sigma < 0.02 \text{ e\AA}^{-2}$ ; hence, more interactions with the left peak of benzene occur.

For the right side of DES  $\sigma$ , any peak from 0 to  $0.01 \text{ e\AA}^{-2}$  interacts with the left peak of benzene ( $-0.006 \text{ e\AA}^{-2}$ ). However, because the SA in the DES is typically a strong hydrogen bond acceptor (e.g., Br<sup>-</sup> and Cl<sup>-</sup>), it is unlikely to interact with benzene through hydrogen bonding because benzene is a nonpolar compound. Therefore, for the positive charge density, instead of SC, the HBD in the DES plays a critical role in interactions with benzene at the nonpolar region. For example, as shown in Figure 4.1, ChBF<sub>4</sub>:Ur

(1:2), ChCl:TUr (1:2) and ChNO<sub>3</sub>:Ur (1:2) showed high selectivity because some peaks exist at  $0 < \sigma < 0.01 \text{ e\AA}^{-2}$  on its  $\sigma$ -profile (Figure 4.4). Taking another example, TBABr:Sulf (1:7) is a DES with the highest PI among all DESs screened. This can be explained through its exclusive  $\sigma$ -profile, which is formed by three major peaks in positive and negative  $\sigma$  values (Figure 4.5). The first peak with a massive area is at  $-0.005 \text{ e\AA}^{-2}$ , which belongs to hydrogen atoms at four butyl groups in the tetrabutylammonium cation. As shown in the profile, this hydrogen can interact with both benzene and cyclohexane at the nonpolar region, which results in a high value of the solvent capacity. In addition, among the DESs studied, TBABr:Sulf also has a high selectivity value (4.78), which is derived from its second peak at  $0.009 \text{ e\AA}^{-2}$ ; it favours an interaction with the left peak of benzene ( $-0.006 \text{ e\AA}^{-2}$ ) in the nonpolar region. As mentioned, the third peak of TBABr:Sulf (1:7) is less crucial for extraction performance because it is derived from the bromide ion in the hydrogen bond acceptor region, thus is unable to interact with benzene in the nonpolar region. Because the values of selectivity and capacity for TBABr:Sulf are relatively high among the others, the highest value of the PI is obtained.

#### 4.1.2.2 Analysis of $\sigma$ -potentials

In COSMO-RS analysis, the  $\sigma$ -potential indicates the affinity of a component in a mixture towards another. In the  $\sigma$ -potential plot, a higher negative value of  $\mu(\sigma)$  indicates an increasing interaction between molecules, whereas a higher positive value signifies an increase in repulsive behaviour. For the horizontal axis, increasing negative and positive values for the hydrogen bonding threshold ( $\pm 0.0084 \text{ e\AA}^{-2}$ ) indicate the region of a molecule where interactions between HBDs and hydrogen bond acceptors occur, respectively. Figure 4.6 shows that both  $\sigma$ -potential curves for benzene and cyclohexane are parabolic in nature, where the interaction can occur only at the nonpolar region.

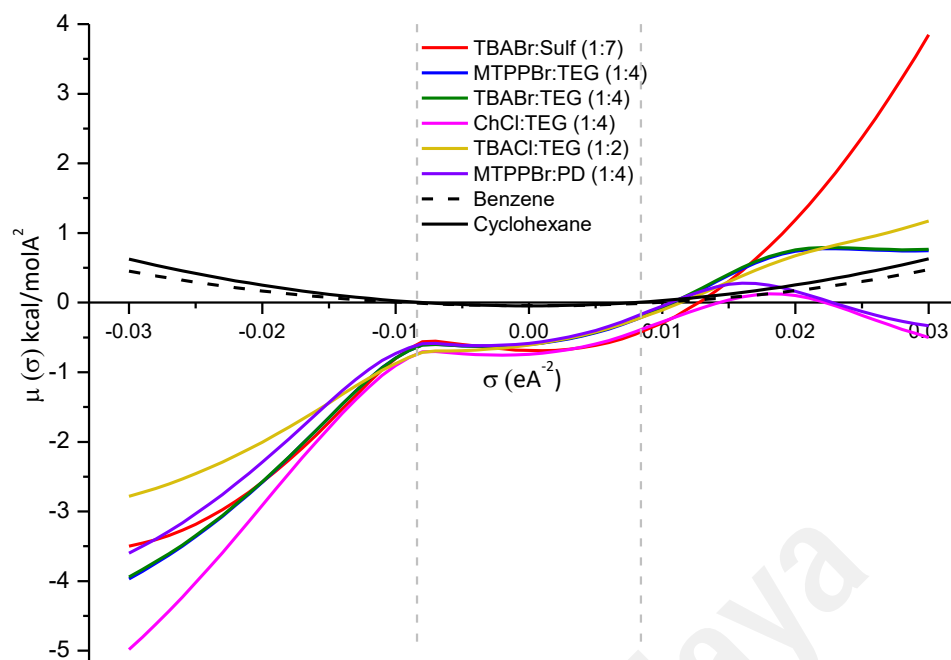


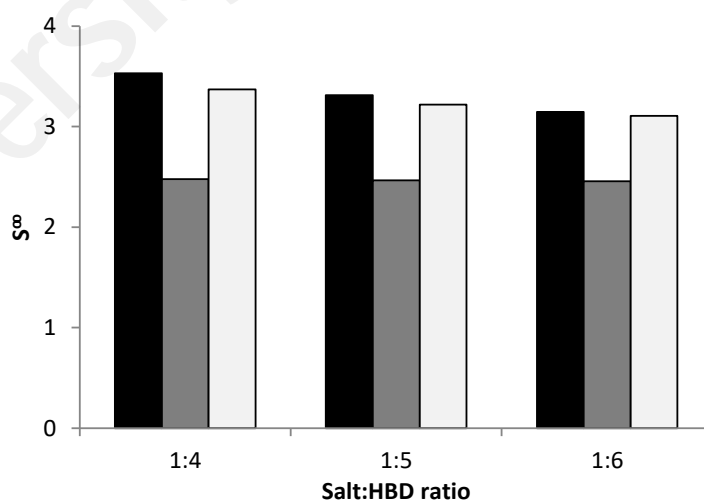
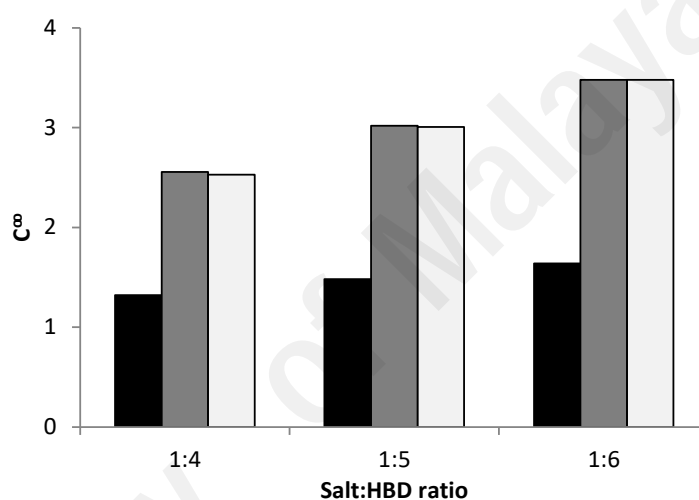
**Figure 4.6:  $\sigma$ -potential of DESs with  $C^\infty$  and  $PI^\infty$**

A critical criterion for selecting a favorable DES for extraction of benzene from cyclohexane is to find one with negative  $\mu(\sigma)$  values at the nonpolar region. As shown in Figure 4.6, all of the selected DESs were found to have strong potential because they have curves with negative values at the nonpolar region, with TBABr:Sulf (1:7) having the highest peak area. The hydrogen bond ability of all DESs in this case is apparently not an advantage, because benzene and cyclohexane both exhibit repulsive behavior at the HBD region.

#### 4.1.3 Effects of salt:HBD ratio

To validate the effect of the ratio on the DES performance, three DESs with different Salt:HBD molar ratios (1:4, 1:5, and 1:6) were selected, and their respective PIs are depicted in Figure 4.7. The superior performance of a DES in extracting benzene from cyclohexane was determined according to a higher salt:HBD ratio. As mentioned, the nonpolar surface parts of an HBD play a critical role in interacting with the left peak of benzene in the  $\sigma$ -profile. A higher concentration (ratio) of the HBD creates a higher peak area in the nonpolar region, indicating a stronger interaction with benzene. However,

apart from stronger DES–benzene interaction, the DES–cyclohexane interaction also increased at higher salt:HBD ratio. This can be explained by the higher HBD peak, which creates higher overlapping area between cyclohexane and benzene at the non-polar region. This condition creates a higher interaction competition and thus reduces the selectivity. As the physical properties of a DES depend on the ratio of its contributing molecules (Abbott et al., 2004), obtaining a DES with the highest ratio, but at a eutectic concentration, is crucial.



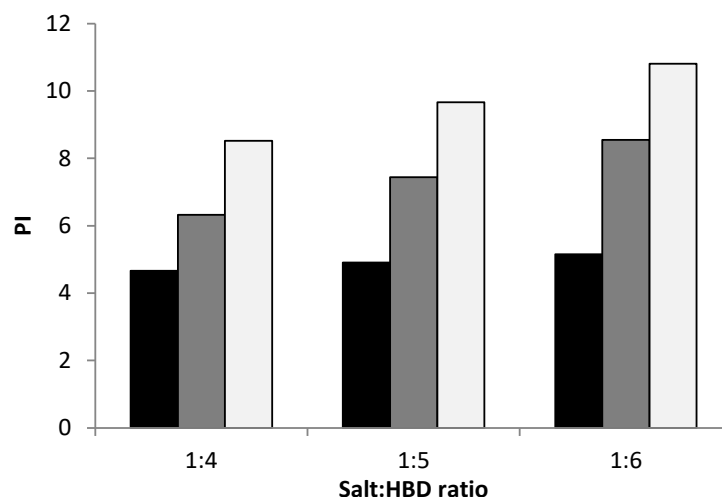


**Figure 4.7: Effect of Salt:HBD ratio towards DESs'  $C^\infty$ ,  $S^\infty$  and  $PI^\infty$ . The black, grey and white colours represent MTPPBr:PD, TBABr:TEG and MTPPBr:TEG, respectively.**

#### 4.1.4 Ternary liquid-liquid equilibrium

The molar compositions of each tie lines for DES + benzene + cyclohexane ternary systems are tabulated in Table 4.1, while the corresponding LLE diagrams are depicted in Figure 4.8 to Figure 4.12. It was observed that all DESs were not present in the raffinate layer, and its concentration in the extract phase is very low. This indicates the minimum cross solubility and easier regeneration of DESs. The selectivity of five DESs increased in the order of MTPPBr:PD (1:4)  $\approx$  TBABr:TEG (1:4) < ChCl:TEG (1:4) < MTPPBr:TEG (1:4) < TBABr:Sulf (1:7), while the benzene distribution ratio increased in the order of ChCl:TEG (1:4) < MTPPBr:PD (1:4) < MTPPBr:TEG (1:4) < TBABr:TEG < TBABr:Sulf (1:7). These orders demonstrated that TBABr:Sulf (1:7) showed the highest values for both selectivity (4.90–13.35) and benzene distribution ratio (0.23–0.19).

**Table 4.1: Molar composition of tie-lines with the distribution ratio and selectivity data for the ternary systems investigated in this work.**

Top layer			Bottom layer			<i>D</i>	<i>S</i>
<i>x</i> <sub>1</sub>	<i>x</i> <sub>2</sub>	<i>x</i> <sub>3</sub>	<i>x</i> <sub>1</sub>	<i>x</i> <sub>2</sub>	<i>x</i> <sub>3</sub>		
<b>benzene (1) + cyclohexane (2) + TBABr:Sulf (1:7) (3)</b>							
0.10	0.899	0.00	0.020	0.013	0.967	0.19	13.354
0.19	0.806	0.000	0.041	0.014	0.944	0.21	11.966
0.28	0.716	0.000	0.059	0.015	0.926	0.20	9.859
0.36	0.634	0.000	0.081	0.017	0.902	0.22	8.164
0.47	0.529	0.000	0.104	0.018	0.878	0.22	6.500
0.56	0.438	0.000	0.134	0.021	0.845	0.23	4.902
<b>benzene (1) + cyclohexane (2) + TBABr:TEG (1:4) (3)</b>							
0.09	0.901	0.000	0.017	0.018	0.965	0.17	8.322
0.20	0.797	0.000	0.028	0.016	0.956	0.13	6.582
0.27	0.721	0.000	0.036	0.019	0.944	0.13	4.831
0.36	0.633	0.000	0.055	0.013	0.931	0.15	7.039
0.47	0.522	0.000	0.070	0.016	0.914	0.14	4.702
0.57	0.424	0.000	0.086	0.015	0.899	0.14	4.257
0.67	0.322	0.000	0.104	0.016	0.880	0.15	3.073
0.77	0.226	0.000	0.128	0.016	0.856	0.16	2.301
<b>benzene (1) + cyclohexane (2) + MTPPBr:TEG (1:4) (3)</b>							
0.10	0.894	0.000	0.011	0.010	0.979	0.10	12.882
0.19	0.803	0.000	0.023	0.007	0.971	0.11	14.102
0.29	0.706	0.000	0.033	0.009	0.958	0.11	9.220
0.38	0.613	0.000	0.041	0.005	0.954	0.10	12.846
0.49	0.508	0.000	0.054	0.007	0.939	0.10	7.868
0.59	0.410	0.000	0.066	0.006	0.928	0.11	7.630
0.69	0.308	0.000	0.081	0.006	0.914	0.11	6.190
0.82	0.172	0.000	0.103	0.005	0.893	0.12	4.493
<b>benzene (1) + cyclohexane (2) + MTPPBr:PD (1:4) (3)</b>							
0.11	0.890	0.000	0.010	0.010	0.980	0.09	8.024
0.21	0.786	0.000	0.018	0.010	0.972	0.08	6.578
0.29	0.702	0.000	0.023	0.010	0.967	0.07	5.526
0.40	0.597	0.000	0.033	0.009	0.958	0.08	5.217
0.50	0.498	0.000	0.044	0.009	0.947	0.08	4.630
0.60	0.398	0.000	0.055	0.008	0.938	0.09	4.741
0.70	0.297	0.000	0.061	0.008	0.931	0.08	3.208
0.79	0.208	0.000	0.077	0.009	0.914	0.09	2.186
<b>benzene (1) + cyclohexane (2) + ChCl:TEG (1:4) (3)</b>							
0.09	0.906	0.000	0.007	0.007	0.986	0.07	9.130
0.19	0.803	0.000	0.014	0.006	0.980	0.07	9.613
0.29	0.708	0.000	0.020	0.004	0.976	0.06	12.091
0.39	0.601	0.000	0.027	0.004	0.969	0.06	9.032
0.50	0.498	0.000	0.032	0.004	0.964	0.06	8.228
0.60	0.393	0.000	0.040	0.004	0.955	0.06	6.100
0.70	0.296	0.000	0.048	0.004	0.948	0.06	4.896
0.80	0.191	0.000	0.057	0.003	0.940	0.07	4.749

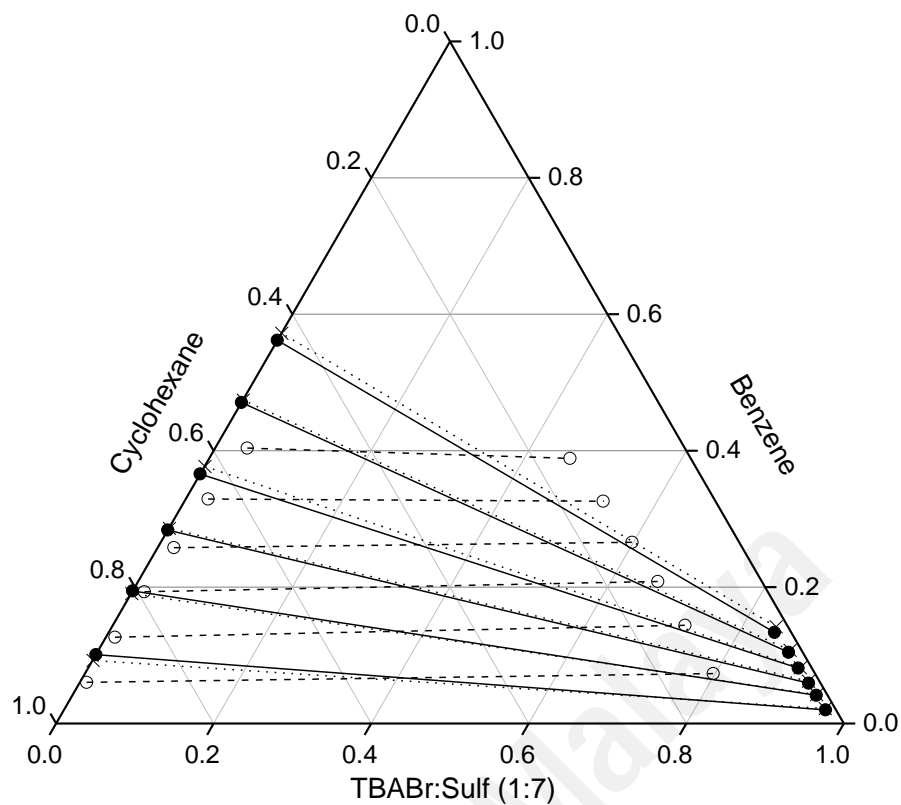


Figure 4.8: Ternary phase diagrams for TBABr:Sulf (1:7) + benzene + cyclohexane at 298.15 K and 1 atm: —●—, experimental; --○--, COSMO-RS; and ···×··, NRTL

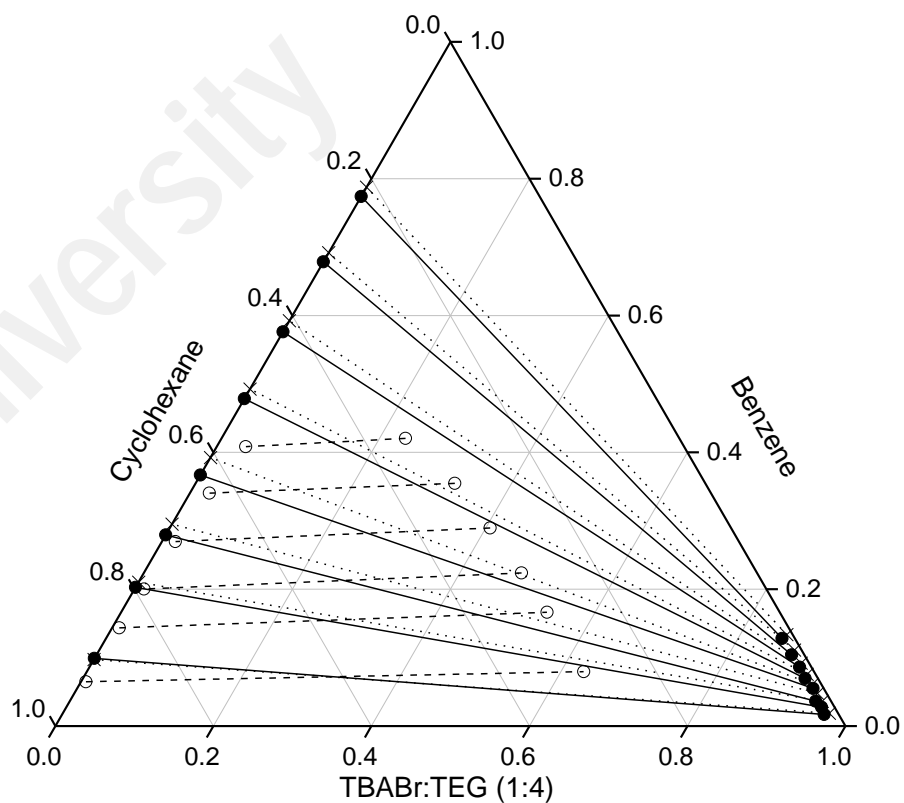


Figure 4.9: Ternary phase diagrams for TBABr:TEG (1:4) + benzene + cyclohexane at 298.15 K and 1 atm: —●—, experimental; --○--, COSMO-RS; and ···×··, NRTL

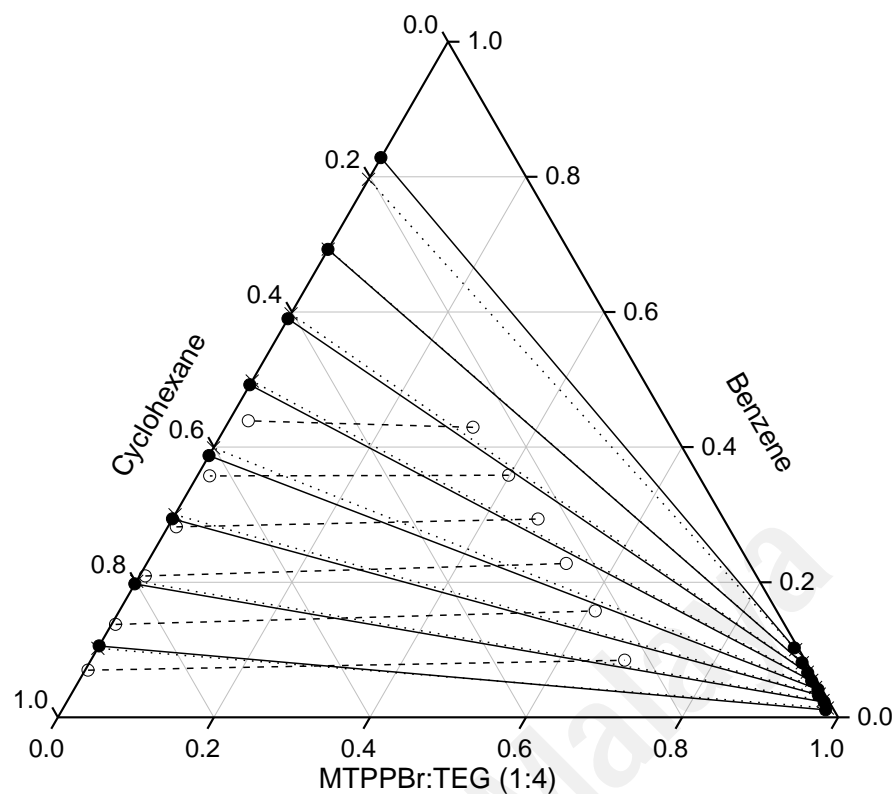


Figure 4.10: Ternary phase diagrams for MTPPBr:TEG (1:4) + benzene + cyclohexane at 298.15 K and 1 atm:  $\bullet$ —, experimental;  $\text{--}\circ\text{--}$ , COSMO-RS; and  $\cdots\times\cdots$ , NRTL

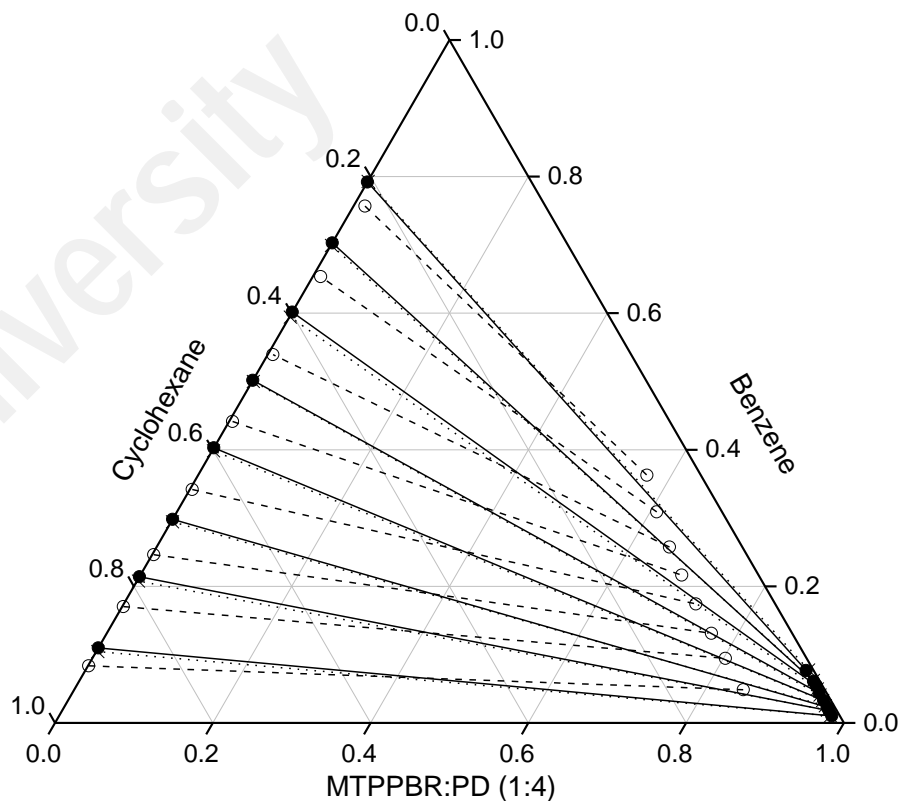
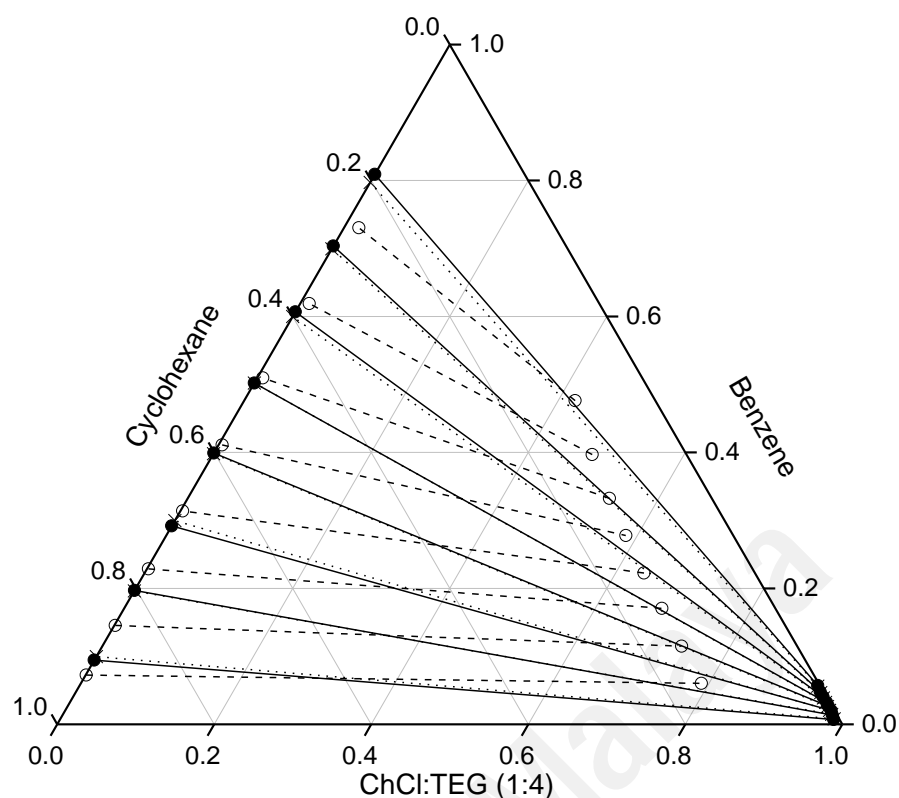


Figure 4.11: Ternary phase diagrams for MTPPBr:PD (1:4) + benzene + cyclohexane at 298.15 K and 1 atm:  $\bullet$ —, experimental;  $\text{--}\circ\text{--}$ , COSMO-RS; and  $\cdots\times\cdots$ , NRTL



**Figure 4.12: Ternary phase diagrams for ChCl:TEG (1:4) + benzene + cyclohexane at 298.15 K and 1 atm: —●—, experimental; --○--, COSMO-RS; and ···×··, NRTL**

All tie-lines in Figure 4.8 to Figure 4.12 showed negative slopes and the gradient of the slopes increased at higher feed concentration of benzene. This result indicates the need of multistage extraction for the process because the affinity of benzene was higher towards cyclohexane than towards the DESs. It is also important to note the discrepancies observed between the experimental and the COSMO-RS tie lines. This finding can be regarded as a computational supportive proof that the separation of benzene and cyclohexane is indeed difficult and unpredictable using COSMO-RS. This inaccuracy could be reasoned by the cyclic nature of cyclohexane, rather straight-chain nature of hydrocarbons such as *n*-hexane and *n*-heptane in other systems reported in literature.

#### 4.1.5 NRTL regression and consistency tests

The RMSD values between the experimental and NRTL-calculated tie lines are listed in Table 4.2. The table shows that all the ternary systems were adequately correlated using the NRTL model according to the average RMSD values, which are less than 1 %. This

close agreement is also observable in Figure 4.8 to 4.12. In addition, the values of the NRTL binary interaction parameters regressed for each ternary system are also listed in Table 4.2. The constancy of the interaction parameters between benzene and cyclohexane is maintained for all ternary systems to conserve the coherence of the regression. The parameters of the Othmer–Tobias and Hand correlations are listed in Table 4.3.

**Table 4.2: NRTL parameters for the ternary systems (benzene + cyclohexane + DES) with RMSD between experimental and calculated data.**

<i>i</i>	<i>j</i>	$\tau_{ij}$	$\tau_{ji}$	<i>RMSD</i> (%)
Benzene	Cyclohexane	-189.57	453.65	
Benzene	TBABr:Sul (1:7)	6565.47	589.99	0.081
Cyclohexane	TBABr:Sul (1:7)	1659.28	812.33	
Benzene	TBABr:TEG (1:4)	4779.40	525.48	0.138
Cyclohexane	TBABr:TEG (1:4)	1932.75	862.49	
Benzene	MTPPBr:TEG (1:4)	5350.47	668.22	0.138
Cyclohexane	MTPPBr:TEG (1:4)	1949.89	993.98	
Benzene	MTPPBr:PD (1:4)	7272.70	865.25	0.041
Cyclohexane	MTPPBr:PD (1:4)	1391.64	807.17	
Benzene	ChCl:TEG (1:4)	6274.22	870.85	0.052
Cyclohexane	ChCl:TEG (1:4)	2285.71	1042.56	

**Table 4.3: Parameters of Othmer–Tobias and Hand correlation for each ternary system and the values of regression coefficient  $R^2$**

Ternary System	Othmer-Tobias			Hand		
	<i>a</i>	<i>b</i>	$R^2$	<i>c</i>	<i>d</i>	$R^2$
<b>Benzene + cyclohexane + DES</b>						
TBABr:Sul (1:7)	3.602	1.462	0.992	3.108	1.197	0.995
TBABr:TEG (1:4)	6.840	2.146	0.992	1.535	5.271	0.990
MTPPBr:TEG (1:4)	7.655	2.095	0.990	5.986	1.571	0.969
MTPPBr:PD (1:4)	7.701	2.231	0.994	5.901	1.596	0.986
ChCl:TEG (1:4)	9.406	2.403	0.994	6.899	1.689	0.976

#### 4.1.6 Experimental selectivity and distribution ratio

Figure 4.13 shows the distribution ratio and selectivity, respectively, as a function of benzene concentration in the raffinate phase.

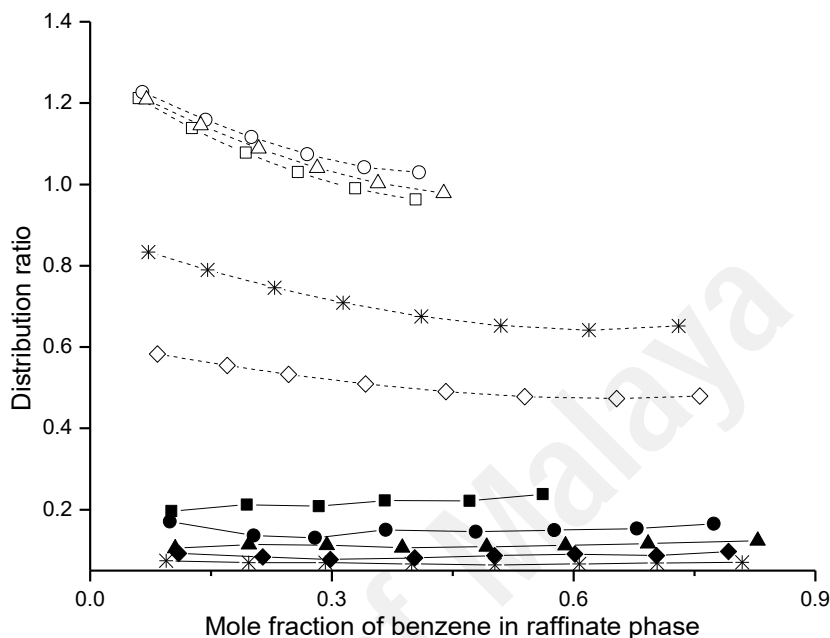


**Figure 4.13: Distribution ratio as a function of benzene concentration in the raffinate phase. The solid-full and dashed-empty data represent the experimental and COSMO-RS results, respectively. The symbols of square, circle, triangle, diamond and star represent TBABr:Sulf (1:7), TBABr:TEG (1:4), MTPPBr:TEG (1:4), MTPPBr:PD (1:4) and ChCl:TEG (1:4), respectively.**

The distribution ratio of benzene at equilibrium typically exhibited a slow increment with an increasing mole fraction of benzene in the raffinate layer. This also means that the distribution ratio increased slightly with a reduction in the benzene mass fraction in the feed. It is inferred that the extraction process is viable not only for low but also for higher feed concentrations of benzene. In addition, the distribution ratio for all systems have values less than unity, which indicates that only a small amount of benzene is extracted in one extraction cycle. This is demonstrated by the negative slope of the tie lines in the ternary diagrams, where the concentration of benzene at equilibrium is higher in the cyclohexane-rich phase. This means that for effective extraction, a large amount of a DES is required for multistage extraction. However, this should be a minor issue after

a DES is considered a reusable and recyclable compound that can be produced using cheap materials.

By contrast, as shown in the analysis of the  $\sigma$ -profile in the earlier section, a DES interacts with both benzene and cyclohexane, which creates interaction competition to an extent. Regarding this condition, selectivity is an accurate measurement that indicates the ability of a DES to selectively extract benzene from cyclohexane, rather than extracting cyclohexane altogether. This means that a DES can efficiently separate benzene from cyclohexane. This is observable in its equation, whereby selectivity is the fraction of the distribution ratio of benzene into that of cyclohexane.

The selectivity of DESs as a function of benzene concentration in the raffinate phase is showed in Figure 4.14.

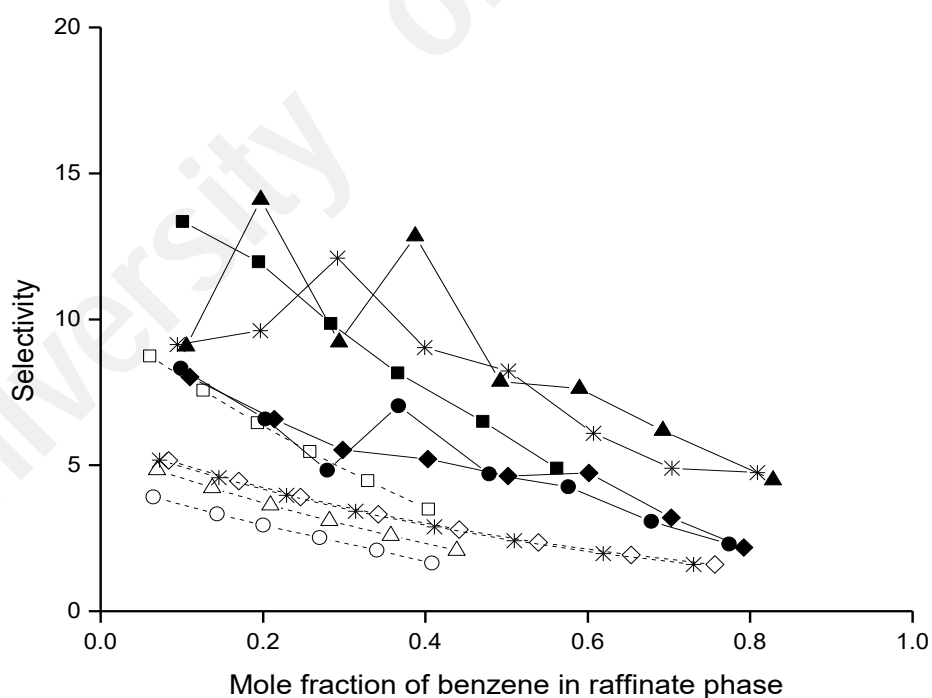


**Figure 4.14: Selectivity as a function of benzene concentration in the raffinate phase. The solid-full and dashed-empty data represent the experimental and COSMO-RS results, respectively. The symbols of square, circle, triangle, diamond and star represent TBABBr:Sulf (1:7), TBABr:TEG (1:4), MTPPBr:TEG (1:4), MTPPBR:PD (1:4) and ChCl:TEG (1:4), respectively.**

DES selectivity typically decreases with an increasing concentration of benzene in the raffinate phase. This trend is in agreement with the results reported for other ternary systems involving DESs as extracting solvents (M. A. Kareem et al., 2012; Kareem et al., 2013; Mulyono et al., 2014). Furthermore, the values of selectivities in all ternary systems studied were greater than unity, indicating that extraction is possible. In addition, as shown in the molar composition tables and ternary diagrams, the equilibrium concentration of DESs in the raffinate layer was zero, indicating a complete non-crossing of the DES into the cyclohexane phase. This can be considered a crucial discovery compared to the critical issue of solvent crossing when using common industrial solvents (e.g., pure sulfolane). Solvent crossing is a considerable drawback to any extraction column because it results in solvent loss and necessitates additional separation steps. This result also revealed that, by transforming the pure industrial solvent into a DES, these disadvantages could be resolved. To further understand the extraction mechanism, the  $^1\text{H}$  NMR peak of the species related were analyzed as the following.

#### 4.1.7 Analysis of extraction mechanism using $^1\text{H}$ NMR

The efficiency of separating aromatic hydrocarbons from aliphatic hydrocarbons through liquid–liquid extraction is not only related to the capacity of the solvent to extract the aromatic hydrocarbon from the aliphatic hydrocarbon layer, but also to the immiscibility between the solvent and the aliphatic hydrocarbon–rich phase. A study of the solvent extraction of benzene from *n*-hexane through LLE for a ternary system (sulfolane + benzene + *n*-hexane) at different ratios revealed the efficacy of sulfolane for removing benzene from the *n*-hexane–rich phase. Nevertheless, sulfolane appeared in the hydrocarbon-rich phase (Mahmoudi & Lotfollahi, 2010).

However, in this study, when sulfolane was combined with TBABr to form the TBABr:sulfolane (1:7) DES, both HPLC and  $^1\text{H}$  NMR analyses of the cyclohexane-rich

phase confirmed the absence of sulfolane in this layer. This result shows that the cyclohexane-rich phase cannot lead to sulfolane dissolution when it is in DES solvent form, and it indicates that TBABr prevents sulfolane from reaching the top layer. To highlight the role of TBABr and the molecular interactions involved in the DES mixture,  $^1\text{H}$  NMR analysis was performed and displayed in Figure 4.15.

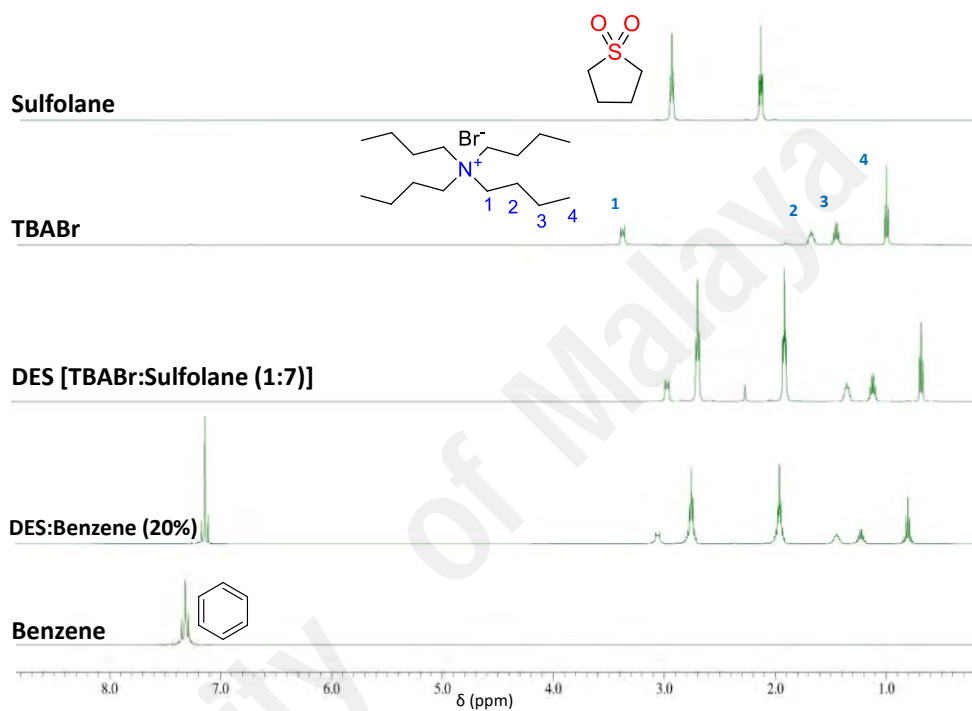


**Figure 4.15:  $^1\text{H}$  NMR spectra of TBABr:Sulf (1:7) and its constituents, in the presence of 20% benzene.**

As displayed above, a comparison of the field shift of the peaks in the DES and its free compounds revealed a significant downfield shift of all hydrogen atoms of TBABr in DES form (from 0.99 and 1.44 to 1.67 ppm, from 3.66 to 0.70 ppm, and from 1.13 and 1.36 to 2.99 ppm), whereas the hydrogen atoms of sulfolane moved to the upfield shift (from 2.13 and 2.94 to 1.93 and 2.72 ppm). These modifications of the field shifts can be explained with the interaction between the bromide anion in TBABr and the sulfur atom in sulfolane. Under the presence of 20% benzene, no critical change in field shift was registered for both hydrogen in sulfolane and TBABr. This result revealed that the TBABr:sulfolane (1:7) DES conserves its structure in the presence of benzene, and

confirmed that TBABr prevents the solubilisation of sulfolane in the cyclohexane-rich phase.

#### **4.1.8 Comparison between COSMO-RS prediction and experimental measurement**

A comparison between the COSMO-RS predictions and experimental results can be analyzed based on the predicted value of capacity at infinite dilution ( $C^\infty$ ) and experimental benzene distribution ratio ( $D_B$ ). Capacity is selected for comparison rather than selectivity, because solvent capacity has a much greater influence on the cost of production than does the selectivity (Zahed A. H., 1992). Figure 4.13 shows that at increased concentration of benzene in raffinate phase, the experimental capacity was almost constant, but the predicted values slightly decreased. Referring back to Figure 4.2, the predicted capacity of the five DESs was ranked as follows: ChCl:TEG (1:4) < MTPPBr:PD (1:4) < MTPPBr:TEG (1:4) < TBABr:TEG (1:4) < TBABr:Sulf (1:7). A comparison of these capacity values with the experimental distribution ratio shown in Figure 4.13 clearly revealed that both COSMO-RS prediction and the experimental data showed the same ranking position. Apart from that, a close value of relative ranking was also observed between MTPPBr:PD (1:4) and ChCl:TEG (1:4) for both COSMO-RS ( $C^\infty$ ) and the experimental results ( $D_B$ ). Meanwhile for the selectivity, as seen in Figure 4.14, both experimental and predicted values are inversely proportional to the concentration of benzene in raffinate phase. In addition, both COSMO-RS and experimental approaches showed similar trend for capacity or selectivity with respect to concentration of benzene in raffinate phase. This result indicated that COSMO-RS can provide good predictions in terms of qualitative screening during the solvent selection process.

#### 4.1.9 Number of extraction stages

In order to determine the number of stages necessary to extract the maximum of benzene from benzene–cyclohexane mixture using TBABr:Sulf (1:7), the top layer (cyclohexane rich phase) was separated from the bottom layer (DES rich phase). Subsequently, the same amount of DES was added to the top layer. This procedure was repeated and the benzene concentration was determined using HPLC analysis. Figure 4.16 shows the HPLC chromatograms of benzene in the raffinate phase after each extraction step. As seen, the peak decreased gradually until reaching a total removal of about 97% after nine extraction cycles. Again, this relatively high number of cycles reflects the difficulty of separating benzene from cyclohexane.

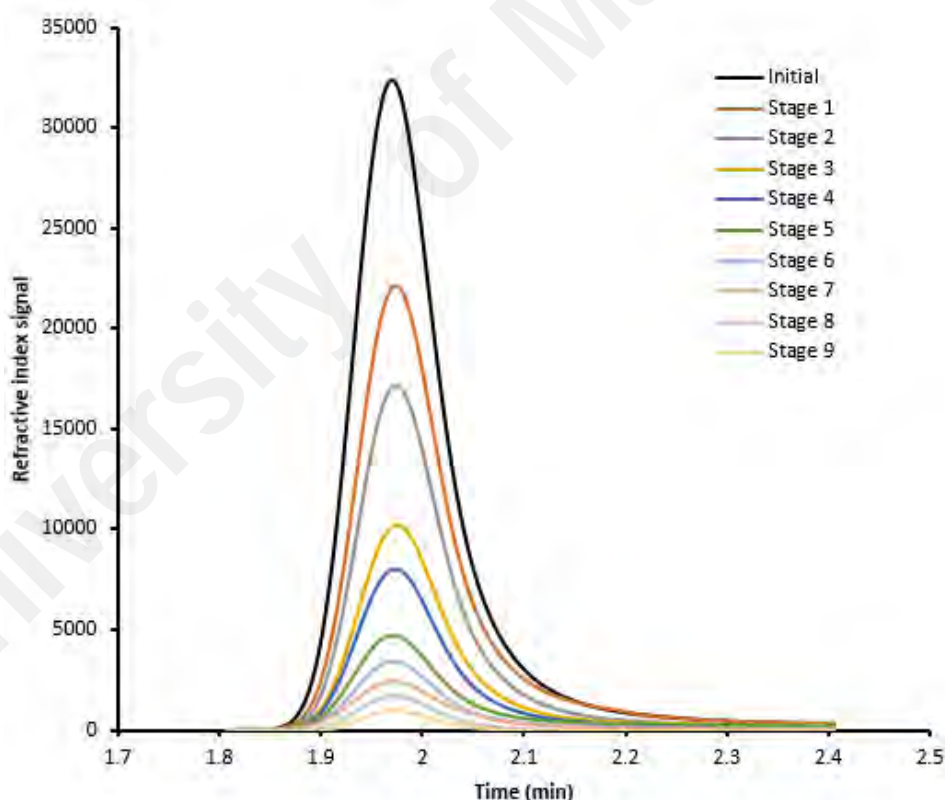


**Figure 4.16: HPLC chromatograms of benzene in the raffinate phase for different extraction stages with TBABr:Sulf (1:7)**

#### 4.1.10 Regeneration of DESs

The regeneration of the extraction solvent and its reuse has economic and environmental benefits. For this purpose, the back extraction and rotary evaporator process were used. In this case, the regeneration of TBABr:Sulf (1:7) DES was performed by using a rotary evaporator under 100 mbar vacuum and 40 °C. After the first extraction, the two phases were separated using a separating funnel and benzene was removed from the bottom layer (DES-rich phase) using a rotary evaporator. Then, the recovered DES was used for new extraction cycle. As seen from Figure 4.17, even after four cycles, the performance of recycled DES was as effective as that of a fresh one. In this figure, the extraction performance reflects the quantity of benzene trapped and is expressed in (%) based on the first extraction cycle. Therefore, these advantages, i.e. easy recycling and maintained extraction efficiency, make this DES an attractive solvent for this challenging separation.

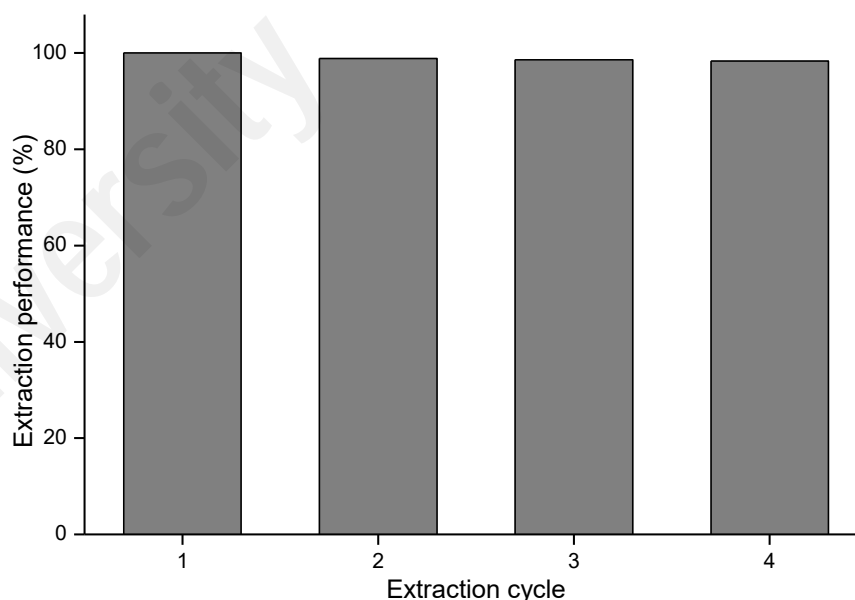


**Figure 4.17: Extraction percentage of benzene using TBABr:Sulf (1:7) after different regeneration cycle.**

## 4.2 Extractive separation of benzene and cyclohexane using ILs

### 4.2.1 COSMO-RS screening

#### 4.2.1.1 $\sigma$ -profiles of industrial organic solvents and ILs

Before selecting the types of cation and anion, the interactions between benzene, cyclohexane and ILs or organic solvents were firstly analyzed by  $\sigma$ -profile analysis. Thus, four organic solvents commonly used for the separation of aromatic–aliphatic mixtures, namely, sulfolane, *N*-methyl-2-pyrrolidinone, ethylene glycol, and tetraethylene glycol, were selected as the benchmarks. The  $\sigma$ -profiles of the industrial solvents and ILs with cyclic cations are illustrated in Figure 4.18 and 4.19. This profile can be categorized into three regions: positive polarity ( $\sigma < -0.0084 \text{ e\AA}^{-2}$ ), non-polar ( $-0.0084 \text{ e\AA}^{-2} \leq \sigma \leq 0.0084 \text{ e\AA}^{-2}$ ), and negative polarity ( $\sigma > 0.0084 \text{ e\AA}^{-2}$ ). The  $y$ -axis represents the surface area of the respective  $\sigma$  regions. The regions in the positive and negative polarities can be viewed as the regions of the hydrogen bond donor and acceptor, respectively. The interactions between the molecules of a system are viewed in terms of a peak area comparison among the curves at negative and positive  $\sigma$  values.

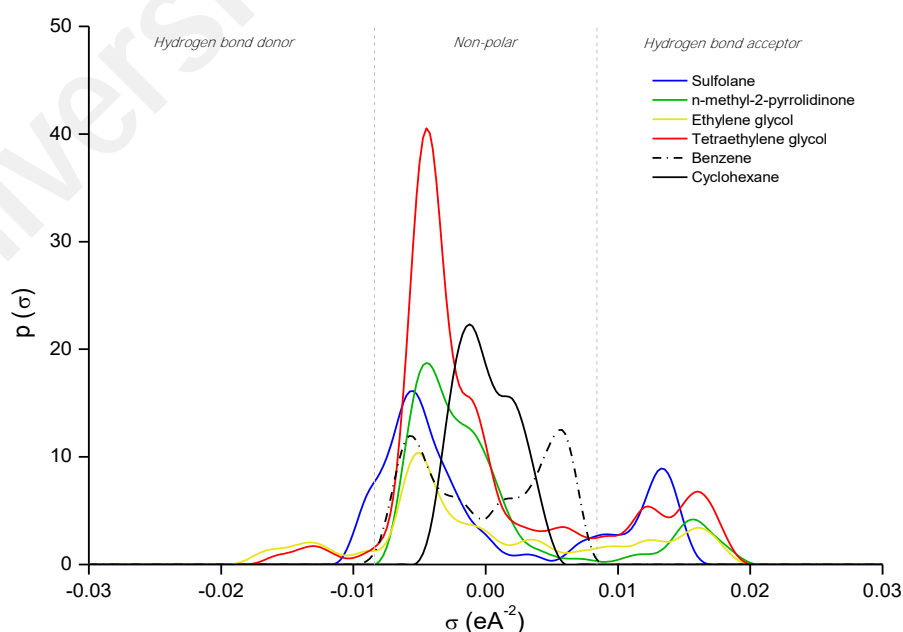
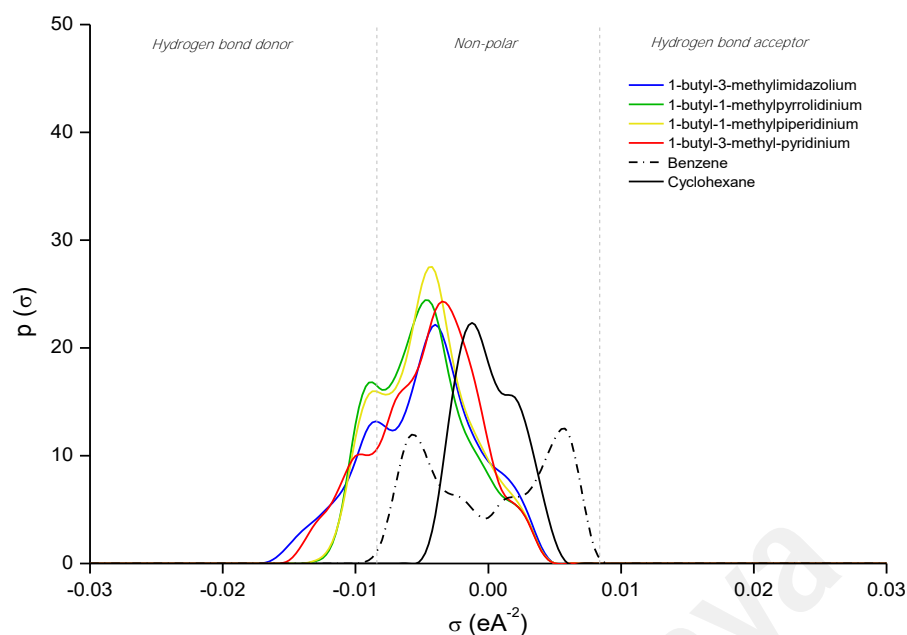


Figure 4.18:  $\sigma$ -profiles of benzene, cyclohexane and industrial organic solvents



**Figure 4.19:  $\sigma$ -profiles of benzene, cyclohexane and ILs with cyclic cations**

As seen in  $\sigma$ -profile graphs, both benzene and cyclohexane have curves in the non-polar region. Therefore, to establish a good interaction with benzene, the extracting solvent should possess a non-polar character as well. Based on Figure 4.18, the selected industrial solvents are capable of interacting with benzene as they show curves with a non-polar character with peaks at approximately  $-0.005 \text{ e}\text{\AA}^{-2}$ . The increase in the alkyl chain from ethylene glycol to tetraethylene glycol led to a higher peak and created a larger interacting area with cyclohexane. In addition to its high interaction with benzene, tetraethylene glycol also exhibits high interaction with cyclohexane. Hence, tetraethylene glycol has a higher capacity but lower selectivity compared to ethylene glycol.

To analyze the interactions in the non-polar region, the  $\sigma$ -profiles of the ILs in Figure 4.19 are represented by cations with same alkyl chains (butyl and methyl). In this work, the screening of cation is narrowed down to the cyclic types as the non-cyclic cations exhibited low performance in the extraction of aromatic compounds (Salleh, Wilfred, & Ibrahim, 2014). Like organic solvents, the major peak for IL cations also existed within the non-polar region. However, these cations also have curves at the polar regions, which indicated that they could be utilized for the extraction of both polar and non-polar solutes.

In the non-polar region, the curves were of similar types and it was difficult to select the suitable cations using only the qualitative  $\sigma$ -profile. Thus, a quantitative screening was carried out in COSMO-RS by calculating the  $\gamma^\infty$  to obtain the value of  $C^\infty$ ,  $S^\infty$  and  $PI^\infty$ .

#### 4.2.1.2 $C^\infty$ , $S^\infty$ and $PI^\infty$

The value of  $C^\infty$ ,  $S^\infty$  and  $PI^\infty$  indicate the quantitative interaction between the three molecules involved at infinite dilution. As shown in Figure 4.20, the capacity of the ILs generally increases with longer cation alkyl chain. For instance, for the IL series  $C_n\text{mimEtSO}_4$  ( $n=2, 4, 6, 8$ ), the capacity increased in the order of  $C_2\text{mimEtSO}_4 < C_4\text{mimEtSO}_4 < C_6\text{mimEtSO}_4 < C_8\text{mimEtSO}_4$ . This could also be evaluated by the change in color for each IL symbol from green (ethyl group) to black (octyl group).

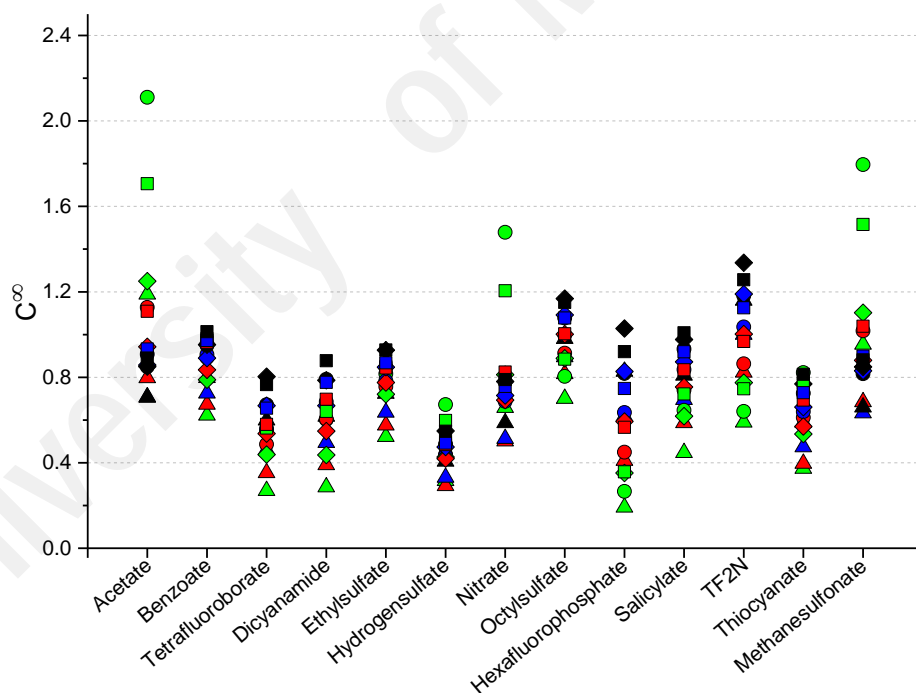


**Figure 4.20: Capacity of the screened ILs at infinite dilution:  $\blacktriangle$ ,  $C_n\text{mim}^+$ ;  $\blacklozenge$ ,  $C_n\text{mpyr}^+$ ;  $\bullet$ ,  $C_n\text{mpyrro}^+$ ;  $\blacksquare$ ,  $C_n\text{mpip}^+$  and the fill colors of green, red, blue and black indicate the cation alkyl length ( $n$ ) from ethyl, butyl, hexyl and octyl, respectively.**

However, some ILs exceptionally showed an arbitrary relation with the cation alkyl chain length, which can be categorized into three groups: 1) imidazolium- and piperidinium-based ILs that contain  $[\text{Ac}]^-$ ; all ILs that contain  $[\text{MeSO}_3]^-$ ; and

piperidinium-based ILs that contain  $[\text{NO}_3]^-$ . This indicates that according to the COSMO-RS calculations, the molecular property (such as polarity, size and structure) of  $[\text{Ac}]^-$ ,  $[\text{MeSO}_3]^-$  and  $[\text{NO}_3]^-$  in the respective cases has an exceptionally stronger effect towards the capacity of ILs, rather than the cation alkyl chain. It also proved that the statistical thermodynamics and quantum chemical approaches used by COSMO-RS may not perfectly satisfy the real nature of all ILs.

On the other hand, the selectivity of the ILs decreased with increasing cation alkyl length, as seen in Figure 4.21. The capacity of an IL reflects its ability to extract other components regardless of their specific structure, while the selectivity evaluates the efficiency of the solvent for extracting a component, or more specifically, the solute (benzene in this case).

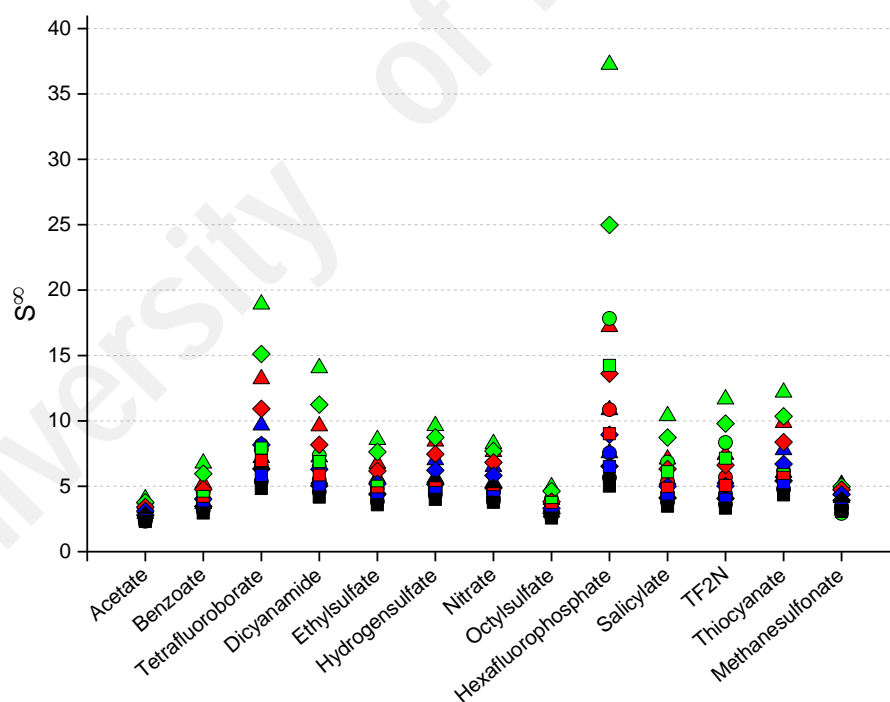


**Figure 4.21: Selectivity of the screened ILs at infinite dilution:  $\blacktriangle$ ,  $\text{C}_n\text{mim}^+$ ;  $\blacklozenge$ ,  $\text{C}_n\text{mpyr}^+$ ;  $\bullet$ ,  $\text{C}_n\text{mpyrro}^+$ ;  $\blacksquare$ ,  $\text{C}_n\text{mpip}^+$  and the fill colors of green, red, blue and black indicate the cation alkyl length (n) from ethyl, butyl, hexyl and octyl, respectively.**

In liquid–liquid extraction process, capacity indicates the amount of solvent required, whereas selectivity evaluates the extraction efficiency. It is ideal to have an extracting

solvent with high capacity and selectivity. However, the capacity of a solvent is generally inversely related to its selectivity, as shown in Figure 4.22 for the ILs involved in this study. This relation makes it difficult to obtain ILs with high values of both capacity and selectivity. Therefore, in solvent-screening process, a conflict exists for either one of these properties.

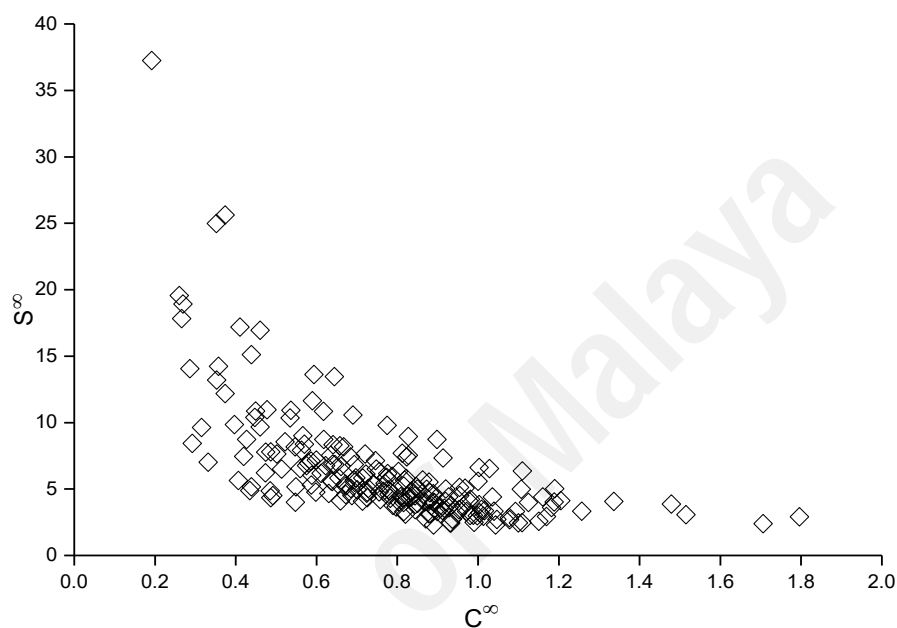


**Figure 4.22:  $S^\infty$  vs  $C^\infty$  for the screened ILs in this study**

The performance index in Figure 4.22 combines both selectivity and capacity by a simple multiplication. Thus, the PI is a mathematical operation that enables evaluation of the overall extraction performance by accommodating the inverse relation between  $C^\infty$  and  $S^\infty$ .

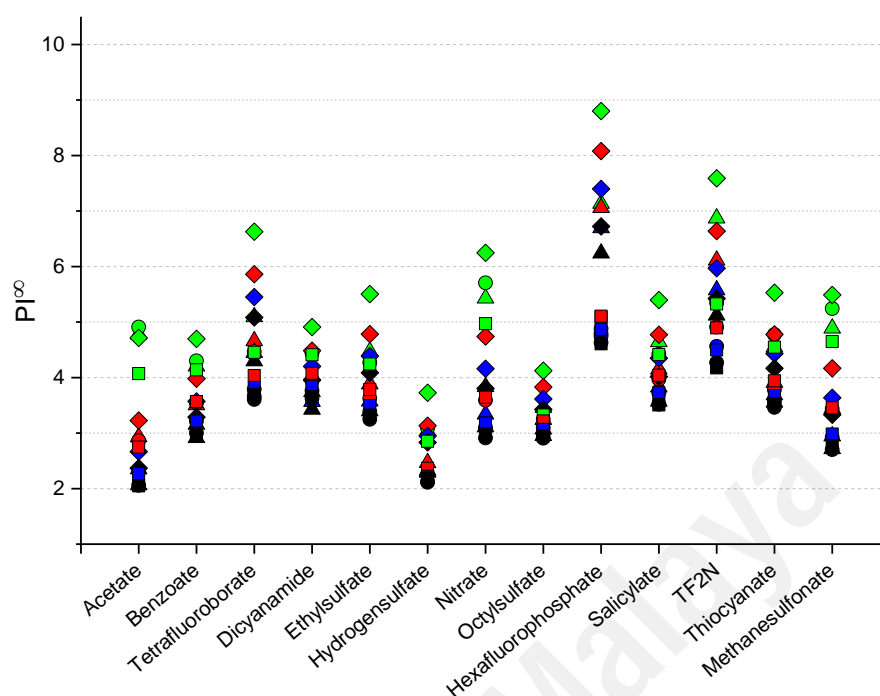


**Figure 4.23: Performance index of the screened ILs at infinite dilution: ▲,  $C_n\text{mim}^+$ ; ◆,  $C_n\text{mpyr}^+$ ; ●,  $C_n\text{mpyrro}^+$ ; ■,  $C_n\text{mpip}^+$  and the fill colors of green, red, blue and black indicate the cation alkyl length (n) from ethyl, butyl, hexyl and octyl, respectively.**

#### 4.2.1.3 Selection of ILs for experimental validation

From the screening result, fifteen ILs for each evaluation criteria were shortlisted in Table 4.4. It is worth noting that the pyrrolidinium- and piperidinium-based ILs showed high  $C^\infty$ , while the imidazolium- and pyridinium-based ILs showed high  $S^\infty$ . This trend validates the effect of aromaticity of the cation towards the capacity and selectivity of ILs. Since benzene is an aromatic compound, the presence of C=C in the ring structure of imidazolium and pyridinium cations enhances the interaction between the cation and benzene via  $\pi$ - $\pi$  interaction, thus increasing the selectivity. In contrast, the C=C bond is not present in the pyrrolidinium and piperidinium structure. This reduces the cation-benzene interactions, thus resulting in an increase in the capacity of the IL. The high value of  $S^\infty$  for  $C_2\text{mimSCN}$  observed in this work is consistent with a previous report wherein a different screening technique (gas liquid chromatography (GLC)) was utilized (Domańska & Marciniak, 2008). Since the COSMO-RS screening is an *a-priori* method

which does not require experimental data, this result proved the reliability and advantage of using COSMO-RS to screen a large number of solvents.

**Table 4.4: The top 15 ILs according to COSMO-RS screening by  $C^\infty$ ,  $S^\infty$  and  $PI^\infty$**

No	Capacity		Selectivity		Performance Index	
	IL	$C^\infty$	IL	$S^\infty$	IL	$PI^\infty$
1	C <sub>2</sub> mpyrroAc	2.11	C <sub>2</sub> mimPF <sub>6</sub>	37.25	C <sub>2</sub> mpyrPF <sub>6</sub>	8.80
2	C <sub>2</sub> mpyrroMeSO <sub>3</sub>	1.80	C <sub>2</sub> mpyrPF <sub>6</sub>	24.98	C <sub>4</sub> mpyrPF <sub>6</sub>	8.08
3	C <sub>2</sub> mpipAc	1.71	C <sub>2</sub> mimBF <sub>4</sub>	18.92	C <sub>2</sub> mpyrTF <sub>2</sub> N	7.59
4	C <sub>2</sub> mpipMeSO <sub>3</sub>	1.52	C <sub>2</sub> mpyrroPF <sub>6</sub>	17.83	C <sub>6</sub> mpyrPF <sub>6</sub>	7.40
5	C <sub>2</sub> mpyrroNO <sub>3</sub>	1.48	C <sub>4</sub> mimPF <sub>6</sub>	17.19	C <sub>2</sub> mimPF <sub>6</sub>	7.13
6	C <sub>8</sub> mpyrTF <sub>2</sub> N	1.34	C <sub>2</sub> mpyrBF <sub>4</sub>	15.12	C <sub>4</sub> mimPF <sub>6</sub>	7.06
7	C <sub>8</sub> mpipTF <sub>2</sub> N	1.26	C <sub>2</sub> mpipPF <sub>6</sub>	14.24	C <sub>2</sub> mimTF <sub>2</sub> N	6.87
8	C <sub>2</sub> mpyrAc	1.25	C <sub>2</sub> mimN(CN) <sub>2</sub>	14.05	C <sub>8</sub> mpyrPF <sub>6</sub>	6.72
9	C <sub>2</sub> mpipNO <sub>3</sub>	1.20	C <sub>4</sub> mpyrPF <sub>6</sub>	13.61	C <sub>6</sub> mimPF <sub>6</sub>	6.69
10	C <sub>6</sub> mpyrTF <sub>2</sub> N	1.19	C <sub>4</sub> mimBF <sub>4</sub>	13.20	C <sub>4</sub> mpyrTF <sub>2</sub> N	6.64
11	C <sub>2</sub> mimAc	1.19	C <sub>2</sub> mimSCN	12.18	C <sub>2</sub> mpyrBF <sub>4</sub>	6.63
12	C <sub>8</sub> mpyrroTF <sub>2</sub> N	1.18	C <sub>2</sub> mimTF <sub>2</sub> N	11.65	C <sub>2</sub> mpyrNO <sub>3</sub>	6.25
13	C <sub>8</sub> mpyrOcSO <sub>4</sub>	1.17	C <sub>2</sub> mpyrN(CN) <sub>2</sub>	11.25	C <sub>8</sub> mimPF <sub>6</sub>	6.24
14	C <sub>8</sub> mimTF <sub>2</sub> N	1.16	C <sub>4</sub> mpyrBF <sub>4</sub>	10.92	C <sub>4</sub> mimTF <sub>2</sub> N	6.11
15	C <sub>8</sub> mpipOcSO <sub>4</sub>	1.15	C <sub>4</sub> mpyrroPF <sub>6</sub>	10.86	C <sub>6</sub> mpyrTF <sub>2</sub> N	5.97

It is known that despite the large number of possible ILs, only some are available in the market or can be possibly produced by laboratory synthesis. A market survey concluded that most of the ILs in Table 4.4 are not available commercially. Although ILs C<sub>2</sub>mimPF<sub>6</sub>, C<sub>4</sub>mimPF<sub>6</sub>, C<sub>2</sub>mpyrroPF<sub>6</sub>, C<sub>4</sub>mpyrroPF<sub>6</sub> and C<sub>2</sub>mpyrroTf<sub>2</sub>N are commercially available, their use is economically limited owing to the extremely high cost. Despite their unavailability, the screening results could still be regarded as a motivation for their synthesis in the future.

Interestingly, four ILs in Table 4.4 are available for purchase at relatively low prices, namely, the high  $C^\infty$  IL (C<sub>2</sub>mimAc), the high  $S^\infty$  ILs (C<sub>2</sub>mimN(CN)<sub>2</sub> and C<sub>2</sub>mimSCN),

and the high  $\text{PI}^\infty$  IL ( $\text{C}_2\text{mimTf}_2\text{N}$ ). Besides, these ILs have also been recognized in other studies for different applications.  $\text{C}_2\text{mimAc}$  was found as a good IL for the dissolution of soft and hard wood (Shiflett et al., 2010) and for an effective conversion of cellulose into cellulose acetate (Köhler et al., 2007).  $\text{C}_2\text{mimSCN}$  was reportedly highly selective in the desulfurization process (Kędra-Królik, Fabrice, & Jaubert, 2011) and was successfully utilized for the separation of aromatic/aliphatic mixtures (Domańska & Marciniak, 2008). The IL  $\text{C}_2\text{mimN}(\text{CN})_2$ , apart from having low viscosity and water-miscible properties (MacFarlane et al., 2001), was shown to be also capable of effectively extracting the heterocyclic sulfur compounds (thiophene and dibenzothiophene) from model oil (Yu et al., 2011). It has been demonstrated that  $\text{C}_2\text{mimTf}_2\text{N}$  has an extremely high capacity for dissolving  $\text{CO}_2$  gas (Schilderman, Raeissi, & Peters, 2007) and shows potential in surfactant technology because of its aggregation behavior with some common non-ionic surfactants (Fletcher & Pandey, 2004). Considering the advantages of ILs over conventional solvents, the selection of these ILs for the separation of benzene and cyclohexane could be more economical and efficient.

#### 4.2.2 Settling time study

Settling time is one of the requirements to ensure an optimal extraction process. In general, the equilibrium condition is characterized by equal values of pressure, temperature, and chemical potential in both phases. This study was performed to determine the minimum time for the top and bottom phases to reach equilibrium after the mixing is stopped. This could be represented by the mean of unchanged concentration of benzene in the extract layer. The ternary system of  $\text{C}_2\text{mimAc}$  + benzene + cyclohexane was taken as an example. As depicted in Figure 4.24, although the mixture was left undisturbed for 3 h, the molar concentration of benzene in the extract layer remained constant or reached equilibrium after 5 mins. The molar concentration of the IL and cyclohexane also remained almost constant throughout this time. The same settling results

were observed for  $C_2mimN(CN)_2$ ,  $C_2mimSCN$ , and  $C_2mimTf_2N$ , indicating a good separation between the two phases after extraction.

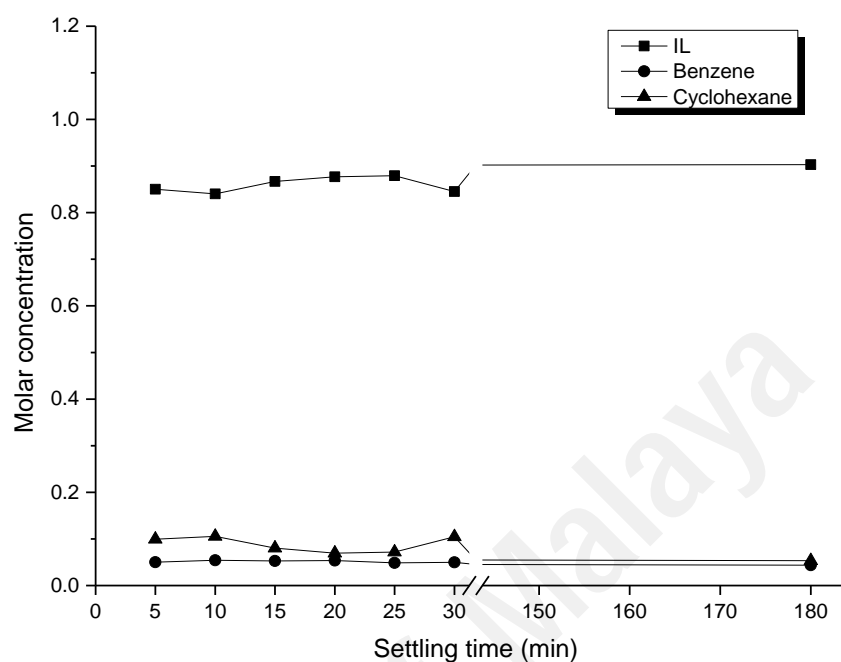


**Figure 4.24: Molar concentration of individual species in extract phase versus time after extraction**

### 4.2.3 Ternary LLE data

The molar composition of the tie-lines for each ternary system are tabulated in Table 4.5. As observed, the absence of IL in the raffinate layer ( $X_{IL,raf} = 0$ ) in all the systems studied indicates a favorable extraction process because the solvent cross-contamination could be avoided. The low concentrations of cyclohexane in the extract layer ( $X_{Ch,ext} < 0.1$ ) indicated an easier regeneration of the IL. In addition, all systems showed feasible extraction process as the experimental selectivity values were far from unity.

**Table 4.5: Molar composition of the tie-lines with the distribution ratio and selectivity data for benzene (1) + cyclohexane (2) + ILs (3) at 25 °C and 1 atm**

Raffinate layer			Extract layer			<i>D</i>	<i>S</i>
<i>x</i> <sub>1</sub>	<i>x</i> <sub>2</sub>	<i>x</i> <sub>3</sub>	<i>x</i> <sub>1</sub>	<i>x</i> <sub>2</sub>	<i>x</i> <sub>3</sub>		
<b>benzene (1) + cyclohexane (2) + C<sub>2</sub>mimAc (3)</b>							
0.085	0.915	0.000	0.036	0.021	0.943	0.42	18.34
0.175	0.825	0.000	0.085	0.069	0.847	0.48	10.33
0.264	0.736	0.000	0.140	0.040	0.820	0.53	10.15
0.360	0.640	0.000	0.180	0.034	0.776	0.50	9.56
0.462	0.538	0.000	0.212	0.033	0.755	0.46	7.44
0.561	0.439	0.000	0.218	0.040	0.742	0.39	4.26
<b>benzene (1) + cyclohexane (2) + C<sub>2</sub>mimN(CN)<sub>2</sub> (3)</b>							
0.073	0.927	0.000	0.049	0.020	0.932	0.67	31.85
0.158	0.842	0.000	0.095	0.018	0.886	0.61	27.94
0.247	0.753	0.000	0.141	0.016	0.844	0.57	27.48
0.339	0.661	0.000	0.184	0.015	0.801	0.54	23.51
0.426	0.574	0.000	0.232	0.016	0.752	0.54	19.23
0.522	0.478	0.000	0.275	0.015	0.710	0.53	16.84
<b>benzene (1) + cyclohexane (2) + C<sub>2</sub>mimSCN (3)</b>							
0.082	0.918	0.000	0.038	0.010	0.953	0.46	44.71
0.168	0.832	0.000	0.077	0.012	0.910	0.46	31.18
0.259	0.741	0.000	0.114	0.010	0.876	0.44	32.73
0.351	0.649	0.000	0.149	0.009	0.842	0.42	30.94
0.450	0.550	0.000	0.184	0.008	0.808	0.41	26.53
0.553	0.447	0.000	0.222	0.007	0.771	0.40	25.22
<b>benzene (1) + cyclohexane (2) + C<sub>2</sub>mimTf<sub>2</sub>N (3)</b>							
0.078	0.922	0.000	0.095	0.059	0.846	1.22	19.09
0.157	0.843	0.000	0.185	0.058	0.757	1.18	17.14
0.243	0.757	0.000	0.259	0.057	0.685	1.07	14.28
0.332	0.668	0.000	0.331	0.054	0.615	1.00	12.36
0.417	0.583	0.000	0.396	0.054	0.549	0.95	10.24
0.518	0.482	0.000	0.459	0.054	0.487	0.89	7.91

The LLE diagrams for the ternary systems of  $C_2mimAc / C_2mimN(CN)_2 / C_2mimSCN$  /  $C_2mimTf_2N + benzene + cyclohexane$  are displayed in Figures 4.24 to 4.27, respectively.

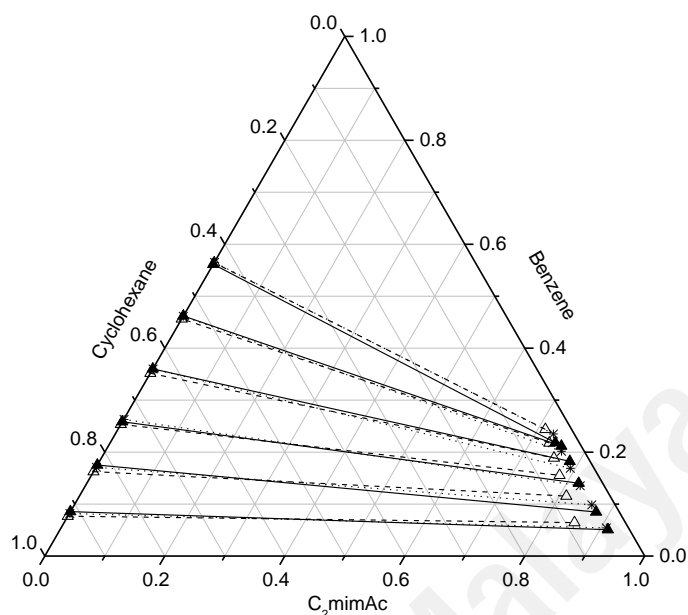


**Figure 4.25: Ternary LLE diagram for  $C_2mimAc + benzene + cyclohexane$  at 25 °C and 1 atm. The symbols are represented by:  $\blacktriangle$ , experimental;  $--\Delta--$ , COSMO-RS; and  $\cdots\times\cdots$ , NRTL.**

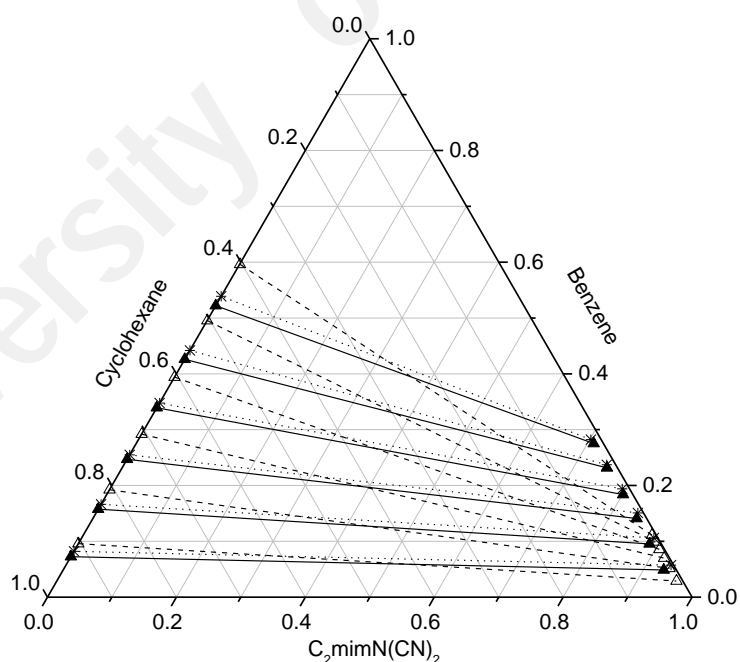


**Figure 4.26: Ternary LLE diagram for  $C_2mimN(CN)_2 + benzene + cyclohexane$  at 25 °C and 1 atm. The symbols are represented by:  $\blacktriangle$ , experimental;  $--\Delta--$ , COSMO-RS; and  $\cdots\times\cdots$ , NRTL.**

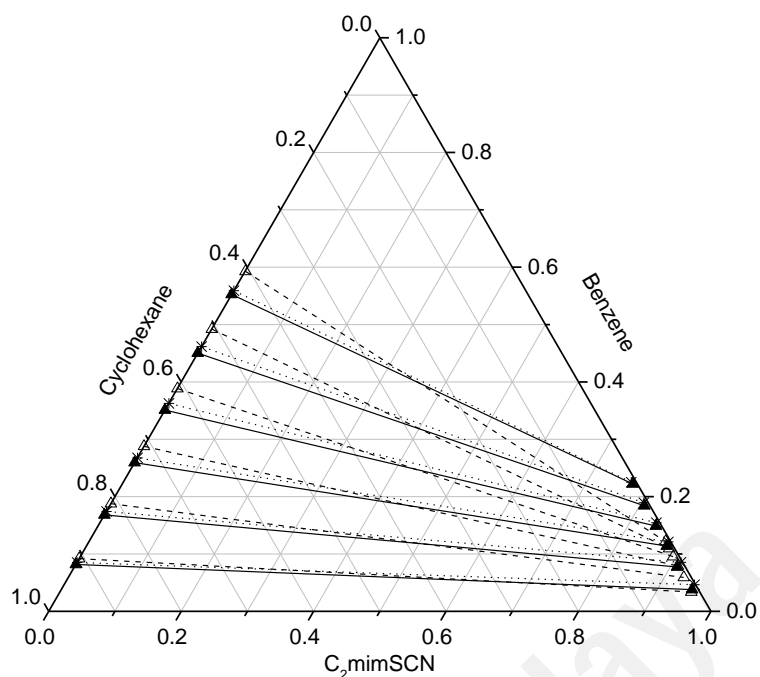


**Figure 4.27: Ternary LLE diagram for  $C_2mimSCN$  + benzene + cyclohexane at 25 °C and 1 atm. The symbols are represented by:  $\blacktriangle$ , experimental;  $\triangle$ , COSMO-RS; and  $\cdot \times \cdot$ , NRTL.**

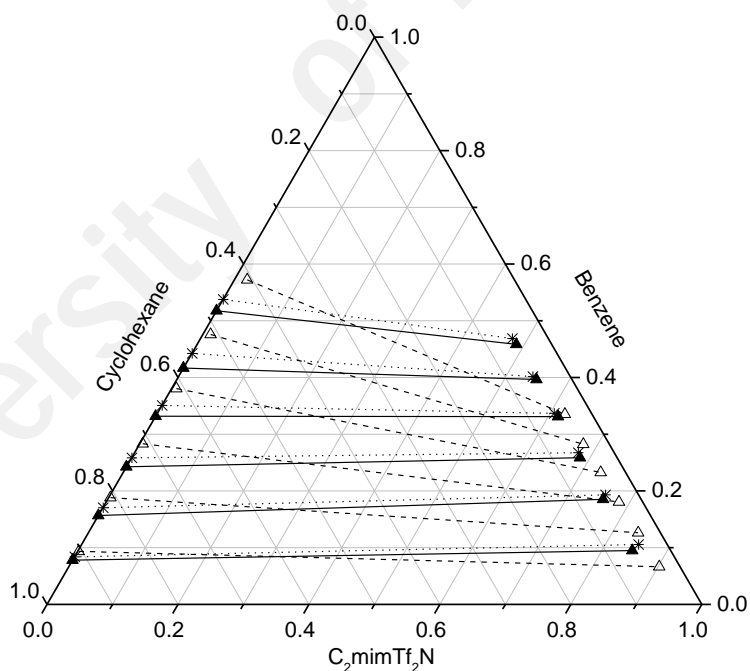


**Figure 4.28: Ternary LLE diagram for  $C_2mimTf_2N$  + benzene + cyclohexane at 25 °C and 1 atm. The symbols are represented by:  $\blacktriangle$ , experimental;  $\triangle$ , COSMO-RS; and  $\cdot \times \cdot$ , NRTL.**

As seen in these figures, the tie lines obtained from the experimental and COSMO-RS approaches showed good agreement for all ternary systems, except for  $C_2mimN(CN)_2$  and  $C_2mimTf_2N$ , which showed deviations. The tie lines for every ternary system were

negative, except in the case of C<sub>2</sub>mimTf<sub>2</sub>N, where a positive slope was observed at higher concentrations of benzene. Again, the absence of ILs in raffinate layer and the low concentration of cyclohexane in extract layer can be visually observed in all ternary systems.

In addition, the value of parameters  $a$ ,  $b$ ,  $c$ ,  $d$ , and  $R^2$  for the consistency tests of each ternary system are listed in Table 4.6. The linearity of each plot (i.e. the value of  $R^2$  close to unity) indicates the excellent degree of consistency for the ternary LLE tie lines reported in this work.

**Table 4.6: Parameters of Othmer-Tobias and Hand correlation for each ternary system and the values of regression coefficient,  $R^2$**

Ternary System	Othmer-Tobias			Hand		
	$a$	$b$	$R^2$	$c$	$d$	$R^2$
C <sub>2</sub> mimAc	1.400	2.297	0.878	1.175	2.142	0.933
C <sub>2</sub> mimN(CN) <sub>2</sub>	1.534	2.624	0.999	1.306	2.261	0.998
C <sub>2</sub> mimSCN	1.481	2.977	0.993	1.320	2.681	0.991
C <sub>2</sub> mimTf <sub>2</sub> N	1.458	2.239	1.000	1.190	1.906	0.996

#### 4.2.4 Comparison between COSMO-RS and experimental results

As seen in Figure 4.25, the COSMO-RS and experimental data for the system involving C<sub>2</sub>mimAc achieved a very good agreement, especially in the raffinate phase. It is worth noting that although the predicted concentration of cyclohexane in the extract decreases steadily with increasing concentration of benzene, the experimental data remains almost constant. Thus, based on the experimental data, the low mutual solubility of cyclohexane with the ILs is constant regardless the concentration of benzene in the feed. This indicates a steady performance of ILs in retaining the low interaction with the cyclohexane, and therefore reduces the cross-contamination effect.

In contrast to  $C_2mimAc$ , the other three ILs showed close values between COSMO-RS and experimental approaches for the concentration of cyclohexane in the extract phase. COSMO-RS also estimated a higher slope than the experimental values for the tie lines in the ternary systems involving  $C_2mimN(CN)_2$  (Figure 4.26). This suggests that COSMO-RS underestimates the affinity of benzene toward the IL and overestimates its affinity toward cyclohexane. The ternary system involving  $C_2mimSCN$  in Figure 4.27 also showed similar results but with lower discrepancies. On the other hand, the predicted tie lines for the ternary system with  $C_2mimTf_2N$  (Figure 4.28) showed negative slope with high magnitude, while the slope of the experimental tie lines were initially positive and changed to negative at higher feed concentrations of benzene. This implies that the actual extraction of benzene using  $C_2mimTf_2N$  at lower feed concentration will produce distribution ratio of greater than unity.

As seen in Figure 4.29, the IL with a high  $PI^\infty$  showed a high distribution ratio. Meanwhile, both COSMO-RS and experimental data gave the same trend of selectivity,  $C_2mimAc < C_2mimTf_2N < C_2mimN(CN)_2 < C_2mimSCN$  (Figure 4.30). Although the experimentally observed selectivity had a higher difference between  $C_2mimN(CN)_2$  and  $C_2mimSCN$  than predicted, it still proves that COSMO-RS is a reliable tool to find ILs with high selectivity.

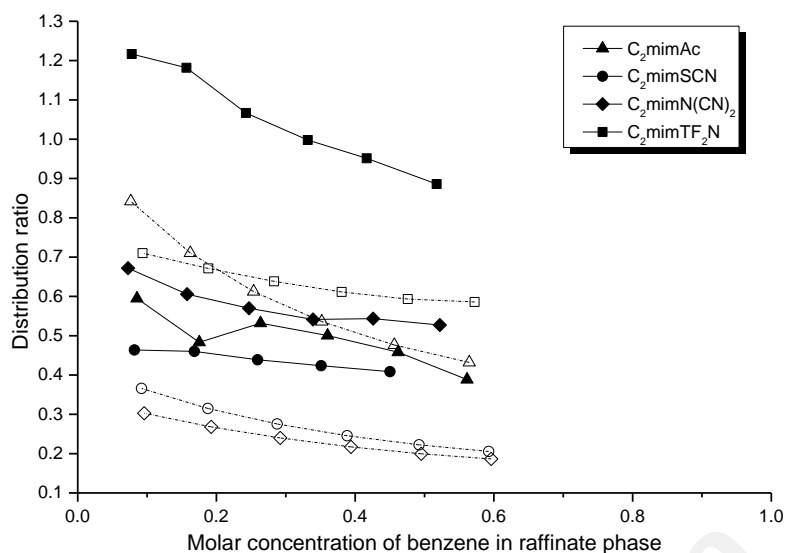


**Figure 4.29: Distribution ratio of benzene versus mole fraction of benzene in raffinate phase for five ternary systems in this study. The solid and dashed lines indicate experimental and COSMO-RS data, respectively.**

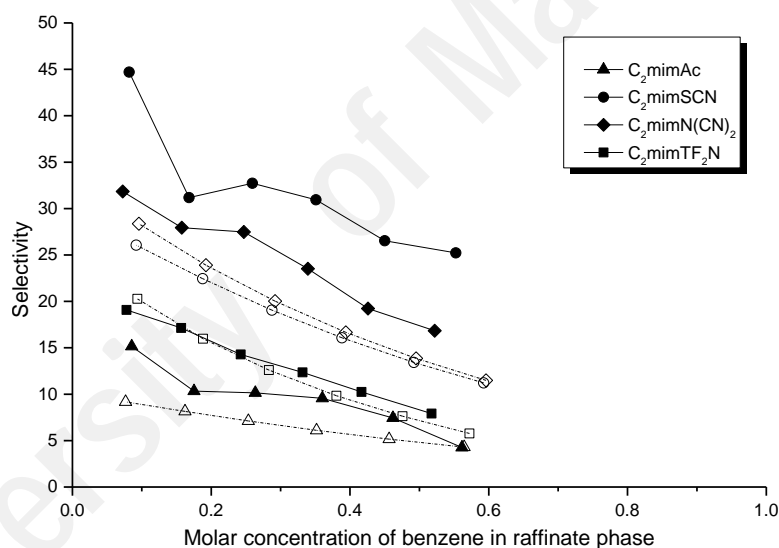


**Figure 4.30: Selectivity of ILs versus mole fraction of benzene in raffinate phase for five ternary systems in this study. The solid and dashed lines indicate experimental and COSMO-RS data, respectively.**

The quantitative comparison between the experimental and COSMO-RS results can be evaluated from their value of RMSD. The molar composition of the tie lines generated by COSMO-RS and the corresponding RMSD values are respectively tabulated in Table 4.7 and Table 4.8. The average RMSD value between the experimental and COSMO-RS was 4.88 %. This agreement can also be visually observed in the ternary diagrams. Considering that COSMO-RS is a fast and an *a priori* method, this value

supports the advantage of COSMO-RS as an assisting tool for thermodynamic properties calculations.

**Table 4.7: Molar composition of the tie-lines predicted by COSMO-RS for benzene (1) + cyclohexane (2) + ILs (3) at 25 °C and 1 atm**

Top layer			Bottom layer		
$x_1$	$x_2$	$x_3$	$x_1$	$x_2$	$x_3$
<b>benzene (1) + cyclohexane (2) + C<sub>2</sub>mimAc (3)</b>					
0.077	0.923	0.000	0.064	0.085	0.851
0.162	0.838	0.000	0.115	0.073	0.812
0.254	0.746	0.000	0.155	0.064	0.781
0.352	0.648	0.000	0.189	0.057	0.755
0.456	0.543	0.000	0.218	0.050	0.732
0.564	0.435	0.000	0.244	0.044	0.713
<b>benzene (1) + cyclohexane (2) + C<sub>2</sub>mimN(CN)<sub>2</sub> (3)</b>					
0.096	0.904	0.000	0.029	0.010	0.961
0.192	0.807	0.000	0.052	0.009	0.939
0.292	0.708	0.000	0.070	0.008	0.922
0.394	0.606	0.000	0.086	0.008	0.907
0.495	0.504	0.000	0.099	0.007	0.894
0.596	0.403	0.001	0.111	0.007	0.882
<b>benzene (1) + cyclohexane (2) + C<sub>2</sub>mimSCN (3)</b>					
0.092	0.908	0.000	0.034	0.013	0.954
0.188	0.812	0.000	0.059	0.011	0.930
0.288	0.712	0.000	0.079	0.010	0.910
0.388	0.611	0.000	0.095	0.009	0.895
0.492	0.507	0.000	0.109	0.008	0.882
0.593	0.407	0.001	0.122	0.007	0.871
<b>benzene (1) + cyclohexane (2) + C<sub>2</sub>mimTf<sub>2</sub>N (3)</b>					
0.094	0.905	0.002	0.066	0.032	0.902
0.188	0.809	0.003	0.126	0.034	0.840
0.283	0.712	0.005	0.181	0.036	0.783
0.381	0.612	0.007	0.233	0.038	0.729
0.476	0.512	0.012	0.282	0.040	0.678
0.572	0.408	0.020	0.335	0.041	0.623

**Table 4.8: RMSD values between the tie lines of COSMO-RS and experimental approaches**

Ternary system	RMSD
C <sub>2</sub> mimAc + benzene + cyclohexane	2.505
C <sub>2</sub> mimN(CN) <sub>2</sub> + benzene + cyclohexane	6.811
C <sub>2</sub> mimSCN + benzene + cyclohexane	3.807
C <sub>2</sub> mimTf <sub>2</sub> N + benzene + cyclohexane	6.410

#### 4.2.5 Comparison of the selected ILs with other solvents

The efficiency of the extraction process can be evaluated from the distribution ratio of solute (benzene in this case) and the selectivity of the solvent. Figure 4.31 and Figure 4.32 compare the values from this work with some of the previous reports that used different types of extracting solvent, namely, organic solvents (Aspi et al., 1998; Chen, Li, & Duan, 2000) and ILs (Calvar et al., 2011; E. González et al., 2010a; Lyu et al., 2014b; Sakal, Shen, & Li, 2012; Zhou et al., 2012a; Zhou et al., 2012b). Additionally, to compare the performance of ILs and DESs, the extraction results using DESs (Salleh et al., 2017b) as discussed in Section 4.1 are included. Sulfolane was involved as a benchmark to represent the performance of the common organic solvents used in industry. The organic solvents with high selectivity (ethylene glycol (EG)) and distribution ratio (dimethylformamide (DMF)) (Aspi et al., 1998) were also included.

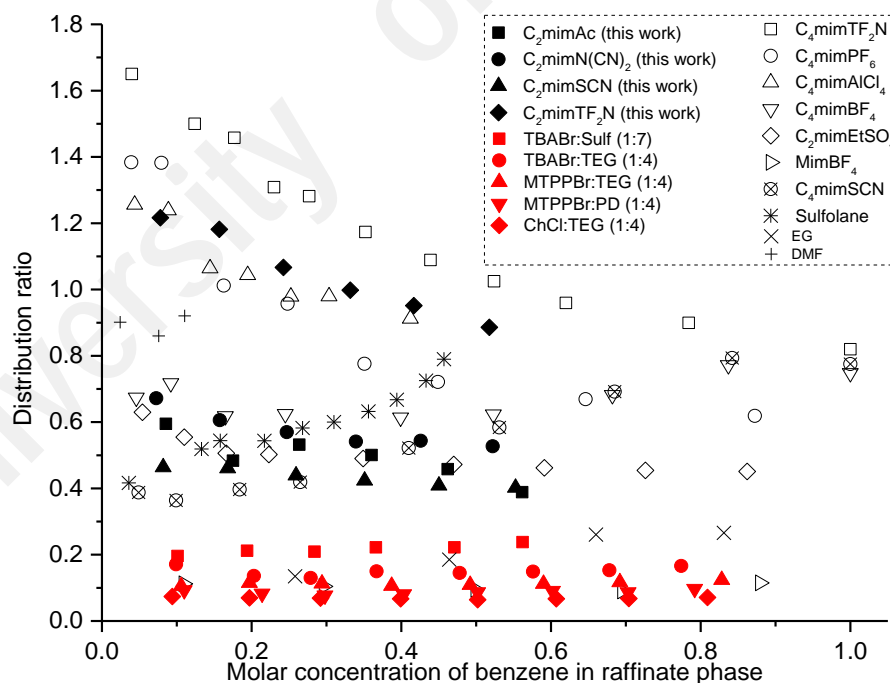
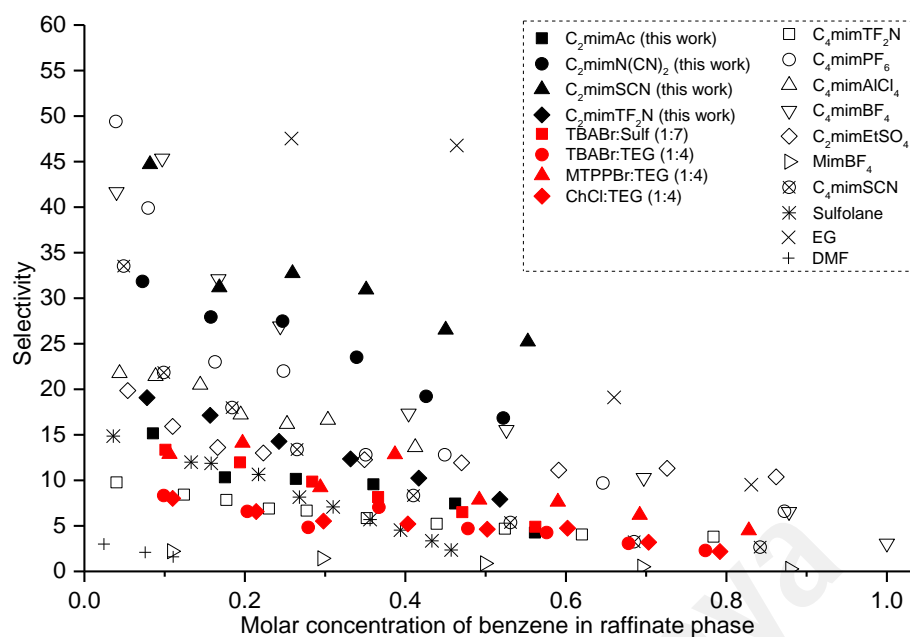


Figure 4.31: Distribution ratio of organic solvents, ILs and DESs for the extractive separation of benzene and cyclohexane



**Figure 4.32: Selectivity of organic solvents, ILs and DESs for the extractive separation of benzene and cyclohexane**

At low concentrations of benzene in the raffinate phase ( $x_{Bz,raff} < 0.3$ ), the distribution ratio for all ILs were higher than that of sulfolane. Furthermore, all ILs in this study displayed higher selectivity than that of sulfolane, confirming the potential of ILs as alternatives solvents. It was also observed that the extraction performances of the ILs were higher than that of the DESs.

These results indicate the advantages and drawbacks of each extracting solvent in the extractive separation of benzene and cyclohexane. Although the organic solvents are cheaper with moderate performance, they are limited by their high volatility and complex process. While ILs have higher extractive performance than organic solvents and DESs, their use is limited because they are expensive and possibly toxic (Zhao, Liao, & Zhang, 2007). On the other hand, although the DESs are cheaper, can be easily synthesized, and environmentally friendly, their extractive performance is rather low. Nevertheless, as shown in Section 4.1, DESs can still be used because of efficient extraction with multiple stages and easy regeneration (Salleh et al., 2017b).

It is noteworthy that three ILs, namely,  $C_4mimTf_2N$ , (Calvar et al., 2011)  $C_4MimPF_6$  (Zhou et al., 2012a) and  $C_4mimAlCl_4$  (Lyu et al., 2014a) showed exceptionally higher distribution ratio than this work. However, the use of each of these ILs as the extracting solvent was associated with significant drawbacks. Although the extraction using  $C_4mimTf_2N$  showed the highest distribution ratio, its selectivity was relatively much lower than that of the other ILs. For the extraction using  $C_nmimPF_6$  ( $n = 4, 5, 6$ ) ( $n = 4, 5, 6$ ) (Zhou et al., 2012a), the high distribution ratio was mitigated by the cost of operation because it is a highly expensive type of IL. The IL  $C_4mimAlCl_4$  is reportedly unstable in humid air, which makes process handling difficult.

#### 4.2.6 NRTL correlation

The RMSD values between experimental and NRTL calculations for both ternary systems are less than 2 %, which indicates that NRTL correlation represents the experimental data very well. This excellent fitting is also obvious from Figure 4.25 to Figure 4.28. Table 4.9 shows the values of NRTL binary interaction parameters regressed for each ternary system. To conserve coherence between this work and the previous one applied to deep eutectic solvents for the same binary mixture, the binary interaction parameters between benzene and cyclohexane, despite the IL used, were taken from Table 4.2 without any adjustment.

**Table 4.9: Binary interaction parameters in NRTL regression for the ternary systems in this study with RMSD between experimental and calculated data.**

<b>Ternary system</b>	<b>i</b>	<b>j</b>	<b><math>\tau_{ij}</math></b>	<b><math>\tau_{ji}</math></b>	<b>RMSD (%)</b>
	Benzene	Cyclohexane	-189.57	453.65	
<b>Benzene + cyclohexane + C<sub>2</sub>MimAc</b>	Benzene	C <sub>2</sub> mimAc	3924.03	64.56	1.174
	Cyclohexane	C <sub>2</sub> mimAc	1780.45	535.69	
<b>Benzene + cyclohexane + C<sub>2</sub>MimN(CN)<sub>2</sub></b>	Benzene	C <sub>2</sub> mimN(CN) <sub>2</sub>	5016.78	148.12	0.881
	Cyclohexane	C <sub>2</sub> mimN(CN) <sub>2</sub>	2108.46	1340.29	
<b>Benzene + cyclohexane + C<sub>2</sub>MimSCN</b>	Benzene	C <sub>2</sub> mimSCN	4424.45	159.42	0.614
	Cyclohexane	C <sub>2</sub> mimSCN	1911.05	1655.71	
<b>Benzene + cyclohexane + C<sub>2</sub>MimTf<sub>2</sub>N</b>	Benzene	C <sub>2</sub> mimTf <sub>2</sub> N	7289.11	110.31	1.174
	Cyclohexane	C <sub>2</sub> mimTf <sub>2</sub> N	1878.57	532.41	

### 4.3 Extractive separation of benzene and cyclohexane using binary ILs

#### 4.3.1 Mixing of IL with organic solvents

The solvent extraction performance in an LLE process can be evaluated through the selectivity and distribution ratio. However, these criteria usually show an inversely proportional relationship. This is the motivation to develop a binary solvent mixture in which the overall extraction performance can be improved by combining a solvent with high capacity with another solvent having high selectivity. EG and DMF reportedly exhibit high selectivity and distribution ratio values, respectively (Aspi et al., 1998). Meanwhile, the results previously described in Section 4.2 demonstrated that  $C_2mimSCN$  has high selectivity and  $C_2mimTf_2N$  has high distribution ratio (Salleh et al., 2018). Because of the inverse relation, the optimum binary molar fraction is indicated by the intersection point of the selectivity and distribution ratio curves. The extraction performances of the binary mixtures of [ $C_2mimSCN$  + DMF] and [ $C_2mimTf_2N$  + EG] at various mixing ratios are depicted in Figure 4.33 and Figure 4.34, respectively.

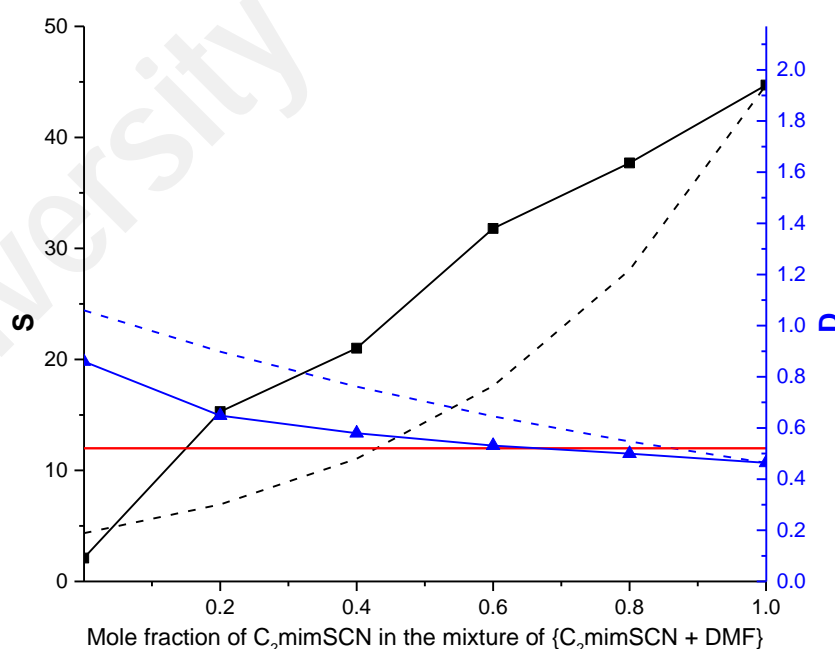


**Figure 4.33: Selectivity of solvent (—■—) and distribution ratio of benzene (—▲—) versus molar fractions of an IL in the respective binary IL mixtures for the pseudo-ternary systems of benzene + cyclohexane + [ $C_2mimSCN$  + DMF] at 25 °C and 1 atm. The solid and dashed lines indicate the experimental and calculated data, respectively. The red line refers to the selectivity and distribution ratio for sulfolane at the same condition.**

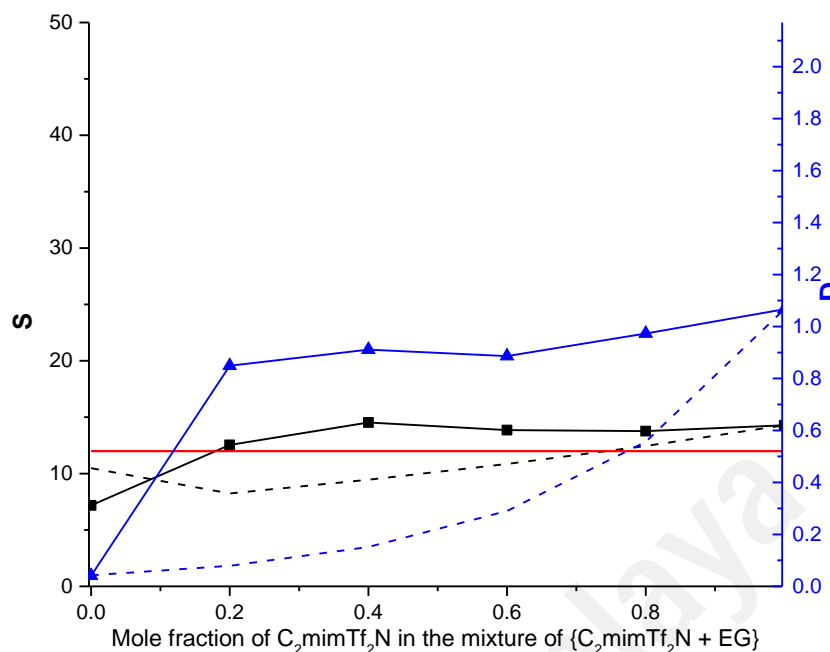


**Figure 4.34: Selectivity of solvent (—■—) and distribution ratio of benzene (—▲—) versus molar fractions of an IL in the respective binary IL mixtures for the pseudo-ternary systems of benzene + cyclohexane + [C<sub>2</sub>mimTf<sub>2</sub>N + EG] at 25 °C and 1 atm. The solid and dashed lines indicate the experimental and calculated data, respectively. The red line refers to the selectivity and distribution ratio for sulfolane at the same condition.**

As seen in Figure 4.33, 20 mol % of C<sub>2</sub>mimSCN in the mixture of [C<sub>2</sub>mimSCN + DMF] resulted in the optimal extraction performance. However, the extraction performance increased only slightly after sulfolane. On the other hand, it is interesting to note in Figure 4.34 that over the whole range of binary ratios, the selectivity of [C<sub>2</sub>mimTf<sub>2</sub>N + EG] was almost constant, while the distribution ratio increased only slightly. Furthermore, although the molar fraction of C<sub>2</sub>mimTf<sub>2</sub>N in the mixture was low, both the selectivity and distribution ratio of the binary mixture were nearly equal to that of pure C<sub>2</sub>mimTf<sub>2</sub>N. This demonstrated that the presence of a small fraction of IL in the binary mixture could dominate the distribution ratio. The mixed solvent showed constant selectivity ( $S_{\text{mix,average}} = 13.7$ ) and a slight increase in the distribution ratio ( $D_{\text{mix,average}} = 0.91$ ), both of which were comparable to the corresponding values in pure C<sub>2</sub>mimTf<sub>2</sub>N ( $S_{\text{IL}}=14.3$ ,  $D_{\text{IL}} = 1.06$ ). Both the selectivity and distribution ratio of [C<sub>2</sub>mimTf<sub>2</sub>N + EG] increased steadily when the molar fraction of IL in the binary mixture ( $X_{\text{IL}}$ ) was 0.2.

These findings showed that EG can be mixed with C<sub>2</sub>mimTf<sub>2</sub>N not only as a co-solvent, but also as a diluting agent. This could result in economic savings, as a small amount of the expensive IL can be mixed with a relatively high amount of inexpensive EG.

To provide a fair comparison between the pure and mixed solvents, the LLE data for pure DMF and EG must be measured under the same operating conditions. Thus, the LLE data for pure DMF and EG were newly measured at 25 °C and 1 atm and tabulated in Table 4.10.

**Table 4.10: Molar composition of the tie-lines with the distribution ratio and selectivity data for benzene (1) + cyclohexane (2) + DMF or EG (3) at 25 °C and 1 atm**

Raffinate layer			Extract layer			<i>D</i>	<i>S</i>
<i>x</i> <sub>1</sub>	<i>x</i> <sub>2</sub>	<i>x</i> <sub>3</sub>	<i>x</i> <sub>1</sub>	<i>x</i> <sub>2</sub>	<i>x</i> <sub>3</sub>		
<b>benzene (1) + cyclohexane (2) + DMF (3)</b>							
0.023	0.858	0.119	0.024	0.207	0.770	1.04	4.34
0.044	0.829	0.126	0.047	0.202	0.751	1.06	4.35
0.066	0.742	0.192	0.070	0.269	0.662	1.05	2.91
0.092	0.708	0.200	0.094	0.273	0.633	1.03	2.66
0.023	0.858	0.119	0.024	0.207	0.770	1.04	4.34
<b>benzene (1) + cyclohexane (2) + EG (3)</b>							
0.094	0.906	0.000	0.004	0.004	0.992	0.04	10.48
0.195	0.805	0.000	0.009	0.006	0.984	0.05	5.92
0.298	0.702	0.000	0.012	0.004	0.984	0.04	7.18
0.402	0.598	0.000	0.016	0.003	0.981	0.04	7.23

The LLE data for the pure ILs were taken from Section 4.2 (Salleh et al., 2018). For the mixed solvents, the LLE data were experimentally measured based on the optimized binary molar fractions, i.e., [0.2 C<sub>2</sub>mimSCN + 0.8 DMF] and [0.2 C<sub>2</sub>mimTf<sub>2</sub>N + 0.8 EG] and are summarized in Table 4.11. The tie lines and pseudo-ternary plots of both systems are shown in Figure 4.35 and Figure 4.36.

**Table 4.11: Molar composition of the tie-lines with the distribution ratio and selectivity data for benzene (1) + cyclohexane (2) + [IL (3) + DMF or EG (4)] at 25 °C and 1 atm**

Raffinate layer				Extract layer				<i>D</i>	<i>S</i>
$x_1$	$x_2$	$x_3$	$x_4$	$x_1$	$x_2$	$x_3$	$x_4$		
<b>benzene (1) + cyclohexane (2) + [C<sub>2</sub>mimSCN (3) + DMF (4)]</b>									
0.064	0.888	0.000	0.049	0.041	0.045	0.192	0.722	0.64	12.80
0.130	0.803	0.000	0.067	0.081	0.046	0.186	0.687	0.62	10.74
0.198	0.710	0.000	0.092	0.123	0.047	0.180	0.650	0.62	9.45
0.275	0.609	0.000	0.116	0.160	0.051	0.177	0.612	0.58	6.95
0.346	0.507	0.000	0.146	0.200	0.053	0.171	0.576	0.58	5.56
<b>benzene (1) + cyclohexane (2) + [C<sub>2</sub>mimTf<sub>2</sub>N (3) + EG (4)]</b>									
0.087	0.913	0.000	0.000	0.071	0.042	0.539	0.348	0.82	17.90
0.175	0.825	0.000	0.000	0.157	0.080	0.509	0.254	0.90	9.25
0.266	0.734	0.000	0.000	0.221	0.064	0.497	0.218	0.83	9.61
0.358	0.642	0.000	0.000	0.286	0.046	0.460	0.208	0.80	11.05
0.451	0.549	0.000	0.000	0.368	0.045	0.425	0.162	0.82	10.07

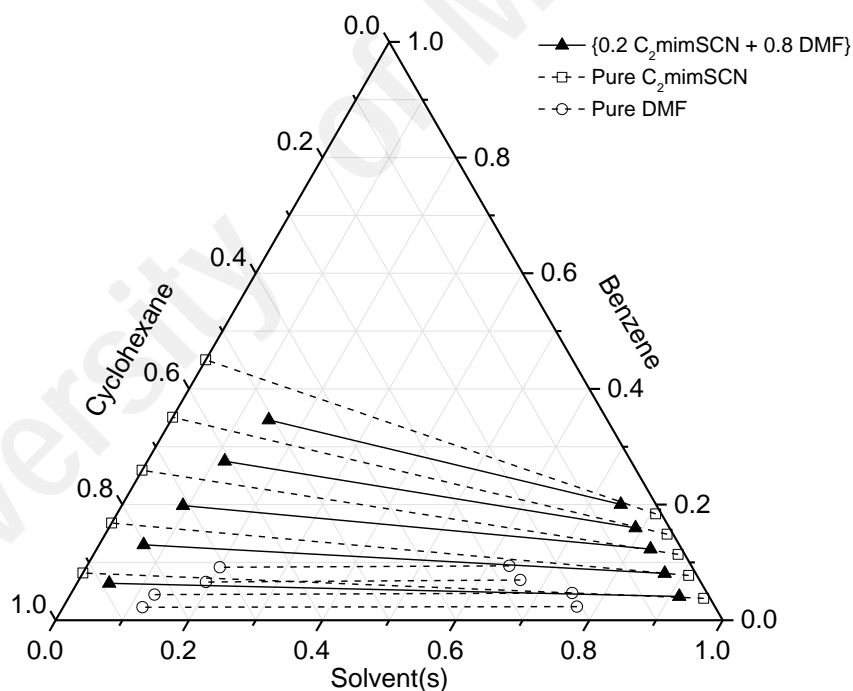


**Figure 4.35: Ternary LLE involving the mixture of [C<sub>2</sub>mimSCN + DMF] in comparison with the individual C<sub>2</sub>mimSCN or DMF.**

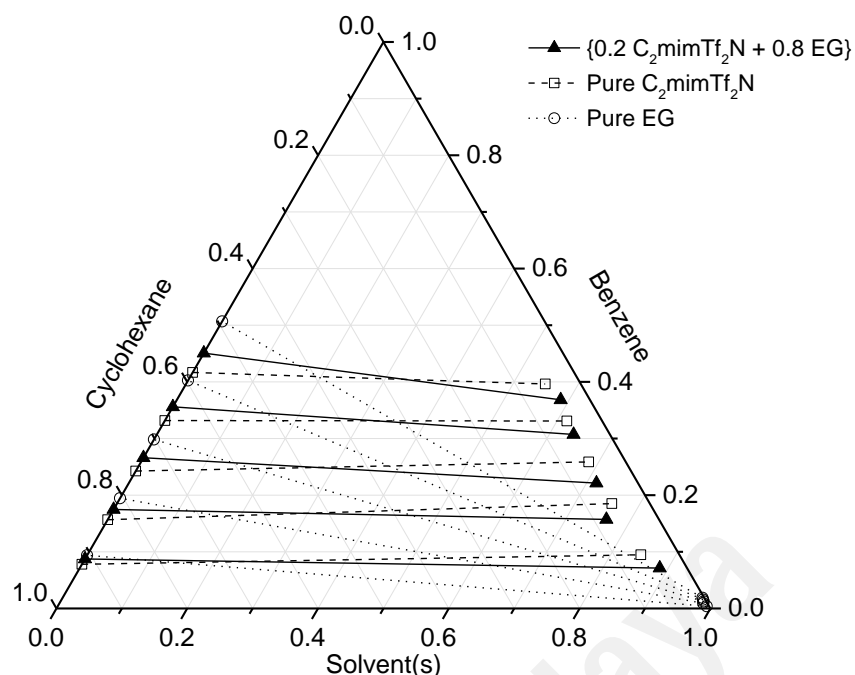


**Figure 4.36: Ternary LLE involving the mixture of [C<sub>2</sub>mimTf<sub>2</sub>N + EG] in comparison with the individual C<sub>2</sub>mimTf<sub>2</sub>N or EG.**

As can be seen, the immiscibility region in the ternary plot of the IL-DMF mixture is much higher than that of pure DMF (Aspi et al., 1998). In addition, the raffinate layers of both systems did not contain any trace of IL. This indicated that after extraction, the IL did not cross-contaminate the raffinate layer. However, the raffinate phase was not free from DMF, indicating that an additional purification step is required to separate DMF from the remaining benzene-cyclohexane mixture. Thus, it was concluded that although the extraction performance of [C<sub>2</sub>mimSCN + DMF] was better than that of pure DMF, the process was more complicated than that using pure C<sub>2</sub>mimSCN.

On the other hand, the phase behavior of the mixture [0.2 C<sub>2</sub>mimSCN + 0.8 EG] was even more interesting. In contrast to the IL-DMF mixture, extraction using [IL-EG] left no trace of either the IL or EG in the raffinate layer, confirming that solvent cross-contamination was completely avoided. This result is consistent with and slightly better than that reported in the previous work for pure EG, in which EG was still detectable in the top layer in a very low concentration ( $X_{EG,raff} = 0.002$ ) (Aspi et al., 1998). In addition,

the plot for the small fraction (20 mol %) of  $C_2mimTf_2N$  in the  $C_2mimSCN$ -EG mixture exhibited tie lines comparable to those for pure  $C_2mimTf_2N$ . This behavior confirmed that the dilution of  $C_2mimTf_2N$  with EG did not lower its extraction performance.

#### 4.3.2 Mixing of an IL with another IL

From the results of COSMO-RS screening previously discussed in section 4.2 (Salleh et al., 2018), the experimental performance of the four selected ILs can be summarized as in Table 4.12.

**Table 4.12: The selectivity and distribution ratio using pure ILs for 10 wt % of benzene in benzene-cyclohexane feed mixture**

IL	S	D
$C_2mimSCN$	44.71	0.46
$C_2mimN(CN)_2$	31.85	0.67
$C_2mimTf_2N$	19.09	1.22
$C_2mimAc$	18.34	0.42

Based on their individual performances, four binary mixtures of IL were created by combining an IL with high selectivity with another IL with high distribution ratio. To determine the optimized binary ratio, the extraction performances of each binary IL mixture at various mixing molar ratios are shown in Figure 4.37 to Figure 4.40. Most of the binary ratios showed much higher extraction performance than sulfolane. This demonstrated the superior performance of the binary ILs compared to conventional organic solvents, while still maintaining moderate selectivity and distribution ratio values.

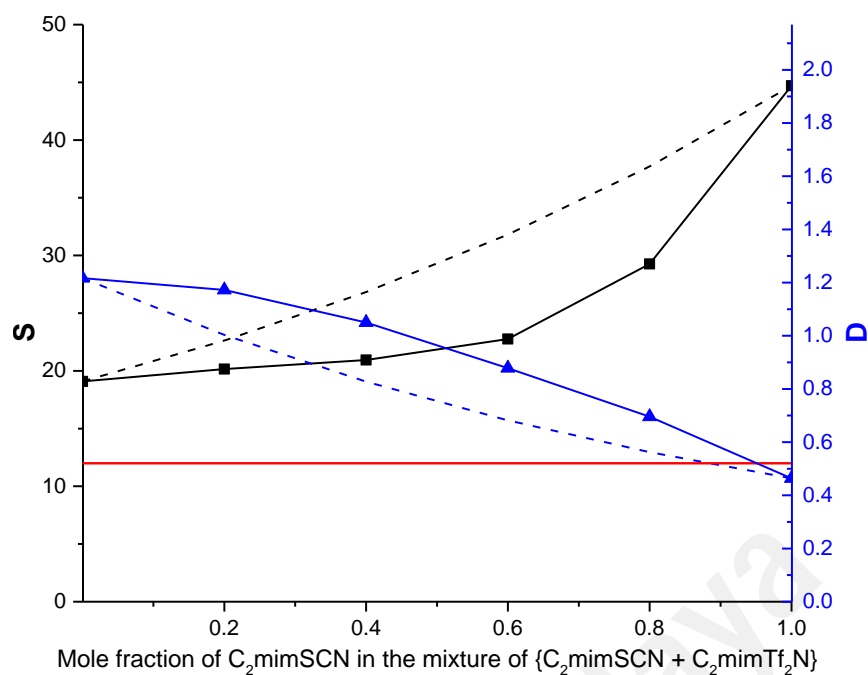


**Figure 4.37: Selectivity of solvent (—■—) and distribution ratio of benzene (—▲—) versus molar fractions of an IL for the pseudo-ternary systems of benzene + cyclohexane + [C<sub>2</sub>mimSCN + C<sub>2</sub>mimTf<sub>2</sub>N] at 298 °C and 1 atm. The solid and dashed lines indicate the experimental and calculated data, respectively. The red line refers to the selectivity and distribution ratio for sulfolane at the same condition.**

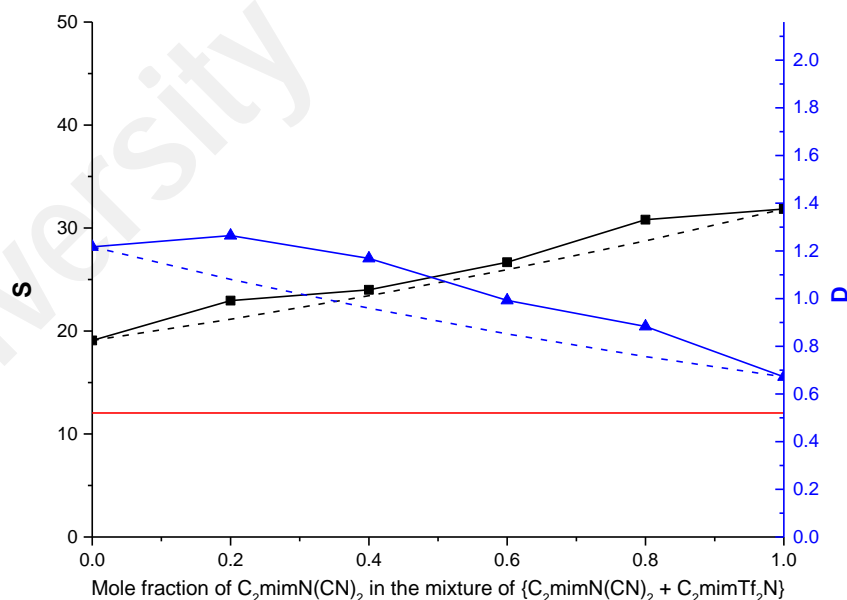


**Figure 4.38: Selectivity of solvent (—■—) and distribution ratio of benzene (—▲—) versus molar fractions of an IL for the pseudo-ternary systems of benzene + cyclohexane + [C<sub>2</sub>mimN(CN)<sub>2</sub> + C<sub>2</sub>mimTf<sub>2</sub>N] at 298 °C and 1 atm. The solid and dashed lines indicate the experimental and calculated data, respectively. The red line refers to the selectivity and distribution ratio for sulfolane at the same condition.**

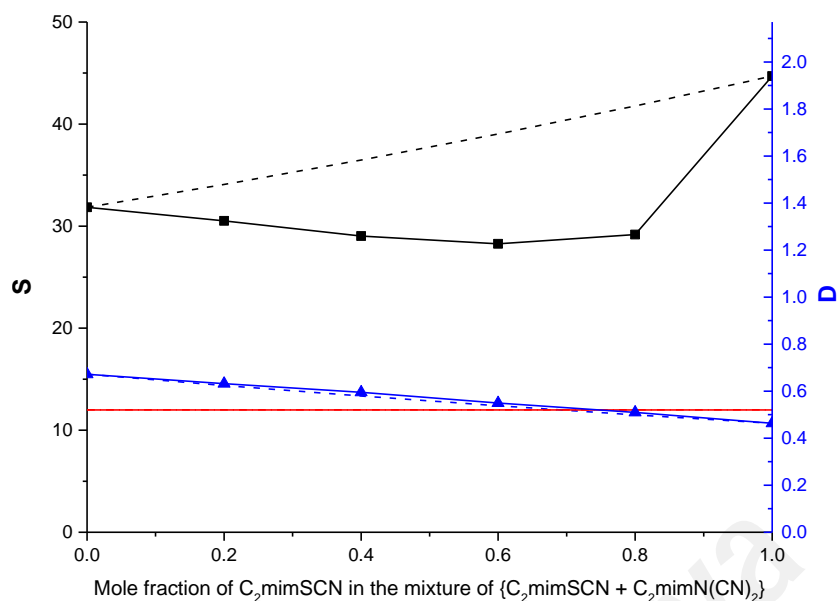


**Figure 4.39: Selectivity of solvent (—■—) and distribution ratio of benzene (—▲—) versus molar fractions of an IL for the pseudo-ternary systems of benzene + cyclohexane + [C<sub>2</sub>mimSCN + C<sub>2</sub>mimN(CN)<sub>2</sub>] at 298 °C and 1 atm. The solid and dashed lines indicate the experimental and calculated data, respectively. The red line refers to the selectivity and distribution ratio for sulfolane at the same condition.**

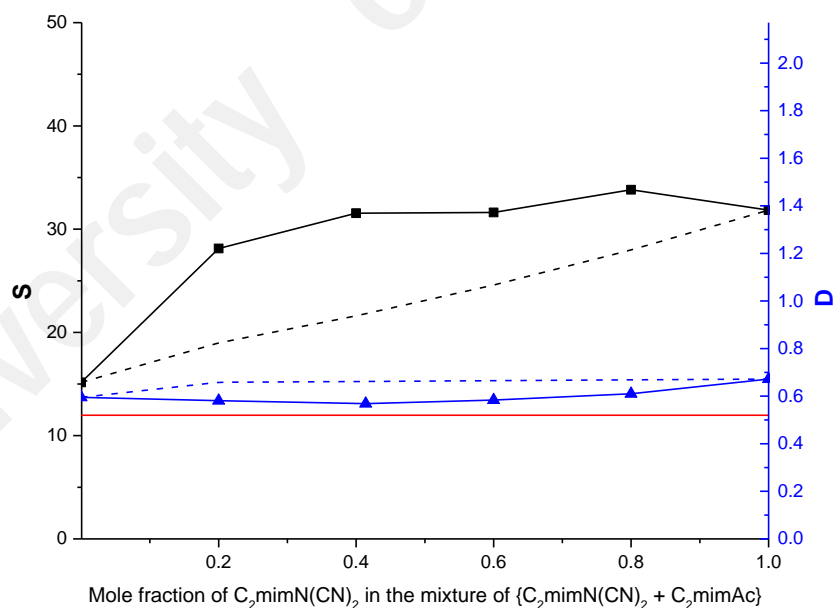


**Figure 4.40: Selectivity of solvent (—■—) and distribution ratio of benzene (—▲—) versus molar fractions of an IL for the pseudo-ternary systems of benzene + cyclohexane + [C<sub>2</sub>mimN(CN)<sub>2</sub> + C<sub>2</sub>mimAc] at 298 °C and 1 atm. The solid and dashed lines indicate the experimental and calculated data, respectively. The red line refers to the selectivity and distribution ratio for sulfolane at the same condition.**

The highest extraction performance for [C<sub>2</sub>mimSCN + C<sub>2</sub>mimTf<sub>2</sub>N] was achieved using an equimolar mixture. Interestingly, an equimolar mixture was also recommended for [C<sub>2</sub>mim(NCN)<sub>2</sub> + C<sub>2</sub>mimTf<sub>2</sub>N], but with different plots of selectivity and distribution ratio. This finding can be explained by the non-ideality factors of the mixed liquids. In liquid state, two solutions are said to be ideal when they have the same nature (structural properties) and size (volume and surface area). Although both binary mixtures consist of the same imidazolium cation, they are still non-ideal because of the different anions. Tf<sub>2</sub>N<sup>-</sup> has a distinct nature and relatively larger size compared to SCN<sup>-</sup> and N(CN)<sub>2</sub><sup>-</sup>. These results were consistent with those of the previous work, which showed a close agreement between the calculated and experimental data when the two ILs involved were almost identical (García et al., 2012b, 2012d).

The extraction performance of the mixed ILs follows the order [C<sub>2</sub>mimN(CN)<sub>2</sub> + C<sub>2</sub>mimTf<sub>2</sub>N] > [C<sub>2</sub>mimSCN + C<sub>2</sub>mimTf<sub>2</sub>N] > [C<sub>2</sub>mimSCN + C<sub>2</sub>mimN(CN)<sub>2</sub>] > [C<sub>2</sub>mimN(CN)<sub>2</sub> + C<sub>2</sub>mimAc]. From this order, it is worth noting the contrary effect between the benzene distribution ratio and selectivity. Firstly, as seen at the intersection point of both curves in Figure 4.37 and Figure 4.38, all mixtures effectively achieved extractive performances superior to that of sulfolane. This demonstrated the viability of mixing the potential ILs to overcome the trade-off between the selectivity and the distribution ratio, thus enhance the extraction performance. Secondly, although [C<sub>2</sub>mimSCN + C<sub>2</sub>mimTf<sub>2</sub>N] consists of the ILs with highest selectivity and highest distribution ratio, its intersection point is lower than that of [C<sub>2</sub>mim(NCN)<sub>2</sub> + C<sub>2</sub>mimTf<sub>2</sub>N]. Thus, mixing the IL with the highest selectivity with the IL with the highest distribution ratio does not automatically result in the best extraction performance. Therefore, to achieve the highest performance, determining the recommended mixing ratio through experimental work is critical.

The remaining two systems (Figure 4.39 and Figure 4.40) showed rather a different mixing behavior compared to the earlier ones. The distribution ratios of the mixed solvents were very close to the corresponding values in the pure ILs. The calculated value of the distribution ratio was also in good agreement with the experimental data. This trend can be explained by the close distribution ratios of the three ILs involved. On the other hand, the selectivity of these mixed solvents seemed to be dominated by one of the two ILs. This can be seen in the respective plots, in which the selectivity of [C<sub>2</sub>mimSCN + C<sub>2</sub>mimN(CN)<sub>2</sub>] was dominated by C<sub>2</sub>mimSCN (Figure 4.39), while the selectivity of [C<sub>2</sub>mimN(CN)<sub>2</sub> + C<sub>2</sub>mimAc] was dominated by C<sub>2</sub>mimN(CN)<sub>2</sub> (Figure 4.40), regardless of the molar mixing ratio. In comparison to sulfolane, both mixed solvents gave higher selectivity but a comparable distribution ratio.

The LLE data were experimentally measured based on the optimized binary molar fractions, i.e., [0.5 C<sub>2</sub>mimSCN + 0.5 C<sub>2</sub>mimTf<sub>2</sub>N], [0.5 C<sub>2</sub>mimN(CN)<sub>2</sub> + 0.5 C<sub>2</sub>mimTf<sub>2</sub>N], [0.2 C<sub>2</sub>mimSCN + 0.8 C<sub>2</sub>mimN(CN)<sub>2</sub>], and [0.2 C<sub>2</sub>mimN(CN)<sub>2</sub> + 0.8 C<sub>2</sub>mimAc], and are summarized in Table 4.13.

**Table 4.13: Molar composition of the tie-lines with the distribution ratio and selectivity data for benzene (1) + cyclohexane (2) + binary mixture of ILs (3) at 25 °C and 1 atm**

Raffinate layer			Extract layer			<i>D</i>	<i>S</i>
<i>x</i> <sub>1</sub>	<i>x</i> <sub>2</sub>	<i>x</i> <sub>3</sub>	<i>x</i> <sub>1</sub>	<i>x</i> <sub>2</sub>	<i>x</i> <sub>3</sub>		
<b>benzene (1) + cyclohexane (2) + [0.5 C<sub>2</sub>mimTf<sub>2</sub>N + 0.5 C<sub>2</sub>mimSCN] (3)</b>							
0.076	0.924	0.000	0.073	0.043	0.883	0.96	20.67
0.157	0.843	0.000	0.145	0.041	0.814	0.92	18.92
0.242	0.758	0.000	0.207	0.046	0.747	0.86	14.23
0.326	0.674	0.000	0.268	0.037	0.695	0.82	15.15
0.421	0.579	0.000	0.326	0.037	0.638	0.77	12.23
<b>benzene (1) + cyclohexane (2) + [0.5 C<sub>2</sub>mimTf<sub>2</sub>N + 0.5 C<sub>2</sub>mimN(CN)<sub>2</sub>] (3)</b>							
0.077	0.923	0.000	0.079	0.043	0.878	1.03	22.11
0.159	0.841	0.000	0.150	0.053	0.797	0.95	15.07
0.243	0.757	0.000	0.215	0.049	0.736	0.88	13.54
0.326	0.674	0.000	0.278	0.044	0.679	0.85	13.17
0.411	0.589	0.000	0.350	0.029	0.621	0.85	17.52
<b>benzene (1) + cyclohexane (2) + [0.2 C<sub>2</sub>mimSCN + 0.8 C<sub>2</sub>mimN(CN)<sub>2</sub>] (3)</b>							
0.079	0.921	0.000	0.047	0.042	0.911	0.60	12.95
0.165	0.835	0.000	0.065	0.025	0.911	0.39	13.21
0.249	0.751	0.000	0.092	0.017	0.892	0.37	16.46
0.342	0.658	0.000	0.175	0.014	0.811	0.51	24.92
0.434	0.566	0.000	0.221	0.013	0.766	0.51	21.98
<b>benzene (1) + cyclohexane (2) + [0.2 C<sub>2</sub>mimN(CN)<sub>2</sub> + 0.8 C<sub>2</sub>mimAc] (3)</b>							
0.083	0.917	0.000	0.039	0.022	0.939	0.47	19.57
0.171	0.829	0.000	0.074	0.034	0.892	0.43	10.72
0.264	0.736	0.000	0.117	0.019	0.864	0.44	17.04
0.349	0.651	0.000	0.143	0.018	0.839	0.41	15.07
0.452	0.548	0.000	0.173	0.019	0.807	0.38	10.88

The tie lines and pseudo-ternary plots of all four systems are depicted in Figure 4.41 to Figure 4.44. As can be seen from all the figures, the mixed ILs generally produced tie lines that fell between the tie lines of the pure ILs, and this intermediary effect became more apparent in the IL-rich region. This finding was consistent with and supported the absence of IL in the raffinate phase in both cases (pure or mixed ILs). Meanwhile, the resulting tie lines for [C<sub>2</sub>mimSCN + C<sub>2</sub>mimN(CN)<sub>2</sub>] and [C<sub>2</sub>mimN(CN)<sub>2</sub> + C<sub>2</sub>mimAc] were almost identical to those of the corresponding pure ILs. However, as shown in Table 4.13, the selectivities of the mixed solvents were actually lower than the pure ones, with the reduction in selectivity being governed by the concentration of cyclohexane in the extract layer.

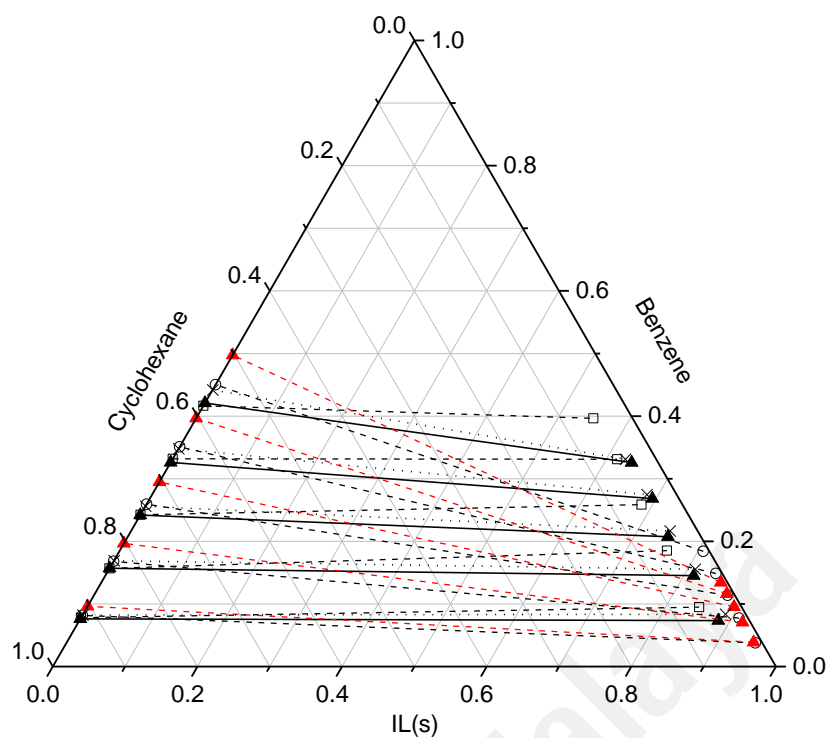


**Figure 4.41: Ternary plots involving the mixture of [C<sub>2</sub>mimSCN + C<sub>2</sub>mimTf<sub>2</sub>N] in comparison with the individual IL: —▲—, experimental (IL mixture); - -▲- -, COSMO-RS (IL mixture); ··×··, NRTL (IL mixture); --○--, pure C<sub>2</sub>mimSCN and --□--, pure C<sub>2</sub>mimTf<sub>2</sub>N**

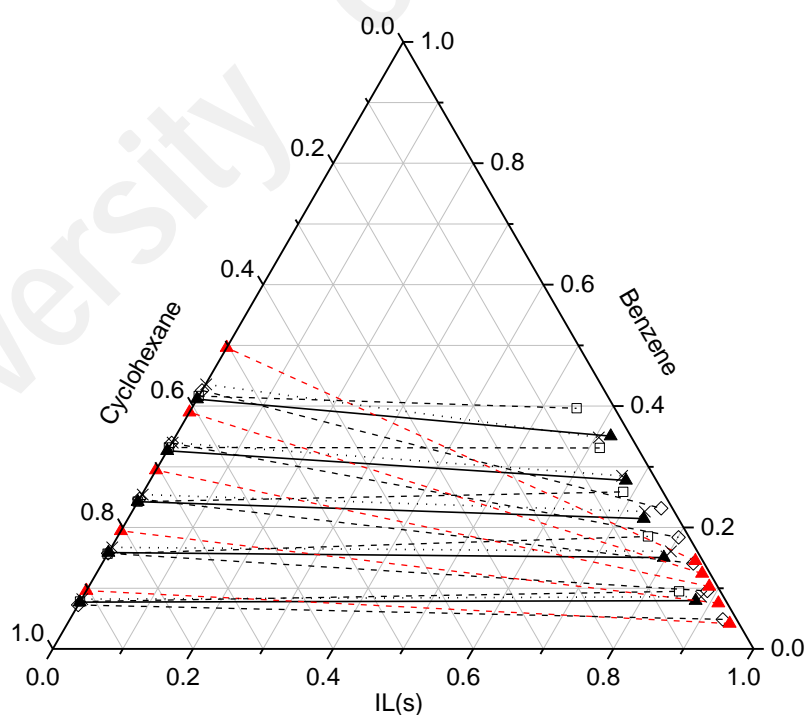


**Figure 4.42: Ternary plots involving the mixture of [C<sub>2</sub>mimN(CN<sub>2</sub>) + C<sub>2</sub>mimTf<sub>2</sub>N] in comparison with the individual IL: —▲—, experimental (IL mixture); - -▲- -, COSMO-RS (IL mixture); ··×··, NRTL (IL mixture); --○--, pure C<sub>2</sub>mimN(CN<sub>2</sub>) and --□--, pure C<sub>2</sub>mimTf<sub>2</sub>N**

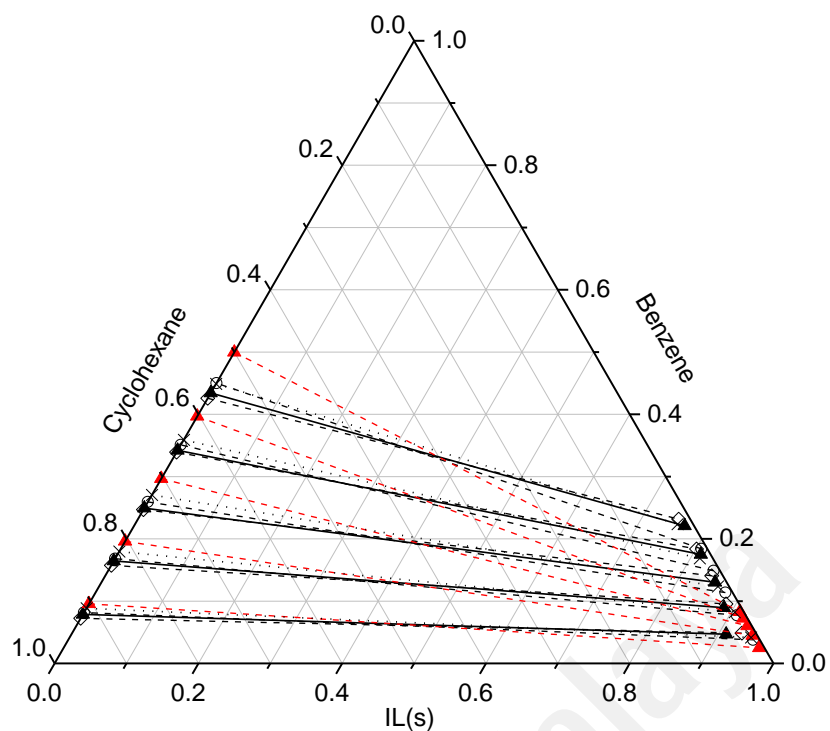


Figure 4.43: Ternary plots involving the mixture of [C<sub>2</sub>mimSCN + C<sub>2</sub>mimN(CN<sub>2</sub>)] in comparison with the individual IL:  $\blacktriangle$ , experimental (IL mixture);  $-\blacktriangle-$ , COSMO-RS (IL mixture);  $\cdot\cdot\times\cdot\cdot$ , NRTL (IL mixture);  $-\circ-$ , pure C<sub>2</sub>mimSCN and  $-\square-$ , pure C<sub>2</sub>mimN(CN<sub>2</sub>)

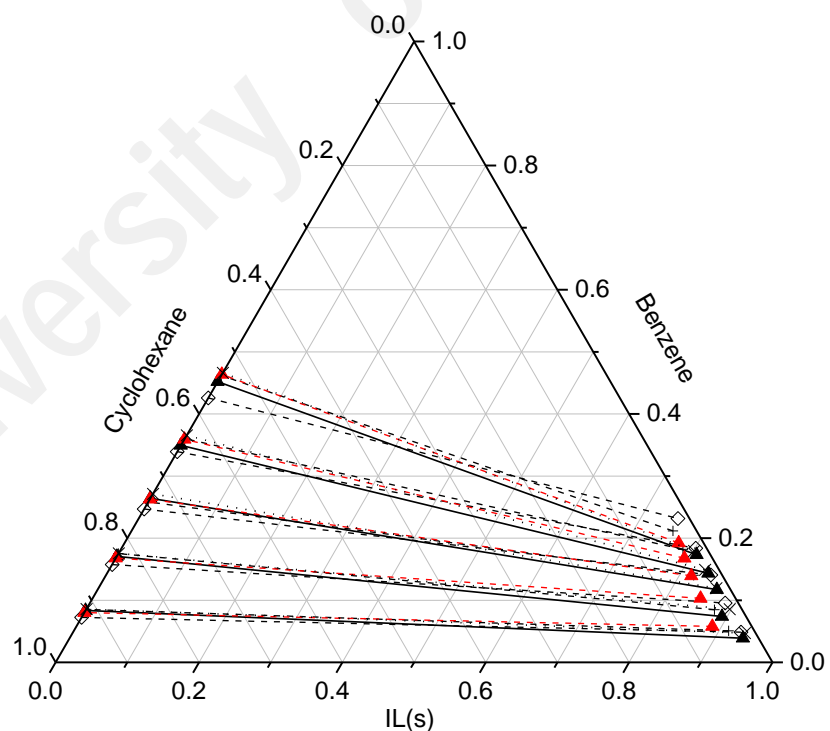
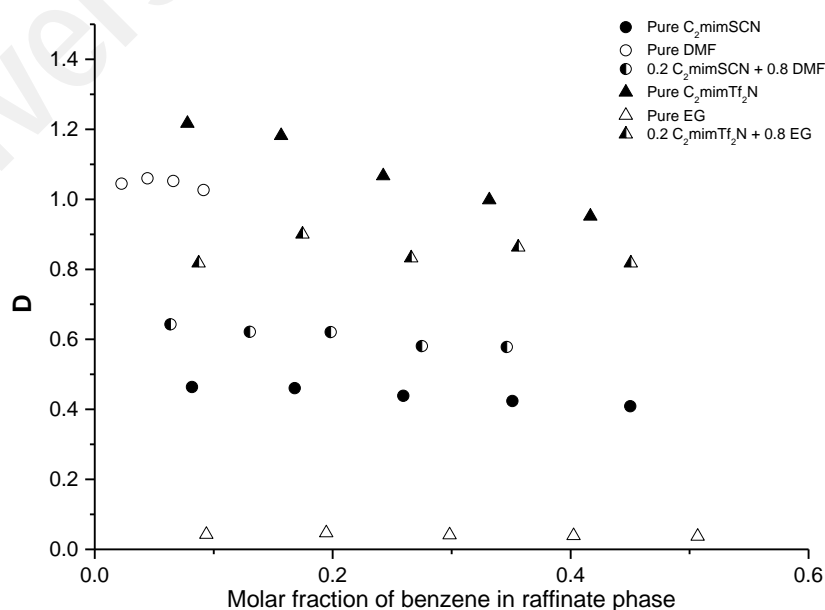


Figure 4.44: Ternary plots involving the mixture of [C<sub>2</sub>mimN(CN<sub>2</sub>) + C<sub>2</sub>mimAc] in comparison with the individual IL:  $\blacktriangle$ , experimental (IL mixture);  $-\blacktriangle-$ , COSMO-RS (IL mixture);  $\cdot\cdot\times\cdot\cdot$ , NRTL (IL mixture);  $-\circ-$ , pure C<sub>2</sub>mimN(CN<sub>2</sub>) and  $-\square-$ , pure C<sub>2</sub>mimAc

### 4.3.3 Comparison between the mixed and pure solvents

A quantitative comparison of the mixed systems with the pure ones is more visible when the selectivity and distribution ratios are plotted separately. The solvent selectivity and the distribution ratio of benzene using the [IL + organic solvent] are depicted in Figure 4.45 and Figure 4.46, respectively. The same comparisons for [IL + IL] mixtures are shown in Figure 4.47 and Figure 4.48. As shown, all the mixed solvents followed the mixing rules, with the selectivity and distribution ratio values appearing in the intermediate region with respect to the pure ones. The distribution ratio showed a steady plot, while the selectivity had some fluctuations. In addition, it is interesting to note that these intermediary results were not simply directly proportional to the molar mixing ratio. For instance, in the [IL + organic solvent] case, 20 mol % of  $C_2mimTf_2N$  in [ $C_2mimTf_2N$  + EG] produced a distribution ratio nearly equal to that of pure  $C_2mimTf_2N$  (Figure 4.45). In the [IL + IL] case, although an equimolar mixture of [ $C_2mimSCN$  +  $C_2mimTf_2N$ ] was used, the selectivity of the mixture was not the average of the individual components, but instead nearly the same as that of pure  $C_2mimTf_2N$  (Figure 4.48). This indicated the versatility of solvent mixing, as the performance of the binary pairs can be customized.



**Figure 4.45: Distribution ratio of benzene using [IL + organic solvent] mixtures in comparison with the respective pure ones.**

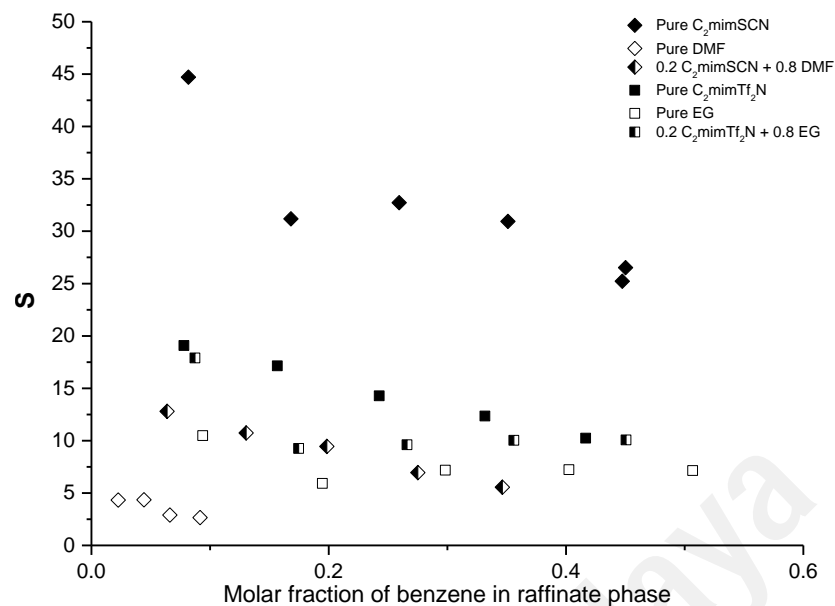


Figure 4.46: Selectivity of [IL + organic solvent] mixtures in comparison with the respective pure ones.

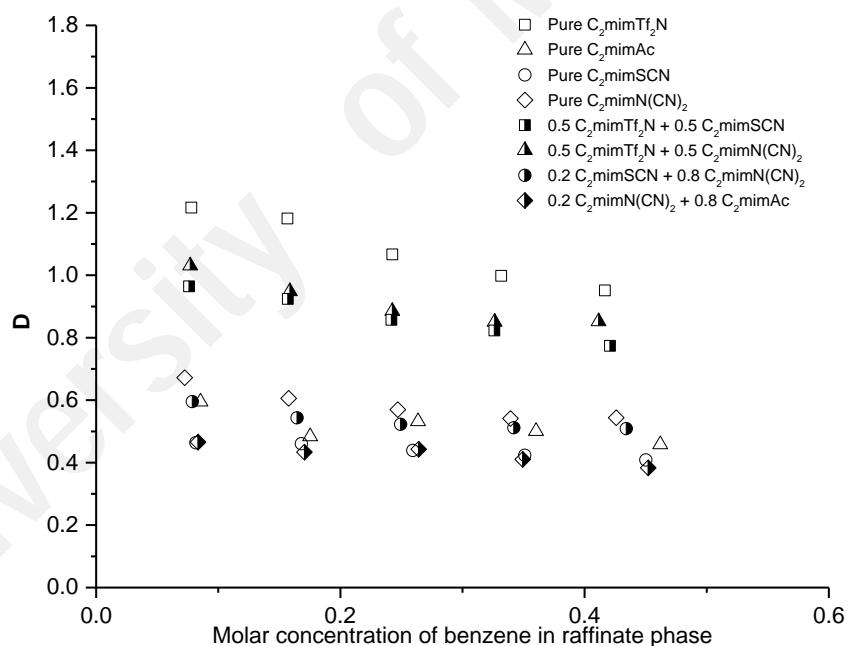
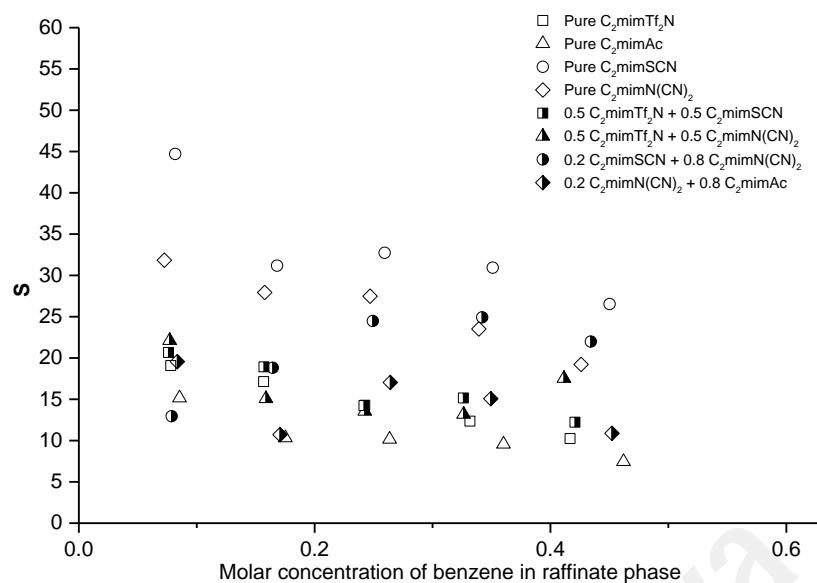


Figure 4.47: Distribution ratio of benzene using binary mixture of ILs in comparison with the respective pure ILs.



**Figure 4.48: Selectivity of [IL + IL] mixtures in comparison with the respective pure ILs.**

#### 4.3.4 The NRTL modelling

The RMSD values between the experimental and NRTL calculations for all ternary systems were less than 2.0 %, which indicates that NRTL correlation represents the experimental data very well. This good agreement is also noticeable in the ternary diagrams (Figure 4.41 to Figure 4.44). Table 4.14 shows the values of the fitting parameters obtained to correlate the experimental LLE data for the pseudo-ternary system. To conserve the coherence, the values of fitting parameter between benzene and cyclohexane were taken as the same with the those using pure ILs and DESs.

**Table 4.14: Binary interaction parameters in NRTL regression for the ternary systems in this study with RMSD between experimental and calculated data**

<i>Ternary system</i>	<i>i</i>	<i>j</i>	$\tau_{ij}$	$\tau_{ji}$	<i>RMSD (%)</i>
	Benzene	Cyclohexane	-189.57	453.65	
<b>Benzene + cyclohexane + C<sub>2</sub>mimTf<sub>2</sub>N + C<sub>2</sub>mimSCN</b>	Benzene	[C <sub>2</sub> mimTf <sub>2</sub> N + C <sub>2</sub> mimSCN]	6109.53	126.15	1.106
	Cyclohexane	[C <sub>2</sub> mimTf <sub>2</sub> N + C <sub>2</sub> mimSCN]	1867.22	664.86	
<b>Benzene + cyclohexane + C<sub>2</sub>mimTf<sub>2</sub>N + C<sub>2</sub>mimN(CN)<sub>2</sub></b>	Benzene	[C <sub>2</sub> mimTf <sub>2</sub> N + C <sub>2</sub> mimN(CN) <sub>2</sub> ]	6598.43	142.41	1.104
	Cyclohexane	[C <sub>2</sub> mimTf <sub>2</sub> N + C <sub>2</sub> mimN(CN) <sub>2</sub> ]	1619.71	608.92	
<b>Benzene + cyclohexane + C<sub>2</sub>mimSCN + C<sub>2</sub>mimN(CN)<sub>2</sub></b>	Benzene	[C <sub>2</sub> mimSCN + C <sub>2</sub> mimN(CN) <sub>2</sub> ]	7031.01	405.53	1.599
	Cyclohexane	[C <sub>2</sub> mimSCN + C <sub>2</sub> mimN(CN) <sub>2</sub> ]	1878.04	927.68	
<b>Benzene + cyclohexane + C<sub>2</sub>mimN(CN)<sub>2</sub> + C<sub>2</sub>mimAc</b>	Benzene	[C <sub>2</sub> mimN(CN) <sub>2</sub> + C <sub>2</sub> mimAc]	3941.60	115.51	0.792
	Cyclohexane	[C <sub>2</sub> mimN(CN) <sub>2</sub> + C <sub>2</sub> mimAc]	1919.24	826.05	

#### 4.4 General insights on the economic and environmental benefits

Based on the results discussed in Section 4.1, 4.2 and 4.3, it can be expected that the extractive separation of benzene and cyclohexane using ILs, DESs or mixture of solvents will produce significant benefits in economic and environmental aspects.

When the volatile organic solvents are replaced with ILs or DESs, solvent cross contamination can be avoided. ILs or DESs were proved to be non-existent in the raffinate phase after extraction. As the product in the raffinate phase consists of only benzene and cyclohexane, the process complexity can be reduced because no additional process is required to purify the raffinate stream. The use of ILs or DESs can also eliminate the environmental concerns associated with the use of organic solvents such as being volatile, toxic and flammable. The advantages of ILs and DESs such as being non-volatile, non-flammable and thermally stable are of great benefits to the industry and environment. Nonetheless, it is not entirely safe to state that ILs or DESs are green solvent unless they are verified in toxicity and corrosivity studies.

The use of solvent binary mixture is also expected to generate significant economic savings. The binary mixture of [C<sub>2</sub>mimTf<sub>2</sub>N + EG] was discovered to potentially compensate the expensiveness of ILs as a small molar composition of C<sub>2</sub>mimTf<sub>2</sub>N in the binary mixture produced the extractive performance nearly the same as the pure C<sub>2</sub>mimTf<sub>2</sub>N. Next, using a correct combination of solvents (IL + organic solvent or IL + IL) in the binary mixture demonstrated the optimized extractive performance in view of selectivity and benzene distribution ratio. Solvent selectivity is generally inversely proportional to solute distribution ratio. The optimized extractive performance indicates the moderation of costs associated with the efficiency of two unit operations, i.e. extraction column (for extraction) and distillation column (for regeneration).

## CHAPTER 5: CONCLUSION AND RECOMMENDATIONS

### 5.1 Conclusion

In this final chapter, the outcomes from each stage of the overall research work are concluded. The following sub-sections will address the objectives of the study. As an overall conclusion, this study shows that the separation of benzene and cyclohexane using new solvents, i.e. ILs and DESs, is highly feasible. The feasibility increased further when the ILs were used in the form of binary mixture. The advantages and drawbacks of using organic solvents, ILs and DESs for the separation of benzene and cyclohexane are also included. Below are the main findings of this study:

#### 5.1.1 The feasibility of using COSMO-RS for solvent screening

In this study, two sets of solvent screening using COSMO-RS were carried out for the separation of benzene and cyclohexane. The screening was achieved based on the comparison of selectivity, capacity and performance index. All these were derived from the activity coefficient at infinite dilution. In addition, the sigma  $\sigma$ -profile and  $\sigma$ -potential of each component were used to analyse the interactions between the different species during the extraction process. The first set considered a total of 40 DESs which were reportedly liquid at ambient temperatures. The second set screened 208 ILs raised from the combination of 16 cations and 13 anions. Each set produced the ranking of DESs/ILs, reflected from the extraction performance. The actual performance of the top-screened ILs/DESs was validated via experimental liquid–liquid extraction process. It was concluded that the ability of COSMO-RS as a tool for selection of ILs/DESs was remarkable because it could predict the trends of ILs/DES performance qualitatively. This work also proved that the COSMO-RS is a fast and assisting tool in solvent screening because it is an *a-priori* method which does not require experimental data. Moreover, good agreement was also observed for the tie lines and the extraction performance between the COSMO-RS and experimental approaches.

### 5.1.2 DESs as a cheaper alternative

The liquid-liquid extraction experiments were carried out at 25 °C and under 1 atm using five DESs selected from the COSMO-RS screening, namely TBABr:Sulf (1:7), TBABr:TEG (1:4), MTPPBr:TEG (1:4), MTPPBr:PD (1:4), and ChCl:TEG (1:4). The new ternary LLE data corresponding to each DES was obtained experimentally and correlated with NRTL model with the RMSD less than 1 %. The findings showed that these DESs were feasible for use as extracting solvents in the separation of benzene and cyclohexane through liquid-liquid extraction. Although the benzene distribution ratio was small, an effective extraction can still be achieved through a multistage process since the DESs were not found in the cyclohexane layer at equilibrium. The extraction using TBABr:Sulf (1:7) was found directly related to the ratio of salt:HBD, indicating that finding the optimum eutectic ratio is crucial. The analysis of extraction mechanism done via <sup>1</sup>H NMR proved that the TBABr:Sulf (1:7) conserves its structure in the presence of benzene. This confirmed that TBABr prevents the solubilisation of sulfolane in the cyclohexane-rich phase. In addition, the TBABr:Sulf (1:7) can also be regenerated into the next extraction stages. The recycled DES was as effective as that of a fresh one as the percentage of benzene extracted remains excellent (>98 %) even after four cycles.

### 5.1.3 The superior performance of ILs

The liquid-liquid extraction experiments with the same condition as in the DES was re-conducted using four ILs suggested by the COSMO-RS screening, namely C<sub>2</sub>mimAc, C<sub>2</sub>mimN(CN)<sub>2</sub>, C<sub>2</sub>mimSCN and C<sub>2</sub>mimTf<sub>2</sub>N. The new ternary LLE data corresponding to each IL was obtained experimentally and correlated with NRTL model with the RMSD less than 2 %. In addition to being commercially available at lower prices, all ILs showed good performance in the extraction of benzene from the benzene-cyclohexane mixture. There was no IL present in the cyclohexane layer and the concentration of cyclohexane in the IL layer was very low. Good agreement was observed for the tie lines between the

COSMO-RS prediction, experimental data and NRTL model. The minimum settling time after extraction was found to be 5 mins only. The comparison of this result with others involving ILs for the same separation showed that these ILs are the most efficient. This work also demonstrated the advantages and drawbacks of each extracting solvent in the extractive separation of benzene and cyclohexane. Although the organic solvents are cheaper with moderate performance, they are limited by their high volatility and complex process. While ILs have higher extractive performance than organic solvents and DESs, their use is limited because they are expensive and possibly toxic. On the other hand, although the DESs are cheaper, can be easily synthesized, and environmentally friendly, their extractive performance is rather low.

#### **5.1.4 The potential of binary ILs mixture**

In the last part of this study, the performance of individual ILs was further developed to produce a customized solvent with optimized value of selectivity and benzene distribution ratio. This was achieved by using binary mixture of the four top-performing ILs. The phase behavior of six quaternary systems, i.e. two [IL + organic solvent] and four [IL + IL] mixtures, were investigated and validated experimentally. All solvent mixtures followed the mixing rule, where the resulting extraction performance was in intermediate region with respect to the corresponding individual solvent. The mixture of [C<sub>2</sub>mimTf<sub>2</sub>N + C<sub>2</sub>mimSCN] remarkably produced the highest extraction performance as reflected by its value of benzene distribution ratio ( $D = 0.96$ ) and selectivity ( $S = 20.7$ ). In addition, ethylene glycol was discovered as a good diluting agent with C<sub>2</sub>mimTf<sub>2</sub>N, which indicated a potential cost saving. The extraction performance was also far more superior to the conventional organic solvents represented by sulfolane. Solvent binary mixture has been proven as a newly efficient and versatile method to optimize the extraction performance.

## 5.2 Recommendations

The findings obtained from this study can be potentially benchmarked to develop a new scope for further studies, especially in the separation of aromatic and aliphatic compounds. This development can be viewed in three contexts, i.e. the improvement of screening process, the design of synthesis for ILs and DESs, and the study of other methods to improve the extraction performance. Hence, the following recommendations are proposed for future research work:

1. While there are numerous type of cations or anions available, the COSMO-RS screening for ILs in this study considered only the common cations and anions. Considering that the types of cations and anions can be further tailor-made for a more specific performance, the effect of their structural design is interesting. For instance, the cations and/or anions that have one or more benzene-like structures are theoretically highly selective towards benzene. The synthesis of novel task-specific ILs (TSILs) – with aromatic functional group attached to the cation or the anion – are also possible to achieve higher selectivity.
2. The COSMO-RS screening in this study has produced a list of top fifteen ILs according to  $C^\infty$ ,  $S^\infty$  and  $PI^\infty$ , as previously seen in Table 4.4. However, despite their potential, these ILs are mostly not available in commercial market. Thus, the acquisition of these ILs through laboratory synthesis is needed to validate their actual performance.
3. Similar to ILs, the pool of candidates for the selection of DESs in this work can also be further expanded by considering new options. Recently, natural deep eutectic solvents (NADES) has gained much attention by the research communities as they are more environmentally benign. In addition, the screening and synthesis of novel aromatic DESs is an interesting option to consider, since there are many salts or HBDs that have aromatic structures.

4. The study of solvent binary mixture is not limited to the six systems that have been presented in this work. Following the consideration of studying other ILs as discussed above, the effect of binary mixture can be consequently investigated with the aim to enhance the extraction performance.
5. The condition of extraction process in this work can be optimized by studying the effect of temperature, pressure, solvent to feed ratio, mixing speed and kinetic study. This may require the use of optimization tools such as the design of experiment (DOE) method by response surface methodology (RSM).
6. The thermodynamic data in this work can be utilized to perform the design of liquid–liquid extraction process for the separation of benzene and cyclohexane using the selected ILs or DESs. This can be achieved using computational simulations such as Aspen or Matlab.

## REFERENCES

- Abbott, A. P., Boothby, D., Capper, G., Davies, D. L., & Rasheed, R. K. (2004). Deep Eutectic Solvents Formed between Choline Chloride and Carboxylic Acids: Versatile Alternatives to Ionic Liquids. *Journal of the American Chemical Society*, 126(29), 9142-9147.
- Abbott, A. P., Capper, G., Davies, D. L., Rasheed, R. K., & Tambyrajah, V. (2003). Novel solvent properties of choline chloride/urea mixtures. *Chemical Communications*(1), 70-71.
- Alberto, A., Martyn, E., Héctor, R., & R., S. K. (2007). Separation of Benzene and Hexane by Solvent Extraction with 1-Alkyl-3-methylimidazolium Bis{(trifluoromethyl)sulfonyl}amide Ionic Liquids: Effect of the Alkyl-Substituent Length. *The Journal of Physical Chemistry B*, 111(18), 4732-4736.
- Albrecht, R. R. R. (1989). *Membrane Processes*. New York: Wiley.
- Anantharaj, R., & Banerjee, T. (2013). Liquid-Liquid Equilibrium Studies on the Removal of Thiophene and Pyridine from Pentane Using Imidazolium-Based Ionic Liquids. *Journal of Chemical & Engineering Data*, 58(4), 829-837.
- Arce, A., Earle, M. J., Katdare, S. P., Rodriguez, H., & Seddon, K. R. (2008). Application of mutually immiscible ionic liquids to the separation of aromatic and aliphatic hydrocarbons by liquid extraction: a preliminary approach. *Physical Chemistry Chemical Physics*, 10(18), 2538-2542.
- Arce, A., Earle, M. J., Rodriguez, H., & Seddon, K. R. (2007). Separation of aromatic hydrocarbons from alkanes using the ionic liquid 1-ethyl-3-methylimidazolium bis{(trifluoromethyl)sulfonyl}amide. *Green Chemistry*, 9(1), 70-74.
- Aspi, Surana, N. M., Ethirajulu, K., & Vennila, V. (1998). Liquid-Liquid Equilibria for the Cyclohexane + Benzene + Dimethylformamide + Ethylene Glycol System. *Journal of Chemical & Engineering Data*, 43(6), 925-927.
- Bancroft, W. D., & George, A. B. (1930). Hydrogenation of Benzene with Nickel and Platinum. *The Journal of Physical Chemistry*, 35(8), 2219-2225.
- Banerjee, T., & Khanna, A. (2006). Infinite dilution activity coefficients for trihexyltetradecyl phosphonium ionic liquids: measurements and COSMO-RS prediction. *Journal of Chemical & Engineering Data*, 51(6), 2170-2177.
- Bank, E. (2017). How benzene is made. Retrieved from <https://sciencing.com> on 10th July, 2018
- Berthod, A., Ruiz-Ángel, M. J., & Carda-Broch, S. (2008). Ionic liquids in separation techniques. *Journal of Chromatography A*, 1184(1-2), 6-18.

- Boon, J. A., Levisky, J. A., Pflug, J. L., & Wilkes, J. S. (1986). Friedel-Crafts reactions in ambient-temperature molten salts. *The Journal of Organic Chemistry*, 51(4), 480-483.
- Brandrup, J. I., E. H. (1989). *Polymer handbook* (3rd edition ed.): Wiley-Interscience.
- Calvar, N., Domínguez, I., Gómez, E., & Domínguez, Á. (2011). Separation of binary mixtures aromatic + aliphatic using ionic liquids: Influence of the structure of the ionic liquid, aromatic and aliphatic. *Chemical Engineering Journal*, 175, 213-221.
- Carroll, F. A. (2011). *Perspectives on Structure and Mechanism in Organic Chemistry*: Wiley.
- Chauvel, A., & Lefebvre, G. (1989). *Petrochemical Processes: Synthesis-gas derivatives and major hydrocarbons* (Vol. 1): Editions Technip.
- Chen, D., Ye, H., & Hao, W. (2007). (Liquid + liquid) equilibria of {heptane + xylene + N-formylmorpholine} ternary system. *The Journal of Chemical Thermodynamics*, 39(12), 1571-1577.
- Chen, D., Ye, H., & Wu, H. (2007). Liquid-liquid equilibria of methylcyclohexane-benzene-N-formylmorpholine at several temperatures. *Fluid Phase Equilibria*, 255(2), 115-120.
- Chen, J., Li, Z., & Duan, L. (2000). Liquid-Liquid Equilibria of Ternary and Quaternary Systems Including Cyclohexane, 1-Heptene, Benzene, Toluene, and Sulfolane at 298.15 K. *Journal of Chemical & Engineering Data*, 45(4), 689-692.
- Cheremisinoff, N. P. (2003). *Industrial Solvents Handbook, Revised And Expanded*: Taylor & Francis.
- Chum, H. L., Koch, V. R., Miller, L. L., & Osteryoung, R. A. (1975). Electrochemical scrutiny of organometallic iron complexes and hexamethylbenzene in a room temperature molten salt. *Journal of the American Chemical Society*, 97(11), 3264-3265.
- Clough, M. T., Crick, C. R., Grasvik, J., Hunt, P. A., Niedermeyer, H., Welton, T., & Whitaker, O. P. (2015). A physicochemical investigation of ionic liquid mixtures. *Chemical Science*, 6(2), 1101-1114.
- De Fré, R. M., & Verhoeve, L. A. (1976). Phase equilibria in systems composed of an aliphatic and an aromatic hydrocarbon and sulpholane. *Journal of Applied Chemistry and Biotechnology*, 26(1), 469-487.
- Dichiarante, V., Betti, C., Fagnoni, M., Maia, A., Landini, D., & Albin, A. (2007). Characterizing Ionic Liquids as Reaction Media through a Chemical Probe. *Chemistry – A European Journal*, 13(6), 1834-1841.
- Diedenhofen, M., Eckert, F., & Klamt, A. (2003). Prediction of Infinite Dilution Activity Coefficients of Organic Compounds in Ionic Liquids Using COSMO-RS†. *Journal of Chemical & Engineering Data*, 48(3), 475-479.

- Diedenhofen, M., & Klamt, A. (2010). COSMO-RS as a tool for property prediction of IL mixtures—A review. *Fluid Phase Equilibria*, 294(1–2), 31-38.
- Domańska, U., & Marciniak, A. (2008). Measurements of activity coefficients at infinite dilution of aromatic and aliphatic hydrocarbons, alcohols, and water in the new ionic liquid [EMIM][SCN] using GLC. *The Journal of Chemical Thermodynamics*, 40(5), 860-866.
- Domínguez, I., González, E. J., Palomar, J., & Domínguez, Á. (2014). Phase behavior of ternary mixtures {aliphatic hydrocarbon+aromatic hydrocarbon+ionic liquid}: Experimental LLE data and their modeling by COSMO-RS. *The Journal of Chemical Thermodynamics*, 77, 222-229.
- Dong, H., Yang, X., Yue, G., Cao, W., & Zhang, J. (2011). Liquid– liquid equilibria for benzene+ cyclohexane+ N, N-dimethylformamide+ ammonium thiocyanate. *Journal of Chemical & Engineering Data*, 56(5), 2664-2668.
- Dong, H., Yang, X., Yue, G., Zhang, W., & Zhang, J. (2013a). (Liquid + liquid) equilibria for benzene + cyclohexane + N,N-dimethylformamide + sodium thiocyanate. *The Journal of Chemical Thermodynamics*, 63, 169-172.
- Dong, H., Yang, X., Yue, G., Zhang, W., & Zhang, J. (2013b). (Liquid+ liquid) equilibria for benzene+ cyclohexane+ N, N-dimethylformamide+ sodium thiocyanate. *The Journal of Chemical Thermodynamics*, 63, 169-172.
- Dong, H., Yang, X., & Zhang, J. (2010a). Liquid– liquid equilibria for benzene+ cyclohexane+ N, N-dimethylformamide+ potassium thiocyanate. *Journal of Chemical & Engineering Data*, 55(9), 3972-3975.
- Dong, H., Yang, X., & Zhang, J. (2010b). Liquid–Liquid Equilibria for Benzene + Cyclohexane + N,N-Dimethylformamide + Potassium Thiocyanate. *Journal of Chemical & Engineering Data*, 55(9), 3972-3975.
- Earle, M. J., Esperanca, J. M. S. S., Gilea, M. A., Canongia Lopes, J. N., Rebelo, L. P. N., Magee, J. W., . . . Widegren, J. A. (2006). The distillation and volatility of ionic liquids. *Nature*, 439(7078), 831-834.
- Earle, M. J., & Seddon, K. R. (2000). Ionic liquids. Green solvents for the future. *Pure and Applied Chemistry*, 72(7), 1391-1398.
- Fang, D.-W., Guan, W., Tong, J., Wang, Z.-W., & Yang, J.-Z. (2008). Study on Physicochemical Properties of Ionic Liquids Based on Alanine [Cnmim][Ala] (n = 2,3,4,5,6). *The Journal of Physical Chemistry B*, 112(25), 7499-7505.
- Feng, L. (2004). Focus on China: Up, up and away? *Chemical Engineer*(762-763), 42-43, 45.
- Ferreira, A. R., Freire, M. G., Ribeiro, J. C., Lopes, F. M., Crespo, J. G., & Coutinho, J. A. P. (2011). An Overview of the Liquid–Liquid Equilibria of (Ionic Liquid + Hydrocarbon) Binary Systems and Their Modeling by the Conductor-like Screening Model for Real Solvents. *Industrial & Engineering Chemistry Research*, 50(9), 5279-5294.

- Ferreira, A. R., Freire, M. G., Ribeiro, J. C., Lopes, F. M., Crespo, J. G., & Coutinho, J. A. P. (2012). Overview of the Liquid–Liquid Equilibria of Ternary Systems Composed of Ionic Liquid and Aromatic and Aliphatic Hydrocarbons, and Their Modeling by COSMO-RS. *Industrial & Engineering Chemistry Research*, 51(8), 3483-3507.
- Ferreira, A. R., Freire, M. G., Ribeiro, J. C., Lopes, F. M., Crespo, J. G., & Coutinho, J. A. P. (2014). Ionic liquids for thiols desulfurization: Experimental liquid–liquid equilibrium and COSMO-RS description. *Fuel*, 128, 314-329.
- Fletcher, K. A., & Pandey, S. (2004). Surfactant Aggregation within Room-Temperature Ionic Liquid 1-Ethyl-3-methylimidazolium Bis(trifluoromethylsulfonyl)imide. *Langmuir*, 20(1), 33-36.
- Fruscella, W. (2000). Benzene *Kirk-Othmer Encyclopedia of Chemical Technology*: John Wiley & Sons, Inc.
- García, S., Larriba, M., García, J., Torrecilla, J. S., & Rodríguez, F. (2012a). Liquid–liquid extraction of toluene from n-heptane using binary mixtures of N-butylpyridinium tetrafluoroborate and N-butylpyridinium bis(trifluoromethylsulfonyl) imide ionic liquids. *Chemical Engineering Journal*, 180, 210-215.
- García, S., Larriba, M., García, J., Torrecilla, J. S., & Rodríguez, F. (2012b). Liquid–liquid extraction of toluene from n-heptane using binary mixtures of N-butylpyridinium tetrafluoroborate and N-butylpyridinium bis(trifluoromethylsulfonyl)imide ionic liquids. *Chemical Engineering Journal*, 180(Supplement C), 210-215.
- García, S., Larriba, M., García, J., Torrecilla, J. S., & Rodríguez, F. (2012c). Separation of toluene from n-heptane by liquid–liquid extraction using binary mixtures of [bpy][BF<sub>4</sub>] and [4bmpy][Tf<sub>2</sub>N] ionic liquids as solvent. *The Journal of Chemical Thermodynamics*, 53, 119-124.
- García, S., Larriba, M., García, J., Torrecilla, J. S., & Rodríguez, F. (2012d). Separation of toluene from n-heptane by liquid–liquid extraction using binary mixtures of [bpy][BF<sub>4</sub>] and [4bmpy][Tf<sub>2</sub>N] ionic liquids as solvent. *The Journal of Chemical Thermodynamics*, 53(Supplement C), 119-124.
- Gómez, E., Domínguez, I., Calvar, N., & Domínguez, Á. (2010a). Separation of benzene from alkanes by solvent extraction with 1-ethylpyridinium ethylsulfate ionic liquid. *The Journal of Chemical Thermodynamics*, 42(10), 1234-1239.
- Gómez, E., Domínguez, I., Calvar, N., Palomar, J., & Domínguez, Á. (2014). Experimental data, correlation and prediction of the extraction of benzene from cyclic hydrocarbons using [Epy][ESO<sub>4</sub>] ionic liquid. *Fluid Phase Equilibria*, 361, 83-92.
- Gómez, E., Domínguez, I., González, B., & Domínguez, Á. (2010b). Liquid–Liquid Equilibria of the Ternary Systems of Alkane + Aromatic + 1-Ethylpyridinium Ethylsulfate Ionic Liquid at T = (283.15 and 298.15) K. *Journal of Chemical & Engineering Data*, 55(11), 5169-5175.

- Gonzalez, A. S. B., Francisco, M., Jimeno, G., de Dios, S. L. G., & Kroon, M. C. (2013). Liquid–liquid equilibrium data for the systems {LTTM + benzene + hexane} and {LTTM + ethyl acetate + hexane} at different temperatures and atmospheric pressure. *Fluid Phase Equilibria*, 360, 54-62.
- González, E., Calvar, N., González, B., & Domínguez, Á. (2010a). Liquid Extraction of Benzene from Its Mixtures Using 1-Ethyl-3-methylimidazolium Ethylsulfate as a Solvent. *Journal of Chemical & Engineering Data*, 55(11), 4931-4936.
- González, E., Domínguez, I., González, B., & Canosa, J. (2010b). Liquid–liquid equilibria for ternary systems of {cyclohexane + aromatic compounds + 1-ethyl-3-methylpyridinium ethylsulfate}. *Fluid Phase Equilibria*, 296(2), 213-218.
- González, E. J., Calvar, N., González, B., & Domínguez, Á. (2010). Liquid Extraction of Benzene from Its Mixtures Using 1-Ethyl-3-methylimidazolium Ethylsulfate as a Solvent. *Journal of Chemical & Engineering Data*, 55(11), 4931-4936.
- González, E. J., Navarro, P., Larriba, M., García, J., & Rodríguez, F. (2016). A comparative study of pure ionic liquids and their mixtures as potential mass agents in the separation of hydrocarbons. *Journal of Molecular Liquids*, 222, 118-124.
- Gouveia, A. S. L., Oliveira, F. S., Kurnia, K. A., & Marrucho, I. M. (2016). Deep Eutectic Solvents as Azeotrope Breakers: Liquid–Liquid Extraction and COSMO-RS Prediction. *ACS Sustainable Chemistry & Engineering*, 4(10), 5640-5650.
- Gruber, D., Langenheim, D., Gmehling, J., & Moollan, W. (1997). Measurement of Activity Coefficients at Infinite Dilution Using Gas–Liquid Chromatography. 6. Results for Systems Exhibiting Gas–Liquid Interface Adsorption with 1-Octanol. *Journal of Chemical & Engineering Data*, 42(5), 882-885.
- H. Davis, J. J. (2004). Task-Specific Ionic Liquids. *Chemistry Letters*, 33(9), 1072-1077.
- Hadj-Kali, M. K., Mulyono, S., Hizaddin, H. F., Wazeer, I., El-Blidi, L., Ali, E., . . . AlNashef, I. M. (2016). Removal of Thiophene from Mixtures with n-Heptane by Selective Extraction Using Deep Eutectic Solvents. *Industrial & Engineering Chemistry Research*, 55(30), 8415-8423.
- Hadj-Kali, M. K., Salleh, Z., Ali, E., Khan, R., & Hashim, M. A. (2017). Separation of aromatic and aliphatic hydrocarbons using deep eutectic solvents: A critical review. *Fluid Phase Equilibria*, 448, 152-167.
- Haghnazarloo, H., Lotfollahi, M. N., Mahmoudi, J., & Asl, A. H. (2013). Liquid–liquid equilibria for ternary systems of (ethylene glycol + toluene + heptane) at temperatures (303.15, 308.15, and 313.15) K and atmospheric pressure: Experimental results and correlation with UNIQUAC and NRTL models. *The Journal of Chemical Thermodynamics*, 60, 126-131.
- Hagiwara, R., & Lee, J. S. (2007). Ionic Liquids for Electrochemical Devices. *Electrochemistry*, 75(1), 23-34.
- Hand, D. B. (1929). Dimeric Distribution. *The Journal of Physical Chemistry*, 34(9), 1961-2000.

- Hayes, J. C. (1972). AROMATIC HYDROGENATION PROCESS: Google Patents.
- Hizaddin, H. F., Hadj-Kali, M. K., Ramalingam, A., & Hashim, M. A. (2015). Extraction of nitrogen compounds from diesel fuel using imidazolium- and pyridinium-based ionic liquids: Experiments, COSMO-RS prediction and NRTL correlation. *Fluid Phase Equilibria*, 405, 55-67.
- Hizaddin, H. F., Ramalingam, A., Hashim, M. A., & Hadj-Kali, M. K. O. (2014). Evaluating the Performance of Deep Eutectic Solvents for Use in Extractive Denitrification of Liquid Fuels by the Conductor-like Screening Model for Real Solvents. *Journal of Chemical & Engineering Data*, 59(11), 3470-3487.
- Holbrey, J., & Seddon, K. (1999). Ionic liquids. *Clean Products and Processes*, 1(4), 223-236.
- Jiao, T., Wang, H., Dai, F., Li, C., & Zhang, S. (2016). Thermodynamics Study on the Separation Process of Cresols from Hexane via Deep Eutectic Solvent Formation. *Industrial & Engineering Chemistry Research*, 55(32), 8848-8857.
- Johann G Stichlmair, & Fair, J. R. (1998). *Distillation: Principles and Practices*: Wiley-VCH.
- Johnson, W. S., Bauer, V. J., Margrave, J. L., Frisch, M. A., Dreger, L. H., & Hubbard, W. N. (1961). The energy difference between the chair and boat forms of cyclohexane. The twist conformation of cyclohexane. *Journal of the American Chemical Society*, 83(3), 606-614.
- K. Weissermel, H.-J. A. (2003). *Industrial Organic Chemistry, 4th Completely Revised edition*. Weinheim: Wiley-VCH.
- Kareem, M., Mjalli, F., Hashim, M. A., Hadj-Kali, M. K. O., Bagh, F. S. G., & Alnashef, I. M. (2012). Phase equilibria of toluene/heptane with tetrabutylphosphonium bromide based deep eutectic solvents for the potential use in the separation of aromatics from naphtha. *Fluid Phase Equilibria*, 333, 47-54.
- Kareem, M. A., Mjalli, F. S., Hashim, M. A., & AlNashef, I. M. (2012). Liquid-liquid equilibria for the ternary system (phosphonium based deep eutectic solvent-benzene-hexane) at different temperatures: A new solvent introduced. *Fluid Phase Equilibria*, 314, 52-59.
- Kareem, M. A., Mjalli, F. S., Hashim, M. A., Hadj-Kali, M. K. O., Ghareh Bagh, F. S., & Alnashef, I. M. (2013). Phase equilibria of toluene/heptane with deep eutectic solvents based on ethyltriphenylphosphonium iodide for the potential use in the separation of aromatics from naphtha. *The Journal of Chemical Thermodynamics*, 65, 138-149.
- Kassel, L. S. (1956). Hydrogenation of benzene to cyclohexane: Patent No. US 2755317 A.
- Kędra-Królik, K., Fabrice, M., & Jaubert, J.-N. (2011). Extraction of Thiophene or Pyridine from n-Heptane Using Ionic Liquids. Gasoline and Diesel

Desulfurization. *Industrial & Engineering Chemistry Research*, 50(4), 2296-2306.

Kędra-Królik, K., Fabrice, M., & Jaubert, J.-N. I. (2011). Extraction of thiophene or pyridine from n-heptane using ionic liquids. Gasoline and diesel desulfurization. *Industrial & Engineering Chemistry Research*, 50(4), 2296-2306.

Kent, J. A. (2013). *Handbook of industrial chemistry and biotechnology*: Springer Science & Business Media.

Klamt, A. (2005). *COSMO-RS: From Quantum Chemistry to Fluid Phase Thermodynamics and Drug Design*: Elsevier.

Klamt, A., & Eckert, F. (2000). COSMO-RS: a novel and efficient method for the a priori prediction of thermophysical data of liquids. *Fluid Phase Equilibria*, 172(1), 43-72.

Köhler, S., Liebert, T., Schöbitz, M., Schaller, J., Meister, F., Günther, W., & Heinze, T. (2007). Interactions of Ionic Liquids with Polysaccharides 1. Unexpected Acetylation of Cellulose with 1-Ethyl-3-methylimidazolium Acetate. *Macromolecular Rapid Communications*, 28(24), 2311-2317.

Kubota, F., & Goto, M. (2006). Application of Ionic Liquids to Solvent Extraction. *Solvent extraction research and development, Japan*, 13, 23-36.

Kurnia, K. A., Athirah, N. A., Candieiro, F. J. M., & Lal, B. (2016). Phase Behavior of Ternary Mixtures {Aliphatic Hydrocarbon + Aromatic Hydrocarbon + Deep Eutectic Solvent}: A Step Forward toward "Greener" Extraction Process. *Procedia Engineering*, 148, 1340-1345.

Kurnia, K. A., Pinho, S. P., & Coutinho, J. A. P. (2014). Designing ionic liquids for absorptive cooling. *Green Chemistry*, 16(8), 3741-3745.

Larkin, J. M., Templeton, J. H., & Champion, D. H. (1993). Process for the production of cyclohexane by liquid phase hydrogenation of benzene: Google Patents.

Larriba, M., Navarro, P., García, J., & Rodríguez, F. (2013a). Liquid-liquid extraction of toluene from heptane using [emim][DCA],[bmim][DCA], and [emim][TCM] ionic liquids. *Industrial & Engineering Chemistry Research*, 52(7), 2714-2720.

Larriba, M., Navarro, P., García, J., & Rodríguez, F. (2013b). Separation of toluene from n-heptane, 2,3-dimethylpentane, and cyclohexane using binary mixtures of [4empy][Tf2N] and [emim][DCA] ionic liquids as extraction solvents. *Separation and Purification Technology*, 120(Supplement C), 392-401.

Larriba, M., Navarro, P., García, J., & Rodríguez, F. (2013c). Separation of toluene from n-heptane, 2, 3-dimethylpentane, and cyclohexane using binary mixtures of [4empy][Tf2N] and [emim][DCA] ionic liquids as extraction solvents. *Separation and purification technology*, 120, 392-401.

- Larriba, M., Navarro, P., García, J. n., & Rodríguez, F. (2014). Liquid–Liquid Extraction of Toluene from n-Alkanes using {[4empty][Tf2N]+[emim][DCA]} Ionic Liquid Mixtures. *Journal of Chemical & Engineering Data*, 59(5), 1692-1699.
- Lerol, J.-C., Masson, J.-C., Renon, H., Fabries, J.-F., & Sannier, H. (1977). Accurate Measurement of Activity Coefficient at Infinite Dilution by Inert Gas Stripping and Gas Chromatography. *Industrial & Engineering Chemistry Process Design and Development*, 16(1), 139-144.
- Liu, H., Fang, R., Li, Z., & Li, Y. (2015). Solventless hydrogenation of benzene to cyclohexane over a heterogeneous Ru–Pt bimetallic catalyst. *Chemical Engineering Science*, 122, 350-359.
- Long, J., Guo, B., Li, X., Jiang, Y., Wang, F., Tsang, S. C., . . . Yu, K. M. K. (2011). One step catalytic conversion of cellulose to sustainable chemicals utilizing cooperative ionic liquid pairs. *Green Chemistry*, 13(9), 2334-2338.
- Lotfi, M., Moniruzzaman, M., Sivapragasam, M., Kandasamy, S., Abdul Mutalib, M. I., Alitheen, N. B., & Goto, M. (2017). Solubility of acyclovir in nontoxic and biodegradable ionic liquids: COSMO-RS prediction and experimental verification. *Journal of Molecular Liquids*.
- Lu, Y., Yang, X., & Luo, G. (2010). Liquid–Liquid Equilibria for Benzene + Cyclohexane + 1-Butyl-3-methylimidazolium Hexafluorophosphate. *Journal of Chemical & Engineering Data*, 55(1), 510-512.
- Lyu, Z., Zhou, T., Chen, L., Ye, Y., Sundmacher, K., & Qi, Z. (2014a). Reprint of: Simulation based ionic liquid screening for benzene–cyclohexane extractive separation. *Chemical Engineering Science*, 115, 186-194.
- Lyu, Z., Zhou, T., Chen, L., Ye, Y., Sundmacher, K., & Qi, Z. (2014b). Simulation based ionic liquid screening for benzene–cyclohexane extractive separation. *Chemical Engineering Science*, 113(0), 45-53.
- M. Reza, S., Lotfollahi, M. N., & Asl, A. H. (2011). (Liquid + liquid) equilibria for mixtures of (ethylene glycol + benzene + cyclohexane) at temperatures (298.15, 308.15, and 318.15) K. *The Journal of Chemical Thermodynamics*, 43(3), 329-333.
- MacFarlane, D. R., Golding, J., Forsyth, S., Forsyth, M., & Deacon, G. B. (2001). Low viscosity ionic liquids based on organic salts of the dicyanamide anion. *Chemical Communications*(16), 1430-1431.
- Mahmoudi, J., & Lotfollahi, M. N. (2010). (Liquid + liquid) equilibria of (sulfolane + benzene + n-hexane), (N-formylmorpholine + benzene + n-hexane), and (sulfolane + N-formylmorpholine + benzene + n-hexane) at temperatures ranging from (298.15 to 318.15) K: Experimental results and correlation. *The Journal of Chemical Thermodynamics*, 42(4), 466-471.
- Manohar, C., Banerjee, T., & Mohanty, K. (2013). Co-solvent effects for aromatic extraction with ionic liquids. *Journal of Molecular Liquids*, 180, 145-153.

- Manohar, C. V., Rabari, D., Kumar, A. A. P., Banerjee, T., & Mohanty, K. (2013). Liquid–liquid equilibria studies on ammonium and phosphonium based ionic liquid–aromatic–aliphatic component at T=298.15K and p=1bar: Correlations and a-priori predictions. *Fluid Phase Equilibria*, 360, 392-400.
- Markit, I. (2017a). *Benzene - Chemical Economics Handbook*. Retrieved from <https://ihsmarkit.com/products/benzene-chemical-economics-handbook.html> on 16th August, 2018
- Markit, I. (2017b). *Cyclohexane - Chemical Economics Handbook*. Retrieved from <https://ihsmarkit.com/products/cyclohexane-chemical-economics-handbook.html> on 16th August, 2018
- McMurry, J. (2011). *Organic Chemistry*: Brooks/Cole Cengage Learning.
- Meindersma, G. W., Hansmeier, A. R., & de Haan, A. B. (2010). Ionic Liquids for Aromatics Extraction. Present Status and Future Outlook. *Industrial & Engineering Chemistry Research*, 49(16), 7530-7540.
- Meindersma, G. W., Podt, A. J., & de Haan, A. B. (2006). Ternary liquid–liquid equilibria for mixtures of toluene+n-heptane+ an ionic liquid. *Fluid Phase Equilibria*, 247(1), 158-168.
- Minami, I. (2009). Ionic Liquids in Tribology. *Molecules*, 14(6), 2286.
- Mohsen-Nia, M., & Doulabi, F. S. M. (2006). Liquid–liquid equilibria for mixtures of (ethylene carbonate + aromatic hydrocarbon + cyclohexane). *Thermochimica Acta*, 445(1), 82-85.
- Mohsen-Nia, M., Modarress, H., Doulabi, F., & Bagheri, H. (2005). Liquid + liquid equilibria for ternary mixtures of (solvent + aromatic hydrocarbon + alkane). *The Journal of Chemical Thermodynamics*, 37(10), 1111-1118.
- Mohsen-Nia, M., Mohammad Doulabi, F. S., & Manousiouthakis, V. I. (2008). (Liquid + liquid) equilibria for ternary mixtures of (ethylene glycol + toluene + n-octane). *The Journal of Chemical Thermodynamics*, 40(8), 1269-1273.
- Mokhtarani, B., Musavi, J., Parvini, M., Sharifi, A., & Mirzaei, M. (2016). Experimental study on liquid–liquid equilibria of ionic liquids+ alkane+ ethyl benzene or p-xylene at 298.15 K. *Fluid Phase Equilibria*, 409, 7-11.
- Moniruzzaman, M., Nakashima, K., Kamiya, N., & Goto, M. (2010). Recent advances of enzymatic reactions in ionic liquids. *Biochemical Engineering Journal*, 48(3), 295-314.
- Mulyono, S., Hizaddin, H. F., Alnashef, I. M., Hashim, M. A., Fakeeha, A. H., & Hadj-Kali, M. K. (2014). Separation of BTEX aromatics from n-octane using a (tetrabutylammonium bromide + sulfolane) deep eutectic solvent - experiments and COSMO-RS prediction. *RSC Advances*, 4(34), 17597-17606.

- Naik, P. K., Dehury, P., Paul, S., & Banerjee, T. (2016). Evaluation of Deep Eutectic Solvent for the selective extraction of toluene and quinoline at  $T = 308.15$  K and  $p = 1$  bar. *Fluid Phase Equilibria*, *423*, 146-155.
- Navarro, P., Larriba, M., García, J., González, E. J., & Rodríguez, F. (2016). Selective recovery of aliphatics from aromatics in the presence of the {[4empy][Tf 2 N]+[emim][DCA]} ionic liquid mixture. *The Journal of Chemical Thermodynamics*, *96*, 134-142.
- Navarro, P., Larriba, M., García, J., & Rodríguez, F. (2014). Thermal stability, specific heats, and surface tensions of ([emim][DCA]+[4empy][Tf 2 N]) ionic liquid mixtures. *The Journal of Chemical Thermodynamics*, *76*, 152-160.
- Navarro, P., Larriba, M., García, J., & Rodríguez, F. (2017). Design of the recovery section of the extracted aromatics in the separation of BTEX from naphtha feed to ethylene crackers using [4empy][Tf2N] and [emim][DCA] mixed ionic liquids as solvent. *Separation and purification technology*, *180*, 149-156.
- Oliveira, F. S., Pereiro, A. B., Rebelo, L. P., & Marrucho, I. M. (2013). Deep eutectic solvents as extraction media for azeotropic mixtures. *Green Chemistry*, *15*(5), 1326-1330.
- Othmer, D., & Tobias, P. (1942). Liquid-Liquid Extraction Data - The Line Correlation. *Industrial & Engineering Chemistry*, *34*(6), 693-696.
- Paduszynski, K. (2017). An overview of performance of COSMO-RS approach in predicting activity coefficients of molecular solutes in ionic liquids and derived properties at infinite dilution. *Physical Chemistry Chemical Physics*.
- Plechkova, N. V., & Seddon, K. R. (2007). Ionic liquids: "designer" solvents for green chemistry. *Methods and Reagents for Green Chemistry*, 105-130.
- Plechkova, N. V., & Seddon, K. R. (2008). Applications of ionic liquids in the chemical industry. *Chemical Society Reviews*, *37*(1), 123-150.
- Potdar, S., Anantharaj, R., & Banerjee, T. (2012). Aromatic Extraction Using Mixed Ionic Liquids: Experiments and COSMO-RS Predictions. *Journal of Chemical & Engineering Data*, *57*(4), 1026-1035.
- Putnam, R., Taylor, R., Klamt, A., Eckert, F., & Schiller, M. (2003). Prediction of infinite dilution activity coefficients using COSMO-RS. *Industrial & Engineering Chemistry Research*, *42*(15), 3635-3641.
- Renon, H., & Prausnitz, J. M. (1968). Local compositions in thermodynamic excess functions for liquid mixtures. *AIChE Journal*, *14*(1), 135-144.
- Robert, O., & Dang, V. Q. (1971). Manufacture of naphthenic hydrocarbons by hydrogenation of the corresponding aromatic hydrocarbons: Patent No. US 3597489 A.
- Rodríguez, N. R., Gerlach, T., Scheepers, D., Kroon, M. C., & Smirnova, I. (2017). Experimental determination of the LLE data of systems consisting of {hexane +

benzene + deep eutectic solvent} and prediction using the Conductor-like Screening Model for Real Solvents. *The Journal of Chemical Thermodynamics*, 104, 128-137.

Rodriguez, N. R., Requejo, P. F., & Kroon, M. C. (2015). Aliphatic–Aromatic Separation Using Deep Eutectic Solvents as Extracting Agents. *Industrial & Engineering Chemistry Research*, 54(45), 11404-11412.

S. Ghannad, S. M. Reza, Lotfollahi, M. N., & Haghghi, A. (2011). Measurement of (liquid + liquid) equilibria for ternary systems of (N-formylmorpholine + benzene + cyclohexane) at temperatures (303.15, 308.15, and 313.15) K. *The Journal of Chemical Thermodynamics*, 43(6), 938-942.

Sakal, S., Shen, C., & Li, C.-x. (2012). (Liquid + liquid) equilibria of {benzene + cyclohexane + two ionic liquids} at different temperature and atmospheric pressure. *The Journal of Chemical Thermodynamics*, 49, 81-86.

Salem, S., Chong, S., & Chun-xi, L. (2012). (Liquid+liquid) equilibria of {benzene+cyclohexane+two ionic liquids} at different temperature and atmospheric pressure. *The Journal of Chemical Thermodynamics*, 49, 81-86.

Salem, S., Shen, C., & Li, C.-x. (2012). (Liquid + liquid) equilibria of {benzene + cyclohexane + two ionic liquids} at different temperature and atmospheric pressure. *The Journal of Chemical Thermodynamics*, 49, 81-86.

Salleh, Z., Hadj-Kali, M., Hashim, M. A., & Mulyono, S. (2018). Ionic liquids for the separation of benzene and cyclohexane – COSMO-RS screening and experimental validation. *Journal of Molecular Liquids*, 266, 51-61.

Salleh, Z., Hadj-Kali, M., Hizaddin, H. F., & Ali Hashim, M. (2017a). Extraction of nitrogen compounds from model fuel using 1-ethyl-3-methylimidazolium methanesulfonate. *Separation and Purification Technology*.

Salleh, Z., Wazeer, I., Mulyono, S., El-blidi, L., Hashim, M. A., & Hadj-Kali, M. (2017b). Efficient removal of benzene from cyclohexane-benzene mixtures using deep eutectic solvents – COSMO-RS screening and experimental validation. *The Journal of Chemical Thermodynamics*, 104, 33-44.

Salleh, Z., Wazeer, I., Mulyono, S., El-blidi, L., Hashim, M. A., & Hadj-Kali, M. K. (2017c). Efficient removal of benzene from cyclohexane-benzene mixtures using deep eutectic solvents – COSMO-RS screening and experimental validation. *The Journal of Chemical Thermodynamics*, 104, 33-44.

Salleh, Z., Wilfred, C., & Ibrahim, A. M. (2014). *Desulfurization of Fuel Using Ionic Liquids: Computational Selection of Cation and Anion*. Paper presented at the Applied Mechanics and Materials.

Sander, A., Rogošić, M., Slivar, A., & Žuteg, B. (2016). Separation of Hydrocarbons by Means of Liquid-Liquid Extraction with Deep Eutectic Solvents. *Solvent Extraction and Ion Exchange*, 34(1), 86-98.

- Schilderman, A. M., Raeissi, S., & Peters, C. J. (2007). Solubility of carbon dioxide in the ionic liquid 1-ethyl-3-methylimidazolium bis(trifluoromethylsulfonyl)imide. *Fluid Phase Equilibria*, 260(1), 19-22.
- Seddon, K. (1995). Room-temperature ionic liquids: neoteric solvents for clean catalysis. *Kinetics and Catalysis*, 37(5), 693-697.
- Seddon, K. R. (1997). Ionic Liquids for Clean Technology. *Journal of Chemical Technology & Biotechnology*, 68(4), 351-356.
- Seyedein Ghannad, S. M., Lotfollahi, M. N., & Haghghi Asl, A. (2011). Measurement of (liquid + liquid) equilibria for ternary systems of (N-formylmorpholine + benzene + cyclohexane) at temperatures (303.15, 308.15, and 313.15) K. *The Journal of Chemical Thermodynamics*, 43(6), 938-942.
- Shen, J., Wang, H., Liu, H., Sun, Y., & Liu, Z. (2008). Brønsted acidic ionic liquids as dual catalyst and solvent for environmentally friendly synthesis of chalcone. *Journal of Molecular Catalysis A: Chemical*, 280(1-2), 24-28.
- Shiau, L.-D., & Yu, C.-C. (2009). Separation of the benzene/cyclohexane mixture by stripping crystallization. *Separation and Purification Technology*, 66(2), 422-426.
- Shiflett, M. B., Drew, D. W., Cantini, R. A., & Yokozeki, A. (2010). Carbon Dioxide Capture Using Ionic Liquid 1-Butyl-3-methylimidazolium Acetate. *Energy & Fuels*, 24(10), 5781-5789.
- Shvedene, N. V., Chernyshov, D. V., & Pletnev, I. V. (2008). Ionic liquids in electrochemical sensors. *Russian Journal of General Chemistry*, 78(12), 2507-2520.
- Simulis®, & thermodynamics. a thermo physical properties calculation server provided by ProSim. <http://www.prosim.net/>.
- Simulis® thermodynamics. Retrieved from <http://www.prosim.net/> on 15th November, 2016
- Smith, E. L., Abbott, A. P., & Ryder, K. S. (2014). Deep Eutectic Solvents (DESs) and Their Applications. *Chemical Reviews*, 114(21), 11060-11082.
- Song, S., Lin, C., & You, N. (2014a). Phase equilibria Study of the (benzene+cyclohexane+ N, N-dimethylformamide+ potassium thiocyanate) quaternary systems. *Fluid Phase Equilibria*, 376, 154-158.
- Song, S., Lin, C., & You, N. (2014b). Phase equilibria Study of the (benzene+cyclohexane+N,N-dimethylformamide+ potassium thiocyanate) quaternary systems. *Fluid Phase Equilibria*, 376, 154-158.
- Song, Z., Zhang, J., Zeng, Q., Cheng, H., Chen, L., & Qi, Z. (2016). Effect of cation alkyl chain length on liquid-liquid equilibria of {ionic liquids + thiophene + heptane}: COSMO-RS prediction and experimental verification. *Fluid Phase Equilibria*, 425, 244-251.

- Sucksmith, I. (1982). Extractive distillation saves energy. *Chem. Eng.(NY);(United States)*, 89(13).
- Tang, B., & Row, K. H. (2013). Recent developments in deep eutectic solvents in chemical sciences. *Monatshefte für Chemie - Chemical Monthly*, 144(10), 1427-1454.
- Tassios, D. (1976). Limitations in Correlating Strongly Nonideal Binary Systems with the NRTL and LEMF Equations. *Industrial & Engineering Chemistry Process Design and Development*, 15(4), 574-578.
- Tefera. (2006). *CEH Marketing Research Report Abstract*. Retrieved from <https://chemical.ihs.com/nl/Public/2006Sept.pdf>
- Thuy Pham, T. P., Cho, C.-W., & Yun, Y.-S. (2010). Environmental fate and toxicity of ionic liquids: A review. *Water Research*, 44(2), 352-372.
- Tonbul, Y., Zahmakiran, M., & Özkar, S. (2014). Iridium(0) nanoparticles dispersed in zeolite framework: A highly active and long-lived green nanocatalyst for the hydrogenation of neat aromatics at room temperature. *Applied Catalysis B: Environmental*, 148-149, 466-472.
- Vangelis, C., Bouriazos, A., Sotiriou, S., Samorski, M., Gutsche, B., & Papadogianakis, G. (2010). Catalytic conversions in green aqueous media: Highly efficient biphasic hydrogenation of benzene to cyclohexane catalyzed by Rh/TPPTS complexes. *Journal of Catalysis*, 274(1), 21-28.
- Verdía, P., González, E. J., Moreno, D., Palomar, J., & Tojo, E. (2017). Deepening of the Role of Cation Substituents on the Extractive Ability of Pyridinium Ionic Liquids of N-Compounds from Fuels. *ACS Sustainable Chemistry & Engineering*, 5(2), 2015-2025.
- Villaluenga, J. P., & Tabe-Mohammadi, A. (2000). A review on the separation of benzene/cyclohexane mixtures by pervaporation processes. *Journal of Membrane Science*, 169(2), 159-174.
- Wang, R., Li, C., Meng, H., Wang, J., & Wang, Z. (2008a). Ternary liquid– liquid equilibria measurement for benzene+ cyclohexane+ N-methylimidazole, or N-ethylimidazole, or N-methylimidazolium dibutylphosphate at 298.2 K and atmospheric pressure. *Journal of Chemical & Engineering Data*, 53(9), 2170-2174.
- Wang, R., Wang, J., Meng, H., Li, C., & Wang, Z. (2008b). Liquid–Liquid Equilibria for Benzene + Cyclohexane + 1-Methyl-3-methylimidazolium Dimethylphosphate or + 1-Ethyl-3-methylimidazolium Diethylphosphate. *Journal of Chemical & Engineering Data*, 53(5), 1159-1162.
- Wang, Z., Xia, S., & Ma, P. (2012). (Liquid + liquid) equilibria for the ternary system of (N-formylmorpholine + ethylbenzene + 2,2,4-trimethylpentane) at temperatures (303.15, 313.15, and 323.15) K. *Fluid Phase Equilibria*, 328, 25-30.

- Weissermel, K., & Arpe, H.-J. (2007). Aromatics — Production and Conversion *Industrial Organic Chemistry* (pp. 311-334): Wiley-VCH Verlag GmbH.
- Welton, T. (1999). Room-temperature ionic liquids. Solvents for synthesis and catalysis. *Chemical Reviews*, 99(8), 2071-2084.
- Wilfred, C., Man, Z., & Chan, Z. (2013). Predicting methods for sulfur removal from model oils using COSMO-RS and partition coefficient. *Chemical Engineering Science*, 102, 373-377.
- Wlazło, M., Alevizou, E. I., Voutsas, E. C., & Domańska, U. (2016). Prediction of ionic liquids phase equilibrium with the COSMO-RS model. *Fluid Phase Equilibria*, 424, 16-31.
- Wypych, G. (2001). *Handbook of Solvents*: ChemTec.
- Yang, X., Zhang, X., Dong, H., Yue, G., & Liu, J. (2015). (Liquid + liquid) equilibria for (benzene + cyclohexane + dimethyl sulfoxide) system at T = (298.15 or 303.15) K: Experimental data and correlation. *The Journal of Chemical Thermodynamics*, 84, 14-17.
- Yin, W., Ding, S., Xia, S., Ma, P., Huang, X., & Zhu, Z. (2010). Cosolvent Selection for Benzene–Cyclohexane Separation in Extractive Distillation. *Journal of Chemical & Engineering Data*, 55(9), 3274-3277.
- You, S.-H., Jeong, I.-Y., & Park, S.-J. (2015). Liquid–liquid equilibria in the ternary systems {hexadecane + BTX aromatics + 2-methoxyethanol or acetonitrile} at 298.15 K. *Fluid Phase Equilibria*, 389, 9-15.
- Yu, G., Li, X., Liu, X., Asumana, C., & Chen, X. (2011). Deep Desulfurization of Fuel Oils Using Low-Viscosity 1-Ethyl-3-methylimidazolium Dicyanamide Ionic Liquid. *Industrial & Engineering Chemistry Research*, 50(4), 2236-2244.
- Zahed A. H., Y. Y., M. A. Gashghari. (1992). Extraction of BTX hydrocarbons from Saudi Arabian refinery platformates. *Eng. Sci*, 4, 101-114.
- Zhang, J., Huang, C., Chen, B., Ren, P., & Lei, Z. (2007). Extraction of Aromatic Hydrocarbons from Aromatic/Aliphatic Mixtures Using Chloroaluminate Room-Temperature Ionic Liquids as Extractants. *Energy & Fuels*, 21(3), 1724-1730.
- Zhang, Q., De Oliveira Vigier, K., Royer, S., & Jerome, F. (2012). Deep eutectic solvents: syntheses, properties and applications. *Chemical Society Reviews*, 41(21), 7108-7146.
- Zhang, Z., Shi-Min, X., & Zhang, W. (2006). Binary mixed solvents for separating benzene-cyclohexane by extractive distillation. *Journal of Tianjin University*, 39, 424-427.
- Zhao, D., Liao, Y., & Zhang, Z. (2007). Toxicity of Ionic Liquids. *CLEAN – Soil, Air, Water*, 35(1), 42-48.

Zhou, T., Wang, Z., Chen, L., Ye, Y., Qi, Z., Freund, H., & Sundmacher, K. (2012a). Evaluation of the ionic liquids 1-alkyl-3-methylimidazolium hexafluorophosphate as a solvent for the extraction of benzene from cyclohexane: (Liquid + liquid) equilibria. *The Journal of Chemical Thermodynamics*, 48, 145-149.

Zhou, T., Wang, Z., Ye, Y., Chen, L., Xu, J., & Qi, Z. (2012b). Deep Separation of Benzene from Cyclohexane by Liquid Extraction Using Ionic Liquids as the Solvent. *Industrial & Engineering Chemistry Research*, 51(15), 5559-5564.

University of Malaya

## LIST OF PUBLICATIONS AND CONFERENCE PROCEEDINGS

### List of main publications in journals:

1. **Zulhaziman, S.**, M.K. Hadj-Kali, M. Ali Hashim, & Mulyono S. (2018). Ionic liquids for the separation of benzene and cyclohexane – COSMO-RS screening and experimental validation. *Journal of Molecular Liquids* 266 (2018) 51-61. DOI: <https://doi.org/10.1016/j.molliq.2018.06.034>, (*ISI-indexed, Q1, IF = 3.648*).
2. **Zulhaziman, S.**, Wazeer, I., Mulyono, S., El-blidi, L., Hashim, M. A., & Hadj-Kali, M. K. (2017). Efficient removal of benzene from cyclohexane-benzene mixtures using deep eutectic solvents – COSMO-RS screening and experimental validation. *The Journal of Chemical Thermodynamics*, 104, 33-44. DOI: <http://dx.doi.org/10.1016/j.jct.2016.09.002>, (*ISI-indexed, Q1, IF = 2.726*).
3. Hadj-Kali, M. K., **Zulhaziman, S.**, Ali, E., Khan, R., & Hashim, M. A. (2017). Separation of aromatic and aliphatic hydrocarbons using deep eutectic solvents: A critical review. *Fluid Phase Equilibria*, 448, 152-167. DOI: <https://doi.org/10.1016/j.fluid.2017.05.011>, (*ISI-indexed, Q1, IF = 2.473*).
4. **Zulhaziman, S.**, Hadj-Kali, M. K., Hizaddin, H. F., & Ali Hashim, M. (2017). Extraction of nitrogen compounds from model fuel using 1-ethyl-3-methylimidazolium methanesulfonate. *Separation and Purification Technology*. DOI: <http://dx.doi.org/10.1016/j.seppur.2017.07.068>, (*ISI-indexed, Q1, IF = 3.359*).
5. **Zulhaziman, S.**, M.K. Hadj-Kali, M. Ali Hashim, & Emadadeen Ali (2018). Extractive separation of benzene and cyclohexane using binary mixtures of emerging solvents. *Chemical Engineering Journal* (under review). (*ISI-indexed, Q1, IF = 3.648*).
6. **Zulhaziman, S.**, M.K. Hadj-Kali, M. Ali Hashim, & Emadadeen Ali (2018). Extractive separation of benzene and cyclohexane using 1-butyl-3-methylimidazolium acetate. IOP Conference Series: Materials Science and Engineering, (*ISI-indexed*).

### List of other publications during this admission:

1. Hayyan, M., Mbous, Y. P., Looi, C. Y., Wong, W. F., Hayyan, A., **Zulhaziman S.**, et al. (2016). Natural deep eutectic solvents: cytotoxic profile. *SpringerPlus*, 5(1), 1-12. doi:10.1186/s40064-016-2575-9.
2. Adeeb H., M. K. Hadj-Kali<sup>c</sup>, **Zulhaziman S.**, S. Rohayu R., Maan H, M. Ali Hashim, M.Y. Zulkifli, Shahidah N. R., Prediction of Deep Eutectic Solvents Solubility in Unsaturated Fatty Acid Using COSMO-RS. *Journal of Molecular Liquids* under review (ISI-indexed, Q1, IF = 3.648).

### List of papers presented in conferences:

1. “*Synthesis and characterisation of imidazolium-based ionic liquids containing nitrile groups*”, – Oral presentation, the 2<sup>nd</sup> International Conference on Purity, Utility Reaction and Environmental Research (PURE) 2015, Golden Horses Palace Hotel, Kuala Lumpur, 9-11<sup>th</sup> November 2015.
2. “*Extraction of nitrogen compounds from model fuel using 1-ethyl-3-methylimidazolium methanesulfonate*”, – Poster presentation, the 3<sup>rd</sup> International Conference on Ionic Liquids in Separation and Purification Technology (ILSEPT) 2017.
3. “*Extractive separation of benzene and cyclohexane using 1-butyl-3-methylimidazolium acetate*”, – Oral presentation, the 5<sup>th</sup> International Conference on Process Engineering and Advanced Materials (ICPEAM), Kuala Lumpur Convention Centre, Kuala Lumpur, 13-15<sup>th</sup> August 2018.



## Ionic liquids for the separation of benzene and cyclohexane – COSMO-RS screening and experimental validation

M. Zulhaziman M. Salleh <sup>a</sup>, Mohamed K. Hadj-Kali <sup>b,\*</sup>, Mohd A. Hashim <sup>a</sup>, Sarwono Mulyono <sup>b</sup>

<sup>a</sup> University of Malaya Centre for Ionic Liquid (UMCIL), Department of Chemical Engineering, Faculty of Engineering, University of Malaya, Kuala Lumpur, Malaysia  
<sup>b</sup> Chemical Engineering Department, King Saud University, P.O. Box 800, Riyadh 11421, Saudi Arabia

### ARTICLE INFO

#### Article history:

Received 6 January 2018  
 Received in revised form 6 June 2018  
 Accepted 8 June 2018  
 Available online 18 June 2018

#### Keywords:

Ionic liquids  
 Benzene  
 Cyclohexane  
 COSMO-RS  
 Liquid-liquid extraction

### ABSTRACT

The separation of benzene and cyclohexane from their mixture is difficult to perform via conventional distillation because of their close boiling points. In this work, liquid-liquid extraction using ionic liquids (ILs) is suggested for this purpose and 16 cations and 13 anions were selected to form 208 possible ILs screened with the Conductor-like Screening Model for Real Solvents (COSMO-RS) module. The screening result was experimentally validated by liquid-liquid extraction using four of the top ranked ILs, namely 1-ethyl-3-methylimidazolium acetate ([C<sub>2</sub>mim][Ac]), 1-ethyl-3-methylimidazolium dicyanamide ([C<sub>2</sub>mim][N(CN)<sub>2</sub>]), 1-ethyl-3-methylimidazolium thiocyanate ([C<sub>2</sub>mim][SCN]) and 1-ethyl-3-methylimidazolium bis(trifluoromethylsulfonyl)imide ([C<sub>2</sub>mim][Tf<sub>2</sub>N]). The ternary liquid-liquid equilibria for these ILs with benzene and cyclohexane were investigated at 25 °C and 1 atm with feed concentration of benzene ranging from 10 to 60 wt%. Good agreement was achieved between the tie-lines obtained from the COSMO-RS model and those obtained experimentally. The performance of ILs used in this study was compared with organic solvents, other ILs, and deep eutectic solvents reported in literature. The results of selectivity and distribution ratio confirmed that COSMO-RS was a reliable method for solvent screening and demonstrated the suitability of the selected ILs as extracting solvents. In all ternary systems, no IL was detected in the cyclohexane layer and the concentration of cyclohexane in the IL layer was very low. This observation indicated that there was minimum cross-contamination between the phases and therefore less energy will be required for the solvent recovery.

© 2018 Elsevier B.V. All rights reserved.

### 1. Introduction

Benzene and cyclohexane are two of the most valuable products that are widely processed in the petrochemical industry. At present, nearly all cyclohexane is produced by the catalytic hydrogenation of benzene [1]. In this process, the cyclohexane with high purity can only be produced via complex process control that involves a complex heat integration and economic study [2, 3]. Therefore, this method usually produces a mixture of benzene and cyclohexane. The unreacted benzene in the reactor's effluent must be removed to produce pure cyclohexane. However, the separation of benzene and cyclohexane by conventional distillation is quite difficult and challenging because they have close boiling points (80.1 °C for benzene and 80.7 °C for cyclohexane).

The conventional techniques employed for the separation of benzene and cyclohexane from their mixture include azeotropic distillation and extractive distillation [4]. In azeotropic distillation, a strongly polar entrainer is introduced to form an azeotropic mixture with cyclohexane, which alters the vapor-liquid equilibrium (VLE) curve for this mixture. Meanwhile, the extractive distillation method uses the entrainer to

reduce the volatility of benzene. Despite their potential at an industrial scale, both processes suffer from several disadvantages such as process complexity, high capital and operating costs, and high energy consumption [5, 6]. Moreover, these processes are carried out by adding a third compound as the entrainer; the removal of the third compound from the distillate introduces higher process complexity and cost to the adopted method. In addition, azeotropic distillation and extractive distillation are only suitable for high (>90%) and medium (65–90%) concentration of benzene, respectively. Liquid-liquid extraction (LLE) is widely used in the industry because of the mild operating conditions and simplicity. Although LLE is suitable for separating low concentrations of benzene (20–65%), there is still no industrial process available for concentrations <20 wt%. While the pervaporation process was reviewed as a potential technique, it was limited by the challenges encountered during economic evaluation [5]. Several reports have demonstrated the excellent performance of industrial organic solvents such as ethylene glycol, tetra-ethylene glycol, sulfolane, and *N*-methylpyrrolidone as extractants [7–9]. However, their application is associated with several challenges because these solvents are usually volatile, toxic and flammable.

Interestingly, ionic liquids (ILs) have become a progressively popular class of solvent in the last decades as their potential in many industrial

\* Corresponding author.

E-mail address: [mhadjkali@ksu.edu.sa](mailto:mhadjkali@ksu.edu.sa) (M.K. Hadj-Kali).



## Efficient removal of benzene from cyclohexane-benzene mixtures using deep eutectic solvents – COSMO-RS screening and experimental validation



Zulhaziman Salleh<sup>a</sup>, Irfan Wazeer<sup>b</sup>, Sarwono Mulyono<sup>b</sup>, Lahssen El-blidi<sup>b</sup>, Mohd Ali Hashim<sup>a</sup>, Mohamed K. Hadj-Kali<sup>b,\*</sup>

<sup>a</sup> University of Malaya Center for Ionic Liquids (UMCIL), Department of Chemical Engineering, Faculty of Engineering, University of Malaya, 50603 Kuala Lumpur, Malaysia

<sup>b</sup> Chemical Engineering Department, King Saud University, P.O. Box 800, Riyadh 11421, Saudi Arabia

### ARTICLE INFO

#### Article history:

Received 9 February 2016  
Received in revised form 17 August 2016  
Accepted 2 September 2016  
Available online 8 September 2016

#### Keywords:

Liquid–liquid extraction  
Deep eutectic solvents  
COSMO-RS  
Benzene  
Cyclohexane

### ABSTRACT

The separation of benzene and cyclohexane is considered one of the most challenging processes in the petrochemical industry. For this study, 40 deep eutectic solvents (DESs) were screened by using the COSMO-RS model. The screening was achieved based on a comparison of selectivity, capacity, and the performance index, all derived from the activity coefficient at infinite dilution. In addition, the sigma  $\sigma$ -profile and  $\sigma$ -potential of each component were used to analyse the interactions between the different species during the extraction process. After screening, five DESs were selected for experimental validation. The liquid–liquid extraction process was conducted, and the ternary diagrams were plotted for the selected DESs at 25 °C under atmospheric pressure. The NRTL model was successfully employed to correlate the experimental tie lines. The results revealed that COSMO-RS was a useful tool for screening potential DESs qualitatively. In addition, observations revealed strong agreement between NRTL and the experiment results, with a root mean square deviation of less than unity for all systems. The findings showed that the selected DESs are feasible for use as extracting solvents for this separation, whereby in all systems no trace of DES was found in the cyclohexane layer.

© 2016 Elsevier Ltd.

### 1. Introduction

Cyclohexane is a critical industrial chemical that can be produced through the catalytic hydrogenation of benzene. To obtain pure cyclohexane, it is necessary to remove unreacted benzene from the reactor's effluent stream, which is entrained into the cyclohexane product [1,2]. One of the most challenging tasks in the chemical industry is the separation of benzene and cyclohexane. Traditional distillation is infeasible for the separation because of their close boiling points ( $\Delta T_b = 0.6$  °C at atmospheric pressure), approximately equal molecular volumes, and the binary azeotrope [3–6]. In the chemical industry, extractive distillation or azeotropic distillation is viable for the separation of benzene and cyclohexane; however, these processes are complex and consume a substantial amount of energy [1,2,6,7].

A typical flow diagram of the industrial process for the production of cyclohexane from benzene is shown in Fig. 1. Liquid–liquid extraction units are most widely employed for the separation of

cyclohexane and benzene because of the low energy consumption, and the key is the extractant [8]. A suitable extractant should have the advantages of high selectivity and solvent capacity, low volatility, easy regeneration, low viscosity, and high thermal stability [4,6,9]. Dimethylsulfoxide, Sulfolane, N-methylpyrrolidone, N-formylmorpholine and methylcarbonate are most widely used as extractants for aromatic compounds [10]. Studies had been carried out to establish the liquid–liquid equilibrium (LLE) data of the ternary systems involving the conventional solvents such as ethylene carbonate [11,12], dimethyl sulfone [13], ethylene glycol [3,14], and N-formylmorpholine [15]. Apart from ternary, the LLE data for quaternary systems had also been reported for N,N-dimethylformamide (DMF) + sodium thiocyanate (NaSCN) [16], and N,N-dimethylformamide + potassium thiocyanate [9]. However, these solvents are typically toxic, flammable, volatile, and difficult to regenerate. In contrast to conventional solvents, ionic liquids (ILs) have been found to be promising solvents for extraction because of their high thermal stability, negligible vapor pressure, nonvolatile nature, and high solution capacity [4,5,17–19]. Several ILs were studied to show good performance in extraction of benzene from cyclohexane including [Bmim][BF<sub>4</sub>] [5], [Bpy]

\* Corresponding author.

E-mail address: [mhadjkali@ksu.edu.sa](mailto:mhadjkali@ksu.edu.sa) (M.K. Hadj-Kali).

<http://dx.doi.org/10.1016/j.jct.2016.09.002>  
0021-9614/© 2016 Elsevier Ltd.



ELSEVIER

Contents lists available at ScienceDirect

## Fluid Phase Equilibria

journal homepage: [www.elsevier.com/locate/fluid](http://www.elsevier.com/locate/fluid)

## Separation of aromatic and aliphatic hydrocarbons using deep eutectic solvents: A critical review



Mohamed K. Hadj-Kali<sup>a,\*</sup>, Zulhaziman Salleh<sup>b,c</sup>, Emad Ali<sup>a</sup>, Rawai Khan<sup>a</sup>,  
Mohd. Ali Hashim<sup>b,c</sup>

<sup>a</sup> Chemical Engineering Department, College of Engineering, King Saud University, P.O.Box 800, Riyadh 11421, Saudi Arabia

<sup>b</sup> Department of Chemical Engineering, Faculty of Engineering, University of Malaya, 50603 Kuala Lumpur, Malaysia

<sup>c</sup> University of Malaya Center for Ionic Liquids (UMCIL), University of Malaya, 50603 Kuala Lumpur, Malaysia

### ARTICLE INFO

#### Article history:

Received 14 March 2017

Received in revised form

5 May 2017

Accepted 12 May 2017

Available online 13 May 2017

#### Keywords:

Deep eutectic solvents

Aliphatics

Aromatics

Liquid-liquid extraction

COSMO-RS

### ABSTRACT

The reported experimental data for the separation of aromatic from aliphatic compounds using green solvents is growing exponentially. This paper surveys the existing data and presents a critical review that helps clarifying the major findings, identifies shortcomings and provides some recommendations. The comparison between deep eutectic solvents (DESs) and both ionic liquids (ILs) and classical organic solvents for this challenging separation is also presented based on experimental selectivity and distribution ratio data. This comparison confirms the capability of DESs to effectively extract aromatic compounds and shows that DESs can compete with ILs and even outclass them in some cases. Moreover, our comprehensive literature survey has revealed that in many cases the use of DESs yields to a minimum cross-contamination between the two phases. This will undeniably facilitate the separation procedure and thus reduce the cost of the separation process. On the other hand, the performance of COSMO-RS to predict ternary liquid-liquid equilibrium diagrams for systems including DESs is also evaluated in this work for all available data. COSMO-RS was able to reproduce the experimental tie-lines with a good accuracy in many cases. Therefore, it represents a cost-effective and time-saving screening tool to evaluate the extraction performance of the unlimited number of possible salt/complexing agents' combinations.

© 2017 Elsevier B.V. All rights reserved.

### 1. Introduction

The separation and purification of aromatics is a challenging task for chemical engineers due to the sharp differences in the boiling points of the various hydrocarbons and the various combinations of azeotropes that may occur [1]. Commercially three techniques for separation are classified according to solution concentration: (i) at low aromatic concentration within 20–65 wt%, the liquid-liquid extraction is mostly used, (ii) for medium aromatic contents ranging from 65 to 90 wt%, the extractive distillation is typically used and (iii) for very high aromatic substances (>90 wt %) azeotropic distillation is applied. But until now, no practical process exist when the separation aromatic content in the feed mixture is below 20 wt% [2]. However, the liquid extraction process is considered to be the best favorable process for aromatic content

of less than 20%. The key advantages of using this process are the low energy consumption and that no change in both physical properties and chemical structure are observed.

Nevertheless, a crucial step in such process is how to select the proper solvent. A perfect solvent should deliver high solute selectivity. Cost-effective solvent should possess great distribution ratio and minimum ratio of feed to solvent. In addition, the physical and thermodynamic characteristics of the solvent such as viscosity, thermal stability, density and surface tension should help its industrial application. Furthermore, the solvent should be environment friendly, easy to regenerate and abundantly available at low cost. Normally organic solvents such as sulfolane, furfuryl alcohol, ethylene glycols, N-methylpyrrolidone (NMP), and N-formylmorpholine (NFM) are used. However, due the high toxicity, flammability, volatile nature and high cost of regeneration of these solvents, researchers are trying to find out alternative solvents with same or better properties.

Around one decade ago, for the first time, a newly emerging

\* Corresponding author.

E-mail address: [mhadjkali@ksu.edu.sa](mailto:mhadjkali@ksu.edu.sa) (M.K. Hadj-Kali).

<http://dx.doi.org/10.1016/j.fluid.2017.05.011>

0378-3812/© 2017 Elsevier B.V. All rights reserved.



## Extraction of nitrogen compounds from model fuel using 1-ethyl-3-methylimidazolium methanesulfonate



M. Zulhaziman M. Salleh<sup>a,b</sup>, Mohamed K. Hadj-Kali<sup>c,\*</sup>, Haneef F. Hizaddin<sup>a,b</sup>, M. Ali Hashim<sup>a,b</sup>

<sup>a</sup> Department of Chemical Engineering, Faculty of Engineering, University of Malaya, 50603 Kuala Lumpur, Malaysia

<sup>b</sup> University Malaya Centre for Ionic Liquids (UMCIL), University of Malaya, 50603 Kuala Lumpur, Malaysia

<sup>c</sup> Chemical Engineering Department, King Saud University, P.O. Box 800, Riyadh 11421, Saudi Arabia

### ARTICLE INFO

**Keywords:**  
Denitrification  
Ionic liquid  
Liquid-liquid extraction  
COSMO-RS  
NRTL

### ABSTRACT

Removal of nitrogen compounds is an essential process in the fuel processing industry. In this work, the extraction performance of 1-ethyl-3-methylimidazolium methanesulfonate ([Emim][MeSO<sub>3</sub>]) ionic liquid in removing pyrrole, indoline, pyridine and quinoline from cyclohexane is investigated. The ternary liquid-liquid equilibria for four systems containing [Emim][MeSO<sub>3</sub>] + pyrrole/indoline/pyridine/quinoline + cyclohexane were predicted using COSMO-RS and validated experimentally at 298.15 K under atmospheric pressure, with feed concentrations of nitrogen compounds ranging from 5 to 50 wt%. Othmer-Tobias and Hand correlations confirmed the consistency of the experimental data. The tie-lines obtained experimentally and predicted with COSMO-RS were in good agreement. Additionally, the non-random two-liquid (NRTL) model was successfully employed to correlate the experimental tie-lines. The effects of basicity of nitrogen compounds toward extraction efficiency were also investigated. The selectivity and distribution ratio results demonstrated the suitability of [Emim][MeSO<sub>3</sub>] as an extraction solvent for removing nitrogen compounds from fuel. Finally, the multi-component extraction confirmed the performance of [Emim][MeSO<sub>3</sub>] for extractive denitrogenation. In all ternary systems investigated in this work, the concentration of cyclohexane in the extract phase was very small and the presence of the IL in the raffinate phase was negligible indicating minimum cross contamination between the extract and raffinate phases.

### 1. Introduction

Removal of nitrogen compounds or denitrogenation is an important process in the fuel processing industry. The presence of aromatic nitrogen compounds in fuels can upset the conventional hydrodesulfurization process through competitive adsorption and catalyst poisoning [1]. Moreover, nitrogen compounds in fuel can also lead to serious environmental effects. The emission of nitrogen oxides into the atmosphere from engine combustion causes air pollution and acid rain. Therefore, stringent regulations have been established by many countries to limit the nitrogen content in fuels. For instance, USA has further limited the nitrogen content in diesel fuel from < 70 ppm in 2003 to < 1 ppm in 2010 [2]. The traditional process for the removal of nitrogen compounds from fuel is known as hydrodenitrogenation (HDN). It is an expensive process not only since it requires an expensive catalyst and a high hydrogen supply but also due to the need for high temperature (600 K) and pressure (300 atm) [3]. Furthermore, HDN is

ineffective in removing refractory aromatic nitrogen compounds such as pyridine, pyrrole and their derivatives.

The nitrogen compounds in fuel oil can be categorized into two types: non-basic and basic. The non-basic nitrogen compounds have a 5-membered ring structure with a lone pair of electrons as part of the aromatic  $\pi$  electron system. The basic compounds are composed of aromatic rings and a lone pair of electrons which are not associated with the aromatic system [4]. Examples of non-basic and basic nitrogen compounds are pyrrole and pyridine, respectively. As more stringent rules are expected in future, the HDN process will be economically unfavorable and challenging to operate with its severe operating conditions. Liquid-liquid extraction (LLE) or, more specifically, extractive denitrogenation (EDN) is an attractive process because it can be operated under ambient operating condition. However, this process requires a careful selection of the extracting solvents. Some studies have investigated this process using common organic solvents such as methanol [5], ethanol [6], N-methylformamide [7], *N,N*-

**Abbreviations:** COSMO-RS, Conductor-like Screening Model for Real Solvents; BP functional, Becke-Perdew functional; DFT, density functional theory; EDN, extractive denitrogenation; HDN, hydrodenitrogenation; IL, ionic liquid; LLE, liquid-liquid extraction; NRTL, non-random two-liquid; RI, resolution of identity; RMSD, root mean square deviation

\* Corresponding author.

E-mail address: [mhadjkali@ksu.edu.sa](mailto:mhadjkali@ksu.edu.sa) (M.K. Hadj-Kali).

<http://dx.doi.org/10.1016/j.seppur.2017.07.068>

Received 8 April 2017; Received in revised form 11 July 2017; Accepted 25 July 2017

Available online 26 July 2017

1383-5866/ © 2017 Elsevier B.V. All rights reserved.

# Extractive separation of benzene and cyclohexane using 1-butyl-3-methylimidazolium acetate

M. Zulhaziman M. Salleh<sup>\*1</sup>, Mohamed K. Hadj-Kali<sup>2</sup>, M. A. Hashim<sup>1</sup>, Emad Ali<sup>2</sup>

<sup>1</sup> University of Malaya Centre for Ionic Liquids (UMCiL), Department of Chemical Engineering, Faculty of Engineering, University of Malaya, Kuala Lumpur, Malaysia.

<sup>2</sup> Chemical Engineering Department, King Saud University, P.O Box 800, Riyadh 11421, Saudi Arabia.

\*Corresponding author: zulhaziman@siswa.um.edu.my

**Abstract.** Separation of benzene and cyclohexane is a challenging process in petrochemical industry due to the difficulty to separate them by a simple distillation. Recognizing ionic liquid as a potential alternative, this work investigated the performance of 1-butyl-3-methylimidazolium acetate ([C<sub>4</sub>Mim][Ac]) as an extracting solvent in the separation of benzene and cyclohexane via liquid–liquid extraction. The ternary liquid–liquid equilibria for this IL with benzene and cyclohexane was investigated at 25 °C and 1 atm, with feed concentration of benzene ranging from 10 to 60 wt %. Good agreement was achieved for the tie-lines obtained from the COSMO-RS model and experimental data. The NRTL model was successfully employed to correlate the experimental tie lines. The performance of [C<sub>4</sub>Mim][Ac] was compared with organic solvent and other ILs reported in literature. The selectivity and distribution ratio of benzene were in the range of 4.17–5.47 and 0.51–0.72, respectively. At equilibrium, no IL was present in the cyclohexane layer and the concentration of cyclohexane in the IL layer was very low. This observation indicated that there was minimum cross-contamination between the phases and less energy was required for solvent recovery.

## 1. Introduction

The separation of benzene and cyclohexane by conventional distillation is difficult and challenging because they have nearly equal boiling points, with the difference of only 0.64 °C. This condition requires an advanced distillation process such as the azeotropic or extractive distillations [1]. Despite their application in industry, both processes suffer from some disadvantages such as process complexity, high capital and operating costs, and high energy consumption [2, 3]. Moreover, these processes are carried out by adding a third compound as the entrainer, in which the removal of the third compound from the distillate causes even higher process complexity and cost. In addition, azeotropic distillation and extractive distillation are only suitable for high (> 90%) and medium (65–90 %) concentration of benzene in the feed, respectively.

Liquid–liquid extraction (LLE) is widely used in the chemical industry because it is a simple process that can be operated at mild conditions. In the case of benzene-cyclohexane mixture, LLE is a suitable method to separate low concentrations of benzene (20–65 %). However, there is still no industrial process available for the concentrations less than 20 wt %. While the pervaporation process was reviewed as a potential technique, it was still limited by the challenges encountered during economic evaluation [2]. Several reports have investigated the performance of industrial organic solvents in LLE process such as ethylene glycol, tetra-ethylene glycol, sulfolane, and *N*-

## APPENDIX

### Appendix A: COSMO-RS prediction data involving $C^\infty$ , $S^\infty$ , $PI^\infty$ , $\sigma$ -profile, $\sigma$ -potential and LLE tie lines

**Table A1:  $C^\infty$ ,  $S^\infty$  and  $PI^\infty$  for 40 DESs studied**

No	DES	$C^\infty$	$S^\infty$	$PI^\infty$
1	TBABr:Sulf (1:7)	4.547	4.297	19.538
2	MTPPBr:TEG (1:4)	2.528	3.371	8.521
3	TBABr:TEG (1:4)	2.550	2.476	6.312
4	MTPPBr:PD (1:4)	1.322	3.529	4.665
5	BTPPBr:EG (1:3)	1.171	3.968	4.646
6	MTPPBr:EG (1:3)	0.996	4.570	4.553
7	BTPPBr:Gly (1:5)	1.181	3.722	4.395
8	BTPPBr:TFA (1:1)	0.752	5.457	4.105
9	ChCl:TEG (1:4)	1.308	3.085	4.036
10	MTPPBr:Gly (1:2)	0.781	4.744	3.705
11	TBACl:TEG (1:2)	1.578	2.336	3.685
12	ChCl:TMUr (1:2)	0.961	3.330	3.199
13	ChCl:LA (1:2)	0.502	5.448	2.735
14	TBABr:PD (1:3)	1.196	2.253	2.695
15	TBABr:Gly (1:4)	0.953	2.607	2.485
16	TMACl:EG (1:2)	0.734	3.204	2.352
17	ChCl:Ac (1:2)	0.553	4.173	2.306
18	TBACl:MA (1:2)	0.724	3.184	2.304
19	TBACl:EG (1:2)	0.957	2.218	2.123
20	ChCl:Ur (1:2)	0.367	5.115	1.878
21	ChCl:PAC (1:1)	0.309	5.695	1.759
22	TBACl:Gly (1:2)	0.783	2.207	1.728
23	ChCl:PPA (1:1)	0.310	5.399	1.675
24	ChCl:MUr (1:2)	0.318	5.248	1.669
25	ChCl:MA (1:1)	0.291	5.565	1.619
26	DEEACl:TFA (1:2)	0.223	7.147	1.595
27	ChCl:OA (1:1)	0.240	6.567	1.577
28	TMACl:Gly (1:2)	0.406	3.779	1.533
29	ChCl:EG (1:2)	0.407	3.494	1.422
30	ChCl:IA (1:1)	0.229	6.126	1.405
31	ChCl:Iso (1:2)	0.281	4.820	1.355
32	ChCl:Gly (1:1)	0.427	3.124	1.334
33	DEEACl:EG (1:2)	0.428	3.090	1.324
34	ChCl:Tur (1:2)	0.078	15.101	1.173
35	DEEACl:Gly (1:2)	0.315	3.376	1.064
36	ChCl:Xy (1:1)	0.257	3.742	0.961
37	ChNO <sub>3</sub> :Ur (1:2)	0.059	14.865	0.874
38	ChCl:Sor (1:1)	0.205	4.162	0.852
39	ChBF <sub>4</sub> :Ur (1:2)	0.023	34.149	0.786
40	ChCl:Glu (1:1)	0.164	4.241	0.695

**Table A2:  $C^\infty$ ,  $S^\infty$  and  $PI^\infty$  for 208 ILs studied**

No	IL	$C^\infty$	$S^\infty$	$PI^\infty$
1	C <sub>2</sub> mimAc	1.188	4.023	4.781
2	C <sub>4</sub> mimAc	0.797	3.673	2.929
3	C <sub>6</sub> mimAc	0.708	3.323	2.351
4	C <sub>8</sub> mimAc	0.706	2.922	2.063
5	C <sub>2</sub> mpyrroAc	2.111	2.326	4.909
6	C <sub>4</sub> mpyrroAc	1.127	2.540	2.864
7	C <sub>6</sub> mpyrroAc	0.907	2.545	2.310
8	C <sub>8</sub> mpyrroAc	0.849	2.424	2.058
9	C <sub>2</sub> mpyrAc	1.250	3.773	4.716
10	C <sub>4</sub> mpyrAc	0.943	3.421	3.224
11	C <sub>6</sub> mpyrAc	0.857	3.108	2.665
12	C <sub>8</sub> mpyrAc	0.850	2.787	2.370
13	C <sub>2</sub> mpipAc	1.706	2.386	4.071
14	C <sub>4</sub> mpipAc	1.109	2.478	2.748
15	C <sub>6</sub> mpipAc	0.933	2.434	2.270
16	C <sub>8</sub> mpipAc	0.890	2.302	2.048
17	C <sub>2</sub> mimbenzoate	0.622	6.757	4.205
18	C <sub>4</sub> mimbenzoate	0.673	5.210	3.505
19	C <sub>6</sub> mimbenzoate	0.726	4.347	3.154
20	C <sub>8</sub> mimbenzoate	0.798	3.653	2.916
21	C <sub>2</sub> mpyrrobenzoate	0.956	4.502	4.303
22	C <sub>4</sub> mpyrrobenzoate	0.892	3.968	3.540
23	C <sub>6</sub> mpyrrobenzoate	0.906	3.548	3.216
24	C <sub>8</sub> mpyrrobenzoate	0.950	3.163	3.003
25	C <sub>2</sub> mpyrbenzoate	0.788	5.958	4.697
26	C <sub>4</sub> mpyrbenzoate	0.835	4.766	3.979
27	C <sub>6</sub> mpyrbenzoate	0.890	4.013	3.571
28	C <sub>8</sub> mpyrbenzoate	0.953	3.450	3.288
29	C <sub>2</sub> mpipbenzoate	0.981	4.221	4.139
30	C <sub>4</sub> mpipbenzoate	0.964	3.701	3.567
31	C <sub>6</sub> mpipbenzoate	0.972	3.309	3.216
32	C <sub>8</sub> mpipbenzoate	1.013	2.956	2.996
33	C <sub>2</sub> mimBF <sub>4</sub>	0.269	18.922	5.092
34	C <sub>4</sub> mimBF <sub>4</sub>	0.353	13.204	4.660
35	C <sub>6</sub> mimBF <sub>4</sub>	0.460	9.668	4.448
36	C <sub>8</sub> mimBF <sub>4</sub>	0.599	7.170	4.296
37	C <sub>2</sub> mpyrroBF <sub>4</sub>	0.547	8.168	4.465
38	C <sub>4</sub> mpyrroBF <sub>4</sub>	0.486	7.789	3.789
39	C <sub>6</sub> mpyrroBF <sub>4</sub>	0.559	6.545	3.659
40	C <sub>8</sub> mpyrroBF <sub>4</sub>	0.672	5.371	3.607
41	C <sub>2</sub> mpyrBF <sub>4</sub>	0.438	15.116	6.627
42	C <sub>4</sub> mpyrBF <sub>4</sub>	0.537	10.923	5.860
43	C <sub>6</sub> mpyrBF <sub>4</sub>	0.667	8.168	5.450
44	C <sub>8</sub> mpyrBF <sub>4</sub>	0.803	6.327	5.082
45	C <sub>2</sub> mpipBF <sub>4</sub>	0.563	7.918	4.456
46	C <sub>4</sub> mpipBF <sub>4</sub>	0.580	6.963	4.037
47	C <sub>6</sub> mpipBF <sub>4</sub>	0.655	5.831	3.822

48	C <sub>8</sub> mpipBF <sub>4</sub>	0.766	4.827	3.696
49	C <sub>2</sub> mimDCN	0.286	14.049	4.025
50	C <sub>4</sub> mimDCN	0.390	9.603	3.743
51	C <sub>6</sub> mimDCN	0.494	7.221	3.567
52	C <sub>8</sub> mimDCN	0.617	5.553	3.425
53	C <sub>2</sub> mpyrroDCN	0.602	7.365	4.437
54	C <sub>4</sub> mpyrroDCN	0.604	6.513	3.934
55	C <sub>6</sub> mpyrroDCN	0.686	5.485	3.760
56	C <sub>8</sub> mpyrroDCN	0.791	4.586	3.627
57	C <sub>2</sub> mpyrDCN	0.437	11.246	4.910
58	C <sub>4</sub> mpyrDCN	0.548	8.179	4.484
59	C <sub>6</sub> mpyrDCN	0.667	6.300	4.202
60	C <sub>8</sub> mpyrDCN	0.786	5.039	3.959
61	C <sub>2</sub> mpipDCN	0.640	6.885	4.410
62	C <sub>4</sub> mpipDCN	0.698	5.845	4.077
63	C <sub>6</sub> mpipDCN	0.777	4.938	3.835
64	C <sub>8</sub> mpipDCN	0.878	4.169	3.659
65	C <sub>2</sub> mimEtSO <sub>4</sub>	0.522	8.559	4.469
66	C <sub>4</sub> mimEtSO <sub>4</sub>	0.576	6.739	3.880
67	C <sub>6</sub> mimEtSO <sub>4</sub>	0.636	5.622	3.574
68	C <sub>8</sub> mimEtSO <sub>4</sub>	0.724	4.689	3.396
69	C <sub>2</sub> mpyrroEtSO <sub>4</sub>	0.816	5.231	4.270
70	C <sub>4</sub> mpyrroEtSO <sub>4</sub>	0.756	4.792	3.623
71	C <sub>6</sub> mpyrroEtSO <sub>4</sub>	0.783	4.317	3.381
72	C <sub>8</sub> mpyrroEtSO <sub>4</sub>	0.846	3.837	3.248
73	C <sub>2</sub> mpyrEtSO <sub>4</sub>	0.721	7.636	5.504
74	C <sub>4</sub> mpyrEtSO <sub>4</sub>	0.775	6.169	4.784
75	C <sub>6</sub> mpyrEtSO <sub>4</sub>	0.847	5.178	4.387
76	C <sub>8</sub> mpyrEtSO <sub>4</sub>	0.927	4.407	4.087
77	C <sub>2</sub> mpipEtSO <sub>4</sub>	0.850	4.995	4.244
78	C <sub>4</sub> mpipEtSO <sub>4</sub>	0.844	4.487	3.785
79	C <sub>6</sub> mpipEtSO <sub>4</sub>	0.868	4.027	3.495
80	C <sub>8</sub> mpipEtSO <sub>4</sub>	0.928	3.585	3.326
81	C <sub>2</sub> mimH <sub>2</sub> SO <sub>4</sub>	0.315	9.629	3.037
82	C <sub>4</sub> mimH <sub>2</sub> SO <sub>4</sub>	0.292	8.438	2.466
83	C <sub>6</sub> mimH <sub>2</sub> SO <sub>4</sub>	0.331	7.012	2.324
84	C <sub>8</sub> mimH <sub>2</sub> SO <sub>4</sub>	0.406	5.641	2.292
85	C <sub>2</sub> mpyrroH <sub>2</sub> SO <sub>4</sub>	0.672	4.588	3.085
86	C <sub>4</sub> mpyrroH <sub>2</sub> SO <sub>4</sub>	0.438	5.157	2.260
87	C <sub>6</sub> mpyrroH <sub>2</sub> SO <sub>4</sub>	0.435	4.887	2.125
88	C <sub>8</sub> mpyrroH <sub>2</sub> SO <sub>4</sub>	0.487	4.344	2.114
89	C <sub>2</sub> mpyrH <sub>2</sub> SO <sub>4</sub>	0.426	8.738	3.727
90	C <sub>4</sub> mpyrH <sub>2</sub> SO <sub>4</sub>	0.420	7.463	3.133
91	C <sub>6</sub> mpyrH <sub>2</sub> SO <sub>4</sub>	0.474	6.225	2.949
92	C <sub>8</sub> mpyrH <sub>2</sub> SO <sub>4</sub>	0.549	5.158	2.832
93	C <sub>2</sub> mpipH <sub>2</sub> SO <sub>4</sub>	0.598	4.772	2.854
94	C <sub>4</sub> mpipH <sub>2</sub> SO <sub>4</sub>	0.485	4.874	2.364
95	C <sub>6</sub> mpipH <sub>2</sub> SO <sub>4</sub>	0.492	4.514	2.221
96	C <sub>8</sub> mpipH <sub>2</sub> SO <sub>4</sub>	0.547	3.998	2.189
97	C <sub>2</sub> mimNO <sub>3</sub>	0.658	8.252	5.428

98	C <sub>4</sub> mimNO <sub>3</sub>	0.501	7.646	3.835
99	C <sub>6</sub> mimNO <sub>3</sub>	0.513	6.504	3.337
100	C <sub>8</sub> mimNO <sub>3</sub>	0.587	5.296	3.108
101	C <sub>2</sub> mpyrroNO <sub>3</sub>	1.479	3.859	5.707
102	C <sub>4</sub> mpyrroNO <sub>3</sub>	0.779	4.608	3.591
103	C <sub>6</sub> mpyrroNO <sub>3</sub>	0.687	4.511	3.101
104	C <sub>8</sub> mpyrroNO <sub>3</sub>	0.713	4.082	2.912
105	C <sub>2</sub> mpyrNO <sub>3</sub>	0.812	7.695	6.247
106	C <sub>4</sub> mpyrNO <sub>3</sub>	0.694	6.833	4.739
107	C <sub>6</sub> mpyrNO <sub>3</sub>	0.715	5.819	4.158
108	C <sub>8</sub> mpyrNO <sub>3</sub>	0.780	4.875	3.804
109	C <sub>2</sub> mpipNO <sub>3</sub>	1.205	4.126	4.971
110	C <sub>4</sub> mpipNO <sub>3</sub>	0.825	4.421	3.646
111	C <sub>6</sub> mpipNO <sub>3</sub>	0.758	4.201	3.182
112	C <sub>8</sub> mpipNO <sub>3</sub>	0.790	3.776	2.982
113	C <sub>2</sub> mimOCSO <sub>4</sub>	0.701	4.940	3.462
114	C <sub>4</sub> mimOCSO <sub>4</sub>	0.816	3.975	3.244
115	C <sub>6</sub> mimOCSO <sub>4</sub>	0.895	3.430	3.071
116	C <sub>8</sub> mimOCSO <sub>4</sub>	0.980	3.011	2.952
117	C <sub>2</sub> mpyrroOCSO <sub>4</sub>	0.805	4.033	3.245
118	C <sub>4</sub> mpyrroOCSO <sub>4</sub>	0.913	3.388	3.092
119	C <sub>6</sub> mpyrroOCSO <sub>4</sub>	0.998	2.996	2.989
120	C <sub>8</sub> mpyrroOCSO <sub>4</sub>	1.078	2.698	2.908
121	C <sub>2</sub> mpyrOCSO <sub>4</sub>	0.889	4.639	4.123
122	C <sub>4</sub> mpyrOCSO <sub>4</sub>	1.002	3.822	3.829
123	C <sub>6</sub> mpyrOCSO <sub>4</sub>	1.092	3.310	3.614
124	C <sub>8</sub> mpyrOCSO <sub>4</sub>	1.169	2.933	3.427
125	C <sub>2</sub> mpipOCSO <sub>4</sub>	0.885	3.759	3.325
126	C <sub>4</sub> mpipOCSO <sub>4</sub>	1.004	3.205	3.217
127	C <sub>6</sub> mpipOCSO <sub>4</sub>	1.078	2.844	3.065
128	C <sub>8</sub> mpipOCSO <sub>4</sub>	1.150	2.567	2.953
129	C <sub>2</sub> mimPF <sub>6</sub>	0.192	37.252	7.135
130	C <sub>4</sub> mimPF <sub>6</sub>	0.411	17.190	7.058
131	C <sub>6</sub> mimPF <sub>6</sub>	0.617	10.842	6.695
132	C <sub>8</sub> mimPF <sub>6</sub>	0.827	7.541	6.240
133	C <sub>2</sub> mpyrroPF <sub>6</sub>	0.266	17.831	4.742
134	C <sub>4</sub> mpyrroPF <sub>6</sub>	0.449	10.858	4.878
135	C <sub>6</sub> mpyrroPF <sub>6</sub>	0.635	7.546	4.791
136	C <sub>8</sub> mpyrroPF <sub>6</sub>	0.818	5.661	4.630
137	C <sub>2</sub> mpyrPF <sub>6</sub>	0.352	24.984	8.801
138	C <sub>4</sub> mpyrPF <sub>6</sub>	0.594	13.612	8.079
139	C <sub>6</sub> mpyrPF <sub>6</sub>	0.827	8.943	7.399
140	C <sub>8</sub> mpyrPF <sub>6</sub>	1.028	6.536	6.722
141	C <sub>2</sub> mpipPF <sub>6</sub>	0.357	14.243	5.089
142	C <sub>4</sub> mpipPF <sub>6</sub>	0.566	9.021	5.105
143	C <sub>6</sub> mpipPF <sub>6</sub>	0.748	6.509	4.866
144	C <sub>8</sub> mpipPF <sub>6</sub>	0.920	5.008	4.608
145	C <sub>2</sub> mimSalicylate	0.447	10.382	4.642
146	C <sub>4</sub> mimSalicylate	0.587	7.070	4.149
147	C <sub>6</sub> mimSalicylate	0.695	5.501	3.826

148	C <sub>8</sub> mimSalicylate	0.809	4.414	3.571
149	C <sub>2</sub> mpyrroSalicylate	0.646	6.846	4.421
150	C <sub>4</sub> mpyrroSalicylate	0.741	5.359	3.968
151	C <sub>6</sub> mpyrroSalicylate	0.836	4.451	3.719
152	C <sub>8</sub> mpyrroSalicylate	0.932	3.778	3.522
153	C <sub>2</sub> mpyrSalicylate	0.618	8.733	5.397
154	C <sub>4</sub> mpyrSalicylate	0.755	6.324	4.772
155	C <sub>6</sub> mpyrSalicylate	0.872	4.985	4.349
156	C <sub>8</sub> mpyrSalicylate	0.977	4.111	4.016
157	C <sub>2</sub> mpipSalicylate	0.722	6.112	4.414
158	C <sub>4</sub> mpipSalicylate	0.835	4.839	4.041
159	C <sub>6</sub> mpipSalicylate	0.919	4.060	3.731
160	C <sub>8</sub> mpipSalicylate	1.008	3.477	3.506
161	C <sub>2</sub> mimTF <sub>2</sub> N	0.590	11.655	6.871
162	C <sub>4</sub> mimTF <sub>2</sub> N	0.823	7.425	6.111
163	C <sub>6</sub> mimTF <sub>2</sub> N	1.000	5.575	5.576
164	C <sub>8</sub> mimTF <sub>2</sub> N	1.160	4.414	5.120
165	C <sub>2</sub> mpyrroTF <sub>2</sub> N	0.641	8.342	5.343
166	C <sub>4</sub> mpyrroTF <sub>2</sub> N	0.863	5.689	4.910
167	C <sub>6</sub> mpyrroTF <sub>2</sub> N	1.036	4.406	4.563
168	C <sub>8</sub> mpyrroTF <sub>2</sub> N	1.182	3.614	4.270
169	C <sub>2</sub> mpyrTF <sub>2</sub> N	0.775	9.793	7.590
170	C <sub>4</sub> mpyrTF <sub>2</sub> N	1.002	6.623	6.639
171	C <sub>6</sub> mpyrTF <sub>2</sub> N	1.190	5.017	5.969
172	C <sub>8</sub> mpyrTF <sub>2</sub> N	1.336	4.058	5.423
173	C <sub>2</sub> mpipTF <sub>2</sub> N	0.746	7.139	5.326
174	C <sub>4</sub> mpipTF <sub>2</sub> N	0.968	5.059	4.895
175	C <sub>6</sub> mpipTF <sub>2</sub> N	1.125	3.997	4.496
176	C <sub>8</sub> mpipTF <sub>2</sub> N	1.257	3.321	4.173
177	C <sub>2</sub> mimSCN	0.373	12.185	4.549
178	C <sub>4</sub> mimSCN	0.397	9.858	3.910
179	C <sub>6</sub> mimSCN	0.474	7.776	3.685
180	C <sub>8</sub> mimSCN	0.588	6.041	3.553
181	C <sub>2</sub> mpyrroSCN	0.822	5.808	4.776
182	C <sub>4</sub> mpyrroSCN	0.612	6.181	3.780
183	C <sub>6</sub> mpyrroSCN	0.639	5.571	3.561
184	C <sub>8</sub> mpyrroSCN	0.725	4.775	3.463
185	C <sub>2</sub> mpyrSCN	0.534	10.345	5.529
186	C <sub>4</sub> mpyrSCN	0.570	8.378	4.776
187	C <sub>6</sub> mpyrSCN	0.661	6.707	4.432
188	C <sub>8</sub> mpyrSCN	0.769	5.416	4.167
189	C <sub>2</sub> mpipSCN	0.774	5.878	4.548
190	C <sub>4</sub> mpipSCN	0.693	5.684	3.940
191	C <sub>6</sub> mpipSCN	0.728	5.049	3.676
192	C <sub>8</sub> mpipSCN	0.814	4.340	3.533
193	C <sub>2</sub> mimMeSO <sub>3</sub>	0.954	5.122	4.887
194	C <sub>4</sub> mimMeSO <sub>3</sub>	0.685	5.026	3.443
195	C <sub>6</sub> mimMeSO <sub>3</sub>	0.632	4.658	2.946
196	C <sub>8</sub> mimMeSO <sub>3</sub>	0.660	4.114	2.715
197	C <sub>2</sub> mpyrroMeSO <sub>3</sub>	1.796	2.919	5.242

<b>198</b>	C <sub>4</sub> mpyrroMeSO <sub>3</sub>	1.017	3.374	3.432
<b>199</b>	C <sub>6</sub> mpyrroMeSO <sub>3</sub>	0.846	3.455	2.922
<b>200</b>	C <sub>8</sub> mpyrroMeSO <sub>3</sub>	0.817	3.309	2.703
<b>201</b>	C <sub>2</sub> mpyrMeSO <sub>3</sub>	1.102	4.978	5.488
<b>202</b>	C <sub>4</sub> mpyrMeSO <sub>3</sub>	0.879	4.738	4.166
<b>203</b>	C <sub>6</sub> mpyrMeSO <sub>3</sub>	0.831	4.376	3.636
<b>204</b>	C <sub>8</sub> mpyrMeSO <sub>3</sub>	0.849	3.923	3.330
<b>205</b>	C <sub>2</sub> mpipMeSO <sub>3</sub>	1.515	3.069	4.650
<b>206</b>	C <sub>4</sub> mpipMeSO <sub>3</sub>	1.039	3.325	3.455
<b>207</b>	C <sub>6</sub> mpipMeSO <sub>3</sub>	0.899	3.317	2.982
<b>208</b>	C <sub>8</sub> mpipMeSO <sub>3</sub>	0.881	3.142	2.769

University of Malaya

**Table A3:  $\sigma$ -profiles and  $\sigma$ -potentials of DESs components**

Salt Cation				Salt Anion				HBD								
$\sigma$	TBA <sup>+</sup>	MTPP <sup>+</sup>	Ch <sup>+</sup>	Br <sup>-</sup>	Cl <sup>-</sup>	BF <sub>4</sub>	NO <sub>3</sub>	Sulf	TEG	Ur	TMUr	TUr	PD	EG	Gly	TFA
-0.03	0.0	0	0	0	0	0	0	0	0	0	0	0	0	0.0	0.0	0.0
-0.029	0.0	0	0	0	0	0	0	0	0	0	0	0	0	0.0	0.0	0.0
-0.028	0.0	0	0	0	0	0	0	0	0	0	0	0	0	0.0	0.0	0.0
-0.027	0.0	0	0	0	0	0	0	0	0	0	0	0	0	0.0	0.0	0.0
-0.026	0.0	0	0	0	0	0	0	0	0	0	0	0	0	0.0	0.0	0.0
-0.025	0.0	0	0	0	0	0	0	0	0	0	0	0	0	0.0	0.0	0.0
-0.024	0.0	0	0	0	0	0	0	0	0	0	0	0	0	0.0	0.0	0.0
-0.023	0.0	0	0	0	0	0	0	0	0	0	0	0	0	0.0	0.0	0.0
-0.022	0.0	0	0	0	0	0	0	0	0	0	0	0	0	0.0	0.0	0.0
-0.021	0.0	0	0	0	0	0	0	0	0	0	0	0	0	0.0	0.0	0.0
-0.02	0.0	0	0.094	0	0	0	0	0	0	0	0	0.016	0.004	0.0	0.036	0.133
-0.019	0.0	0	0.483	0	0	0	0	0	0	0	0	0.475	0.22	0.081	0.319	0.918
-0.018	0.0	0	1.053	0	0	0	0	0	0.006	0.286	0	2.053	0.78	0.503	0.854	2.096
-0.017	0.0	0	1.236	0	0	0	0	0	0.309	1.526	0	4.349	1.041	1.136	1.025	2.761
-0.016	0.0	0	1.087	0	0	0	0	0	0.799	3.664	0	5.485	0.938	1.44	0.85	2.895
-0.015	0.0	0	1.132	0	0	0	0	0	1.011	4.832	0	4.916	1.334	1.598	1.243	2.38
-0.014	0.0	0	1.524	0	0	0	0	0	1.466	4.657	0	4.261	1.787	1.917	1.797	1.577
-0.013	0.0	0.107	2.049	0	0	0	0	0	1.785	4.765	0	3.597	1.737	2.038	1.726	1.392
-0.012	0.846	0.969	4.742	0	0	0	0	0	1.241	4.349	0	2.674	1.462	1.583	1.624	1.377
-0.011	4.481	3.421	11.268	0	0	0	0	0.397	0.756	2.834	0	2.235	1.055	0.934	1.666	1.027
-0.01	8.973	8.044	18.615	0	0	0	0	2.955	0.662	1.751	0	1.814	0.837	0.903	1.8	0.898
-0.009	10.586	17.146	21.543	0	0	0	0	6.415	0.918	1.888	0	1.538	0.993	1.263	1.959	1.038
-0.008	11.825	29.809	18.155	0	0	0	0	8.47	1.95	2.432	0.18	1.62	1.425	1.413	2.711	1.177
-0.007	14.405	34.036	12.761	0	0	0	0	11.755	5.849	1.982	2.668	1.332	2.766	3.553	7.145	1.35

<b>-0.006</b>	18.85	25.672	11.108	0	0	0	0	15.68	16.374	1.234	9.941	1.267	6.257	8.331	12.929	1.568
<b>-0.005</b>	30.979	19.12	12.827	0	0	0	0	15.355	28.309	1.191	18.45	1.552	10.531	10.376	12.614	2.371
<b>-0.004</b>	44.215	19.182	10.653	0	0	0	0.154	11.71	28.234	1.202	21.178	1.235	11.939	7.951	7.876	2.96
<b>-0.003</b>	46.17	17.721	4.891	0	0	0	0.523	8.741	17.841	1.362	17.515	0.904	9.525	5.188	5.239	2.972
<b>-0.002</b>	38.473	16.487	1.696	0	0	0	0.724	6.102	11.696	1.664	15.615	0.982	6.433	3.987	4.923	3.559
<b>-0.001</b>	28.759	18.973	0.91	0	0	0	0.673	3.947	11.419	1.781	17.873	1.033	5.456	3.658	4.366	4.216
<b>0</b>	23.001	21.42	0.76	0	0	0	0.973	2.788	9.195	2.357	16.138	1.457	5.645	3.126	3.227	6.447
<b>0.001</b>	21.626	25.638	0.758	0	0	0	1.233	1.462	5.073	2.985	9.669	2.491	6.089	2.143	2.483	10.853
<b>0.002</b>	21.509	30.248	0.7	0	0	0	0.851	0.827	3.442	3.019	4.655	3.69	5.488	1.829	2.458	14.888
<b>0.003</b>	15.242	23.44	0.506	0	0	0	0.53	0.938	3.53	2.68	2.639	4.7	2.96	2.242	2.116	14.039
<b>0.004</b>	4.595	8.446	0.468	0	0	0.055	0.361	0.706	3.34	2.308	1.962	4.888	1.179	2.186	1.614	7.096
<b>0.005</b>	0.041	0.674	0.805	0	0	0.521	0.643	0.332	3.359	2.246	1.478	3.841	1.355	1.489	1.93	2.114
<b>0.006</b>	0.0	0	0.917	0	0	1.384	1.308	0.898	3.088	2.02	1.528	2.936	1.976	1.074	2.048	1.357
<b>0.007</b>	0.0	0	0.642	0	0	1.595	1.172	1.932	2.128	1.631	1.956	3.707	1.79	1.226	2.06	0.97
<b>0.008</b>	0.0	0	0.426	0	0	1.776	0.776	2.511	1.714	1.282	1.528	4.947	1.535	1.403	2.65	0.891
<b>0.009</b>	0.0	0	0.731	0	0	5.185	1.062	2.802	2.11	0.896	0.557	4.062	1.674	1.653	2.668	1.148
<b>0.01</b>	0.0	0	1.102	0	0	15.167	2.269	2.744	2.415	1.698	0.256	2.308	1.422	1.699	2.089	1.472
<b>0.011</b>	0.0	0	0.769	0	0	27.114	4.272	3.307	3.204	3.191	0.467	2.484	1.285	1.754	2.206	2.558
<b>0.012</b>	0.0	0	0.572	0	0	25.523	6.461	5.816	4.214	2.847	0.576	4.376	1.609	2.203	2.567	3.748
<b>0.013</b>	0.0	0	0.896	0	0	10.87	9.059	8.707	4.048	1.607	0.679	6.238	2.153	2.215	2.821	3.573
<b>0.014</b>	0.0	0	1.112	0	0	1.38	10.443	7.903	3.639	1.678	1.053	5.957	2.878	2.128	3.506	2.474
<b>0.015</b>	0.0	0	1.067	0	0	0	8.695	3.806	4.39	2.725	1.905	3.611	3.027	2.819	3.959	1.196
<b>0.016</b>	0.0	0	0.826	13.833	0	0	6.779	0.788	5.256	3.69	3.023	1.205	2.77	3.425	3.752	0.269
<b>0.017</b>	0.0	0	0.424	28.491	0.848	0	6.395	0	4.403	3.817	3.537	0.108	2.609	2.931	2.922	0.004
<b>0.018</b>	0.0	0	0.092	15.481	14.051	0	5.755	0	2.363	2.973	3.041	0	1.7	1.657	1.515	0.0
<b>0.019</b>	0.0	0	0	0.824	25.557	0	3.845	0	0.671	1.579	1.786	0	0.519	0.47	0.357	0.0
<b>0.02</b>	0.0	0	0	0	12.354	0	1.32	0	0.017	0.441	0.558	0	0.054	0.006	0.0	0.0
<b>0.021</b>	0.0	0	0	0	0	0	0.072	0	0	0.035	0.05	0	0	0.0	0.0	0.0
<b>0.022</b>	0.0	0	0	0	0	0	0	0	0	0	0	0	0	0.0	0.0	0.0

<b>0.023</b>	0.0	0	0	0	0	0	0	0	0	0	0	0	0	0.0	0.0	0.0
<b>0.024</b>	0.0	0	0	0	0	0	0	0	0	0	0	0	0	0.0	0.0	0.0
<b>0.025</b>	0.0	0	0	0	0	0	0	0	0	0	0	0	0	0.0	0.0	0.0
<b>0.026</b>	0.0	0	0	0	0	0	0	0	0	0	0	0	0	0.0	0.0	0.0
<b>0.027</b>	0.0	0	0	0	0	0	0	0	0	0	0	0	0	0.0	0.0	0.0
<b>0.028</b>	0.0	0	0	0	0	0	0	0	0	0	0	0	0	0.0	0.0	0.0
<b>0.029</b>	0.0	0	0	0	0	0	0	0	0	0	0	0	0	0.0	0.0	0.0
<b>0.03</b>	0.0	0	0	0	0	0	0	0	0	0	0	0	0	0.0	0.0	0.0

University of Malaya

**Table A4:  $\sigma$ -profile of solute (benzene) and carrier (cyclohexane)**

$\sigma$	Benzene	Cyclohexane
-0.03	0.0	0.0
-0.029	0.0	0.0
-0.028	0.0	0.0
-0.027	0.0	0.0
-0.026	0.0	0.0
-0.025	0.0	0.0
-0.024	0.0	0.0
-0.023	0.0	0.0
-0.022	0.0	0.0
-0.021	0.0	0.0
-0.02	0.0	0.0
-0.019	0.0	0.0
-0.018	0.0	0.0
-0.017	0.0	0.0
-0.016	0.0	0.0
-0.015	0.0	0.0
-0.014	0.0	0.0
-0.013	0.0	0.0
-0.012	0.0	0.0
-0.011	0.0	0.0
-0.01	0.0	0.0
-0.009	0.319	0.0
-0.008	2.221	0.0
-0.007	7.21	0.0
-0.006	11.683	0.0
-0.005	10.952	0.419
-0.004	7.942	4.473
-0.003	6.499	13.016
-0.002	6.081	20.338
-0.001	4.79	22.16
0	4.242	18.578
0.001	5.728	15.775
0.002	6.155	15.423
0.003	6.616	12.165
0.004	8.762	6.93
0.005	11.592	2.207
0.006	12.176	0.0
0.007	6.98	0.0
0.008	1.423	0.0
0.009	0.0	0.0
0.01	0.0	0.0
0.011	0.0	0.0
0.012	0.0	0.0
0.013	0.0	0.0

---

<b>0.014</b>	0.0	0.0
<b>0.015</b>	0.0	0.0
<b>0.016</b>	0.0	0.0
<b>0.017</b>	0.0	0.0
<b>0.018</b>	0.0	0.0
<b>0.019</b>	0.0	0.0
<b>0.02</b>	0.0	0.0
<b>0.021</b>	0.0	0.0
<b>0.022</b>	0.0	0.0
<b>0.023</b>	0.0	0.0
<b>0.024</b>	0.0	0.0
<b>0.025</b>	0.0	0.0
<b>0.026</b>	0.0	0.0
<b>0.027</b>	0.0	0.0
<b>0.028</b>	0.0	0.0
<b>0.029</b>	0.0	0.0
<b>0.03</b>	0.0	0.0

---

University of Malaya

Table A5:  $\sigma$ -profile of the top-screened DESs

$\sigma$	TBABr:Sulf (1:7)	MTPPBr:TEG (1:4)	TBABr:TEG (1:4)	ChCl:TEG (1:4)	ChCl:TMUr (1:2)	TBACl:TEG (1:2)	MTPPBr:PD (1:4)	CHCl:Tur (1:2)	CHBF4:Ur (1:2)	ChNO3:Ur (1:2)
-0.03	0	0	0	0	0	0	0	0	0	0
-0.029	0	0	0	0	0	0	0	0	0	0
-0.028	0	0	0	0	0	0	0	0	0	0
-0.027	0	0	0	0	0	0	0	0	0	0
-0.026	0	0	0	0	0	0	0	0	0	0
-0.025	0	0	0	0	0	0	0	0	0	0
-0.024	0	0	0	0	0	0	0	0	0	0
-0.023	0	0	0	0	0	0	0	0	0	0
-0.022	0	0	0	0	0	0	0	0	0	0
-0.021	0	0	0	0	0	0	0	0	0	0
-0.02	0	0	0	0.094	0.094	0	0.016	0.126	0.094	0.094
-0.019	0	0	0	0.483	0.483	0	0.88	1.433	0.483	0.483
-0.018	0	0.024	0.024	1.077	1.053	0.012	3.12	5.159	1.625	1.625
-0.017	0	1.236	1.236	2.472	1.236	0.618	4.164	9.934	4.288	4.288
-0.016	0	3.196	3.196	4.283	1.087	1.598	3.752	12.057	8.415	8.415
-0.015	0	4.044	4.044	5.176	1.132	2.022	5.336	10.964	10.796	10.796
-0.014	0	5.864	5.864	7.388	1.524	2.932	7.148	10.046	10.838	10.838
-0.013	0	7.247	7.14	9.189	2.049	3.57	7.055	9.243	11.579	11.579
-0.012	0.846	5.933	5.81	9.706	4.742	3.328	6.817	10.09	13.44	13.44
-0.011	7.26	6.445	7.505	14.292	11.268	5.993	7.641	15.738	16.936	16.936
-0.01	29.658	10.692	11.621	21.263	18.615	10.297	11.392	22.243	22.117	22.117
-0.009	55.491	20.818	14.258	25.215	21.543	12.422	21.118	24.619	25.319	25.319
-0.008	71.115	37.609	19.625	25.955	18.515	15.725	35.509	21.395	23.019	23.019
-0.007	96.69	57.432	37.801	36.157	18.097	26.103	45.1	15.425	16.725	16.725
-0.006	128.61	91.168	84.346	76.604	30.99	51.598	50.7	13.642	13.576	13.576

-0.005	138.464	132.356	144.215	126.063	49.727	87.597	61.244	15.931	15.209	15.209
-0.004	126.185	132.118	157.151	123.589	53.009	100.683	66.938	13.123	13.057	13.211
-0.003	107.357	89.085	117.534	76.255	39.921	81.852	55.821	6.699	7.615	8.138
-0.002	81.187	63.271	85.257	48.48	32.926	61.865	42.219	3.66	5.024	5.748
-0.001	56.388	64.649	74.435	46.586	36.656	51.597	40.797	2.976	4.472	5.145
0	42.517	58.2	59.781	37.54	33.036	41.391	44	3.674	5.474	6.447
0.001	31.86	45.93	41.918	21.05	20.096	31.772	49.994	5.74	6.728	7.961
0.002	27.298	44.016	35.277	14.468	10.01	28.393	52.2	8.08	6.738	7.589
0.003	21.808	37.56	29.362	14.626	5.784	22.302	35.28	9.906	5.866	6.396
0.004	9.537	21.806	17.955	13.828	4.392	11.275	13.162	10.244	5.139	5.445
0.005	2.365	14.11	13.477	14.241	3.761	6.759	6.094	8.487	5.818	5.94
0.006	6.286	12.352	12.352	13.269	3.973	6.176	7.904	6.789	6.341	6.265
0.007	13.524	8.512	8.512	9.154	4.554	4.256	7.16	8.056	5.499	5.076
0.008	17.577	6.856	6.856	7.282	3.482	3.428	6.14	10.32	4.766	3.766
0.009	19.614	8.44	8.44	9.171	1.845	4.22	6.696	8.855	7.708	3.585
0.01	19.208	9.66	9.66	10.762	1.614	4.83	5.688	5.718	19.665	6.767
0.011	23.149	12.816	12.816	13.585	1.703	6.408	5.14	5.737	34.265	11.423
0.012	40.712	16.856	16.856	17.428	1.724	8.428	6.436	9.324	31.789	12.727
0.013	60.949	16.192	16.192	17.088	2.254	8.096	8.612	13.372	14.98	13.169
0.014	55.321	14.556	14.556	15.668	3.218	7.278	11.512	13.026	5.848	14.911
0.015	26.642	17.56	17.56	18.627	4.877	8.78	12.108	8.289	6.517	15.212
0.016	19.349	34.857	34.857	21.85	6.872	10.512	24.913	3.236	8.206	14.985
0.017	28.491	46.103	46.103	18.884	8.346	9.654	38.927	1.488	8.058	14.453
0.018	15.481	24.933	24.933	23.595	20.225	18.777	22.281	14.143	6.038	11.793
0.019	0.824	3.508	3.508	28.241	29.129	26.899	2.9	25.557	3.158	7.003
0.02	0	0.068	0.068	12.422	13.47	12.388	0.216	12.354	0.882	2.202
0.021	0	0	0	0	0.1	0	0	0	0.07	0.142
0.022	0	0	0	0	0	0	0	0	0	0
0.023	0	0	0	0	0	0	0	0	0	0

0.024	0	0	0	0	0	0	0	0	0	0	0
0.025	0	0	0	0	0	0	0	0	0	0	0
0.026	0	0	0	0	0	0	0	0	0	0	0
0.027	0	0	0	0	0	0	0	0	0	0	0
0.028	0	0	0	0	0	0	0	0	0	0	0
0.029	0	0	0	0	0	0	0	0	0	0	0
0.03	0	0	0	0	0	0	0	0	0	0	0

University Of Malaya

**Table A6:  $\sigma$ -potential of the top-screened DESs**

$\sigma$	TBABr:Sulf (1:7)	MTPPBr:TEG (1:4)	TBABr:TEG (1:4)	ChCl:TEG (1:4)	ChCl:TMUr (1:2)	TBACl:TEG (1:2)	MTPPBr:PD (1:4)	CHCl:Tur (1:2)	CHBF <sub>4</sub> :Ur (1:2)	ChNO <sub>3</sub> :Ur (1:2)
-0.03	-3.499	-3.968	-3.939	-4.983	-3.937	-2.784	-3.6	-2.435	-2.088	-3.15
-0.029	-3.454	-3.86	-3.833	-4.804	-3.806	-2.728	-3.5	-2.37	-2.002	-3.021
-0.028	-3.407	-3.745	-3.721	-4.619	-3.671	-2.668	-3.397	-2.301	-1.913	-2.89
-0.027	-3.344	-3.628	-3.607	-4.431	-3.531	-2.605	-3.284	-2.227	-1.818	-2.752
-0.026	-3.27	-3.5	-3.481	-4.232	-3.384	-2.534	-3.164	-2.146	-1.719	-2.61
-0.025	-3.186	-3.361	-3.344	-4.023	-3.233	-2.457	-3.033	-2.061	-1.613	-2.462
-0.024	-3.085	-3.219	-3.204	-3.811	-3.075	-2.376	-2.899	-1.973	-1.505	-2.311
-0.023	-2.975	-3.071	-3.058	-3.594	-2.914	-2.291	-2.759	-1.88	-1.392	-2.155
-0.022	-2.855	-2.911	-2.901	-3.368	-2.75	-2.199	-2.607	-1.784	-1.276	-1.997
-0.021	-2.724	-2.749	-2.74	-3.142	-2.584	-2.104	-2.453	-1.686	-1.16	-1.839
-0.02	-2.577	-2.58	-2.573	-2.913	-2.417	-2.004	-2.292	-1.587	-1.041	-1.678
-0.019	-2.426	-2.403	-2.398	-2.683	-2.249	-1.899	-2.127	-1.491	-0.925	-1.521
-0.018	-2.259	-2.221	-2.217	-2.454	-2.086	-1.789	-1.957	-1.4	-0.813	-1.367
-0.017	-2.089	-2.031	-2.029	-2.227	-1.925	-1.675	-1.783	-1.313	-0.708	-1.221
-0.016	-1.909	-1.843	-1.842	-2.011	-1.769	-1.559	-1.607	-1.233	-0.611	-1.084
-0.015	-1.719	-1.652	-1.652	-1.801	-1.619	-1.441	-1.436	-1.159	-0.523	-0.956
-0.014	-1.527	-1.459	-1.46	-1.593	-1.469	-1.32	-1.267	-1.089	-0.443	-0.836
-0.013	-1.338	-1.27	-1.272	-1.394	-1.32	-1.199	-1.106	-1.022	-0.374	-0.728
-0.012	-1.145	-1.095	-1.096	-1.212	-1.176	-1.083	-0.959	-0.958	-0.315	-0.632
-0.011	-0.965	-0.933	-0.935	-1.045	-1.039	-0.974	-0.833	-0.897	-0.272	-0.552
-0.01	-0.803	-0.797	-0.799	-0.904	-0.912	-0.875	-0.729	-0.838	-0.239	-0.484
-0.009	-0.666	-0.689	-0.692	-0.793	-0.805	-0.789	-0.649	-0.779	-0.22	-0.431
-0.008	-0.561	-0.608	-0.61	-0.707	-0.717	-0.714	-0.588	-0.719	-0.209	-0.388
-0.007	-0.552	-0.599	-0.602	-0.702	-0.702	-0.696	-0.587	-0.702	-0.224	-0.388
-0.006	-0.577	-0.611	-0.612	-0.719	-0.707	-0.693	-0.603	-0.697	-0.246	-0.402

-0.005	-0.602	-0.621	-0.622	-0.734	-0.71	-0.689	-0.613	-0.688	-0.264	-0.412
-0.004	-0.622	-0.627	-0.627	-0.746	-0.71	-0.681	-0.619	-0.676	-0.281	-0.421
-0.003	-0.647	-0.627	-0.626	-0.751	-0.707	-0.668	-0.619	-0.659	-0.293	-0.426
-0.002	-0.663	-0.624	-0.623	-0.753	-0.701	-0.653	-0.612	-0.641	-0.302	-0.427
-0.001	-0.682	-0.619	-0.616	-0.752	-0.69	-0.634	-0.603	-0.618	-0.309	-0.426
0	-0.685	-0.602	-0.599	-0.741	-0.675	-0.61	-0.586	-0.593	-0.311	-0.421
0.001	-0.691	-0.583	-0.578	-0.726	-0.654	-0.581	-0.563	-0.564	-0.312	-0.414
0.002	-0.688	-0.553	-0.547	-0.701	-0.631	-0.547	-0.529	-0.533	-0.308	-0.403
0.003	-0.669	-0.521	-0.514	-0.673	-0.601	-0.51	-0.493	-0.501	-0.301	-0.389
0.004	-0.647	-0.482	-0.474	-0.638	-0.566	-0.468	-0.45	-0.466	-0.291	-0.372
0.005	-0.615	-0.432	-0.423	-0.592	-0.526	-0.419	-0.4	-0.428	-0.277	-0.35
0.006	-0.572	-0.379	-0.368	-0.544	-0.48	-0.367	-0.339	-0.388	-0.26	-0.326
0.007	-0.521	-0.315	-0.304	-0.484	-0.428	-0.309	-0.275	-0.344	-0.239	-0.299
0.008	-0.452	-0.245	-0.232	-0.417	-0.371	-0.245	-0.201	-0.299	-0.214	-0.268
0.009	-0.374	-0.168	-0.154	-0.345	-0.309	-0.177	-0.124	-0.255	-0.187	-0.235
0.01	-0.294	-0.085	-0.07	-0.278	-0.254	-0.106	-0.049	-0.236	-0.185	-0.226
0.011	-0.198	0.004	0.02	-0.207	-0.197	-0.03	0.028	-0.223	-0.184	-0.219
0.012	-0.085	0.097	0.113	-0.139	-0.139	0.049	0.101	-0.217	-0.187	-0.217
0.013	0.031	0.192	0.209	-0.076	-0.084	0.13	0.168	-0.22	-0.198	-0.221
0.014	0.164	0.294	0.312	-0.014	-0.03	0.216	0.222	-0.232	-0.215	-0.232
0.015	0.305	0.39	0.408	0.036	0.022	0.3	0.262	-0.25	-0.234	-0.246
0.016	0.456	0.485	0.503	0.081	0.075	0.385	0.277	-0.273	-0.259	-0.266
0.017	0.623	0.57	0.588	0.111	0.129	0.466	0.274	-0.297	-0.284	-0.286
0.018	0.8	0.642	0.66	0.126	0.186	0.542	0.25	-0.322	-0.307	-0.305
0.019	0.987	0.697	0.715	0.121	0.247	0.61	0.213	-0.345	-0.331	-0.324
0.02	1.19	0.738	0.756	0.102	0.314	0.673	0.162	-0.366	-0.352	-0.341
0.021	1.403	0.763	0.78	0.064	0.382	0.728	0.107	-0.384	-0.369	-0.354
0.022	1.626	0.773	0.791	0.014	0.458	0.779	0.049	-0.398	-0.382	-0.365
0.023	1.864	0.774	0.791	-0.047	0.539	0.825	-0.014	-0.407	-0.391	-0.37

0.024	2.112	0.769	0.786	-0.112	0.626	0.87	-0.071	-0.412	-0.395	-0.371
0.025	2.371	0.76	0.777	-0.184	0.718	0.914	-0.128	-0.414	-0.396	-0.37
0.026	2.645	0.752	0.769	-0.252	0.816	0.96	-0.18	-0.41	-0.392	-0.364
0.027	2.93	0.748	0.765	-0.318	0.92	1.009	-0.228	-0.4	-0.383	-0.353
0.028	3.224	0.742	0.759	-0.384	1.03	1.059	-0.27	-0.386	-0.366	-0.335
0.029	3.528	0.743	0.76	-0.443	1.145	1.114	-0.305	-0.365	-0.348	-0.316
0.03	3.849	0.746	0.764	-0.5	1.266	1.172	-0.334	-0.34	-0.324	-0.292

University of Malaya

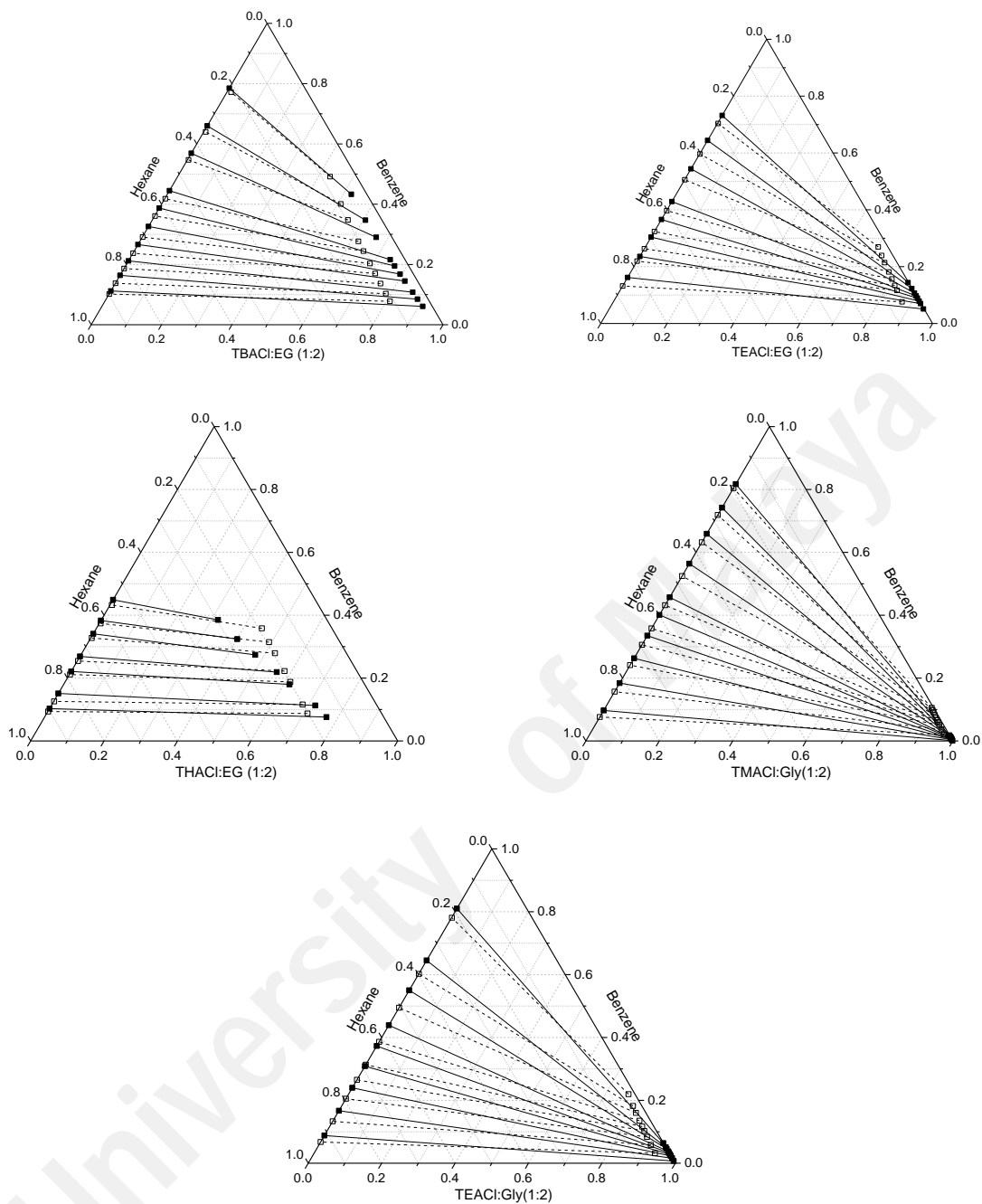


**Figure A1: The COSMO-RS predicted tie lines based on experimental data by Rodriguez et al. (2017). Solid and dashed lines represent experimental and COSMO-RS result, respectively**

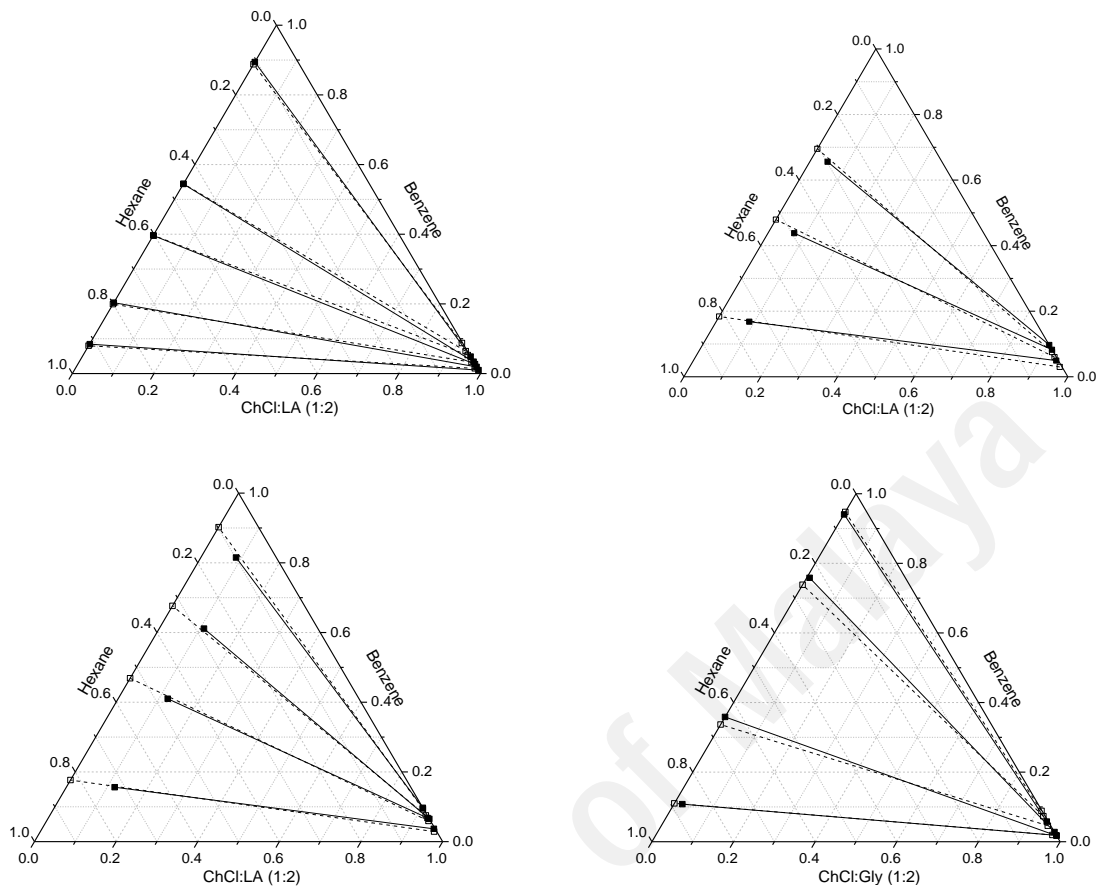


**Figure A2: The COSMO-RS predicted tie lines based on experimental data by Gonzalez et al. (2013). Solid and dashed lines represent experimental and COSMO-RS result, respectively.**

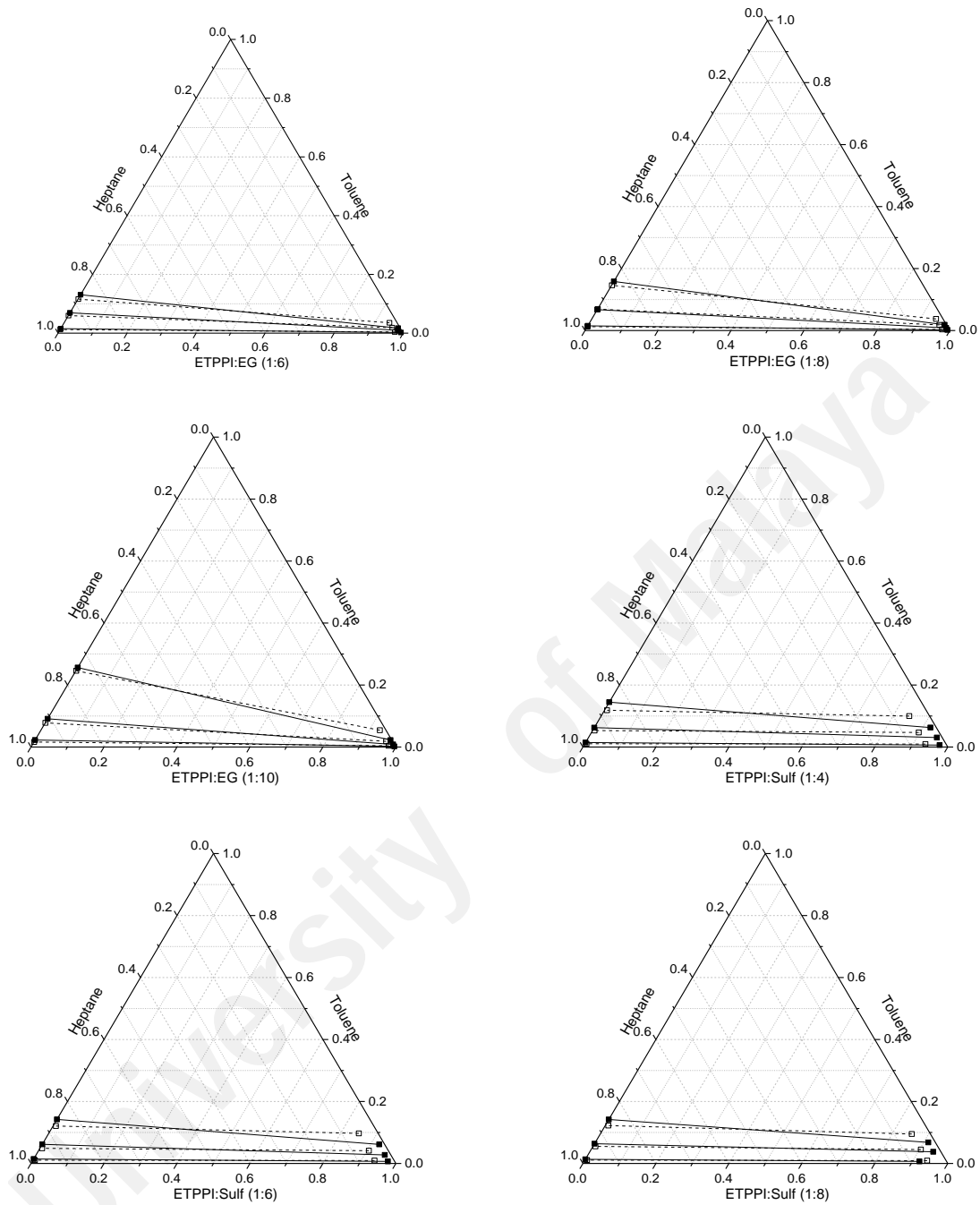


**Figure A3: The COSMO-RS predicted tie lines based on experimental data by Kareem et al. (2013). Solid and dashed lines represent experimental and COSMO-RS result, respectively.**

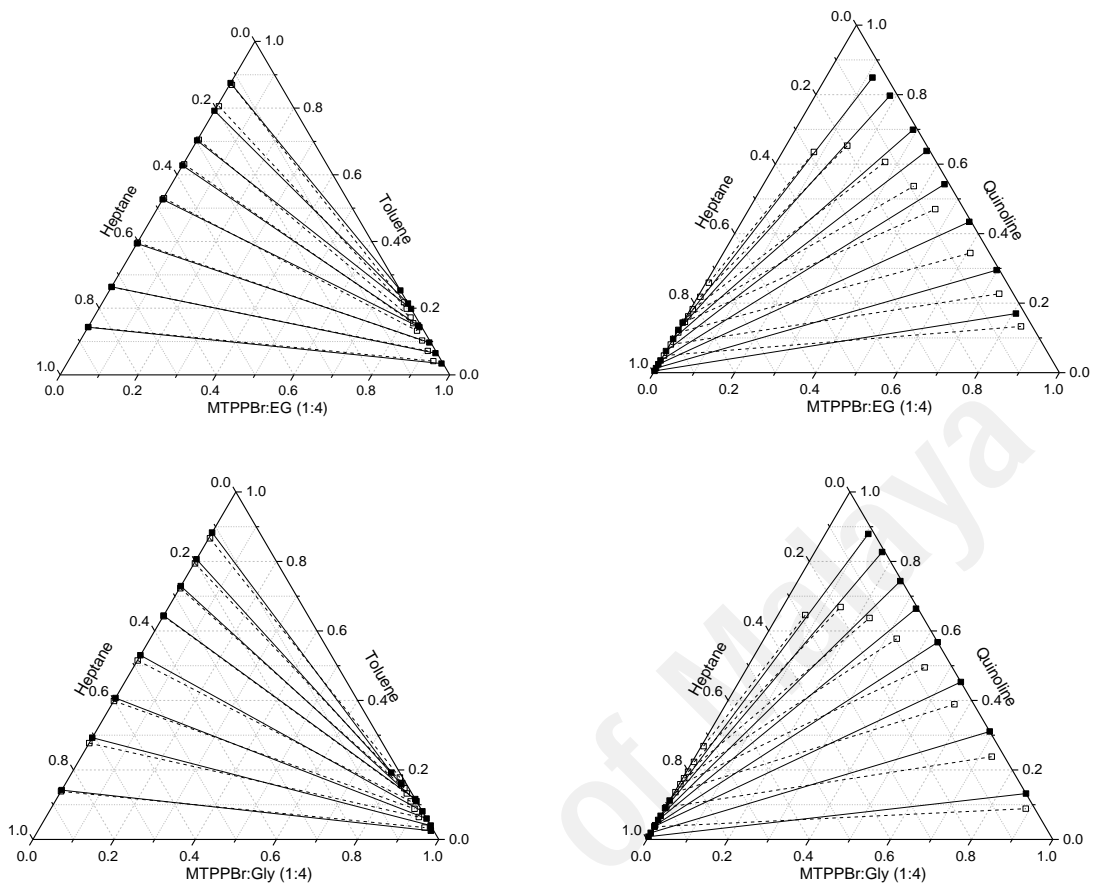


**Figure A 4: The COSMO-RS predicted tie lines based on experimental data by P. K. Naik et al. (2016). Solid and dashed lines represent experimental and COSMO-RS result, respectively.**

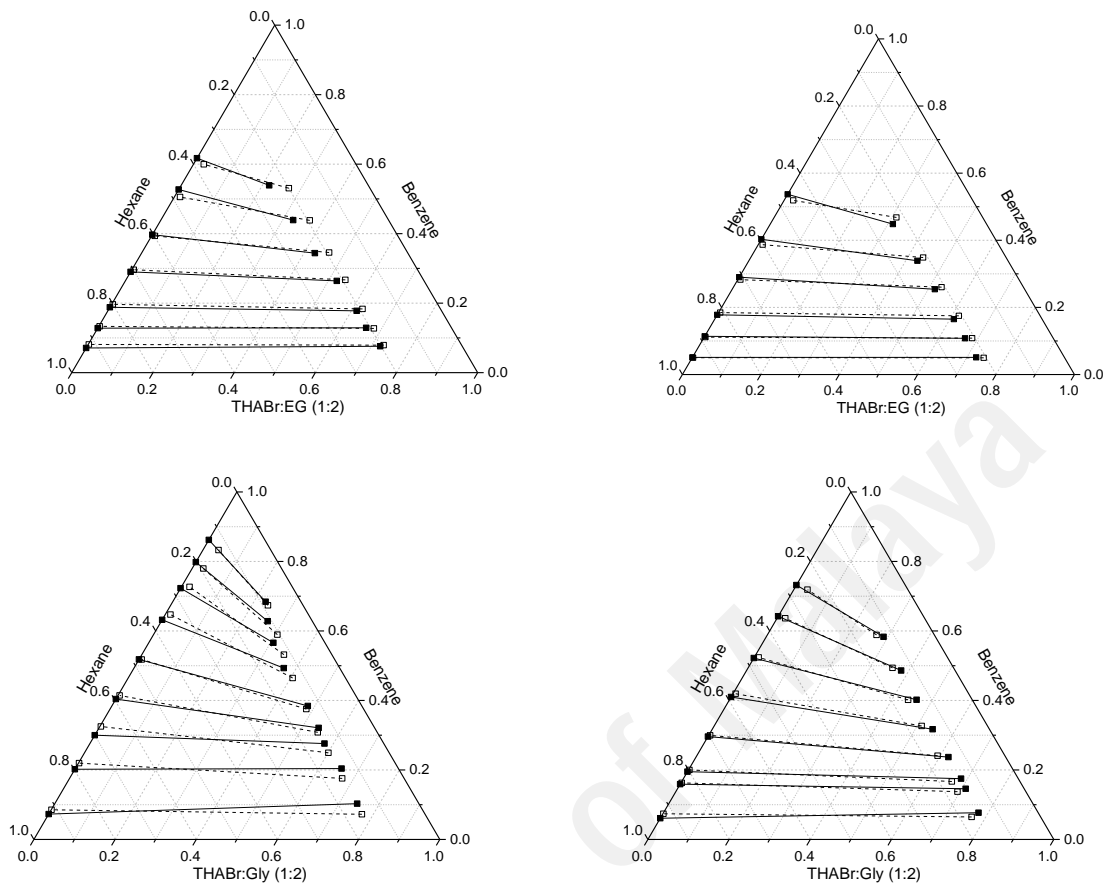


**Figure A5: The COSMO-RS predicted tie lines based on experimental data by Rodriguez et al. (2015). Solid and dashed lines represent experimental and COSMO-RS result, respectively.**

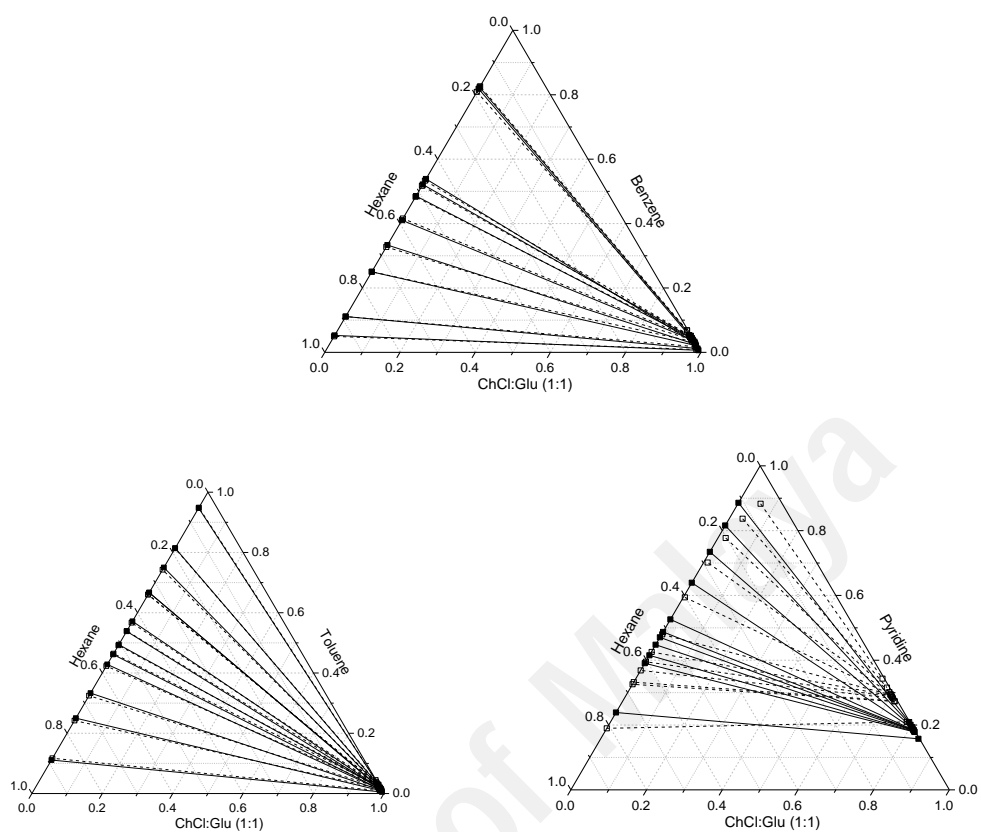


**Figure A6: The COSMO-RS predicted tie lines based on experimental data by Kurnia et al. (2016). Solid and dashed lines represent experimental and COSMO-RS result, respectively.**

**Table A7: Molar composition of the tie-lines predicted by COSMO-RS for ternary systems of benzene (1) + cyclohexane (2) + DESs (3) at 25 °C and 1 atm**

Top layer			Bottom layer		
$x_1$	$x_2$	$x_3$	$x_1$	$x_2$	$x_3$
<b>benzene (1) + cyclohexane (2) + TBABr:Sulf (1:7) (3)</b>					
0.060	0.931	0.009	0.073	0.129	0.798
0.126	0.862	0.012	0.144	0.130	0.726
0.193	0.791	0.015	0.208	0.132	0.660
0.258	0.722	0.021	0.266	0.136	0.598
0.329	0.642	0.028	0.326	0.142	0.532
0.404	0.555	0.041	0.389	0.153	0.458
<b>benzene (1) + cyclohexane (2) + TBABr:TEG (1:4) (3)</b>					
0.064	0.929	0.006	0.079	0.291	0.629
0.143	0.847	0.009	0.166	0.294	0.539
0.200	0.787	0.011	0.223	0.298	0.478
0.269	0.713	0.016	0.289	0.304	0.405
0.340	0.634	0.024	0.354	0.317	0.328
0.408	0.554	0.036	0.420	0.346	0.232
<b>benzene (1) + cyclohexane (2) + MTPPBr:TEG (1:4) (3)</b>					
0.069	0.926	0.003	0.084	0.231	0.684
0.137	0.857	0.005	0.157	0.232	0.610
0.209	0.783	0.007	0.227	0.234	0.537
0.281	0.707	0.010	0.293	0.237	0.468
0.357	0.626	0.015	0.358	0.243	0.398
0.438	0.536	0.024	0.429	0.253	0.317
<b>benzene (1) + cyclohexane (2) + MTPPBr:PD (1:4) (3)</b>					
0.083	0.915	0.000	0.048	0.103	0.848
0.170	0.828	0.001	0.094	0.103	0.802
0.246	0.751	0.001	0.131	0.102	0.766
0.341	0.655	0.002	0.174	0.100	0.725
0.441	0.554	0.004	0.216	0.097	0.686
0.539	0.454	0.006	0.257	0.092	0.650
0.653	0.336	0.010	0.309	0.082	0.608
0.756	0.228	0.014	0.362	0.068	0.568
<b>benzene (1) + cyclohexane (2) + ChCl:TEG (1:4) (3)</b>					
0.072	0.926	0.000	0.060	0.149	0.790
0.145	0.853	0.001	0.114	0.147	0.738
0.228	0.769	0.001	0.170	0.144	0.684
0.313	0.683	0.002	0.222	0.141	0.636
0.411	0.584	0.004	0.277	0.136	0.585
0.509	0.483	0.007	0.332	0.130	0.537
0.619	0.369	0.011	0.396	0.120	0.483
0.730	0.250	0.018	0.476	0.102	0.421

**Table A8: Molar composition of the tie-lines predicted by COSMO-RS for ternary systems of benzene (1) + cyclohexane (2) + ILs (3) at 25 °C and 1 atm**

Raffinate layer			Extract layer		
$x_1$	$x_2$	$x_3$	$x_1$	$x_2$	$x_3$
<b>benzene (1) + cyclohexane (2) + C<sub>2</sub>mimAc (3)</b>					
0.082	0.917	0.001	0.054	0.037	0.909
0.171	0.829	0.001	0.098	0.039	0.862
0.263	0.736	0.001	0.135	0.040	0.825
0.360	0.640	0.001	0.169	0.040	0.792
0.461	0.538	0.000	0.202	0.038	0.760
0.565	0.435	0.000	0.235	0.035	0.730
<b>benzene (1) + cyclohexane (2) + C<sub>2</sub>mimN(CN)<sub>2</sub> (3)</b>					
0.082	0.918	0.000	0.057	0.004	0.939
0.166	0.834	0.000	0.106	0.006	0.888
0.255	0.745	0.000	0.151	0.009	0.840
0.348	0.652	0.000	0.194	0.011	0.794
0.442	0.558	0.000	0.237	0.014	0.749
0.539	0.461	0.000	0.282	0.016	0.702
<b>benzene (1) + cyclohexane (2) + C<sub>2</sub>mimSCN (3)</b>					
0.085	0.914	0.000	0.046	0.001	0.952
0.174	0.826	0.000	0.086	0.003	0.912
0.268	0.732	0.000	0.121	0.004	0.875
0.363	0.637	0.000	0.155	0.005	0.840
0.461	0.538	0.000	0.189	0.007	0.804
0.559	0.441	0.000	0.225	0.008	0.767
<b>benzene (1) + cyclohexane (2) + C<sub>2</sub>mimTf<sub>2</sub>N (3)</b>					
0.084	0.916	0.001	0.106	0.044	0.851
0.170	0.829	0.001	0.193	0.050	0.756
0.258	0.741	0.001	0.268	0.055	0.678
0.351	0.649	0.000	0.337	0.057	0.606
0.442	0.557	0.000	0.402	0.057	0.541
0.538	0.462	0.000	0.469	0.055	0.476

## APPENDIX B: $^1\text{H}$ NMR spectroscopy of samples from extract and raffinate layers

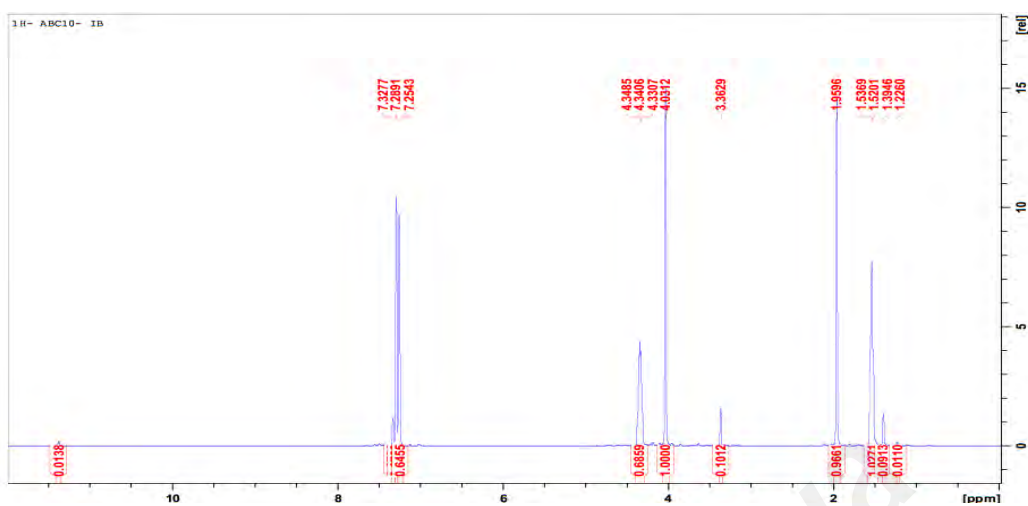


Figure B1: Extract layer of  $\text{C}_2\text{mimAc}$  + benzene + cyclohexane (10% benzene in feed)

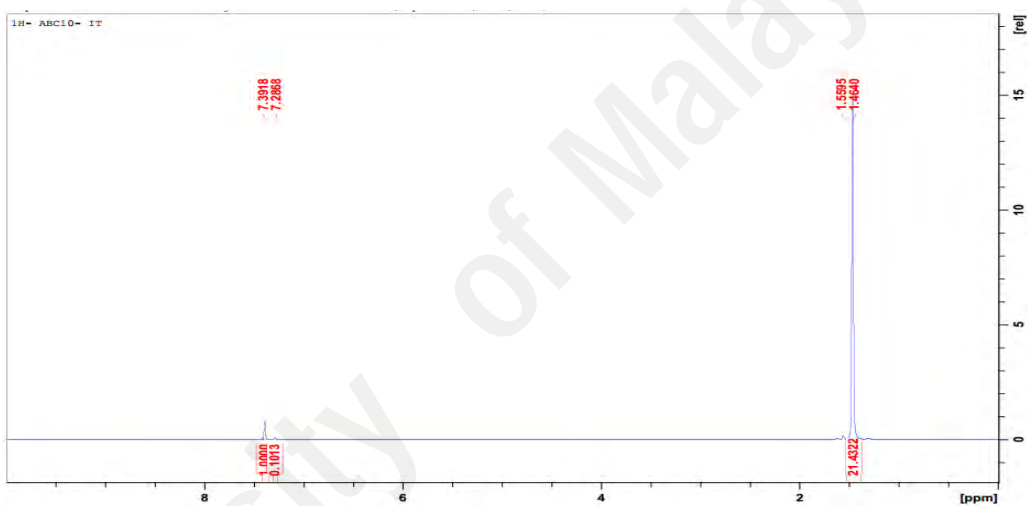


Figure B2: Raffinate layer of  $\text{C}_2\text{mimAc}$  + benzene + cyclohexane (10% benzene in feed)

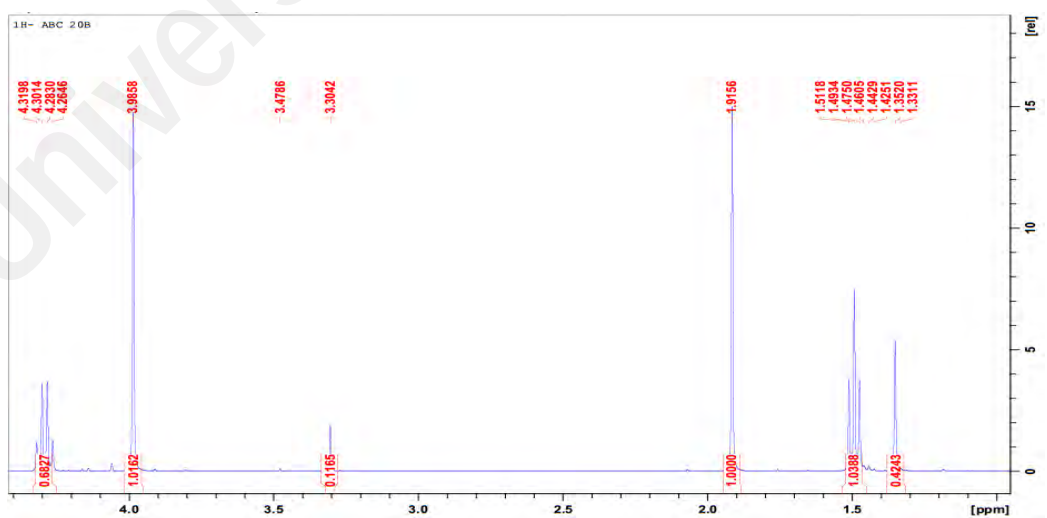


Figure B3: Extract layer of  $\text{C}_2\text{mimAc}$  + benzene + cyclohexane (20% benzene in feed)

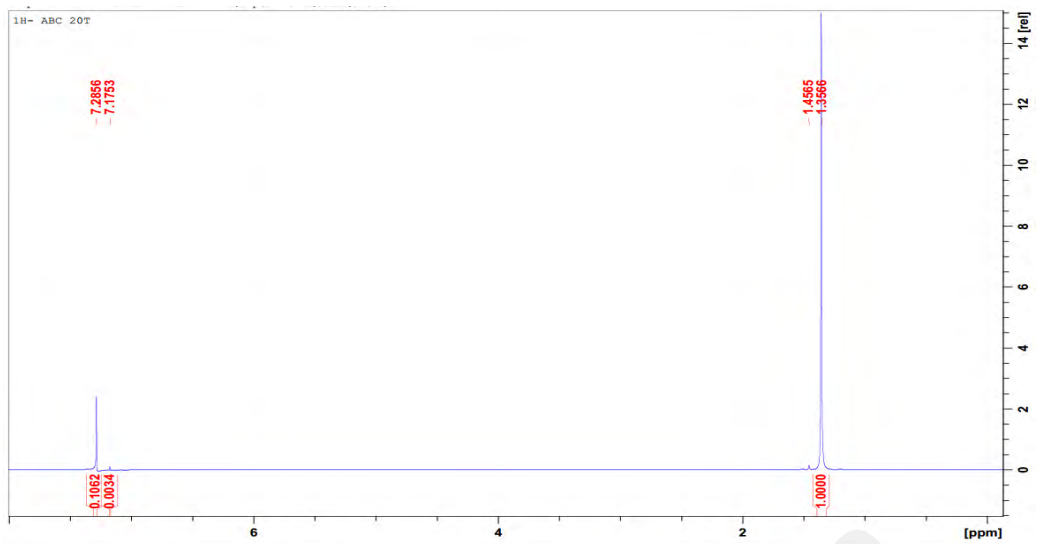


Figure B4: Raffinate layer of  $C_2mimAc$  + benzene + cyclohexane (20% benzene in feed)

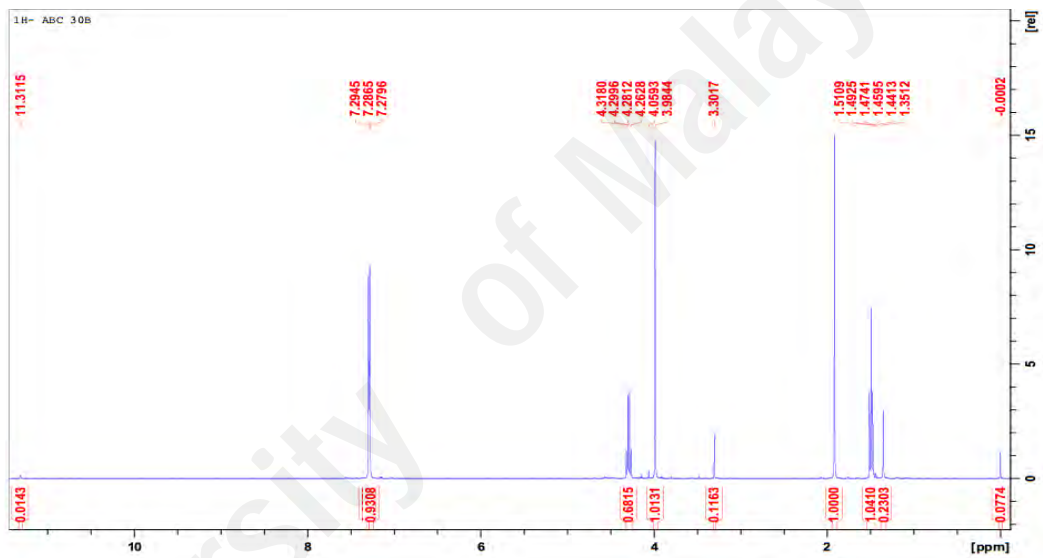


Figure B5: Extract layer of  $C_2mimAc$  + benzene + cyclohexane (30% benzene in feed)

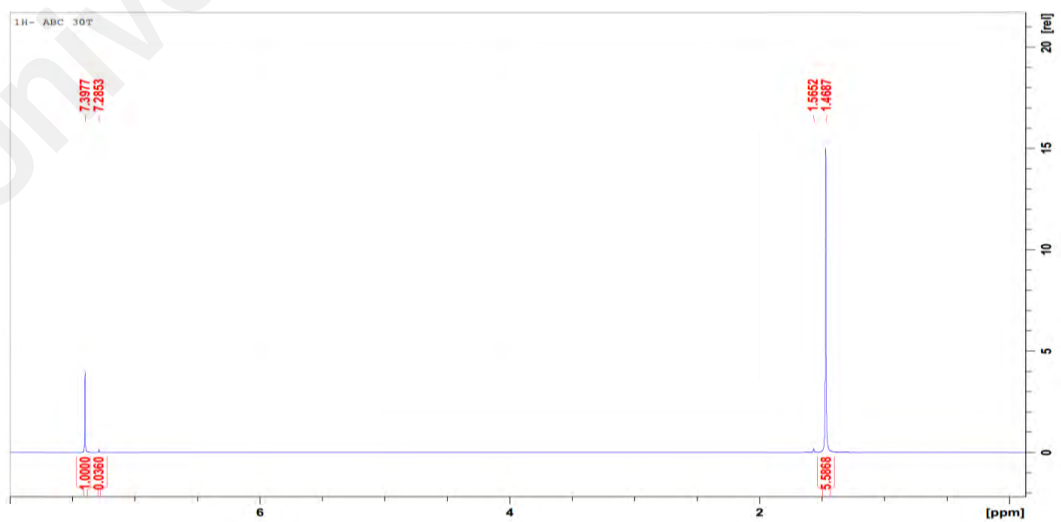


Figure B6: Raffinate layer of  $C_2mimAc$  + benzene + cyclohexane (30% benzene in feed)

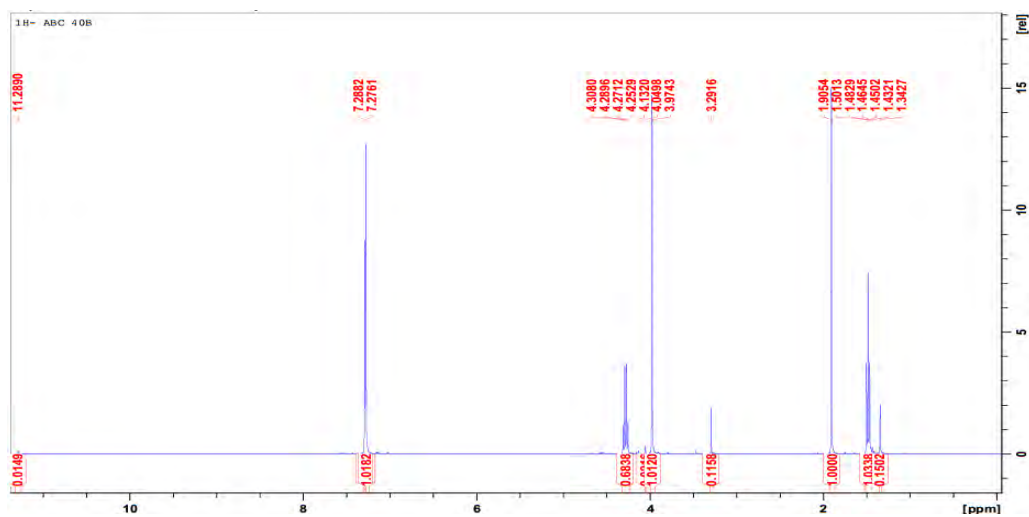


Figure B7: Extract layer of C<sub>2</sub>mimAc + benzene + cyclohexane (40% benzene in feed)

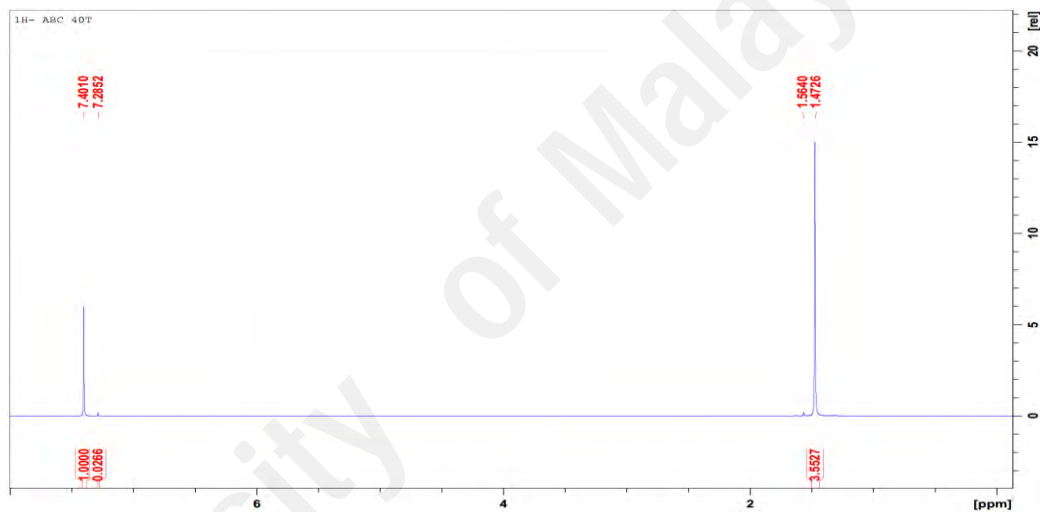


Figure B8: Raffinate layer of C<sub>2</sub>mimAc + benzene + cyclohexane (40% benzene in feed)

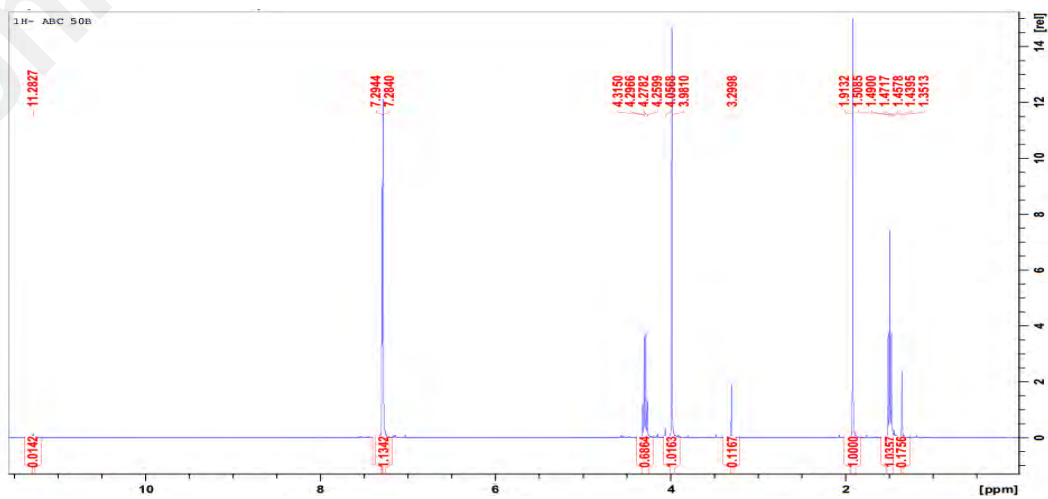


Figure B9: Extract layer of C<sub>2</sub>mimAc + benzene + cyclohexane (50% benzene in feed)

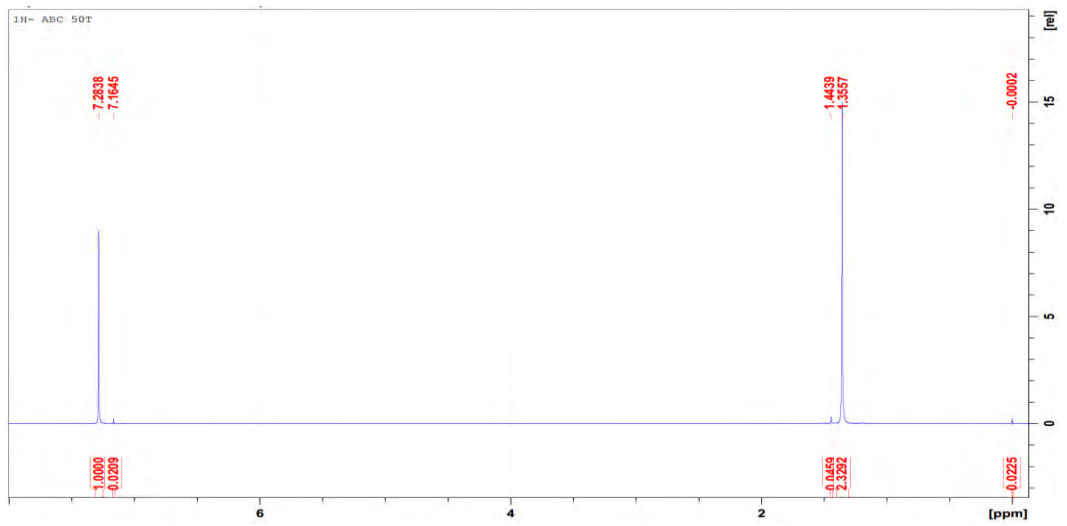


Figure B10: Raffinate layer of C<sub>2</sub>mimAc + benzene + cyclohexane (50% benzene in feed)

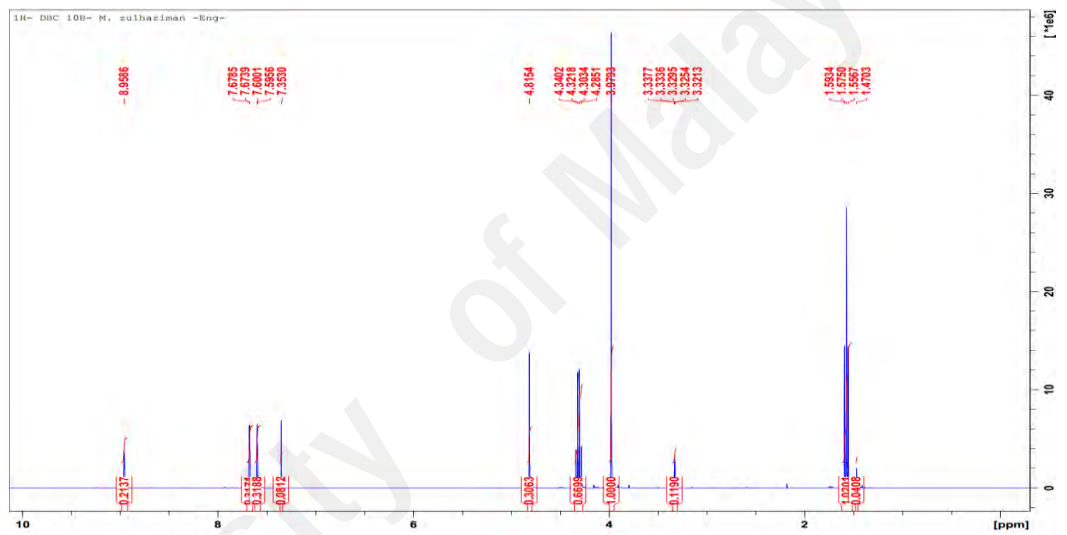


Figure B11: Extract layer of C<sub>2</sub>mimSCN + benzene + cyclohexane (10% benzene in feed)

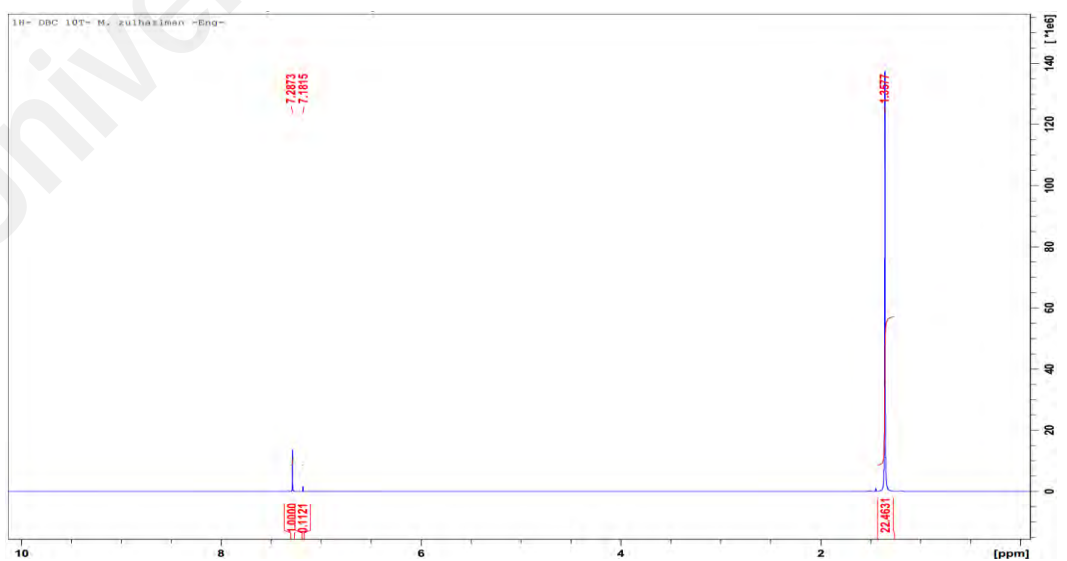


Figure B12: Raffinate layer of C<sub>2</sub>mimSCN + benzene + cyclohexane (10% benzene in feed)

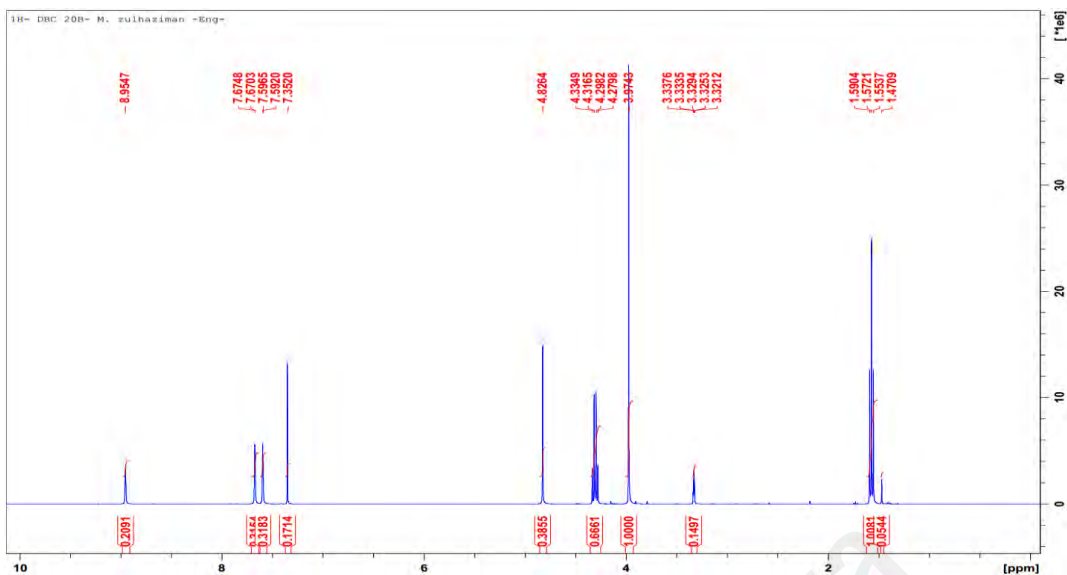


Figure B13: Extract layer of C<sub>2</sub>mimSCN + benzene + cyclohexane (20% benzene in feed)

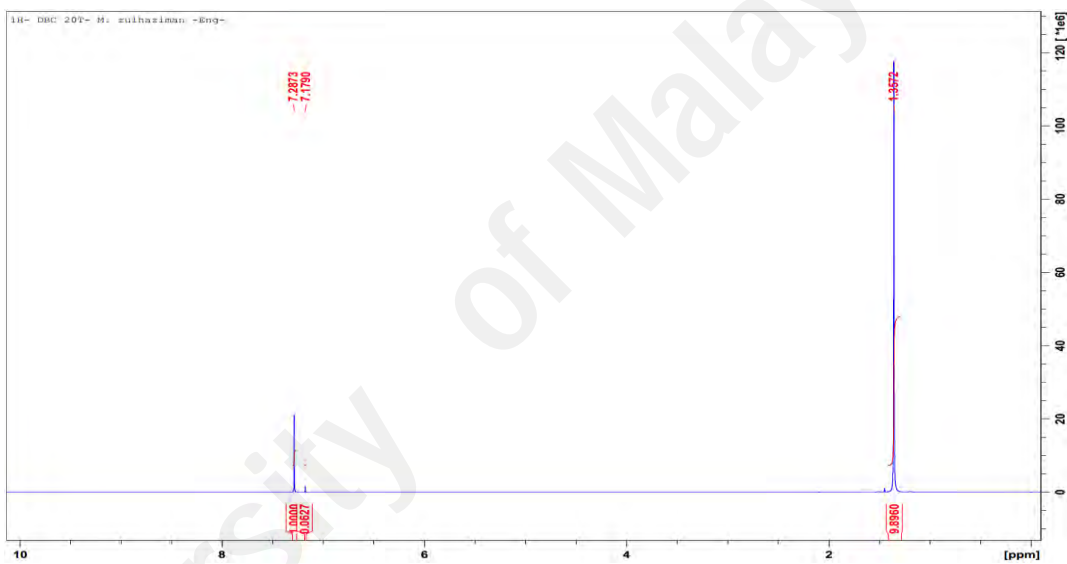


Figure B14: Raffinate layer of C<sub>2</sub>mimSCN + benzene + cyclohexane (20% benzene in feed)

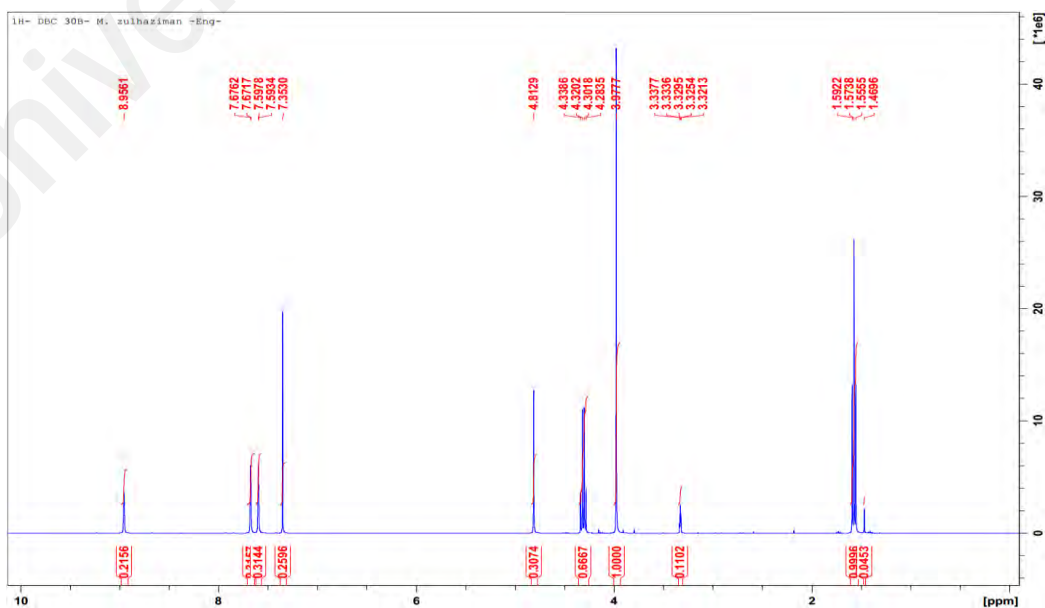


Figure B15: Extract layer of C<sub>2</sub>mimSCN + benzene + cyclohexane (30% benzene in feed)

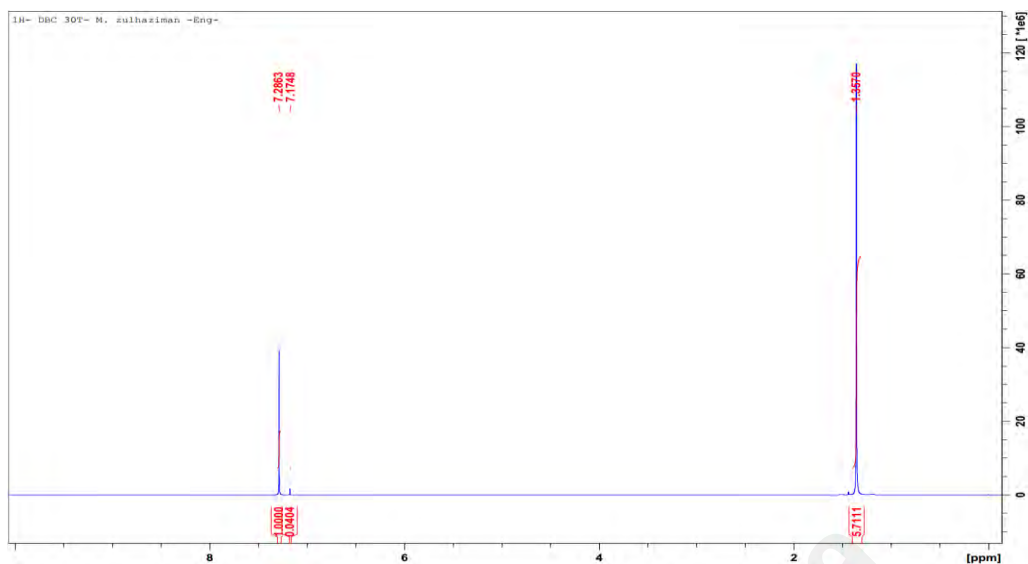


Figure B16: Raffinate layer of C<sub>2</sub>mimSCN + benzene + cyclohexane (30% benzene in feed)

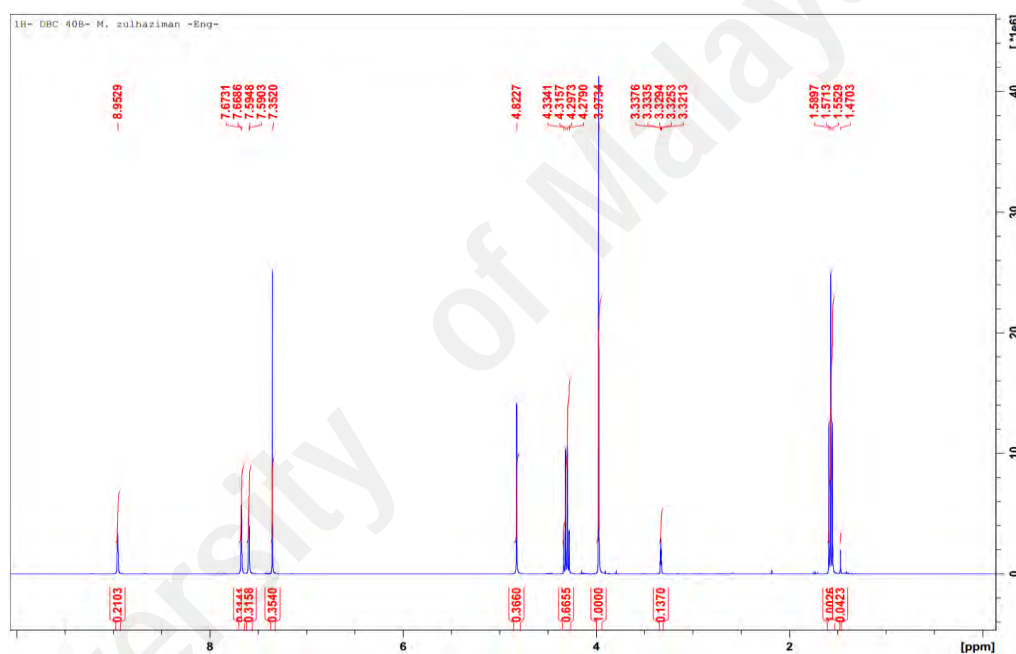


Figure B17: Extract layer of C<sub>2</sub>mimSCN + benzene + cyclohexane (40% benzene in feed)

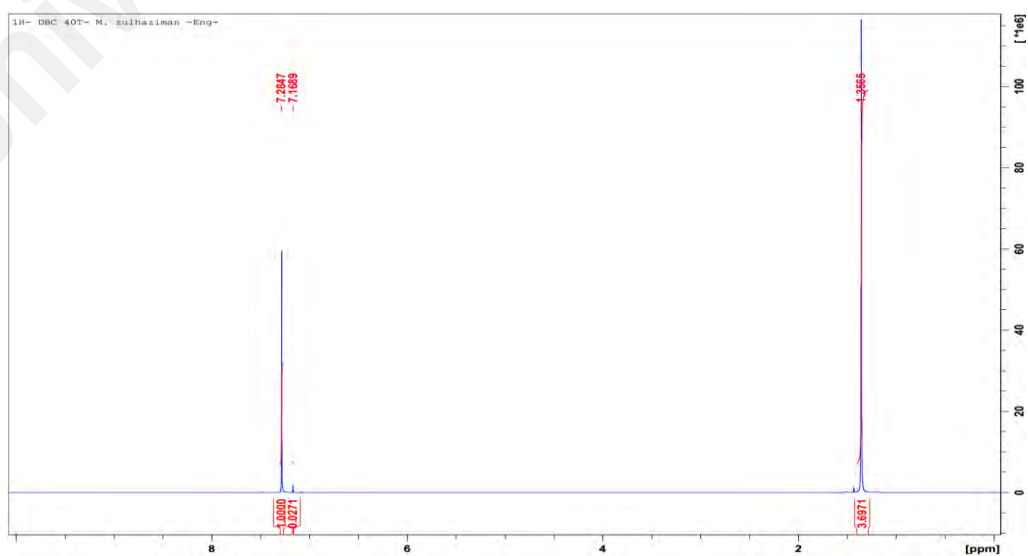


Figure B18: Raffinate layer of C<sub>2</sub>mimSCN + benzene + cyclohexane (40% benzene in feed)

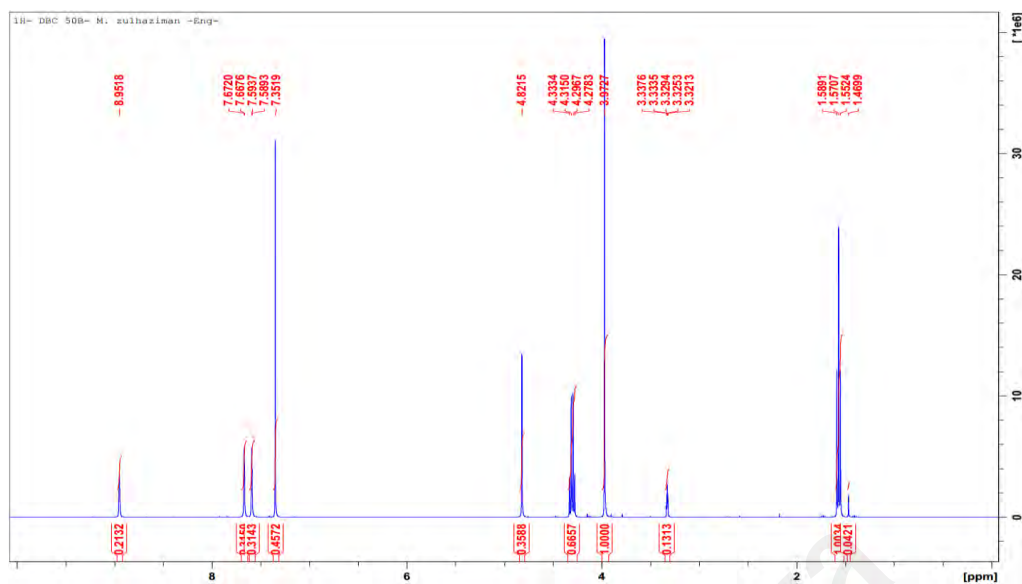


Figure B19: Extract layer of C<sub>2</sub>mimSCN + benzene + cyclohexane (50% benzene in feed)

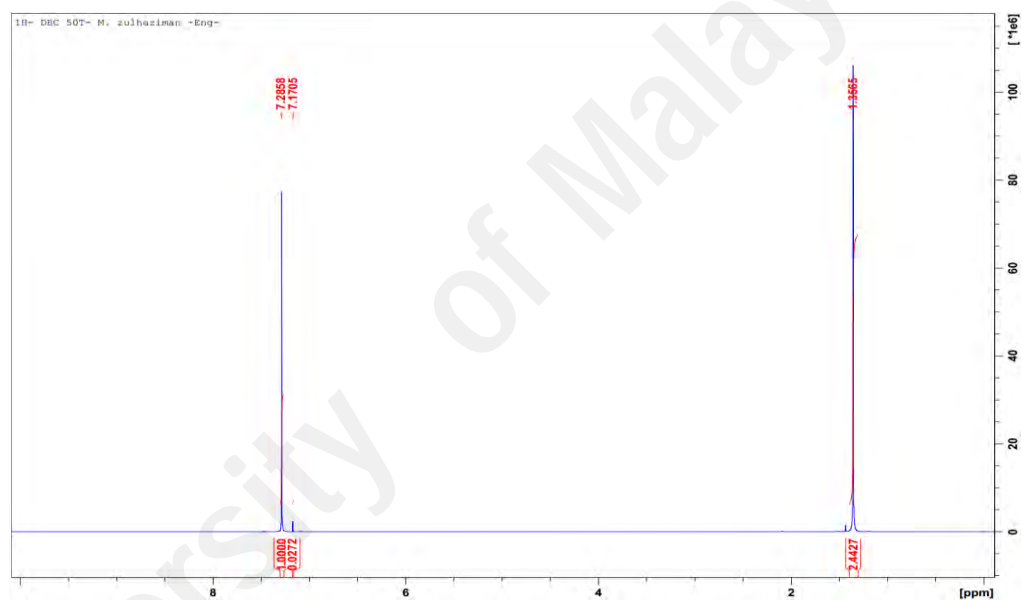


Figure B20: Raffinate layer of C<sub>2</sub>mimSCN + benzene + cyclohexane (50% benzene in feed)

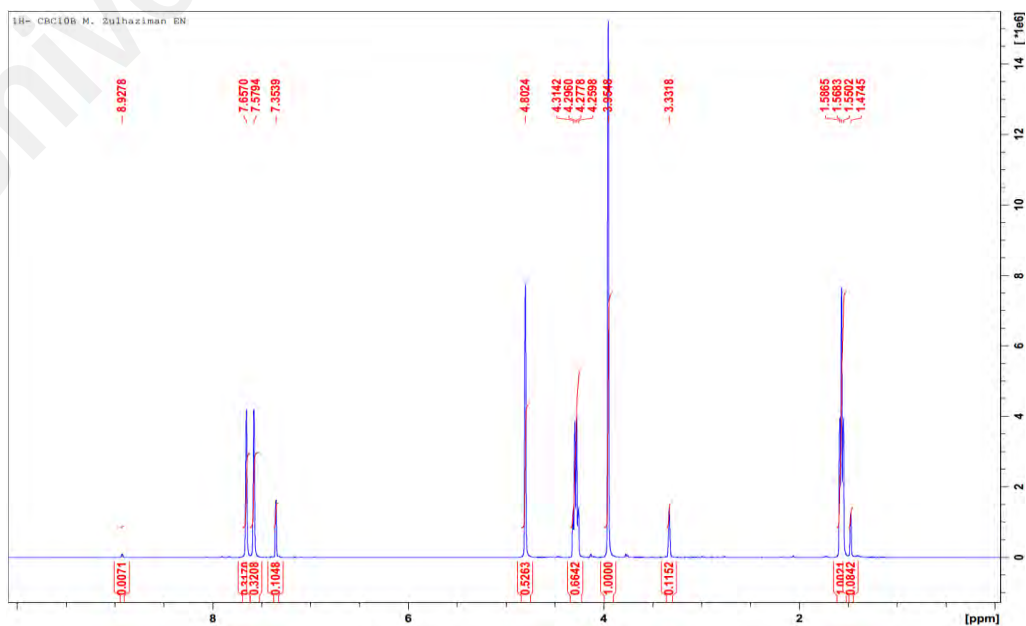


Figure B21: Extract layer of C<sub>2</sub>mimN(CN)<sub>2</sub> + benzene + cyclohexane (10% benzene in feed)

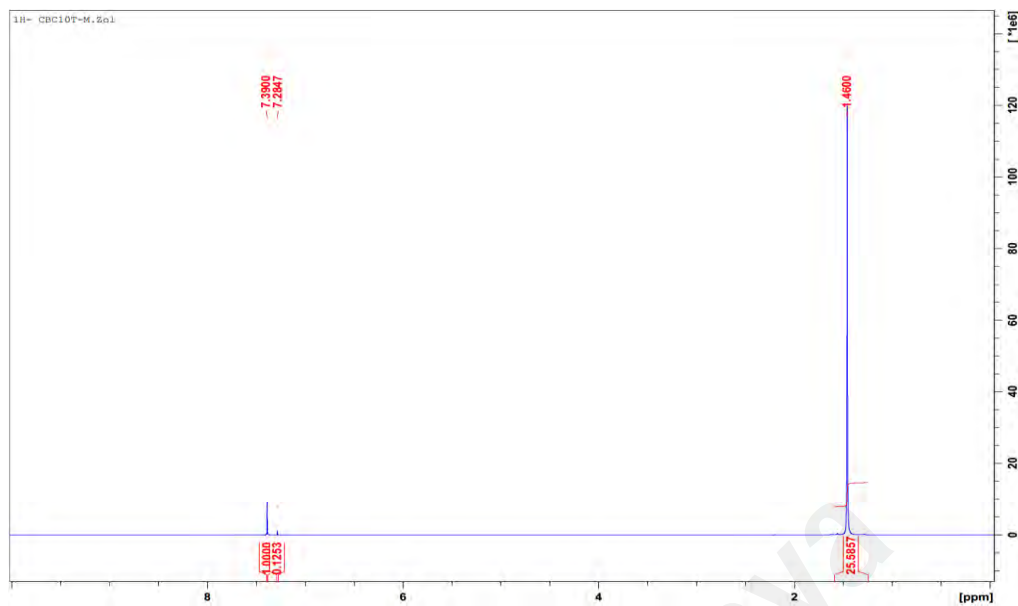


Figure B22: Raffinate layer of  $C_2mimN(CN)_2$  + benzene + cyclohexane (10% benzene in feed)

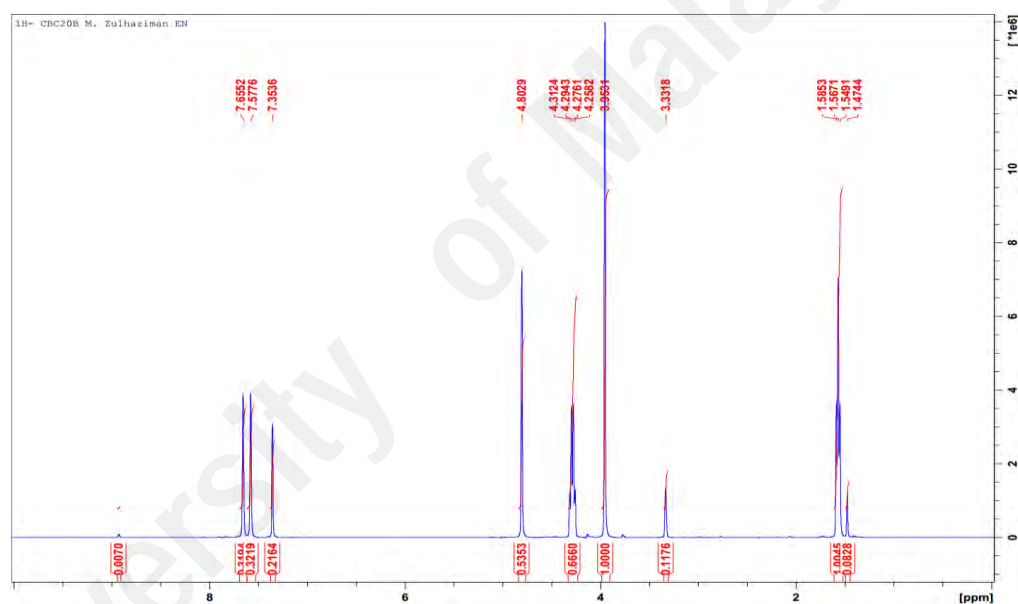


Figure B23: Extract layer of  $C_2mimN(CN)_2$  + benzene + cyclohexane (20% benzene in feed)

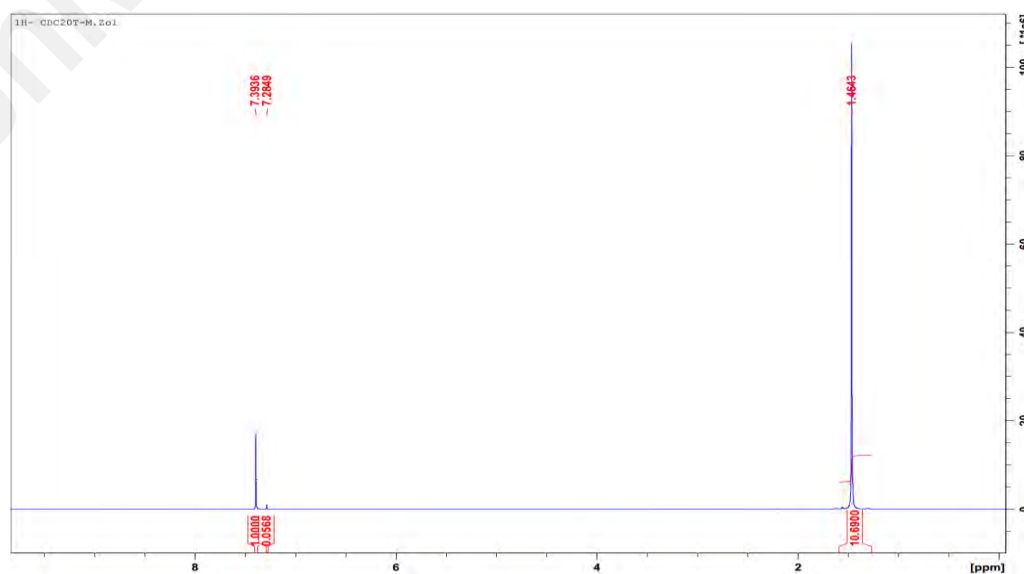


Figure B24: Raffinate layer of  $C_2mimN(CN)_2$  + benzene + cyclohexane (20% benzene in feed)

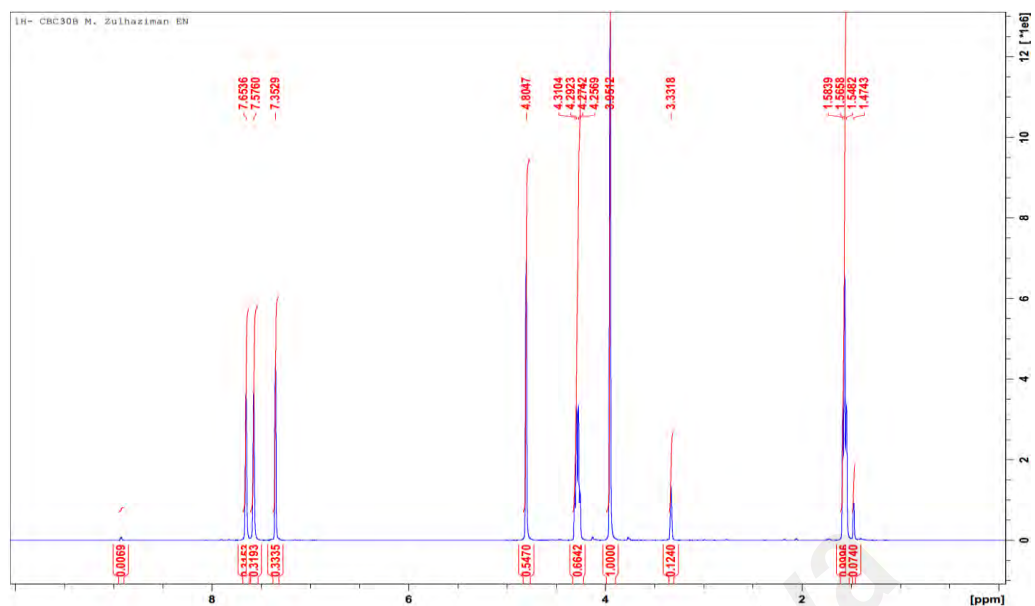


Figure B25: Extract layer of  $C_2mimN(CN)_2$  + benzene + cyclohexane (30% benzene in feed)

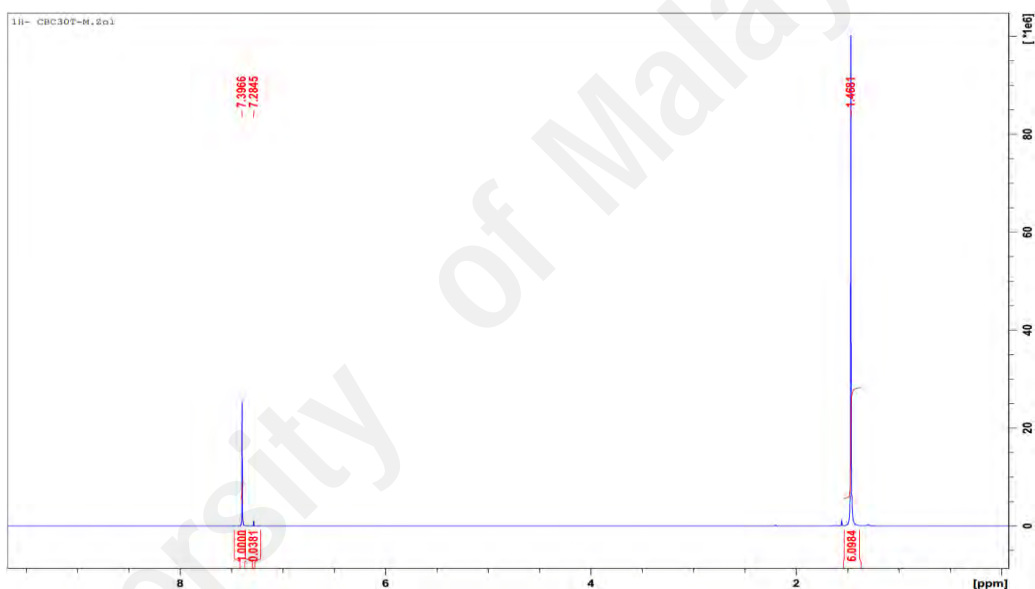


Figure B26: Raffinate layer of  $C_2mimN(CN)_2$  + benzene + cyclohexane (30% benzene in feed)

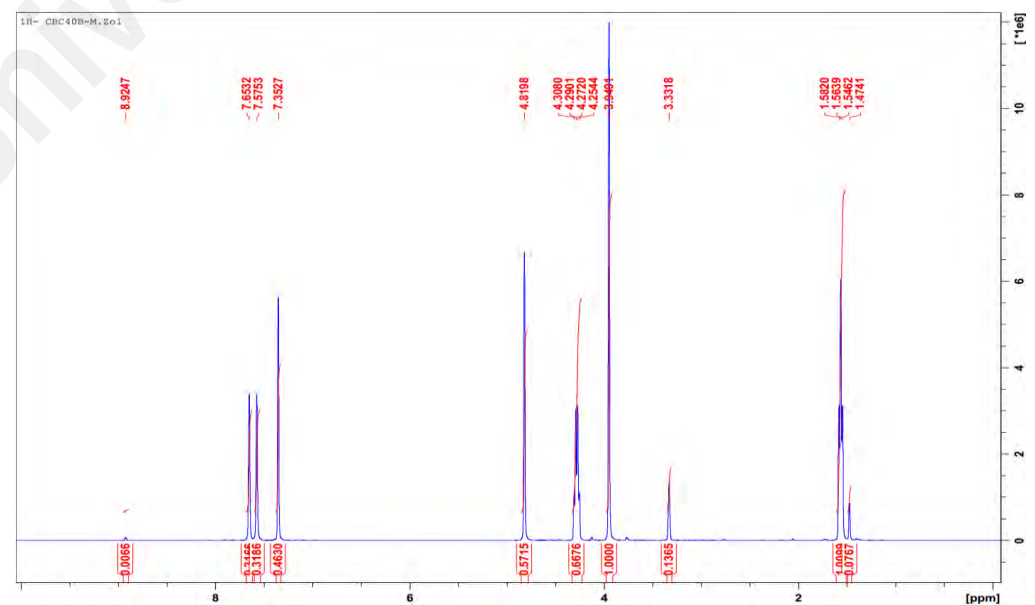


Figure B27: Extract layer of  $C_2mimN(CN)_2$  + benzene + cyclohexane (40% benzene in feed)

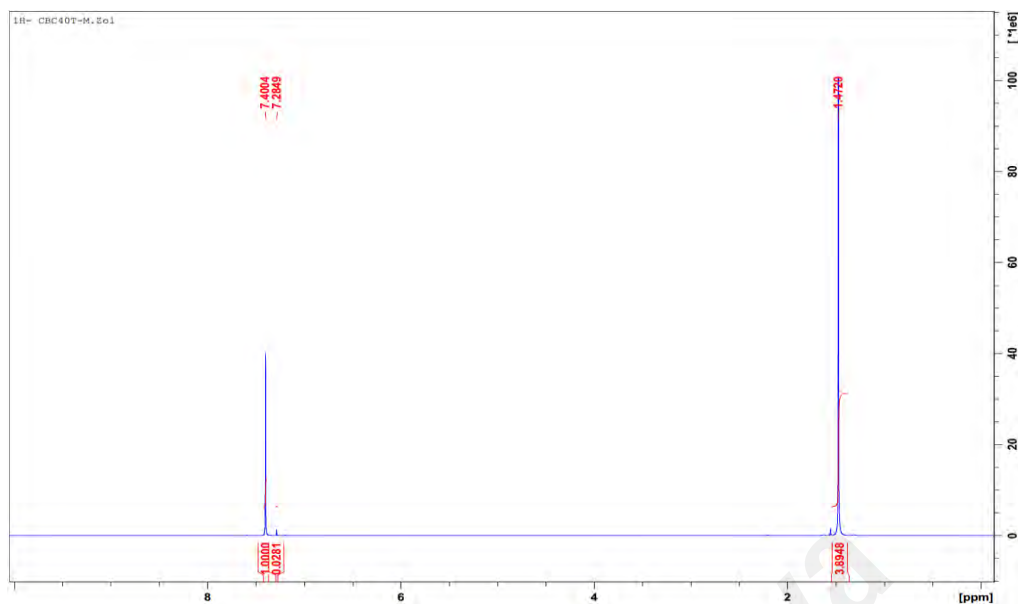


Figure B28: Raffinate layer of  $\text{C}_2\text{mimN}(\text{CN})_2$  + benzene + cyclohexane (40% benzene in feed)

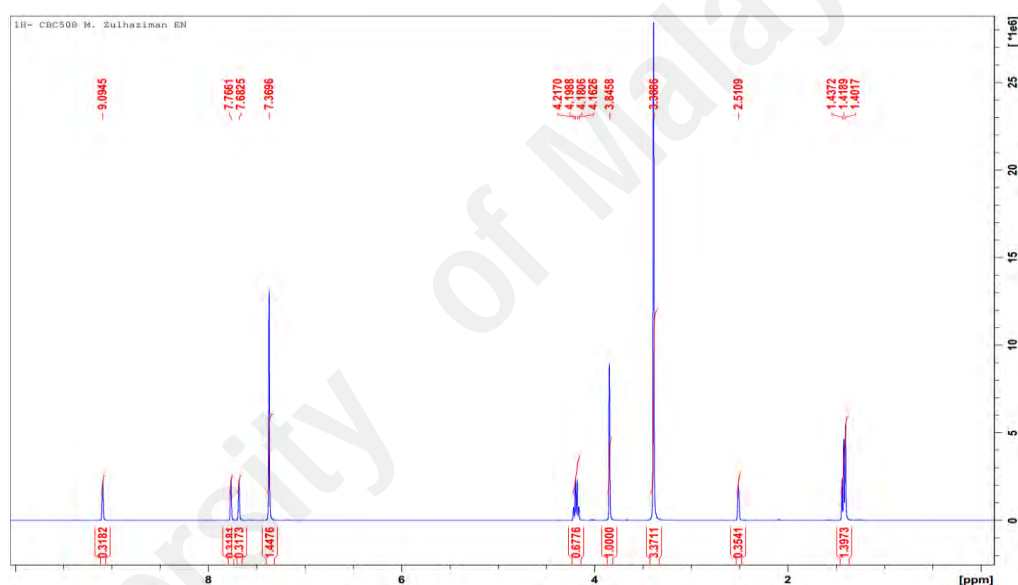


Figure B29: Extract layer of  $\text{C}_2\text{mimN}(\text{CN})_2$  + benzene + cyclohexane (50% benzene in feed)

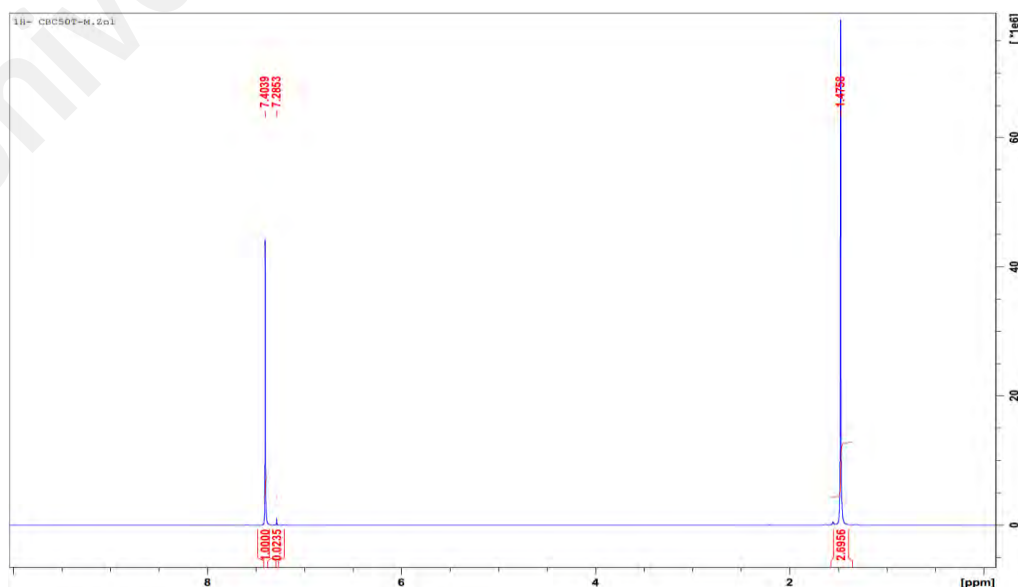


Figure B30: Raffinate layer of  $\text{C}_2\text{mimN}(\text{CN})_2$  + benzene + cyclohexane (50% benzene in feed)

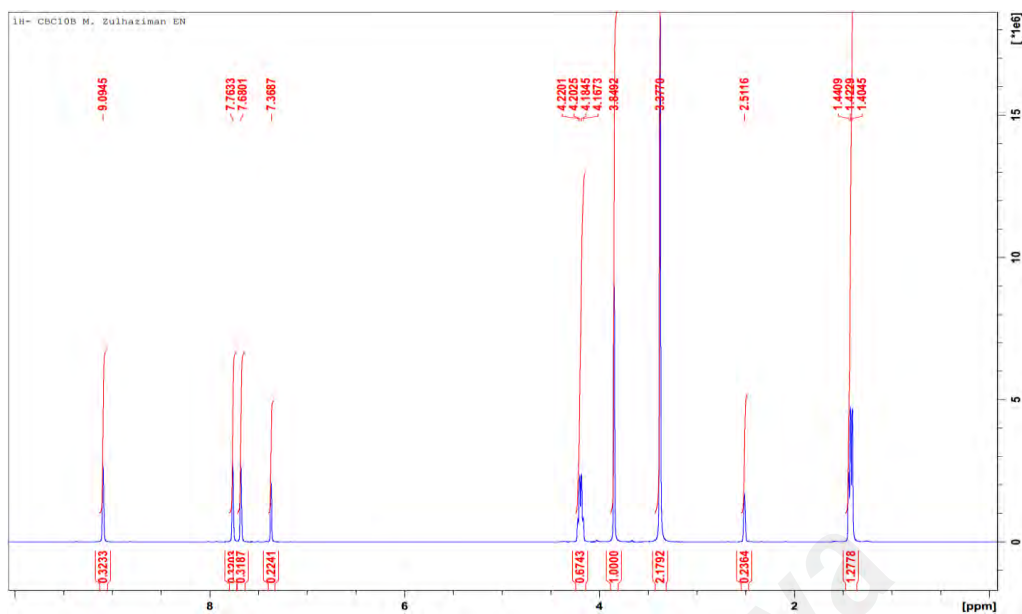


Figure B31: Extract layer of  $C_2mimTf_2N^+$  benzene + cyclohexane (10% benzene in feed)

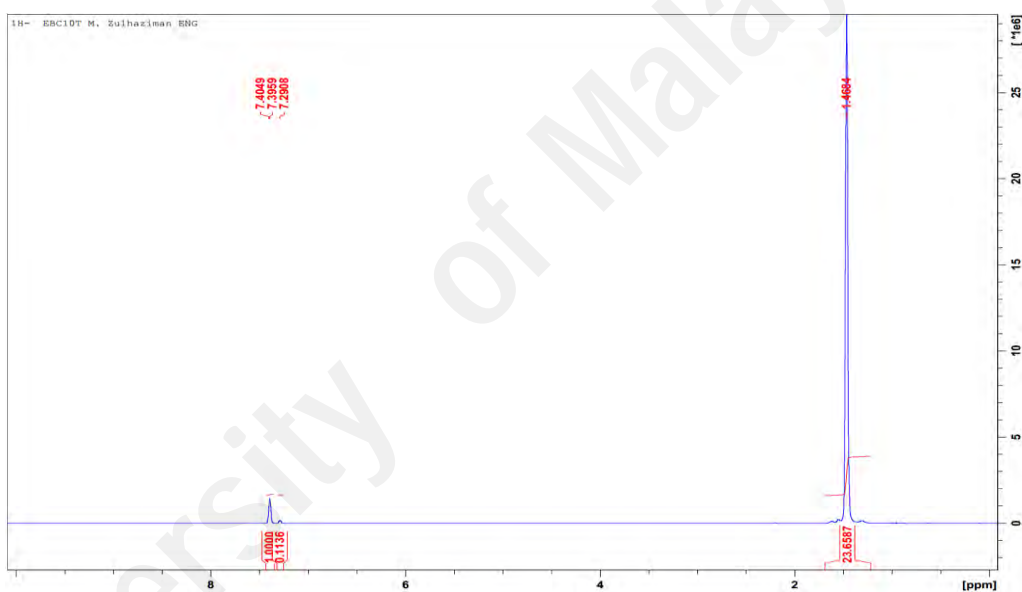


Figure B32: Raffinate layer of  $C_2mimTf_2N^+$  benzene + cyclohexane (10% benzene in feed)

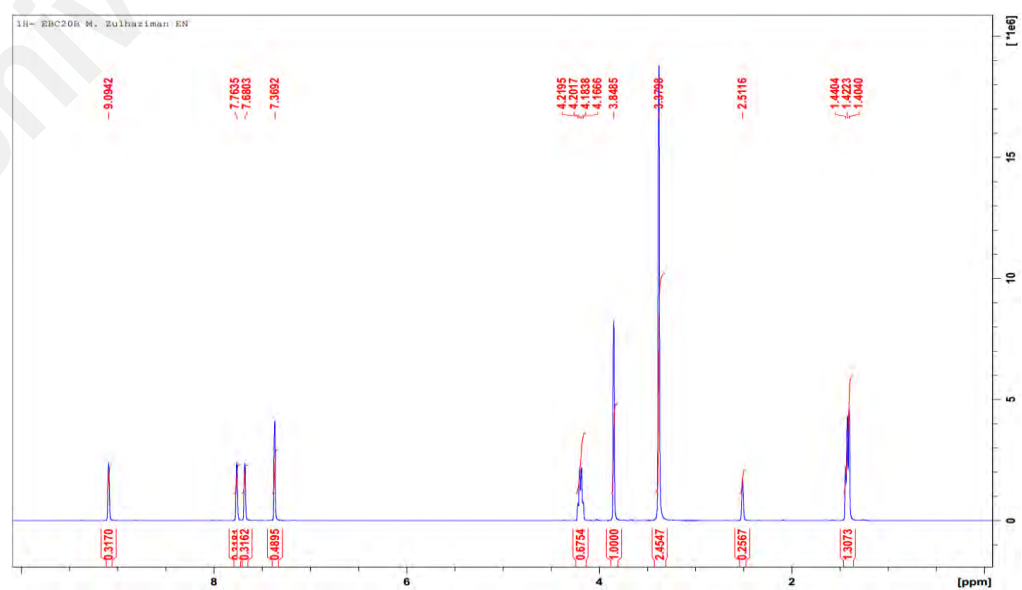


Figure B33: Extract layer of  $C_2mimTf_2N^+$  benzene + cyclohexane (20% benzene in feed)

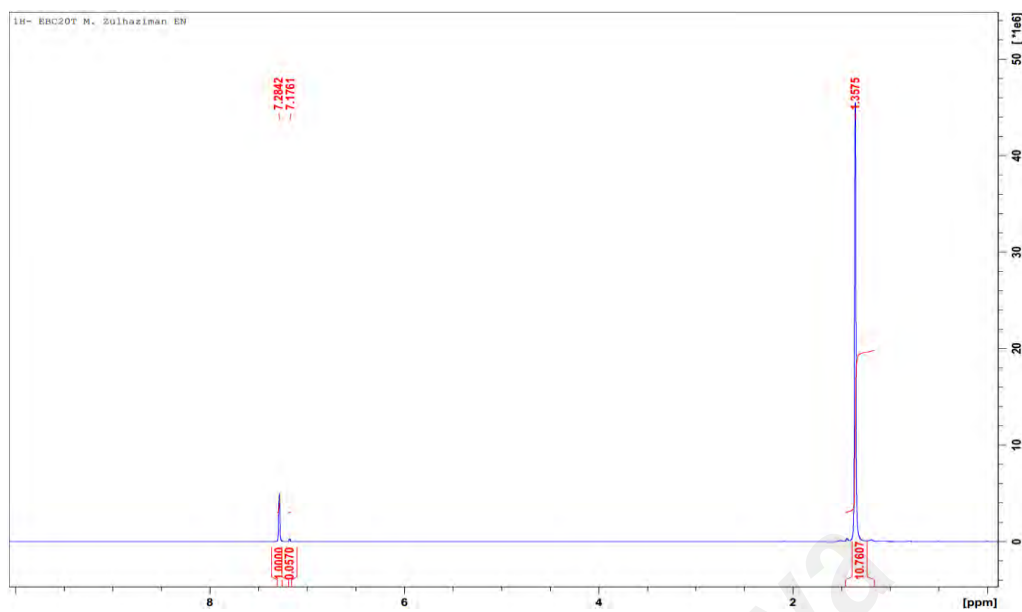


Figure B34: Raffinate layer of  $C_2mimTf_2N$  + benzene + cyclohexane (20% benzene in feed)

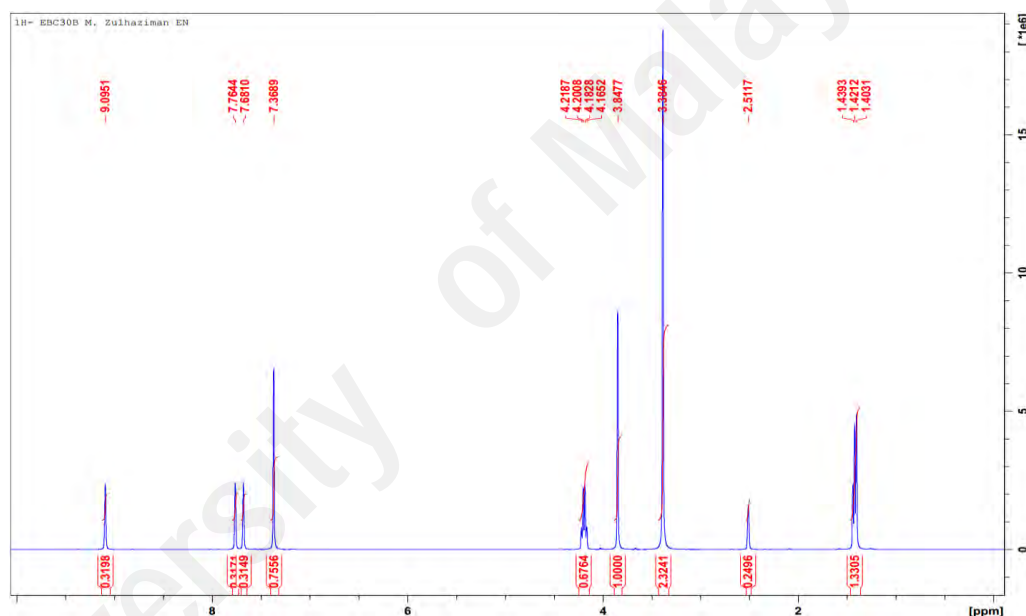


Figure B35: Extract layer of  $C_2mimTf_2N$  + benzene + cyclohexane (30% benzene in feed)

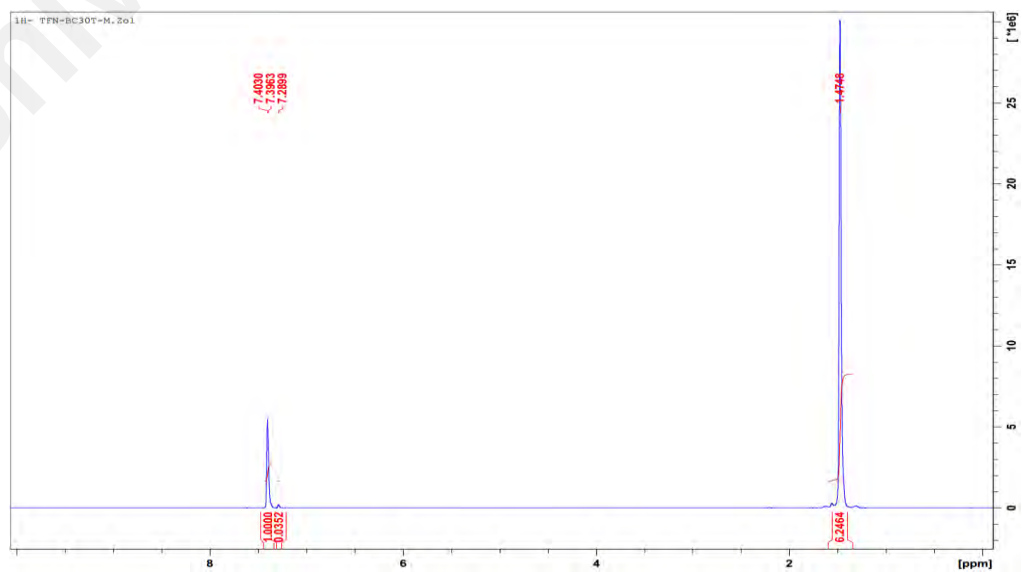


Figure B36: Raffinate layer of  $C_2mimTf_2N$  + benzene + cyclohexane (30% benzene in feed)

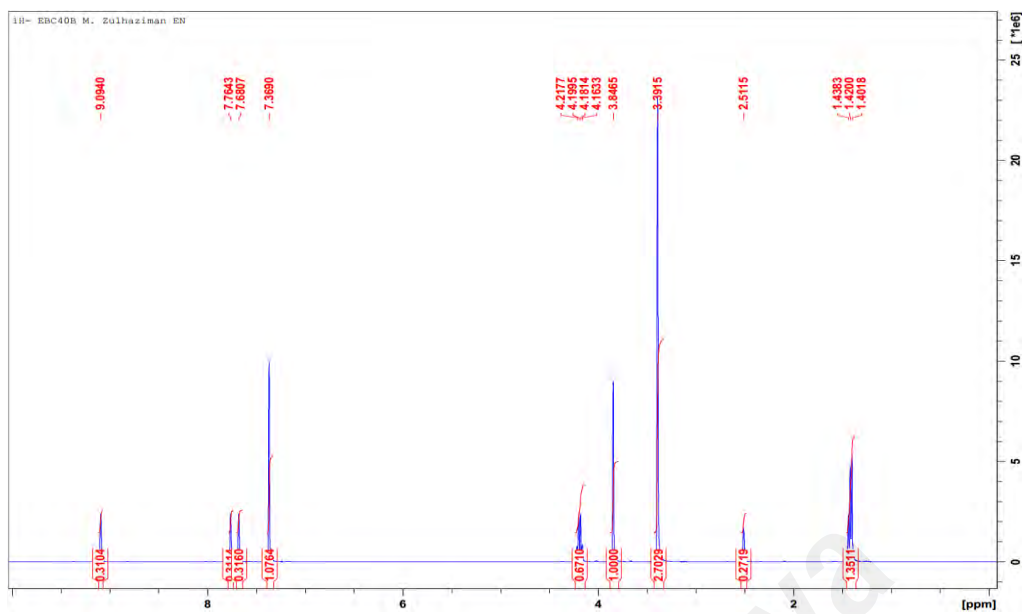


Figure B37: Extract layer of C<sub>2</sub>mimTf<sub>2</sub>N + benzene + cyclohexane (40% benzene in feed)

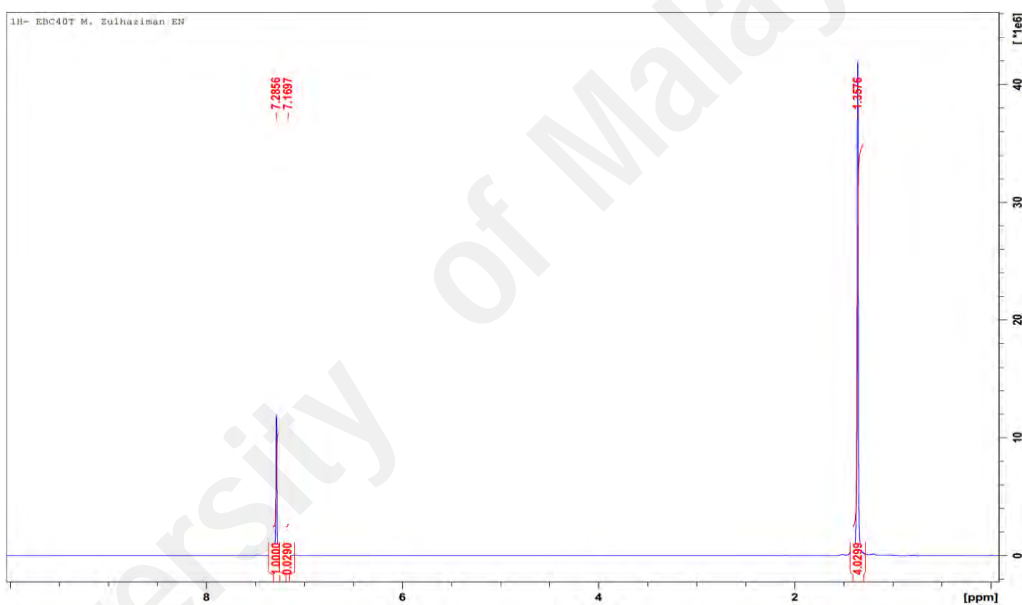


Figure B38: Raffinate layer of C<sub>2</sub>mimTf<sub>2</sub>N + benzene + cyclohexane (40% benzene in feed)

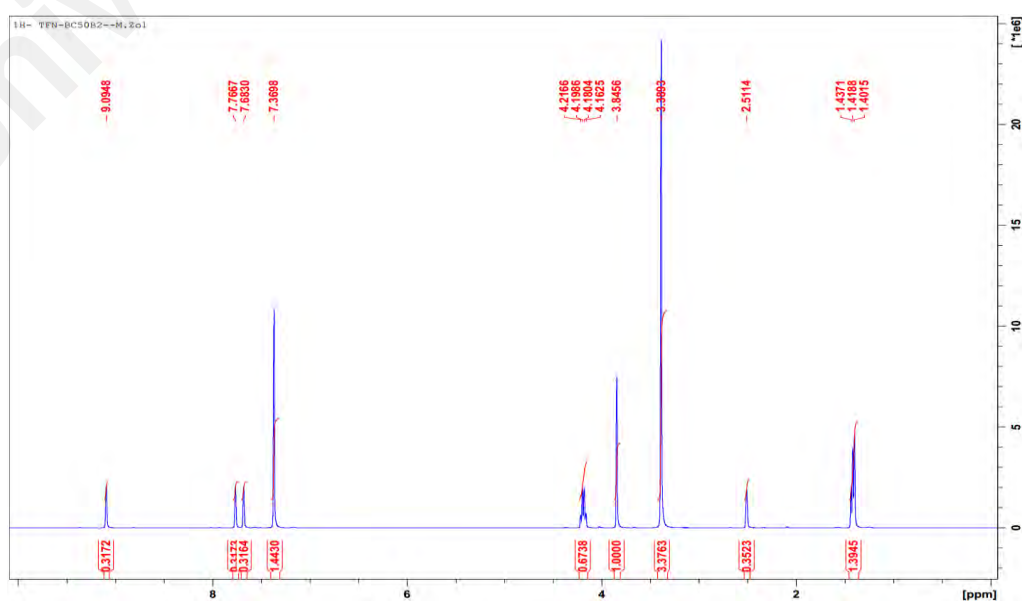


Figure B39: Extract layer of C<sub>2</sub>mimTf<sub>2</sub>N + benzene + cyclohexane (50% benzene in feed)

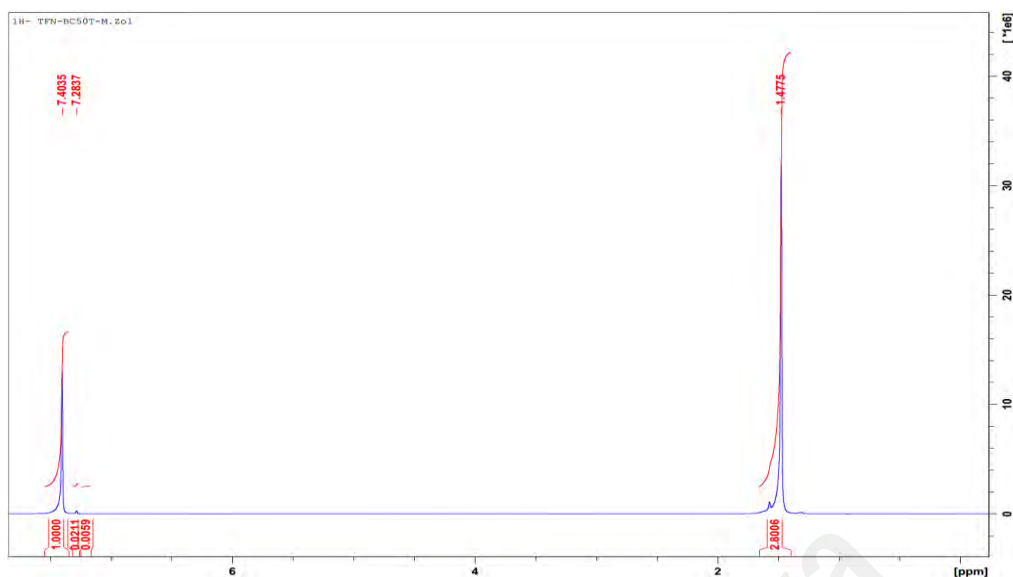


Figure B40: Raffinate layer of  $C_2mimTf_2N$  + benzene + cyclohexane (50% benzene in feed)

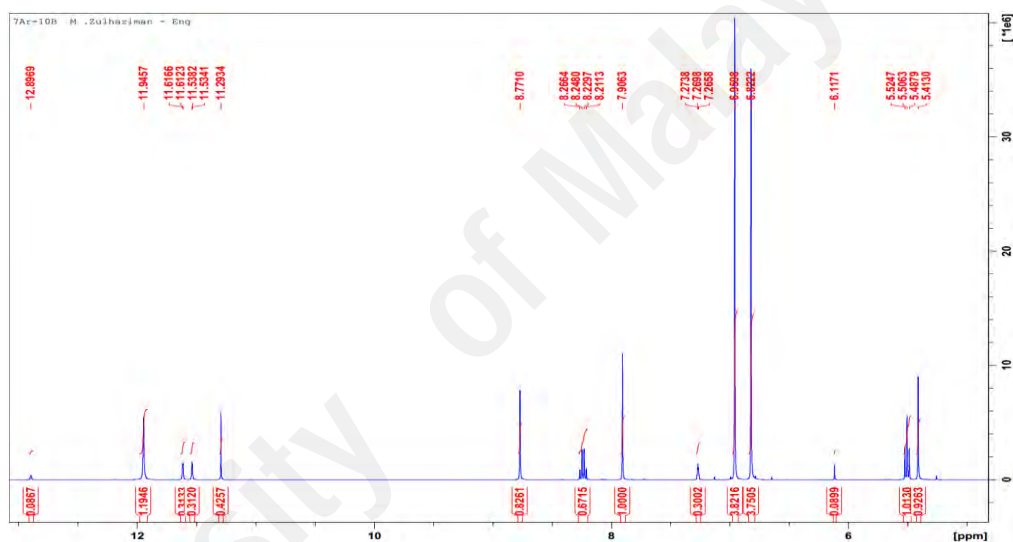


Figure B41: Extract layer of  $[C_2mimSCN + DMF]$  + benzene + cyclohexane (10% benzene in feed)

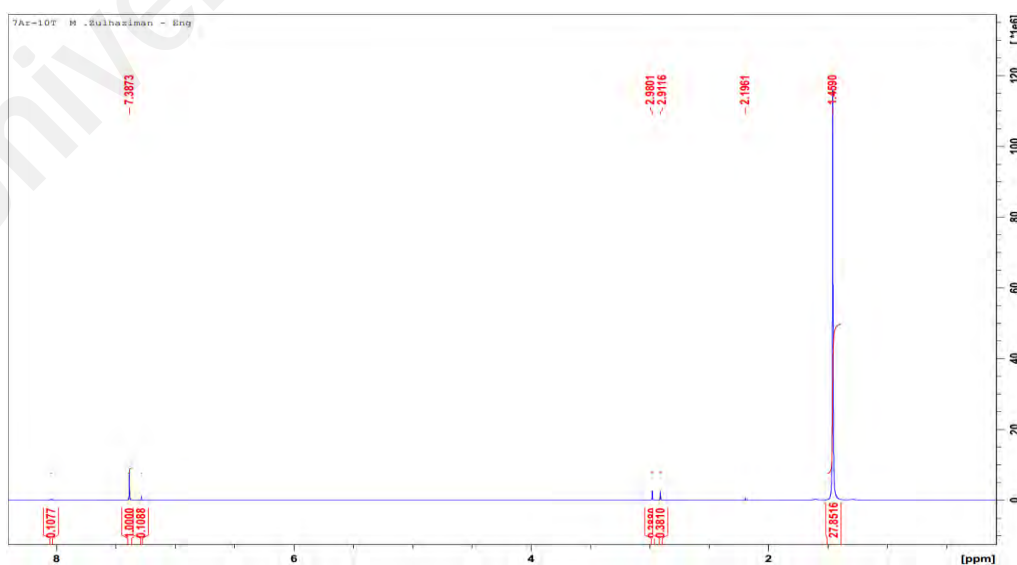


Figure B42: Raffinate layer of  $[C_2mimSCN + DMF]$  + benzene + cyclohexane (10% benzene in feed)

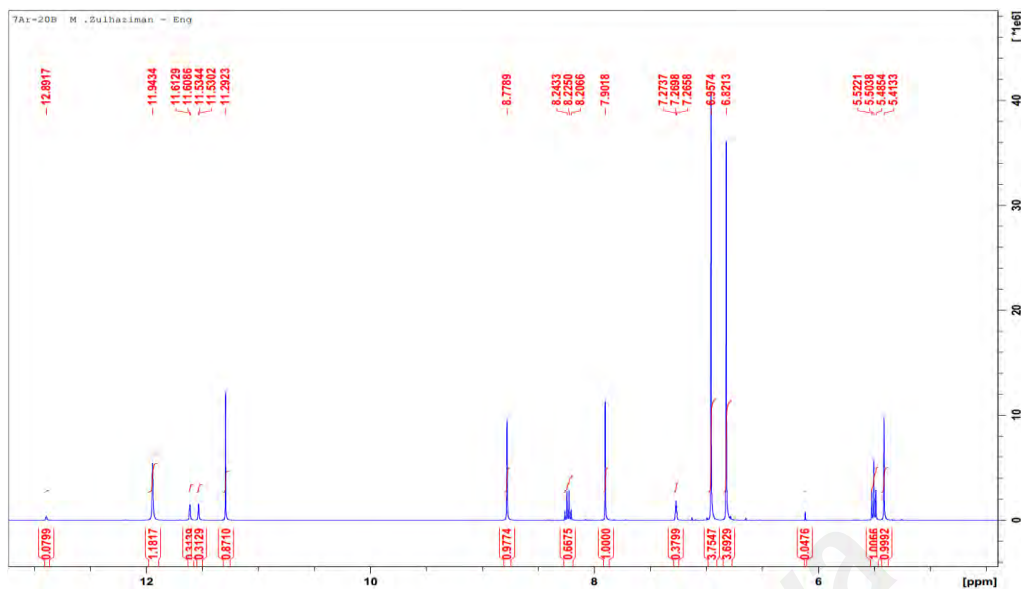


Figure B43: Extract layer of [C<sub>2</sub>mimSCN + DMF] + benzene + cyclohexane (20% benzene in feed)

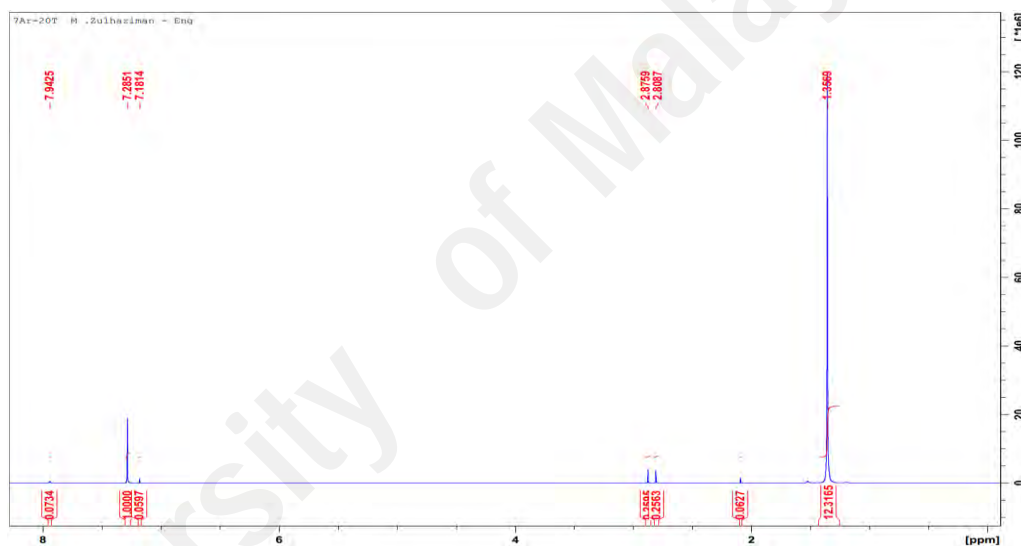


Figure B44: Raffinate layer of [C<sub>2</sub>mimSCN + DMF] + benzene + cyclohexane (20% benzene in feed)

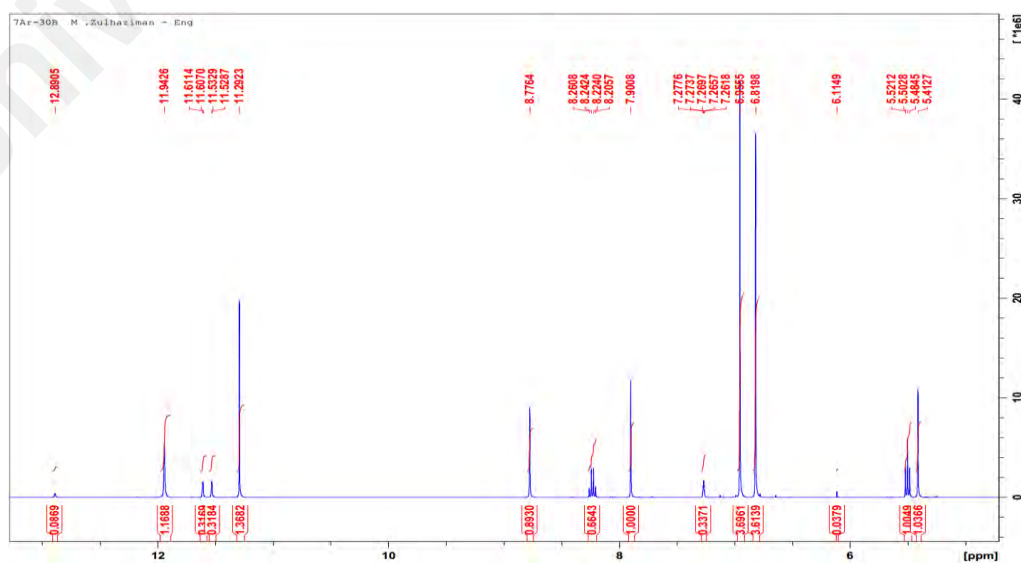


Figure B45: Extract layer of [C<sub>2</sub>mimSCN + DMF] + benzene + cyclohexane (30% benzene in feed)

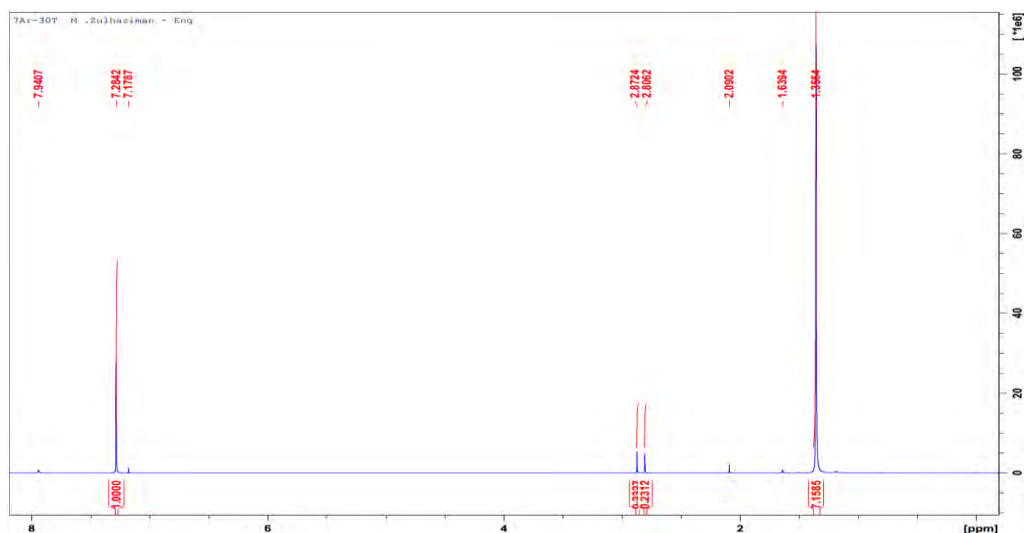


Figure B46: Raffinate layer of [C<sub>2</sub>mimSCN + DMF] + benzene + cyclohexane (30% benzene in feed)

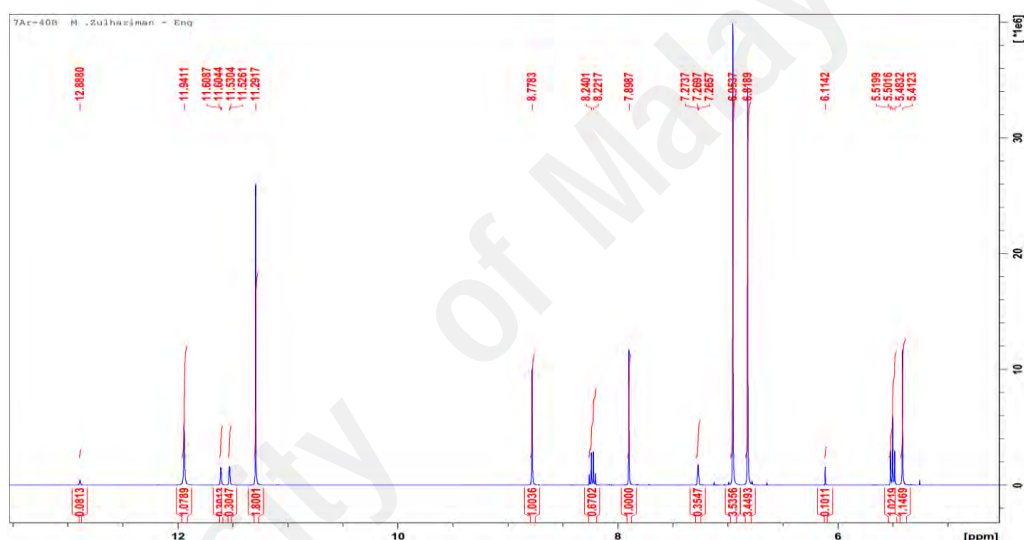


Figure B47: Extract layer of [C<sub>2</sub>mimSCN + DMF] + benzene + cyclohexane (40% benzene in feed)

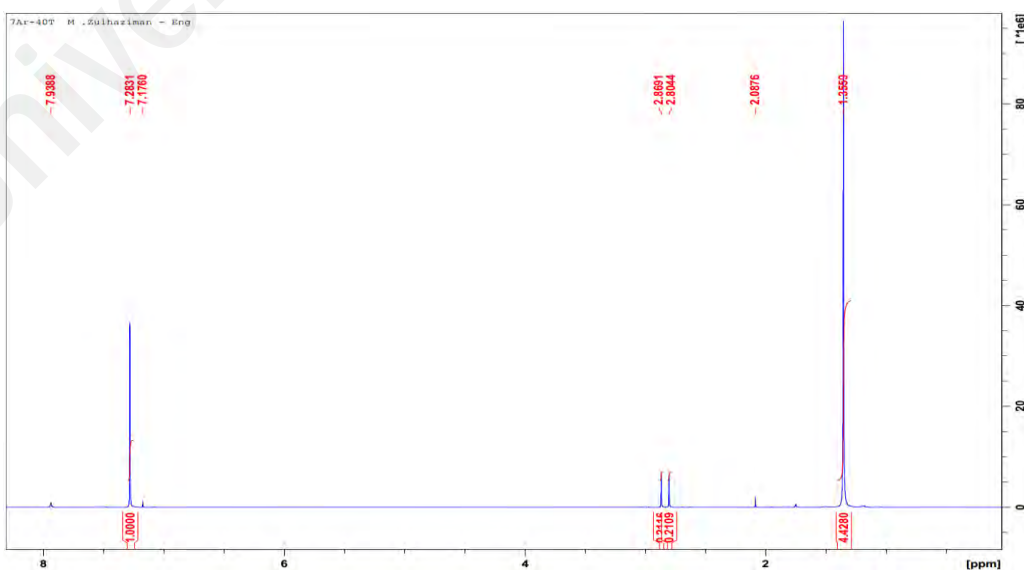


Figure B48: Raffinate layer of [C<sub>2</sub>mimSCN + DMF] + benzene + cyclohexane (40% benzene in feed)

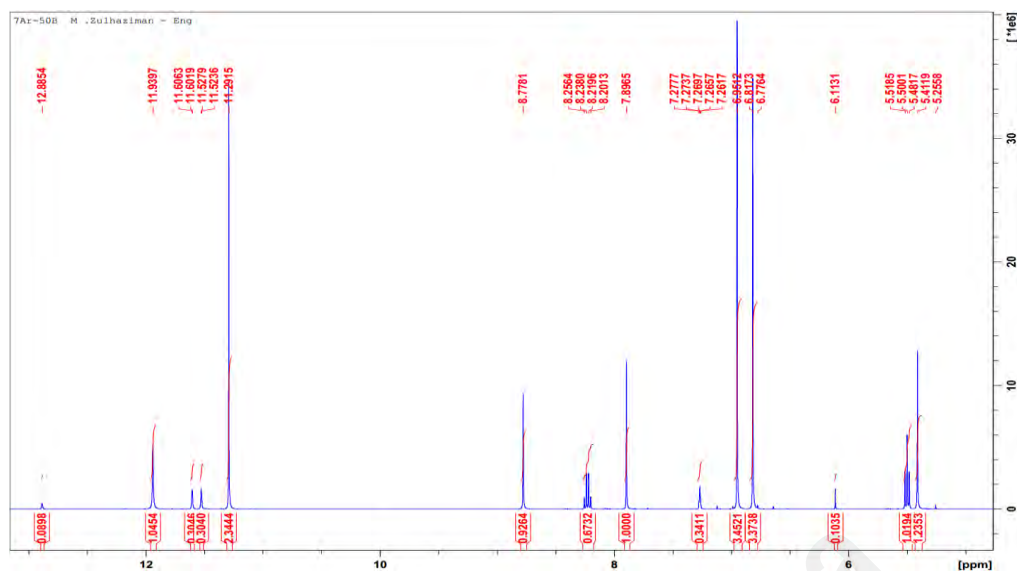


Figure B49: Extract layer of [C<sub>2</sub>mimSCN + DMF] + benzene + cyclohexane (50% benzene in feed)

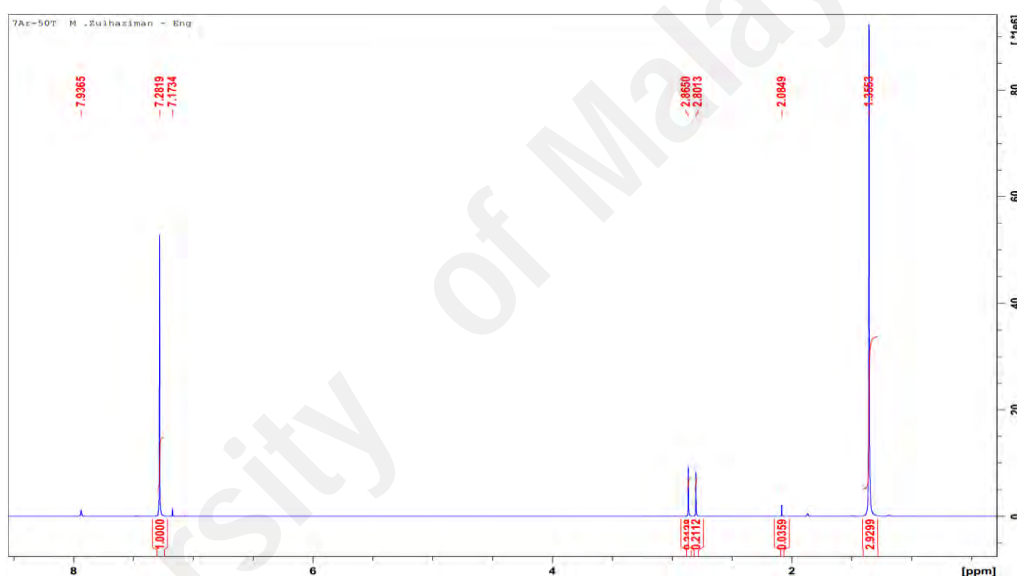


Figure B50: Raffinate layer of [C<sub>2</sub>mimSCN + DMF] + benzene + cyclohexane (50% benzene in feed)

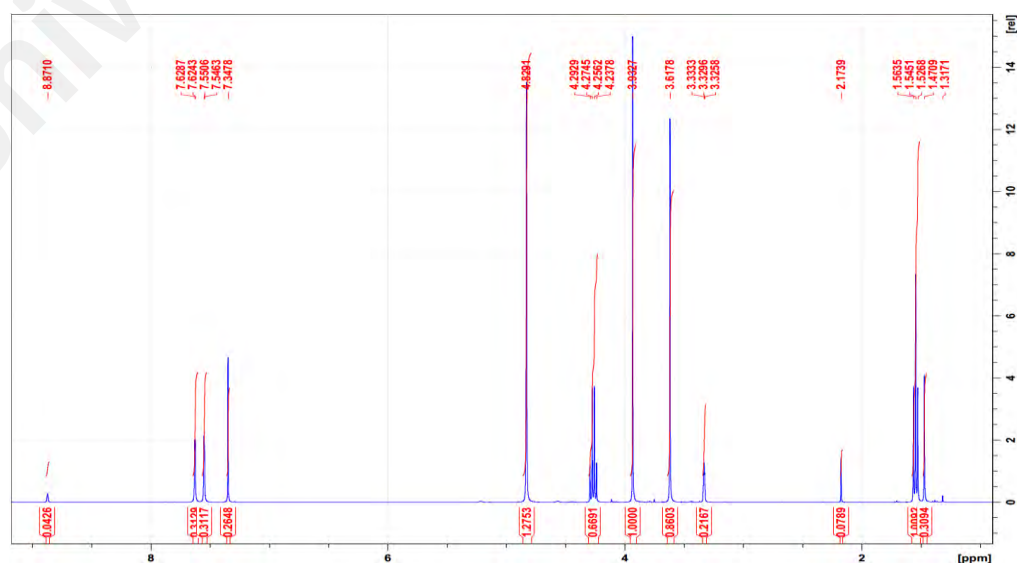


Figure B51: Extract layer of [C<sub>2</sub>mimTf<sub>2</sub>N + EG] + benzene + cyclohexane (10% benzene in feed)

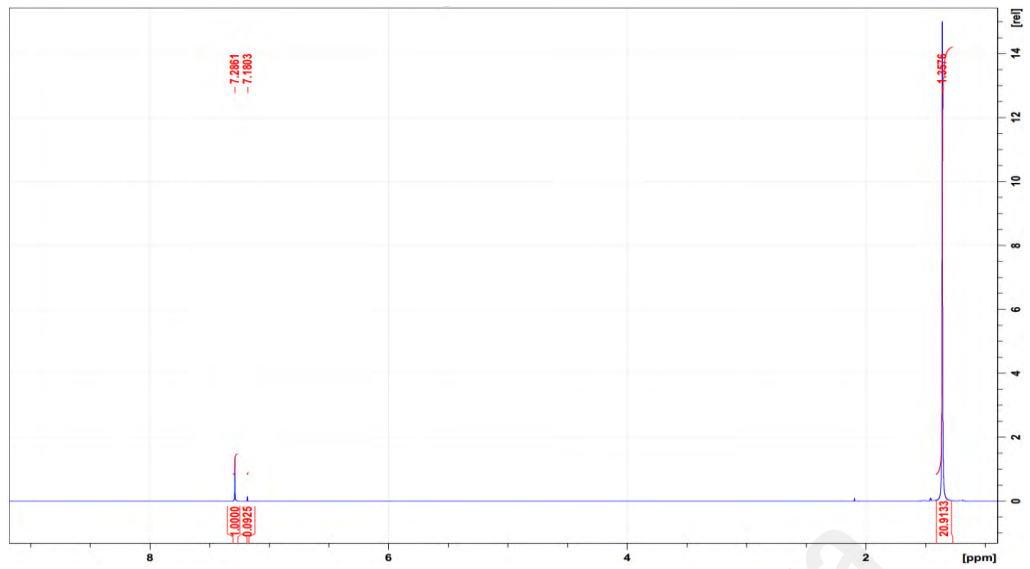


Figure B52: Raffinate layer of [C<sub>2</sub>mimTf<sub>2</sub>N + EG] + benzene + cyclohexane (10% benzene in feed)

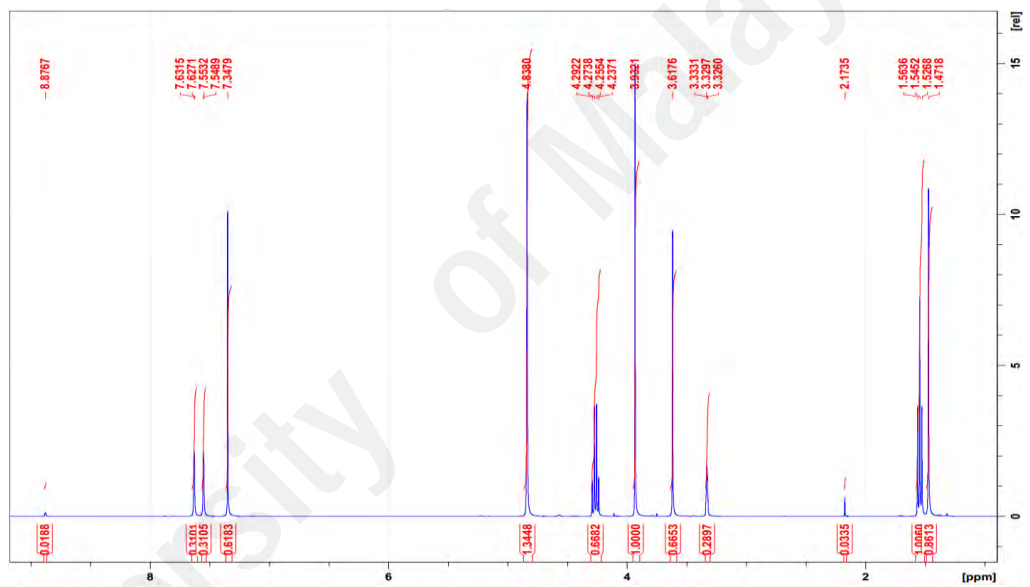


Figure B53: Extract layer of [C<sub>2</sub>mimTf<sub>2</sub>N + EG] + benzene + cyclohexane (20% benzene in feed)

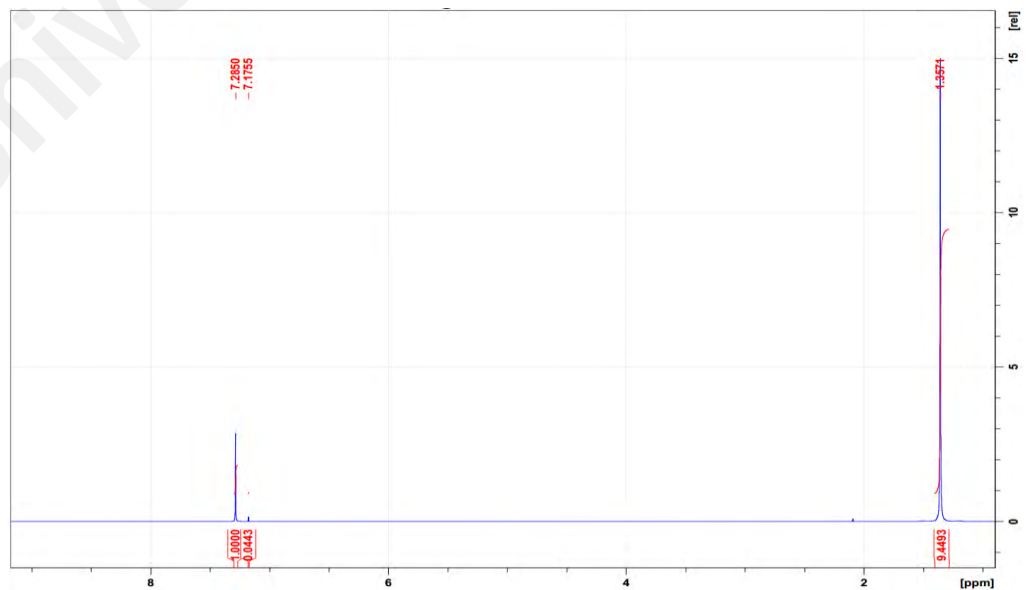


Figure B54: Raffinate layer of [C<sub>2</sub>mimTf<sub>2</sub>N + EG] + benzene + cyclohexane (20% benzene in feed)

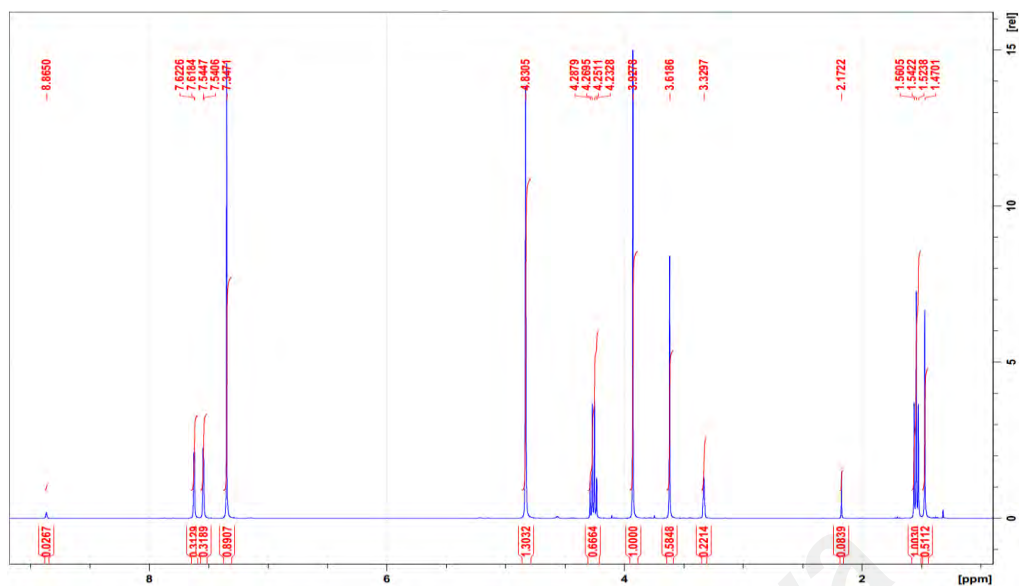


Figure B55: Extract layer of [C<sub>2</sub>mimTf<sub>2</sub>N + EG] + benzene + cyclohexane (30% benzene in feed)

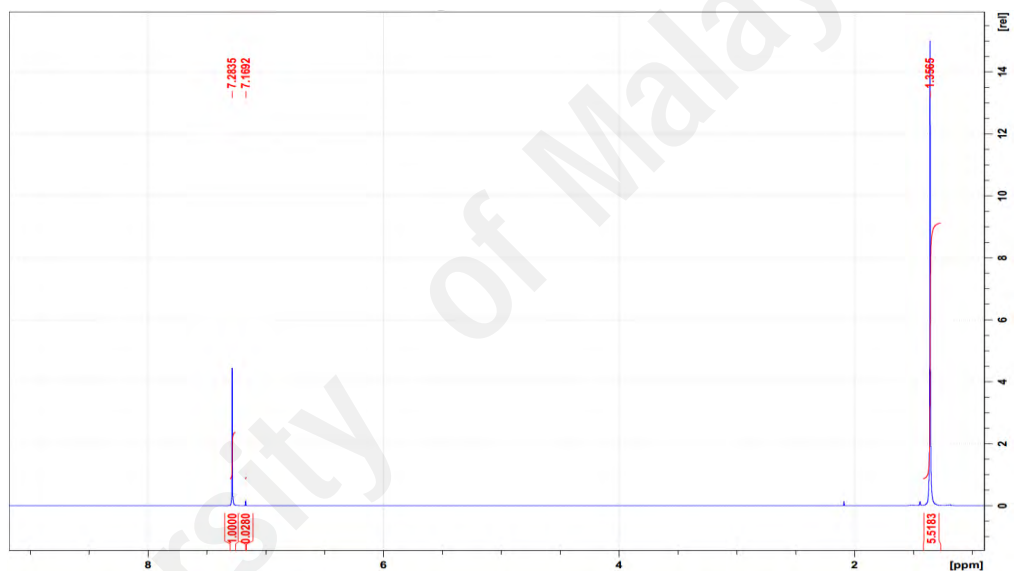


Figure B56: Raffinate layer of [C<sub>2</sub>mimTf<sub>2</sub>N + EG] + benzene + cyclohexane (30% benzene in feed)

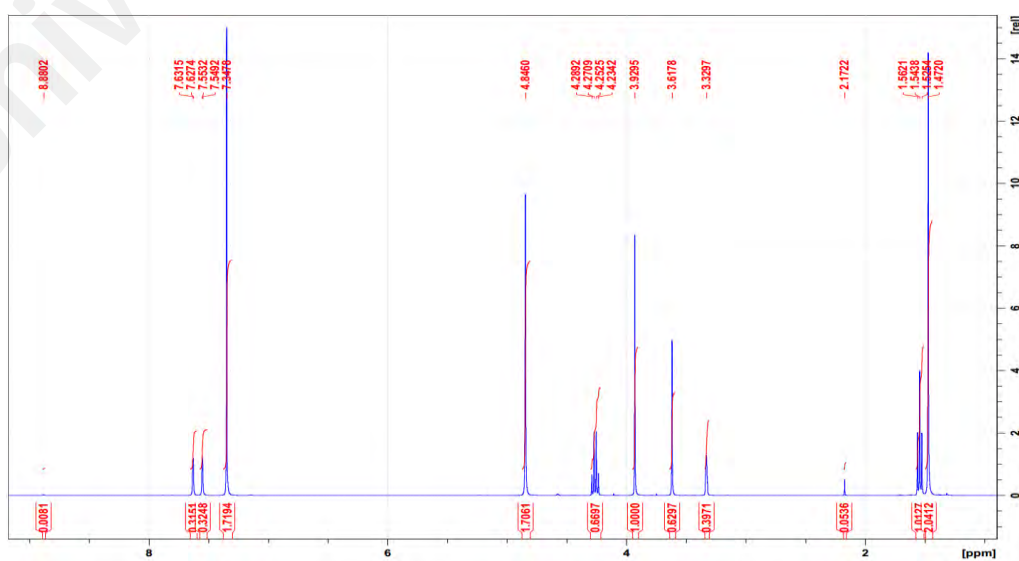


Figure B57: Extract layer of [C<sub>2</sub>mimTf<sub>2</sub>N + EG] + benzene + cyclohexane (40% benzene in feed)

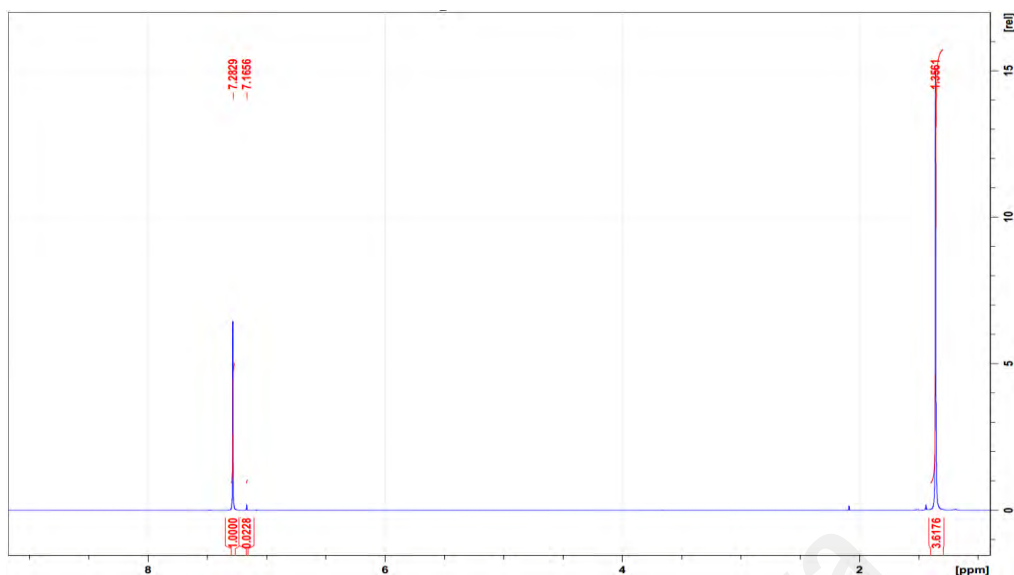


Figure B58: Raffinate layer of [C<sub>2</sub>mimTf<sub>2</sub>N + EG] + benzene + cyclohexane (40% benzene in feed)

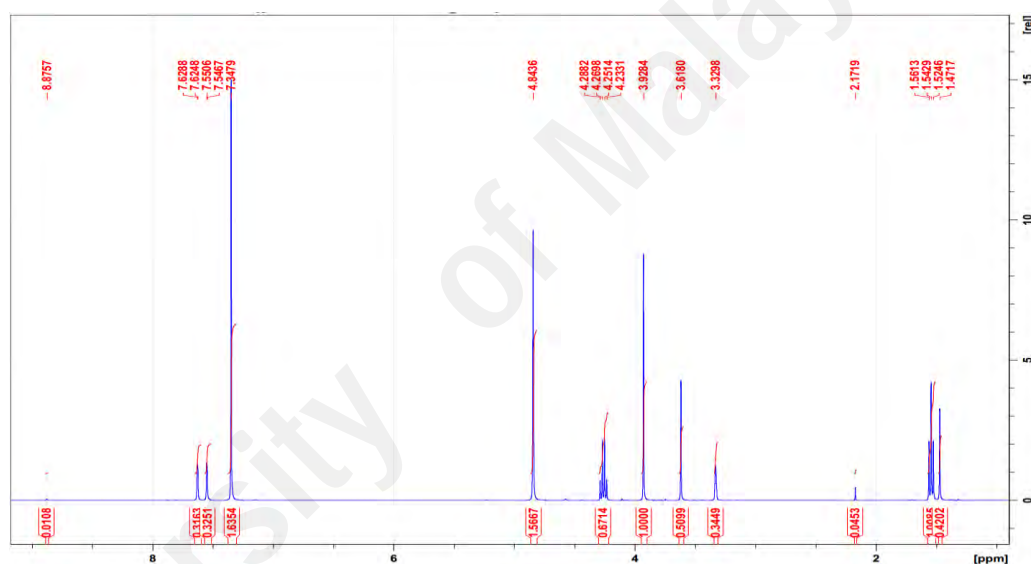


Figure B59: Extract layer of [C<sub>2</sub>mimTf<sub>2</sub>N + EG] + benzene + cyclohexane (50% benzene in feed)

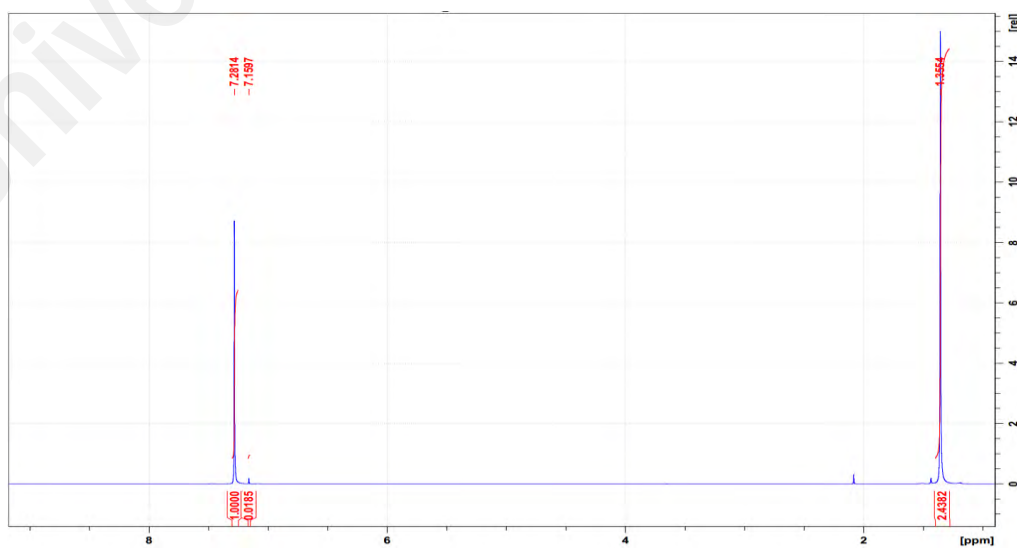


Figure B60: Raffinate layer of [C<sub>2</sub>mimTf<sub>2</sub>N + EG] + benzene + cyclohexane (50% benzene in feed)

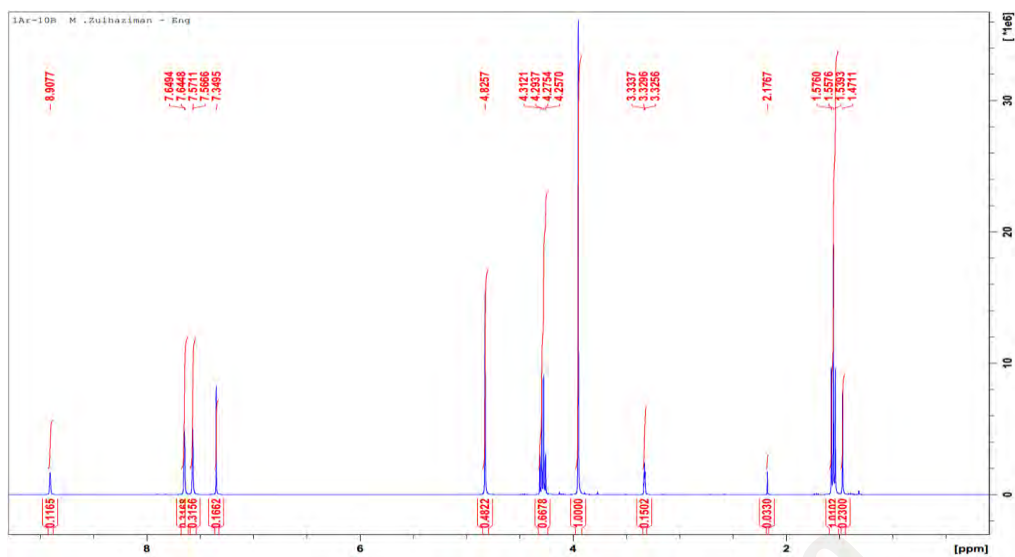


Figure B61: Extract layer of [C<sub>2</sub>mimSCN + C<sub>2</sub>mimTf<sub>2</sub>N] + benzene + cyclohexane (10% benzene in feed)

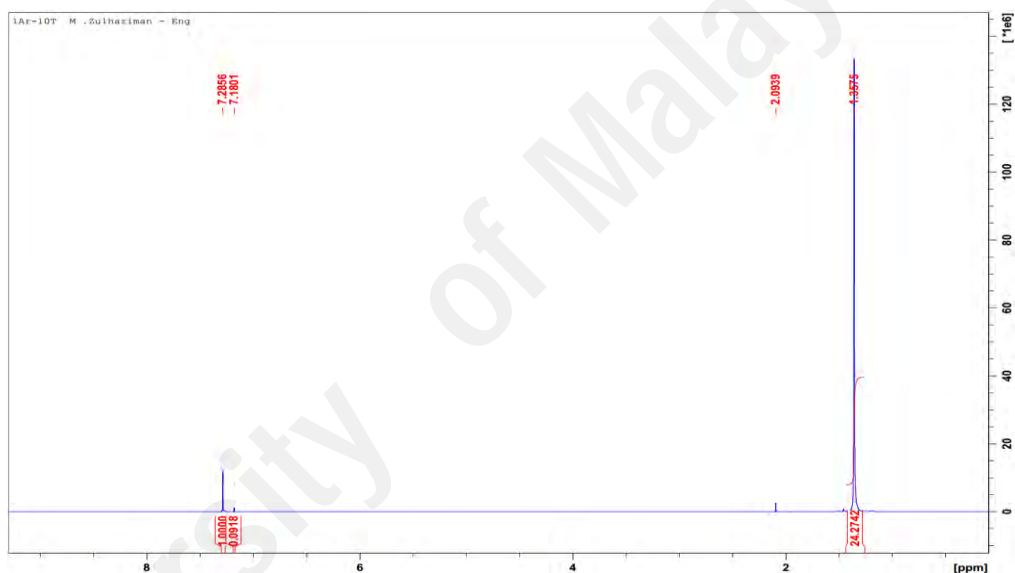


Figure B62: Raffinate layer of [C<sub>2</sub>mimSCN + C<sub>2</sub>mimTf<sub>2</sub>N] + benzene + cyclohexane (10% benzene in feed)

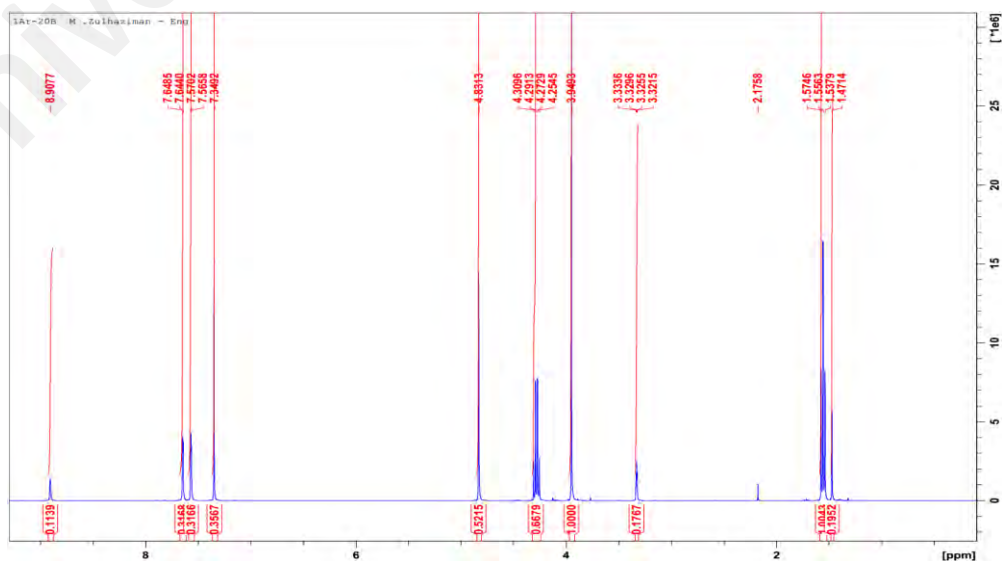


Figure B63: Extract layer of [C<sub>2</sub>mimSCN + C<sub>2</sub>mimTf<sub>2</sub>N] + benzene + cyclohexane (20% benzene in feed)

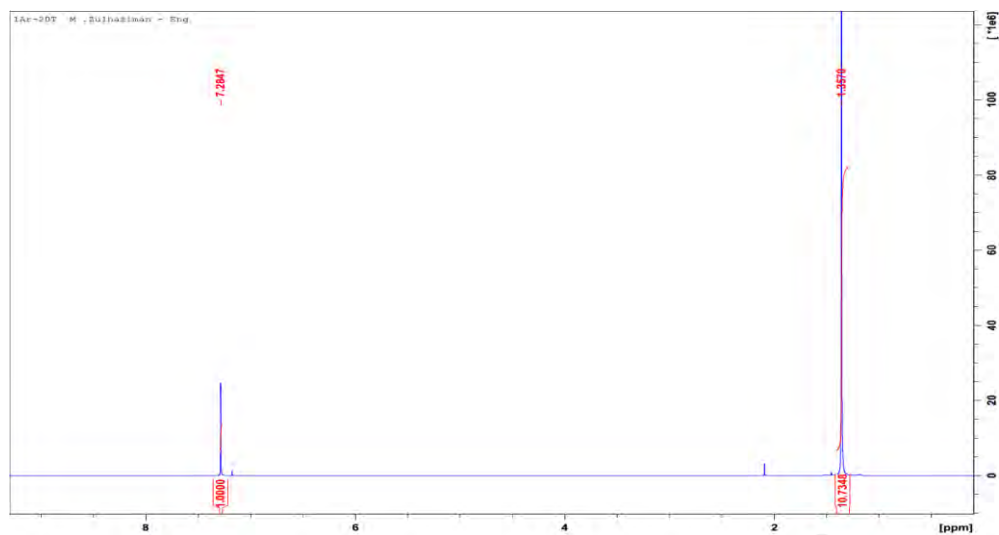


Figure B64: Raffinate layer of [C<sub>2</sub>mimSCN + C<sub>2</sub>mimTf<sub>2</sub>N] + benzene + cyclohexane (20% benzene in feed)

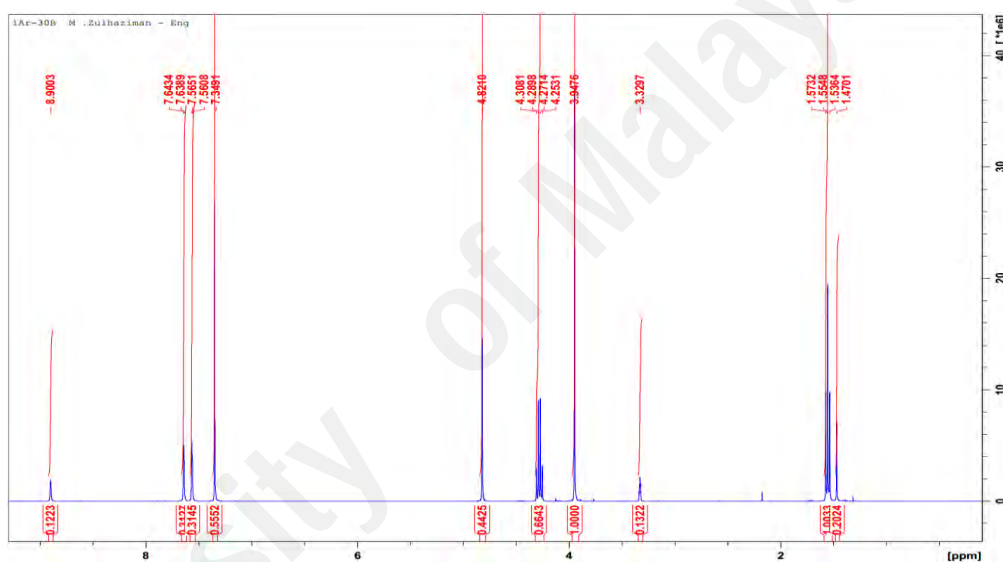


Figure B65: Extract layer of [C<sub>2</sub>mimSCN + C<sub>2</sub>mimTf<sub>2</sub>N] + benzene + cyclohexane (30% benzene in feed)

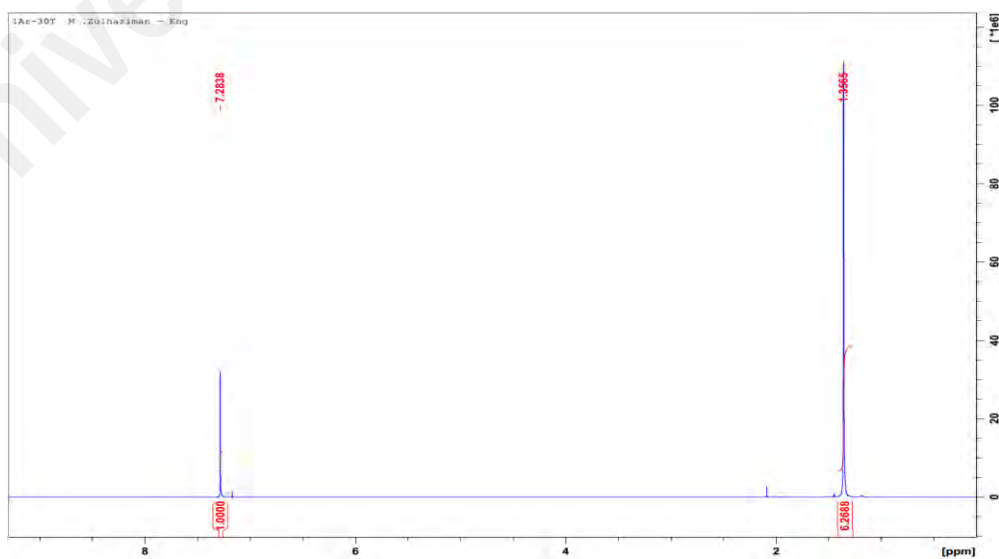


Figure B66: Raffinate layer of [C<sub>2</sub>mimSCN + C<sub>2</sub>mimTf<sub>2</sub>N] + benzene + cyclohexane (30% benzene in feed)

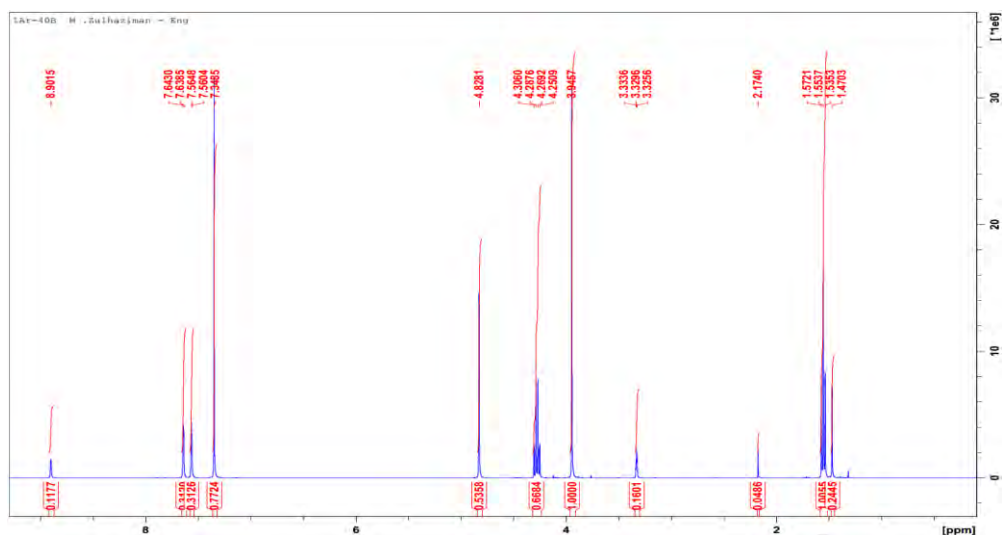


Figure B67: Extract layer of [C<sub>2</sub>mimSCN + C<sub>2</sub>mimTf<sub>2</sub>N] + benzene + cyclohexane (40% benzene in feed)

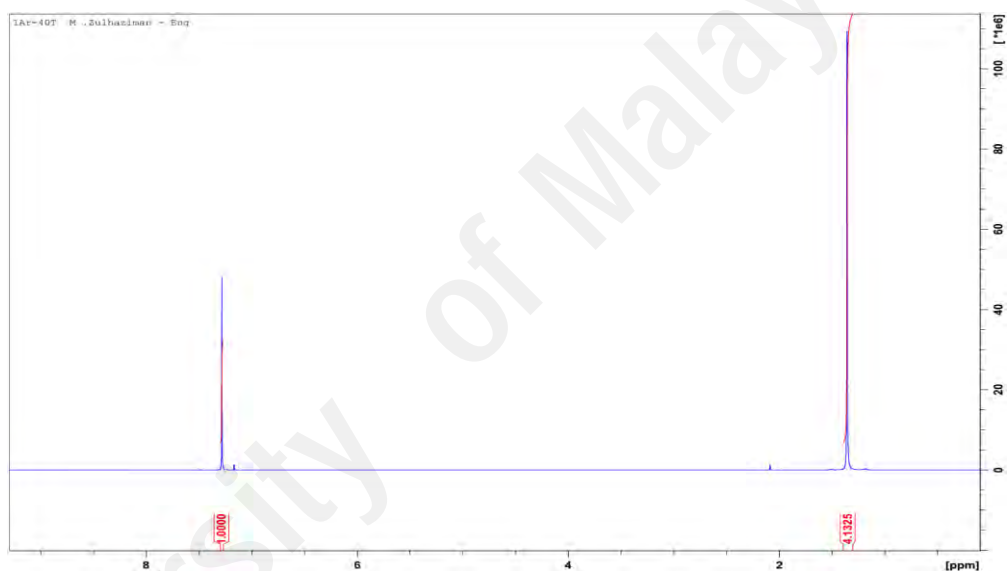


Figure B68: Raffinate layer of [C<sub>2</sub>mimSCN + C<sub>2</sub>mimTf<sub>2</sub>N] + benzene + cyclohexane (40% benzene in feed)

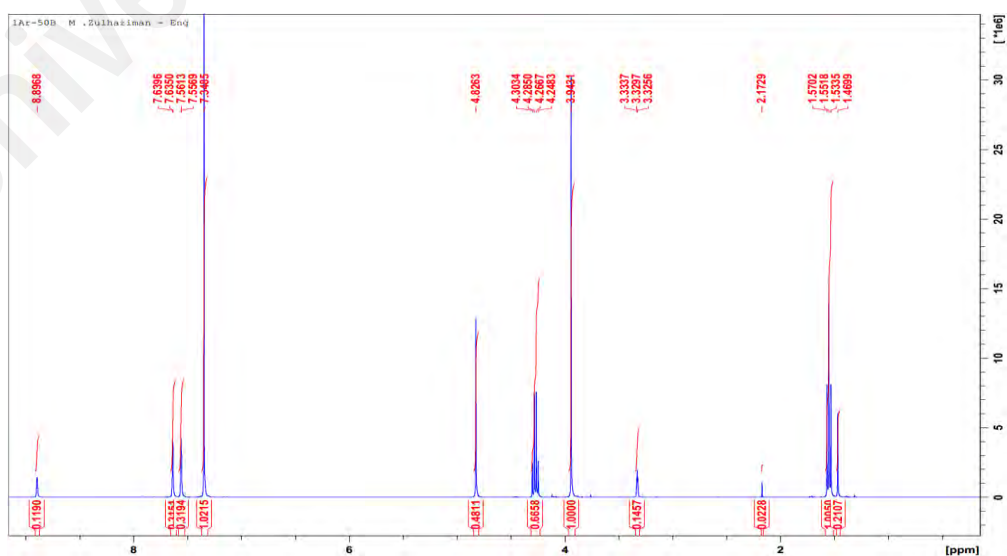


Figure B69: Extract layer of [C<sub>2</sub>mimSCN + C<sub>2</sub>mimTf<sub>2</sub>N] + benzene + cyclohexane (50% benzene in feed)

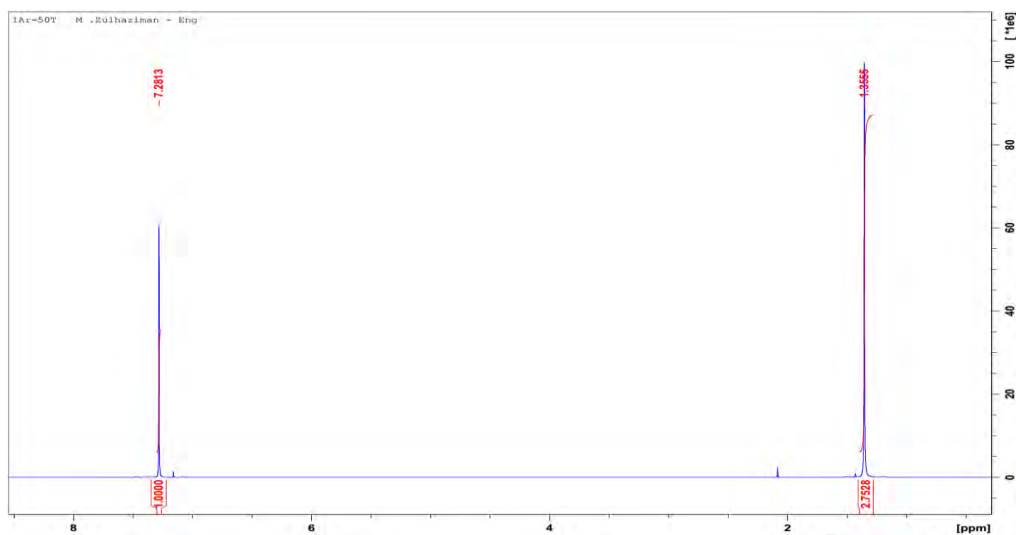


Figure B70: Raffinate layer of  $[C_2mimSCN + C_2mimTf_2N]$  + benzene + cyclohexane (50% benzene in feed)

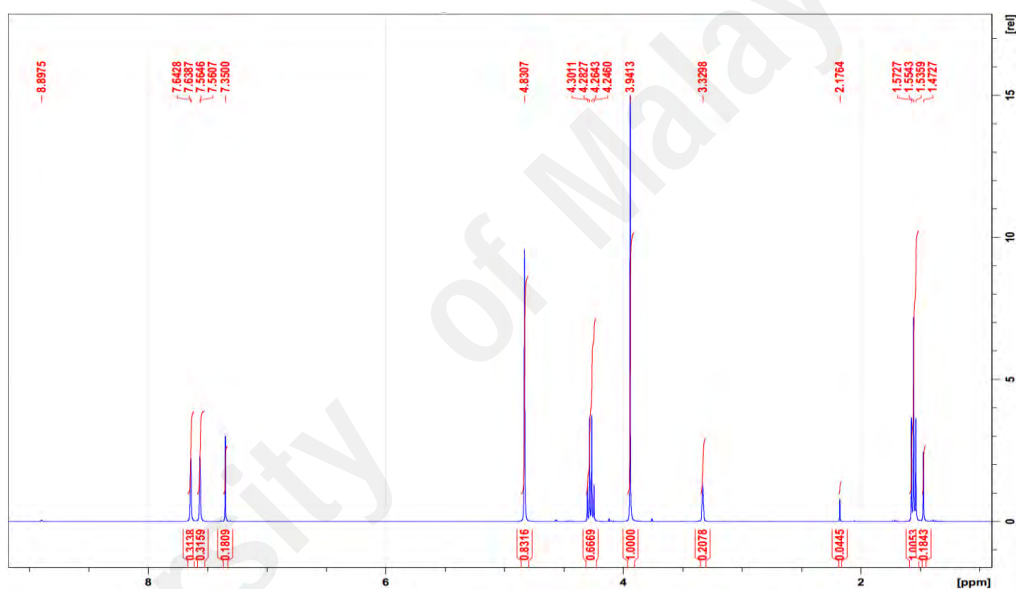


Figure B71: Extract layer of  $[C_2mimN(CN)_2 + C_2mimTf_2N]$  + benzene + cyclohexane (10% benzene in feed)

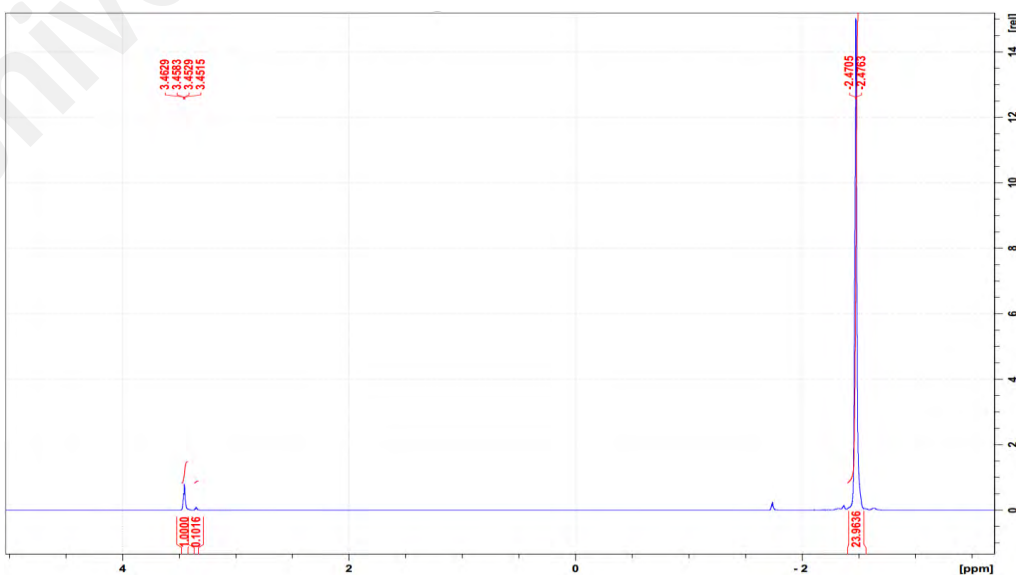


Figure B72: Raffinate layer of  $[C_2mimN(CN)_2 + C_2mimTf_2N]$  + benzene + cyclohexane (10% benzene in feed)

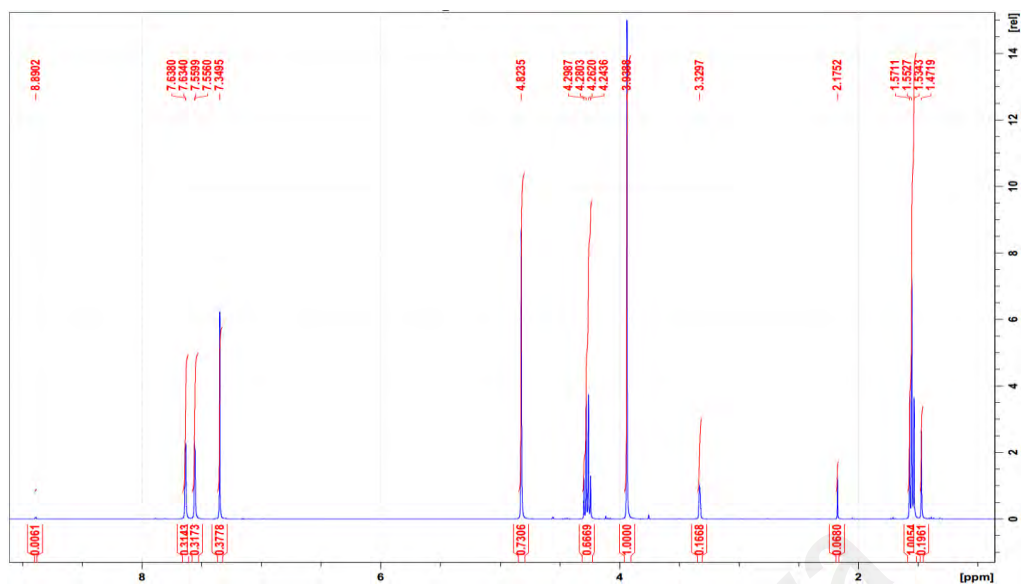


Figure B73: Extract layer of  $[\text{C}_2\text{mimN}(\text{CN})_2 + \text{C}_2\text{mimTf}_2\text{N}] + \text{benzene} + \text{cyclohexane}$  (20% benzene in feed)

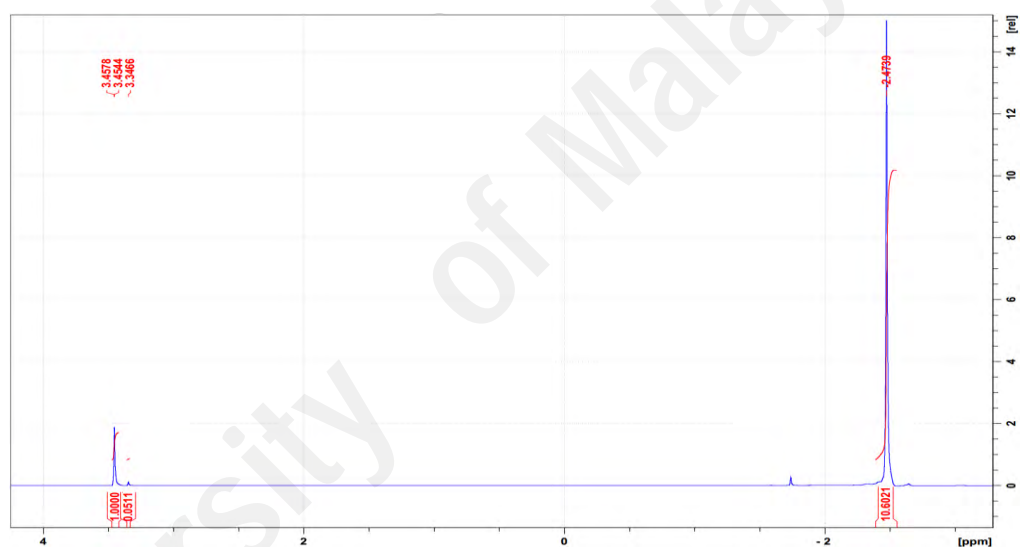


Figure B74: Raffinate layer of  $[\text{C}_2\text{mimN}(\text{CN})_2 + \text{C}_2\text{mimTf}_2\text{N}] + \text{benzene} + \text{cyclohexane}$  (20% benzene in feed)

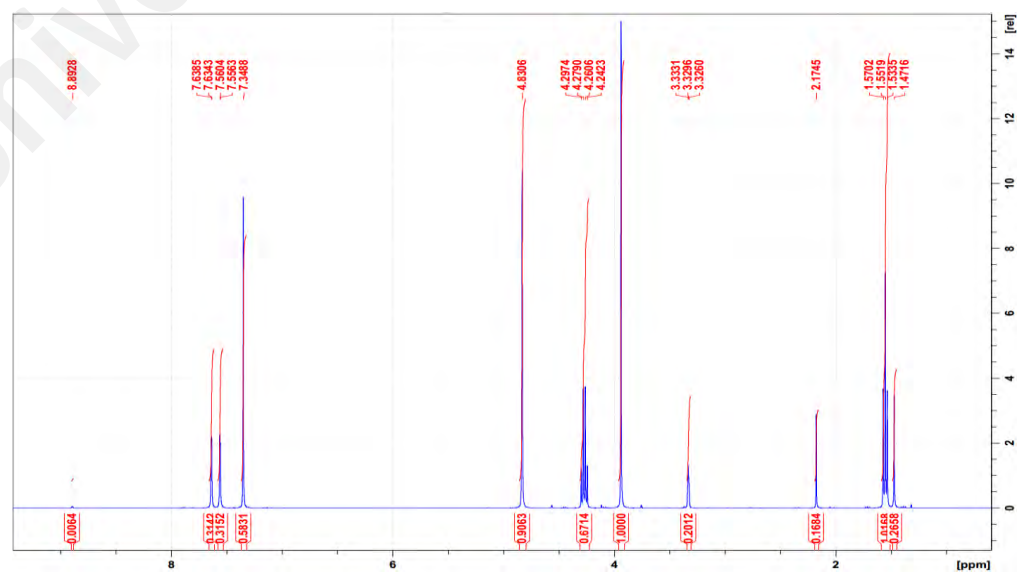


Figure B75: Extract layer of  $[\text{C}_2\text{mimN}(\text{CN})_2 + \text{C}_2\text{mimTf}_2\text{N}] + \text{benzene} + \text{cyclohexane}$  (30% benzene in feed)

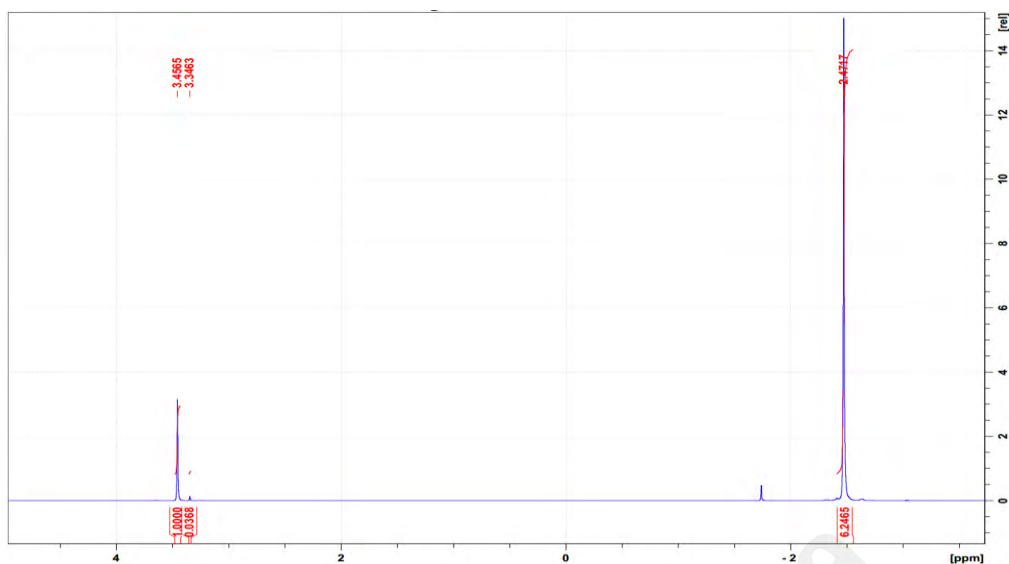


Figure B76: Raffinate layer of  $[\text{C}_2\text{mimN}(\text{CN})_2 + \text{C}_2\text{mimTf}_2\text{N}] + \text{benzene} + \text{cyclohexane}$  (30% benzene in feed)

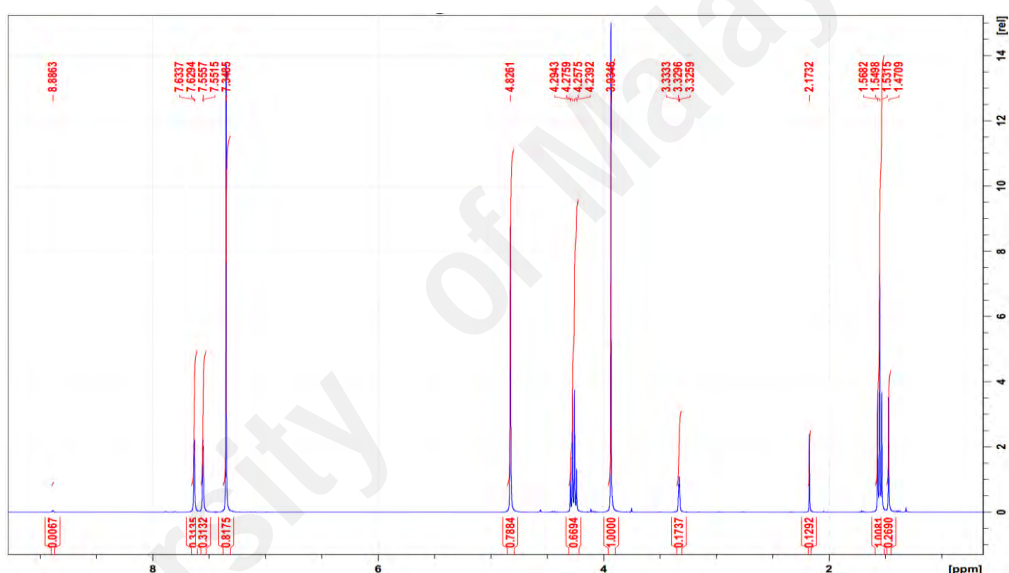


Figure B77: Extract layer of  $[\text{C}_2\text{mimN}(\text{CN})_2 + \text{C}_2\text{mimTf}_2\text{N}] + \text{benzene} + \text{cyclohexane}$  (40% benzene in feed)

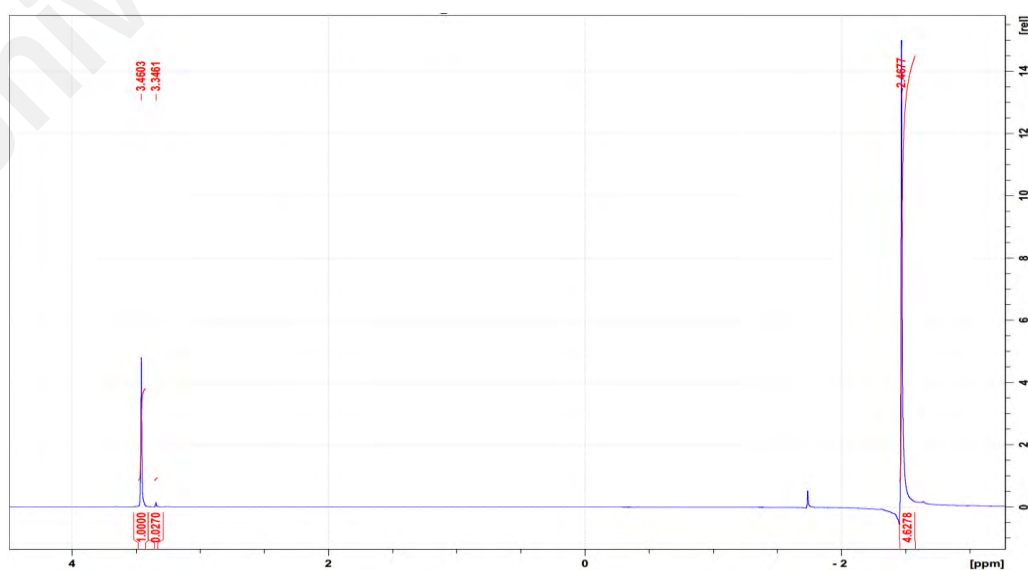


Figure B78: Raffinate layer of  $[\text{C}_2\text{mimN}(\text{CN})_2 + \text{C}_2\text{mimTf}_2\text{N}] + \text{benzene} + \text{cyclohexane}$  (40% benzene in feed)

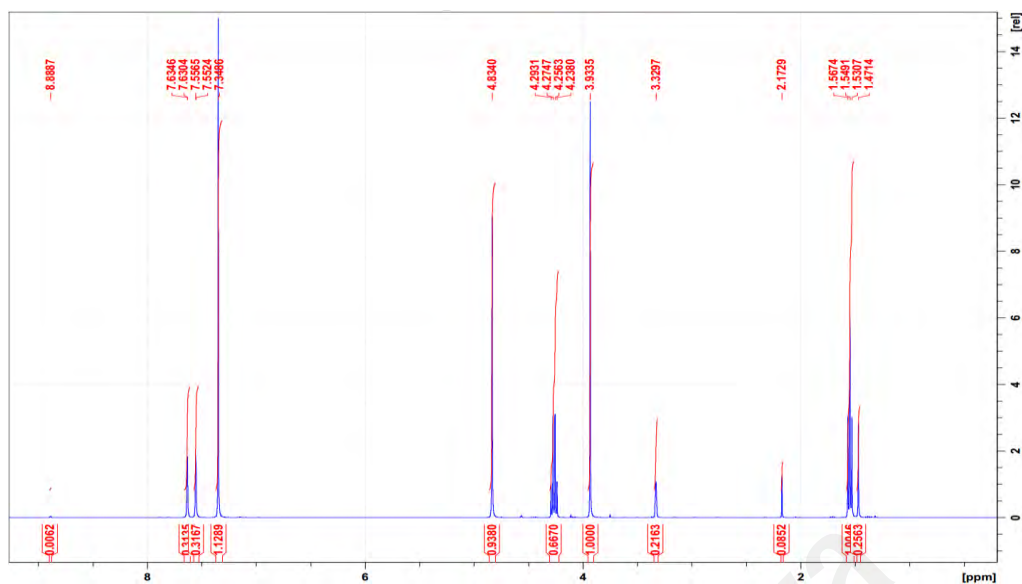


Figure B79: Extract layer of  $[C_2mimN(CN)_2 + C_2mimTf_2N]$  + benzene + cyclohexane (50% benzene in feed)

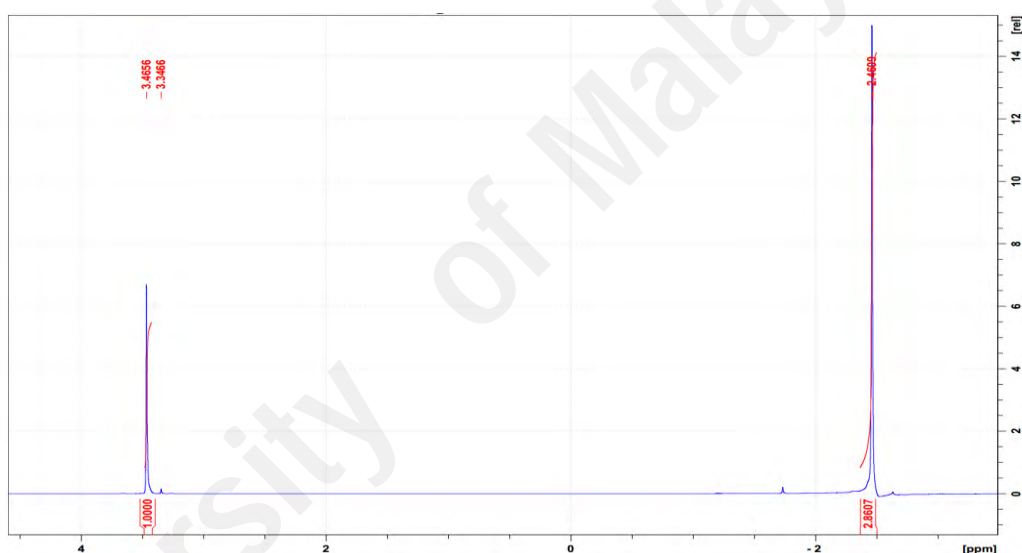


Figure B80: Raffinate layer of  $[C_2mimN(CN)_2 + C_2mimTf_2N]$  + benzene + cyclohexane (50% benzene in feed)

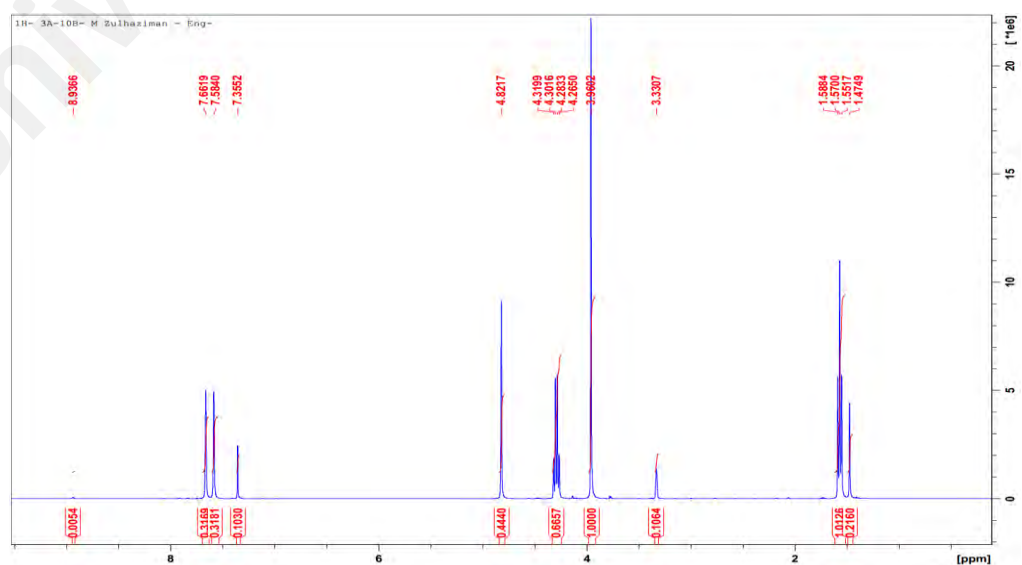


Figure B81: Extract layer of  $[C_2mimSCN + C_2mimN(CN)_2]$  + benzene + cyclohexane (10% benzene in feed)

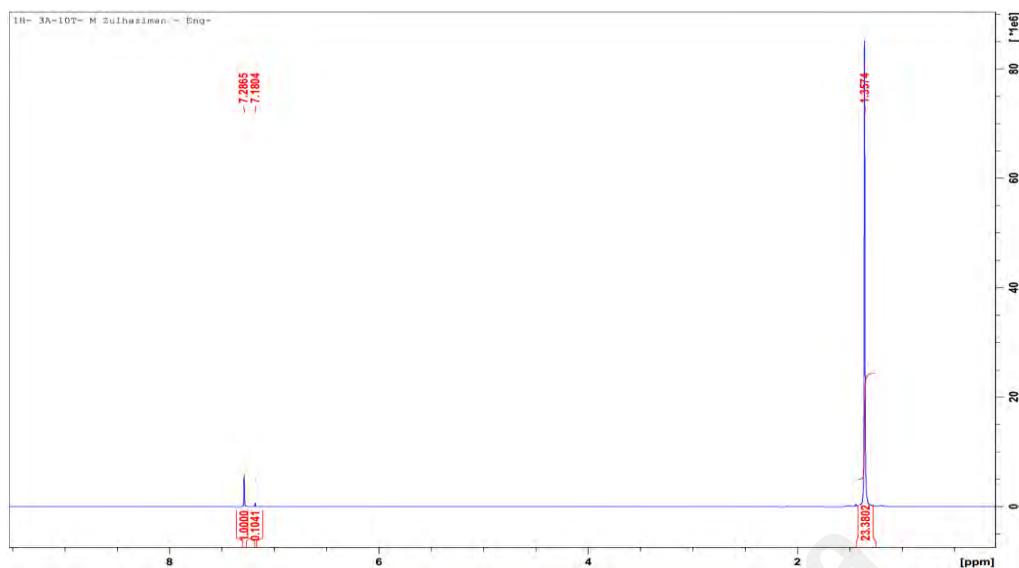


Figure B82: Raffinate layer of  $[C_2mimSCN + C_2mimN(CN)_2]$  + benzene + cyclohexane (10% benzene in feed)

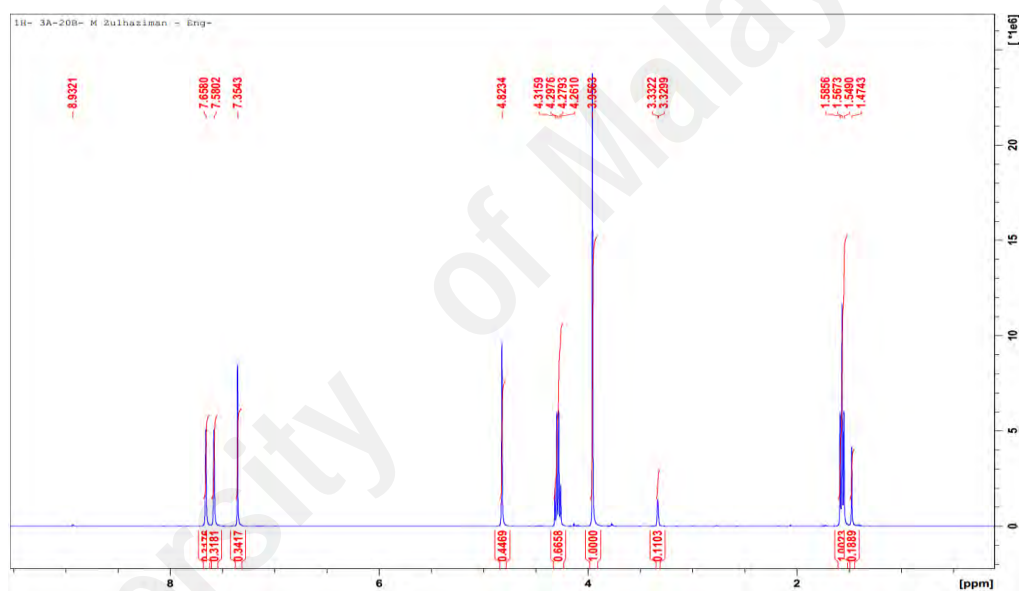


Figure B83: Extract layer of  $[C_2mimSCN + C_2mimN(CN)_2]$  + benzene + cyclohexane (20% benzene in feed)

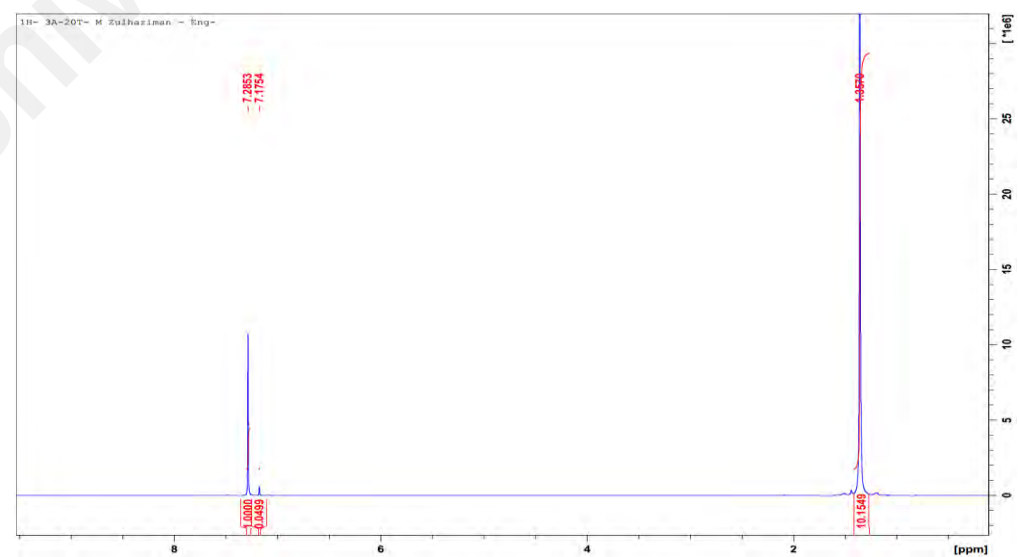


Figure B84: Raffinate layer of  $[C_2mimSCN + C_2mimN(CN)_2]$  + benzene + cyclohexane (20% benzene in feed)

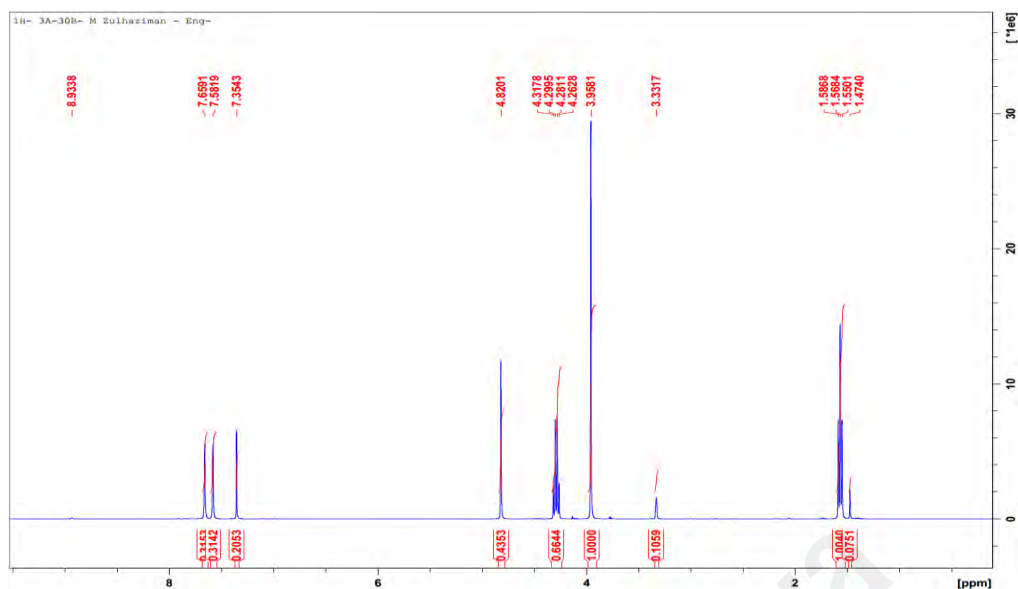


Figure B85: Extract layer of  $[C_2mimSCN + C_2mimN(CN)_2]$  + benzene + cyclohexane (30% benzene in feed)

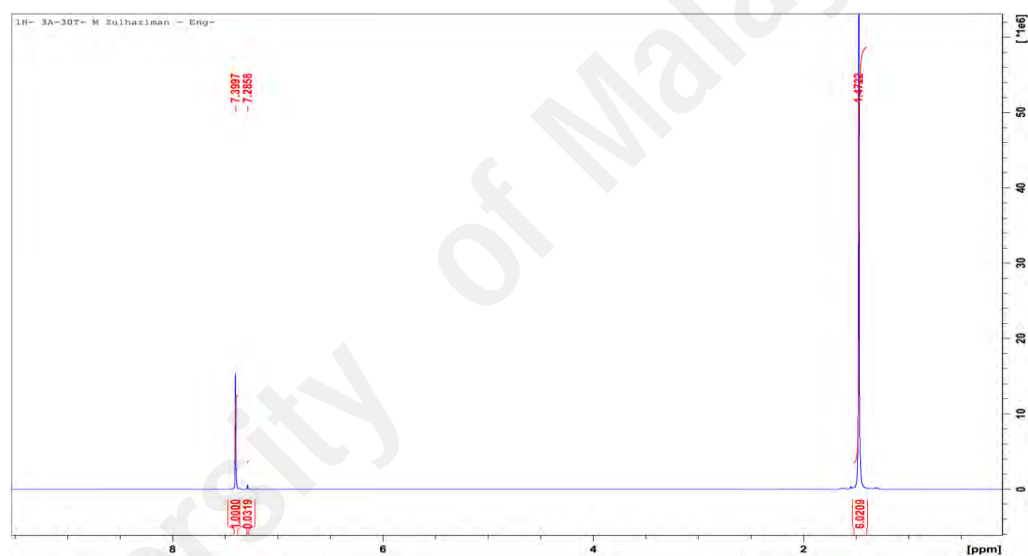


Figure B86: Raffinate layer of  $[C_2mimSCN + C_2mimN(CN)_2]$  + benzene + cyclohexane (30% benzene in feed)

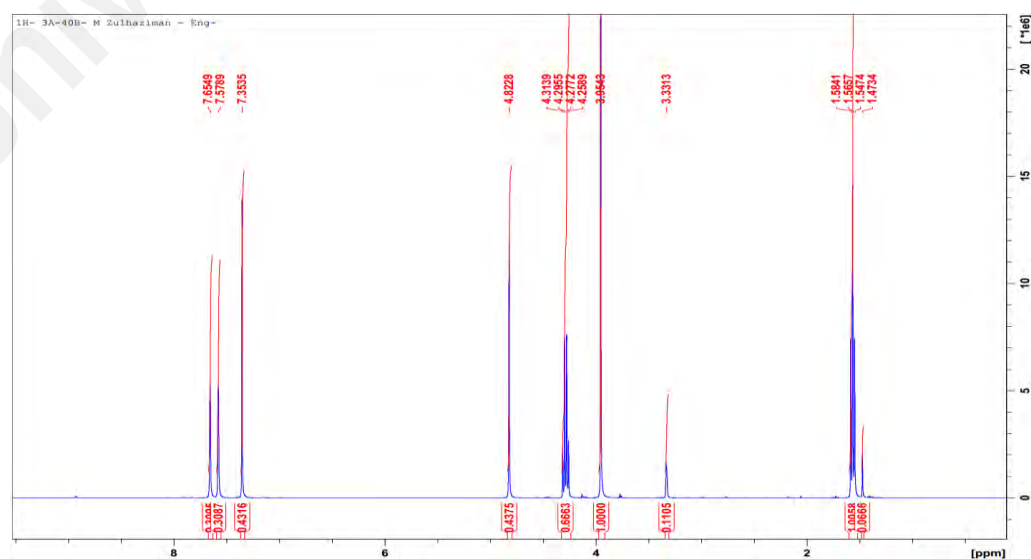


Figure B87: Extract layer of  $[C_2mimSCN + C_2mimN(CN)_2]$  + benzene + cyclohexane (40% benzene in feed)

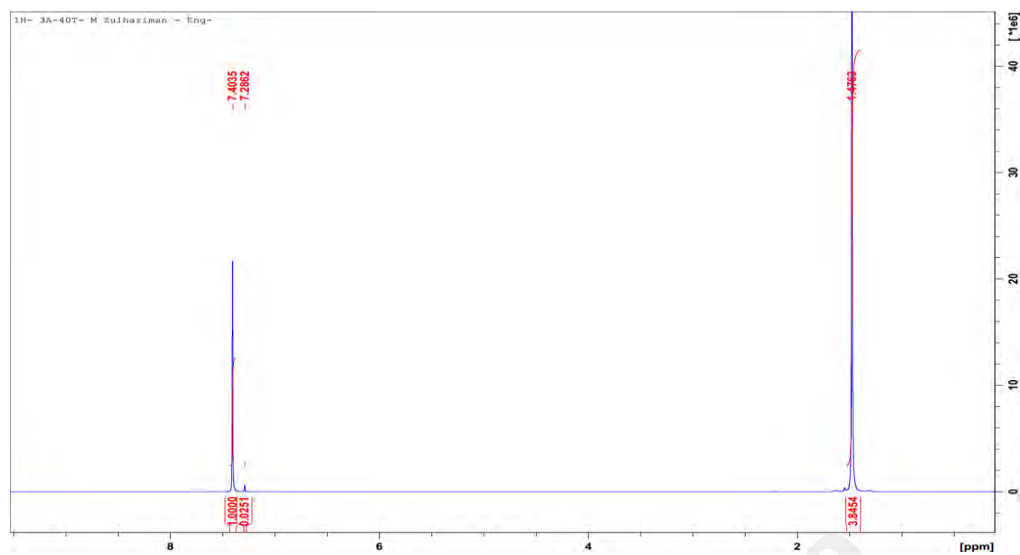


Figure B88: Raffinate layer of  $[C_2mimSCN + C_2mimN(CN)_2]$  + benzene + cyclohexane (40% benzene in feed)

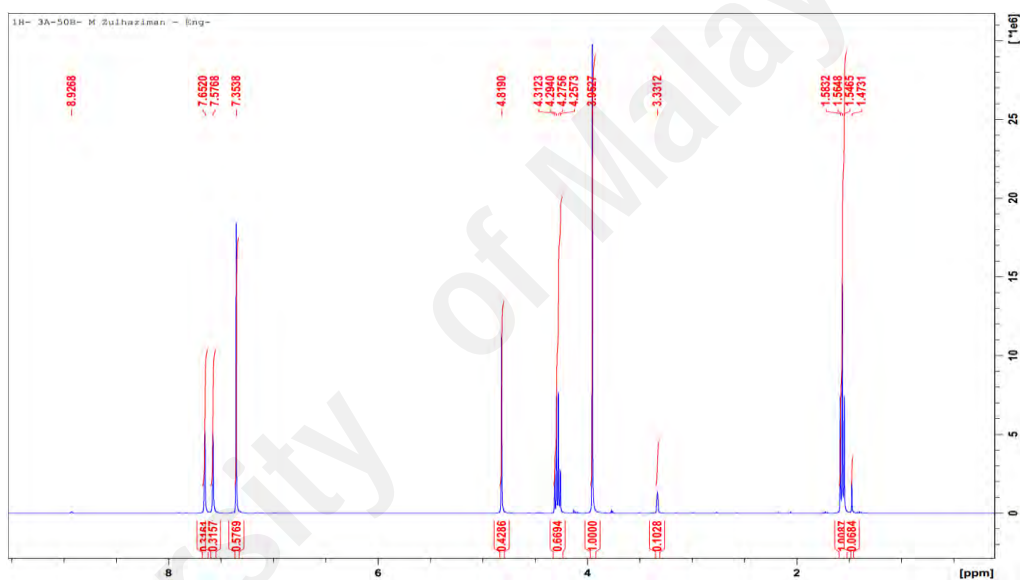


Figure B89: Extract layer of  $[C_2mimSCN + C_2mimN(CN)_2]$  + benzene + cyclohexane (50% benzene in feed)

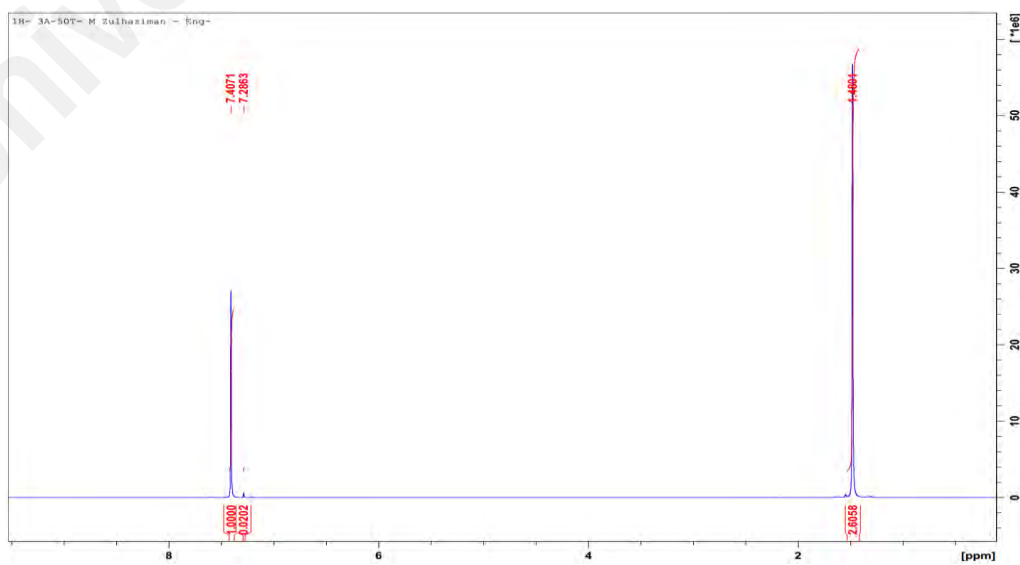


Figure B90: Raffinate layer of  $[C_2mimN(CN)_2 + C_2mimAc]$  + benzene + cyclohexane (50% benzene in feed)

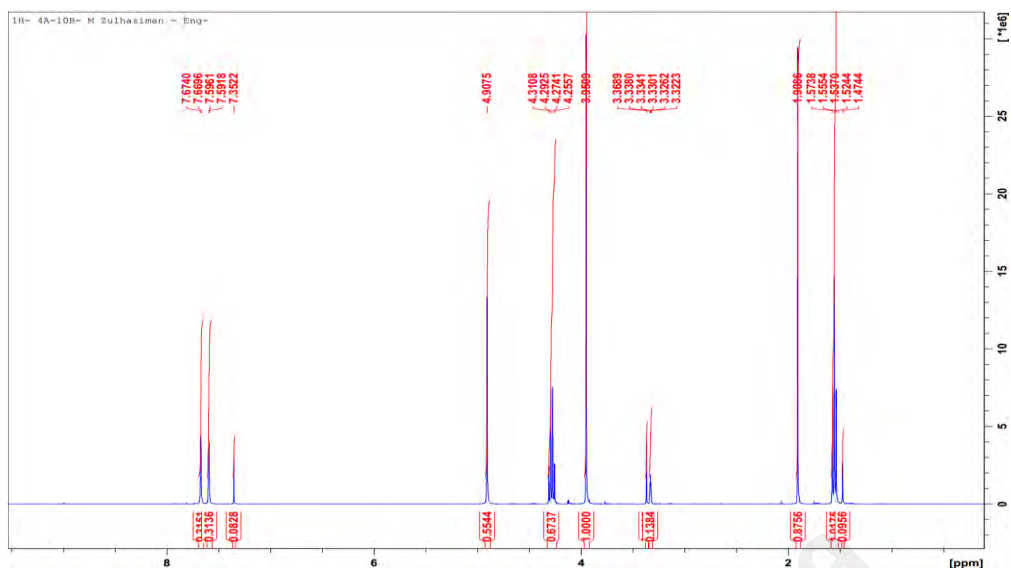


Figure B91: Extract layer of  $[C_2mimN(CN)_2 + C_2mimAc]$  + benzene + cyclohexane (10% benzene in feed)

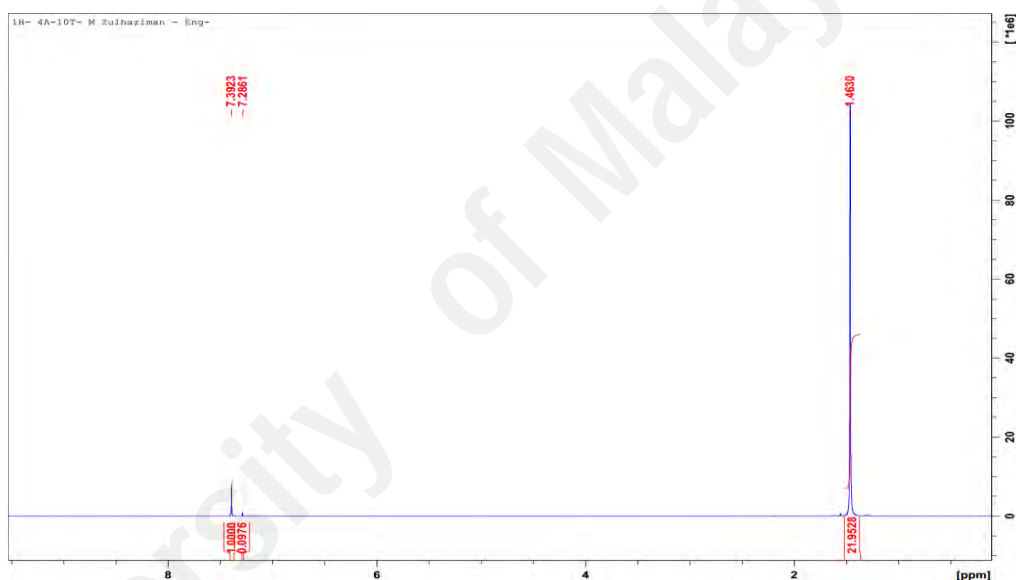


Figure B92: Raffinate layer of  $[C_2mimN(CN)_2 + C_2mimAc]$  + benzene + cyclohexane (10% benzene in feed)

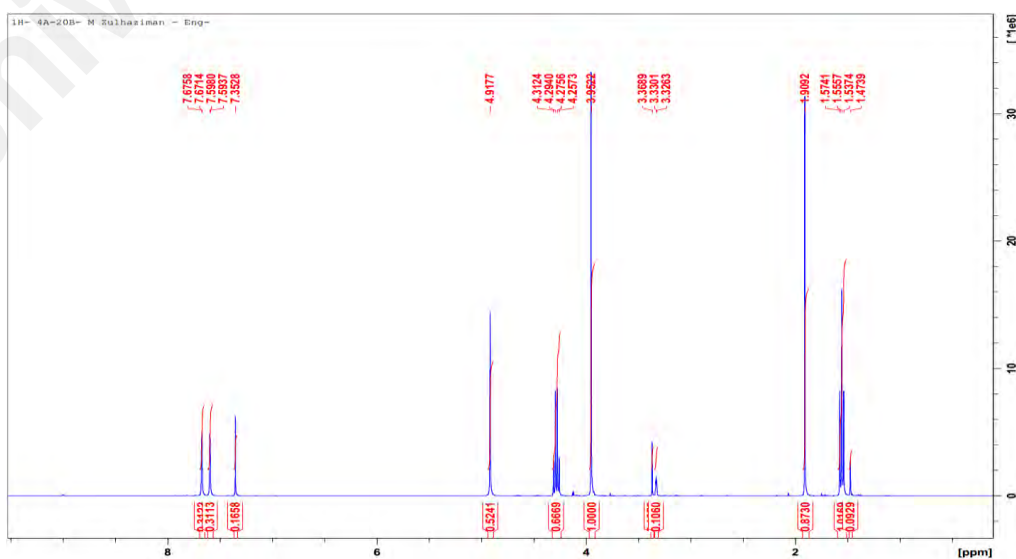


Figure B93: Extract layer of  $[C_2mimN(CN)_2 + C_2mimAc]$  + benzene + cyclohexane (20% benzene in feed)

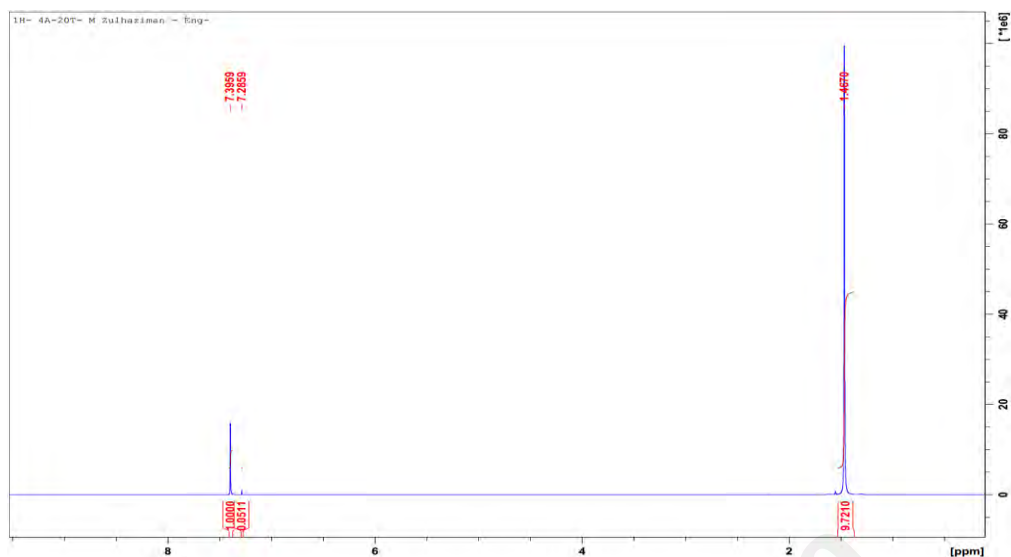


Figure B94: Raffinate layer of  $[\text{C}_2\text{mimN}(\text{CN})_2 + \text{C}_2\text{mimAc}] + \text{benzene} + \text{cyclohexane}$  (20% benzene in feed)

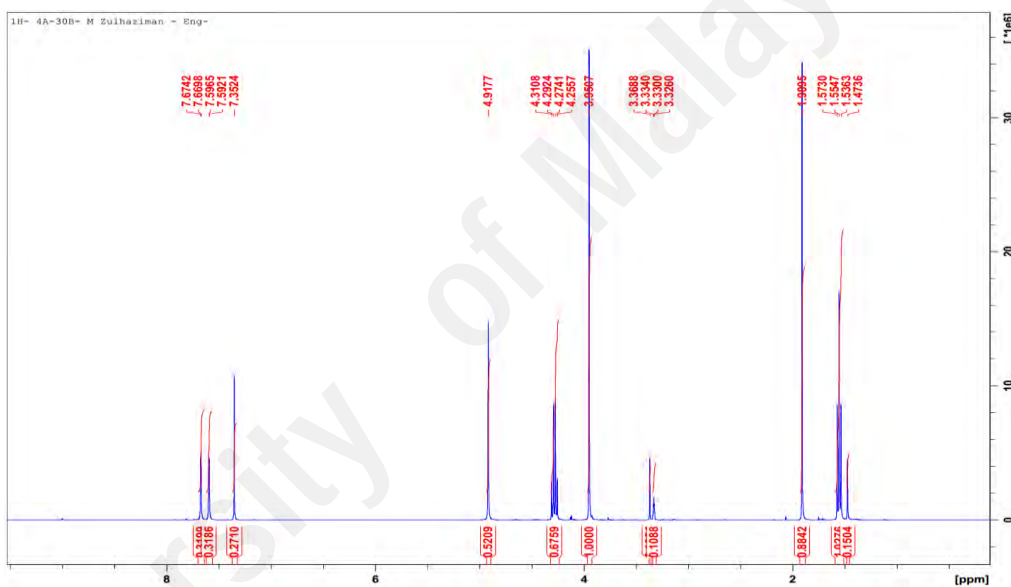


Figure B95: Extract layer of  $[\text{C}_2\text{mimN}(\text{CN})_2 + \text{C}_2\text{mimAc}] + \text{benzene} + \text{cyclohexane}$  (30% benzene in feed)

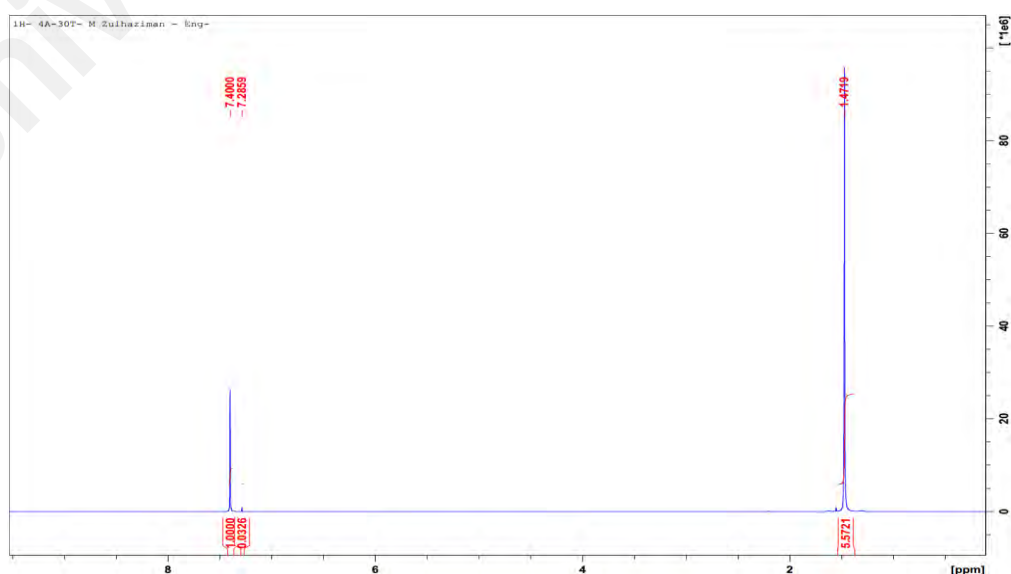


Figure B96: Raffinate layer of  $[\text{C}_2\text{mimN}(\text{CN})_2 + \text{C}_2\text{mimAc}] + \text{benzene} + \text{cyclohexane}$  (30% benzene in feed)

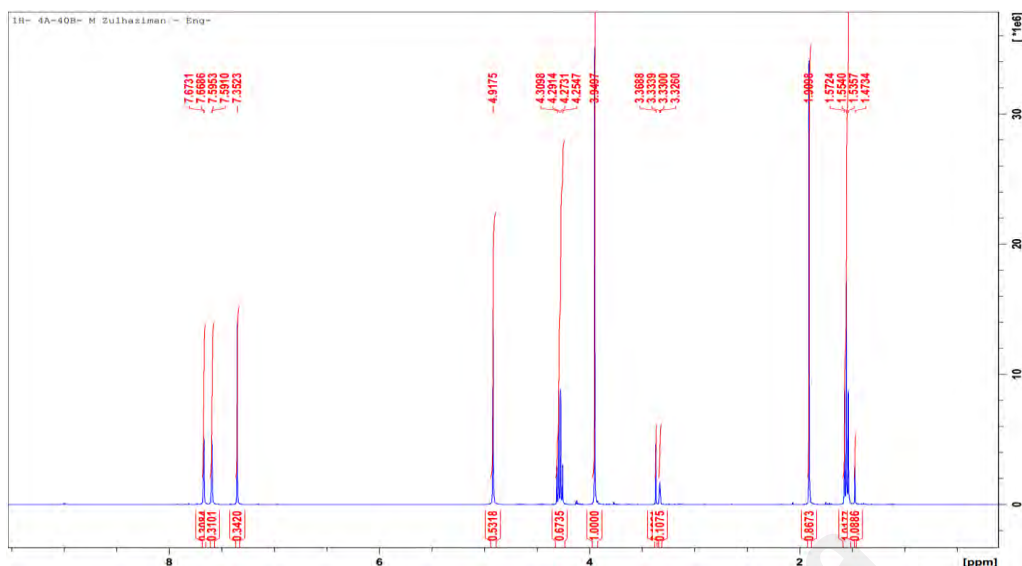


Figure B97: Extract layer of  $[\text{C}_2\text{mimN}(\text{CN})_2 + \text{C}_2\text{mimAc}] + \text{benzene} + \text{cyclohexane}$  (40% benzene in feed)

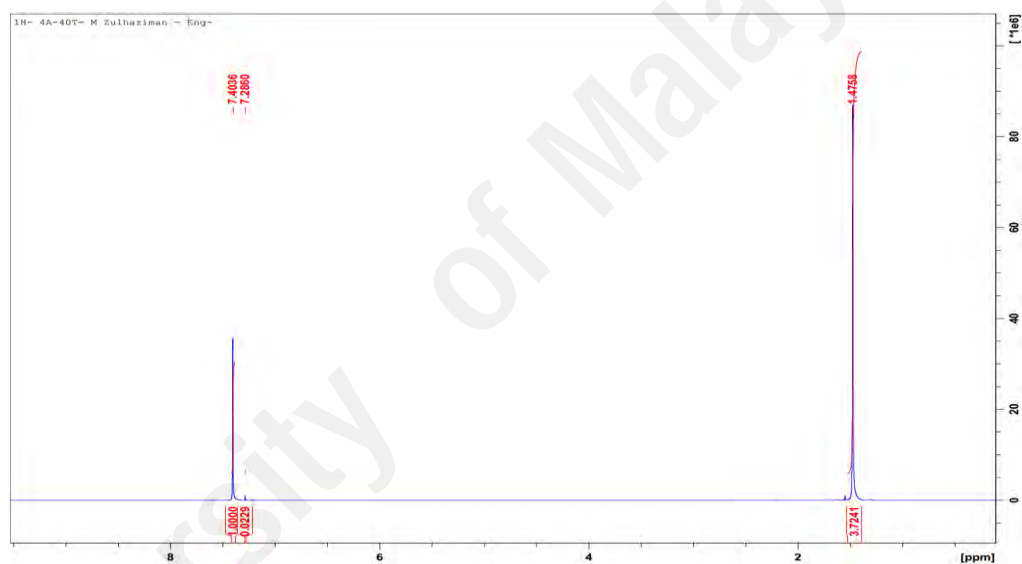


Figure B98: Raffinate layer of  $[\text{C}_2\text{mimN}(\text{CN})_2 + \text{C}_2\text{mimAc}] + \text{benzene} + \text{cyclohexane}$  (40% benzene in feed)

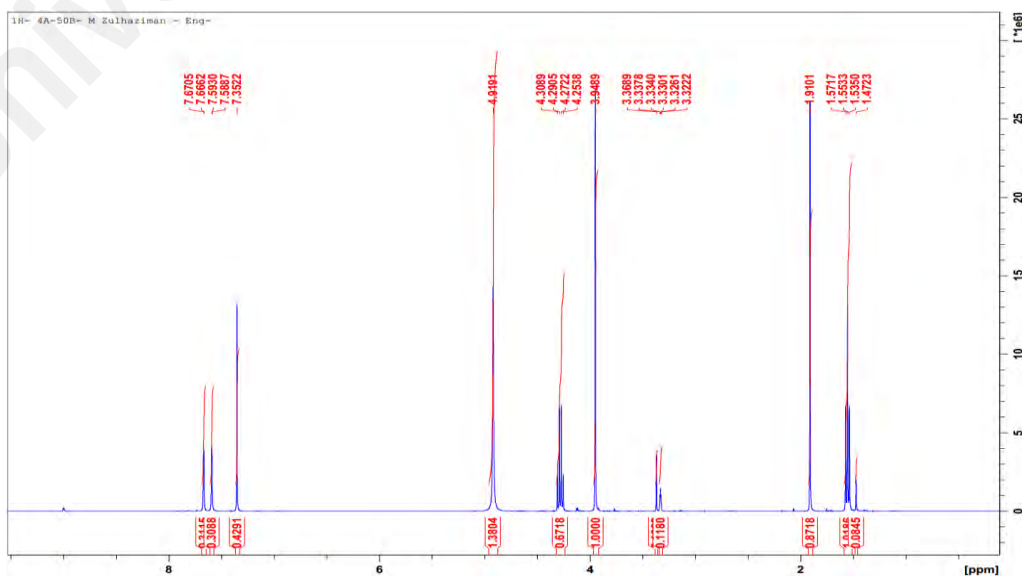


Figure B99: Extract layer of  $[\text{C}_2\text{mimN}(\text{CN})_2 + \text{C}_2\text{mimAc}] + \text{benzene} + \text{cyclohexane}$  (50% benzene in feed)

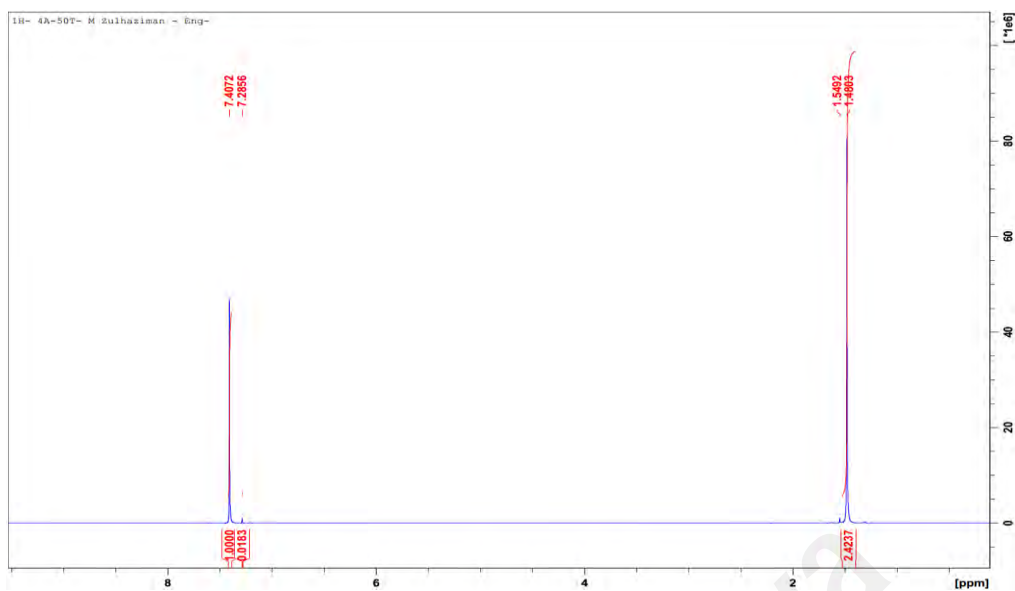


Figure B100: Raffinate layer of  $[\text{C}_2\text{mimN}(\text{CN})_2 + \text{C}_2\text{mimAc}] + \text{benzene} + \text{cyclohexane}$  (50% benzene in feed)

University of Malaysia